

# X-ray Imaging

Chris Jacobsen

Department of Physics & Astronomy

Stony Brook University, NY, USA

[Chris.Jacobsen@stonybrook.edu](mailto:Chris.Jacobsen@stonybrook.edu)

Slides at **<http://tinyurl.com/nceg6r>**

# X-ray microscopy group at Stony Brook

Xiaojing Huang,  
Johanna Nelson,  
Christian Holzner,  
Robert Towers,  
Simon Moser, Sue  
Wirick, Chris  
Jacobsen, Bjorg  
Larson, Jan  
Steinbrener, Josh  
Turner, Holger  
Fleckenstein  
**Many alumni and  
collaborators!**



**Funding: DoE (method development), NIH (application to cells, phase contrast), NYSTAR (coherent optics and applications)**

Wilhelm Röntgen  
Universität Würzburg  
Dec. 1895



Michael Pupin  
Columbia University/New York  
Feb. 1896



“This is of the hand of a gentleman resident in New York, who, while on a hunting trip in England a few months ago, was so unfortunate as to discharge his gun into his right hand, no less than forty shot lodging in the palm and fingers. The hand has since healed completely; but the shot remain in it, the doctors being unable to remove them, because unable to determine their exact location. The result is that the hand is almost useless, and often painful.” - Cleveland Moffett, McClure’s Magazine, April 1896

# The X-ray Microscope

It would be a big improvement on microscopes using light or electrons, for X-rays combine short wavelengths, giving fine resolution, and penetration. The main problems standing in the way have now been solved.

# SCIENTIFIC AMERICAN

Established 1845

CONTENTS FOR MARCH 1949

VOLUME 180, NUMBER 3

SCIENTIFIC AMERICAN is copyrighted 1949 in the U. S. and Berne Convention countries by Scientific American, Inc.

## THE X-RAY MICROSCOPE

by Paul Kirkpatrick

It would be a useful complement to microscopes using light or electrons, for X-rays combine short wavelengths, giving fine resolution, and penetration. The main problems standing in the way have now been solved. **44**

Some further problems were solved after 1949...

Grazing incidence mirror optics: Kirkpatrick and Baez, 1949; Wolter 1952

Zone plate optics: Baez 1960; Schmahl and Rudolph 1969; Ceglio 1980

Synchrotron radiation: Horowitz and Howell 1972; Aoki *et al.*, 1972; Niemann, Schmahl *et al.*, 1976

Scanning: Horowitz and Howell 1972; Rarback, Kirz *et al.*, 1980

Fluorescence: Horowitz and Howell 1972; Sparks 1980

Cryo: Schneider *et al.*, 1995; Maser, Jacobsen *et al.*, 1996

Tomography: Haddad *et al.*, 1994; Schneider, Weiss *et al.* 1998

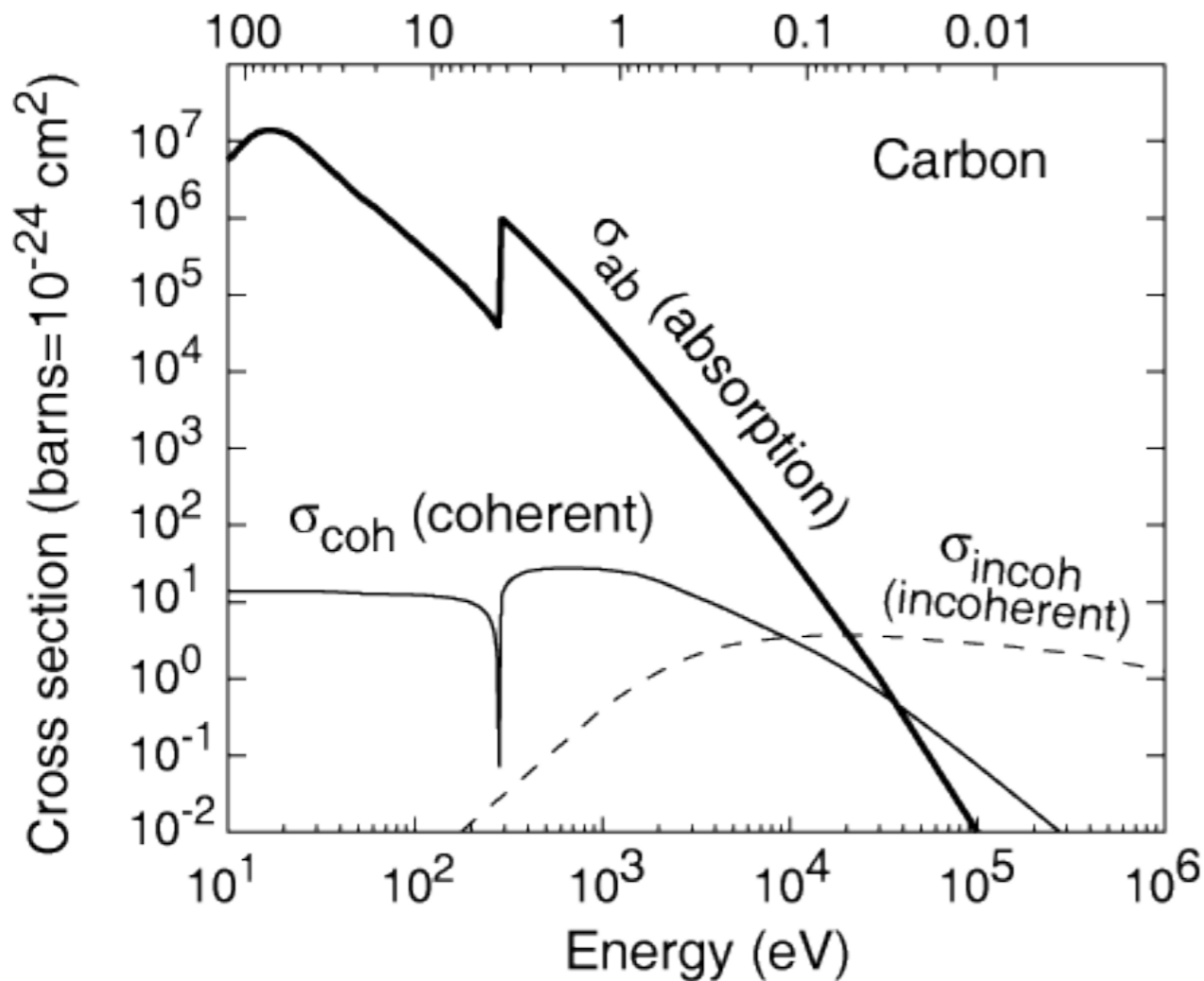
NEXAFS spectromicroscopy: Ade, Kirz *et al.*, 1992

# Historical comments

- Following Röntgen: use visible light microscopes to examine detail of x-ray micrographs on film.
- 1940's & 1950's: reflective optics (Kirkpatrick & Baez; Wolter)
- 1960's: point source projection (Cosslett, Nixon and others)
- “modern” era with zone plates:
  - UV holography for fabrication, full-field imaging using synchrotron: Schmahl et al., Göttingen [Optik **29**, 577--585 (1969); Applied Optics **15**, 1883--1884 (1976)]
  - Electron beam lithography for zone plate fabrication: proposed by Sayre [IBM technical report RC 3974 (#17965), 1972], and first implemented by Ceglio et al., *J. Vac. Sci. Tech. B* **1**, 1285 (1983) and Kern et al., *SPIE* **447**, 204 (1984).
  - Scanning microscopy with zone plates: Kirz et al., Stony Brook [Scanned Image Microscopy, E.A. Ash, Editor. 1980: London. p. 449]

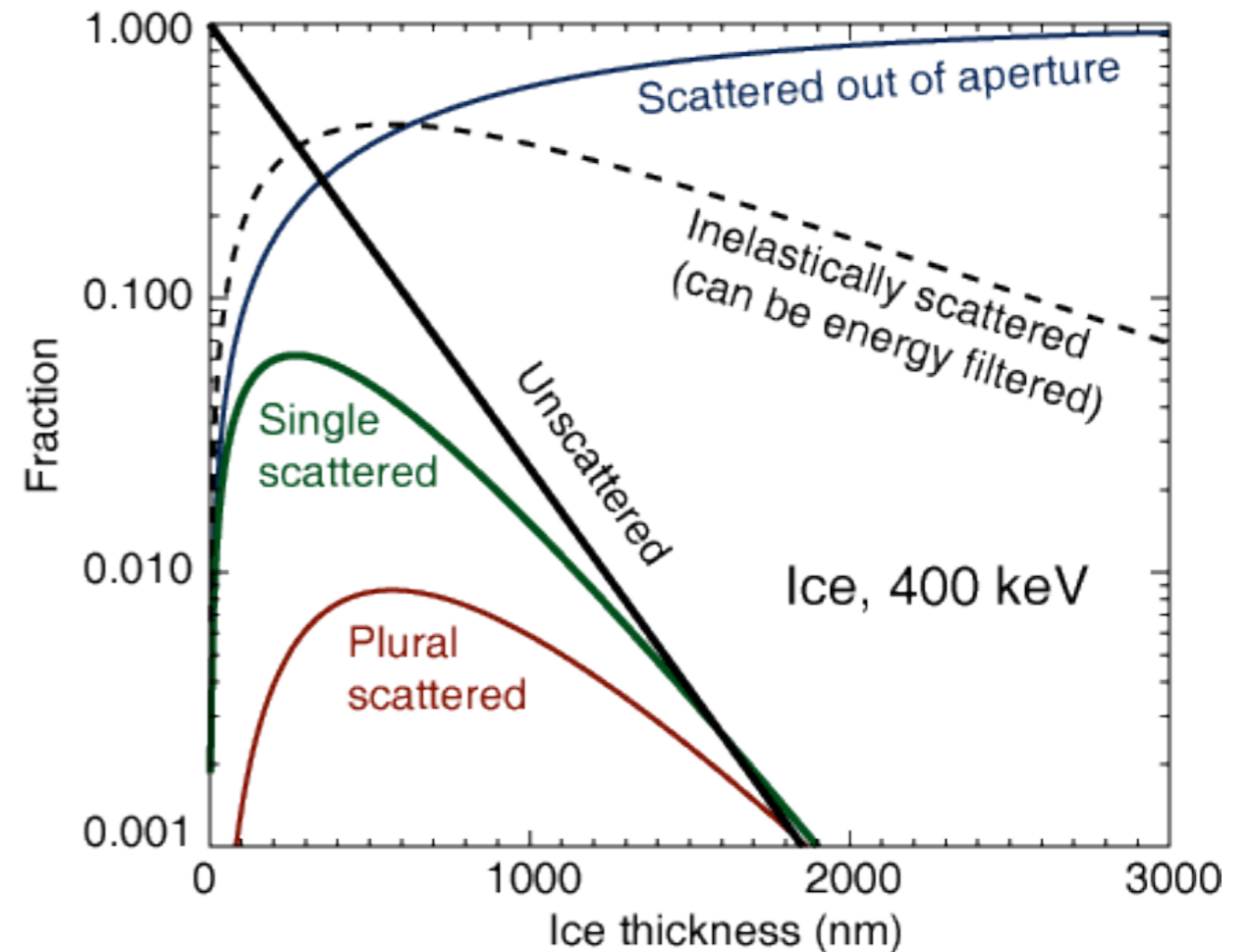
# X rays

$\lambda$  (nm)



- Absorption dominates
- Inelastic scattering is weak
- No multiple scattering

# Electrons

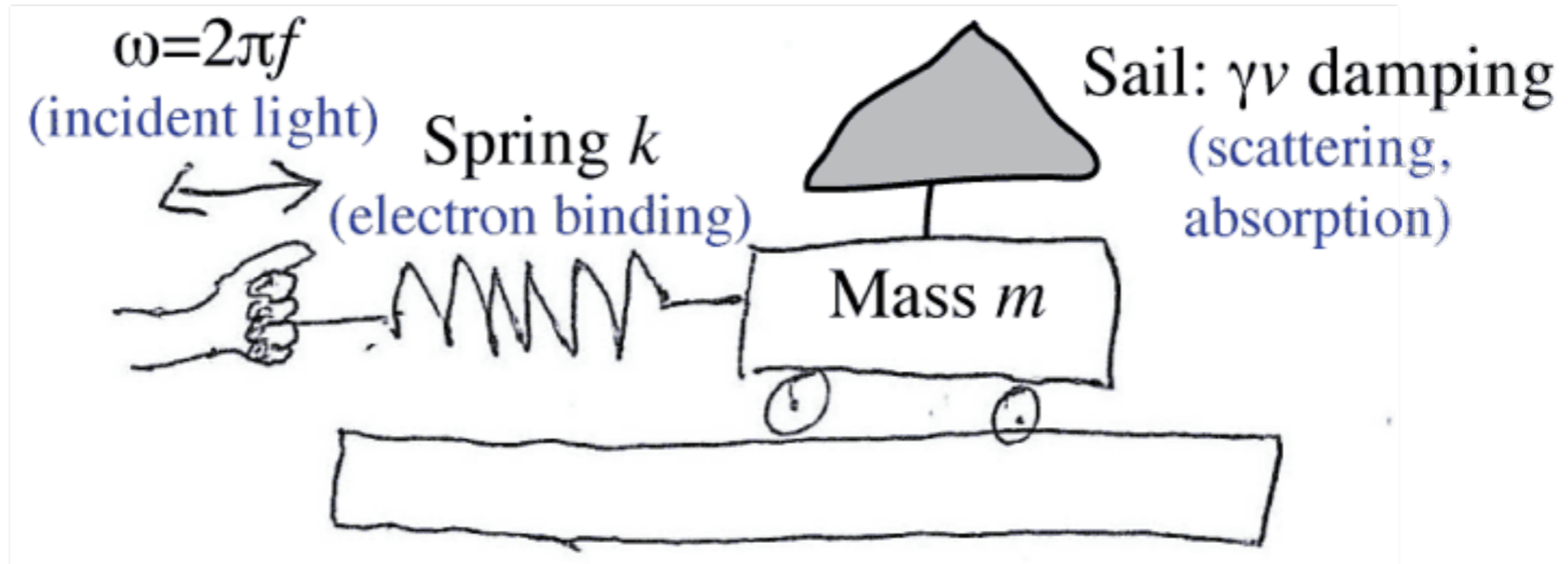


- Inelastic scattering dominates (energy filters)
- Multiple scattering often present
- High contrast from small things

# The refractive index

- Damped, driven harmonic oscillator

Driving frequency



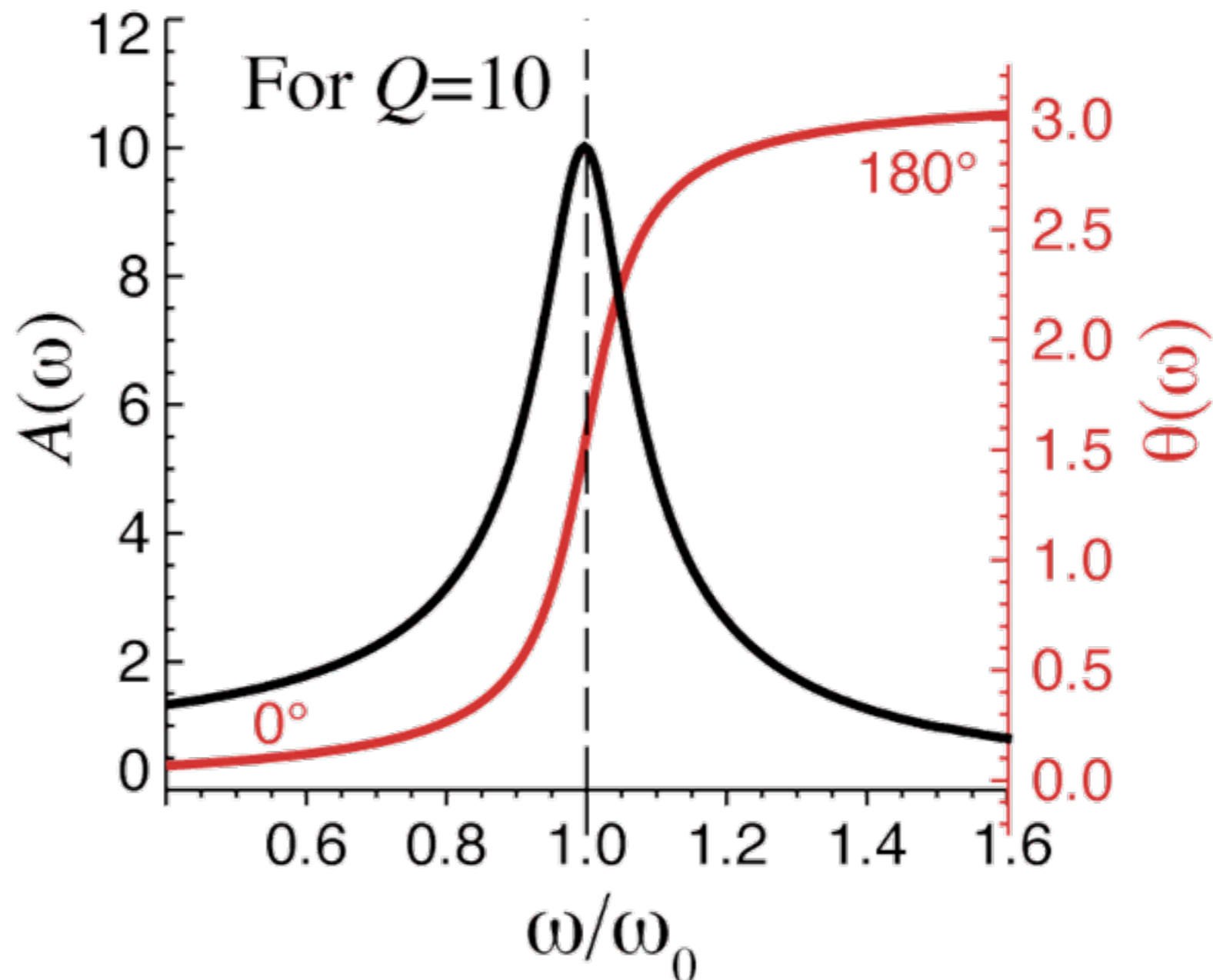
- Damping: scattering, absorption
- Driving: incident electromagnetic wave  $\omega$
- Harmonic oscillator: electron quantum state with energy  $\hbar\omega_0 = \hbar\sqrt{k/m}$



# Damped, driven harmonic oscillator

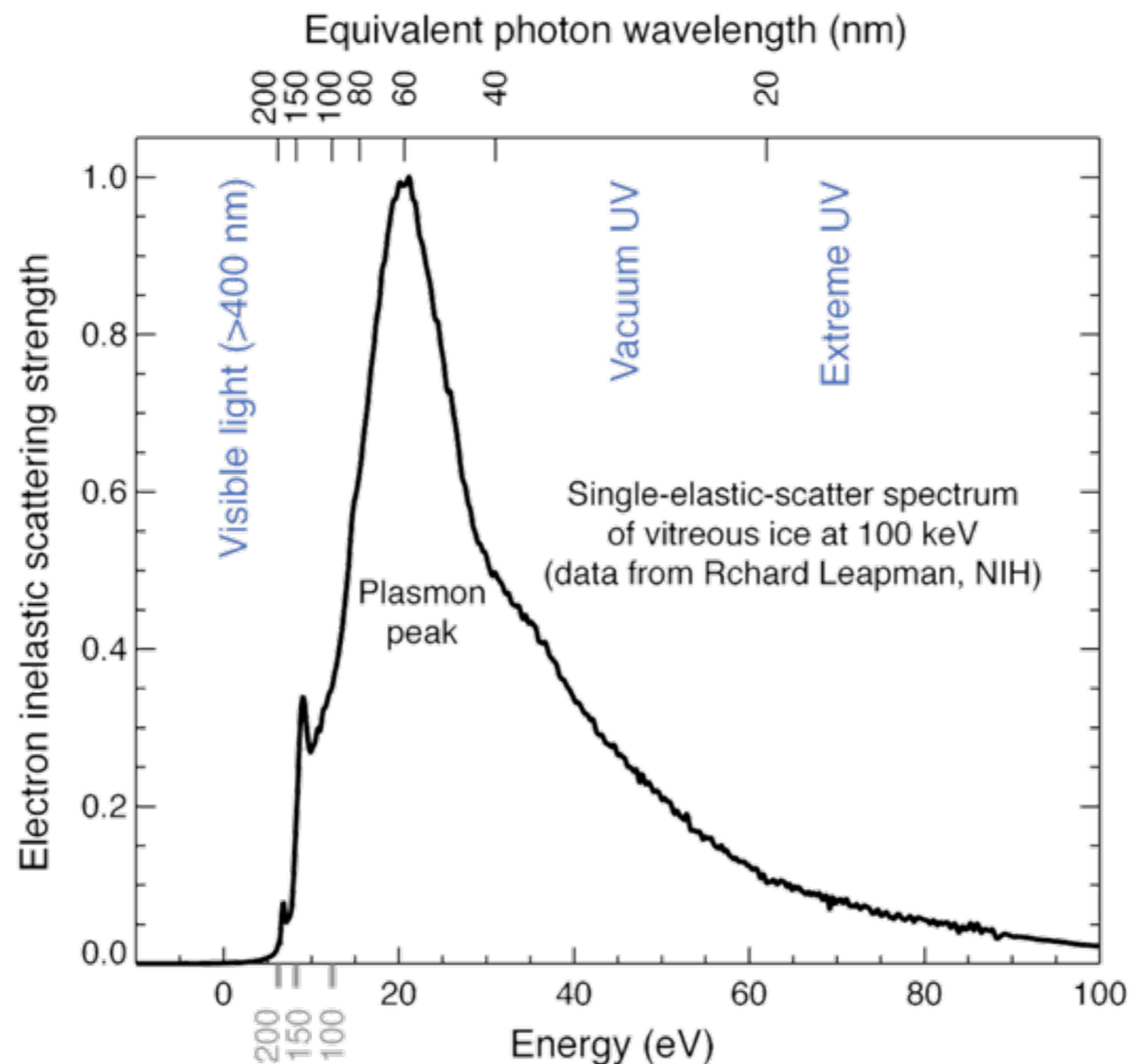
- Single resonance: absorption peak, **phase shift across resonance**

$$Q = \omega_0 / \gamma$$



# The preponderance of plasmons

Dividing line between low and high frequency limits of refractive index



# Mysteries of the refractive index

Write refractive index as

$$n = 1 - \frac{n_a r_e}{2\pi} \lambda^2 (f_1 + if_2) = 1 - \alpha \lambda^2 (f_1 + if_2)$$

Phase velocity is faster than light in vacuum!

$$v_p = \frac{\omega}{k} \approx c(1 + \alpha f_1 \lambda^2)$$

Prisms refract x rays the opposite way from visible light!

Phase is advanced rather than retarded! Total external reflection with critical angle

$$\theta_c \approx \sqrt{2\alpha \lambda^2 f_1}$$

But group velocity is OK:

$$v_g = \frac{d\omega}{dk} \approx c(1 - \alpha f_1 \lambda^2)$$

*Lassen sich Brechungsexponenten der Körper für Röntgenstrahlen experimentell ermitteln?*

Von A. Einstein.

(Eingegangen am 21. März 1918.)

Vor einigen Tagen erhielt ich von Herrn Prof. A. KÖHLER (Wiesbaden) eine kurze Arbeit<sup>1)</sup>, in welcher eine auffallende Erscheinung bei Röntgenaufnahmen geschildert ist, die sich bisher nicht hat deuten lassen. Die reproduzierten Aufnahmen — zu meist menschliche Gliedmaßen darstellend — zeigen an der Kontur einen hellen Saum von etwa 1 mm Breite, in welchem die Platte heller bestrahlt zu sein scheint als in der (nicht beschatteten) Umgebung des Röntgenbildes.

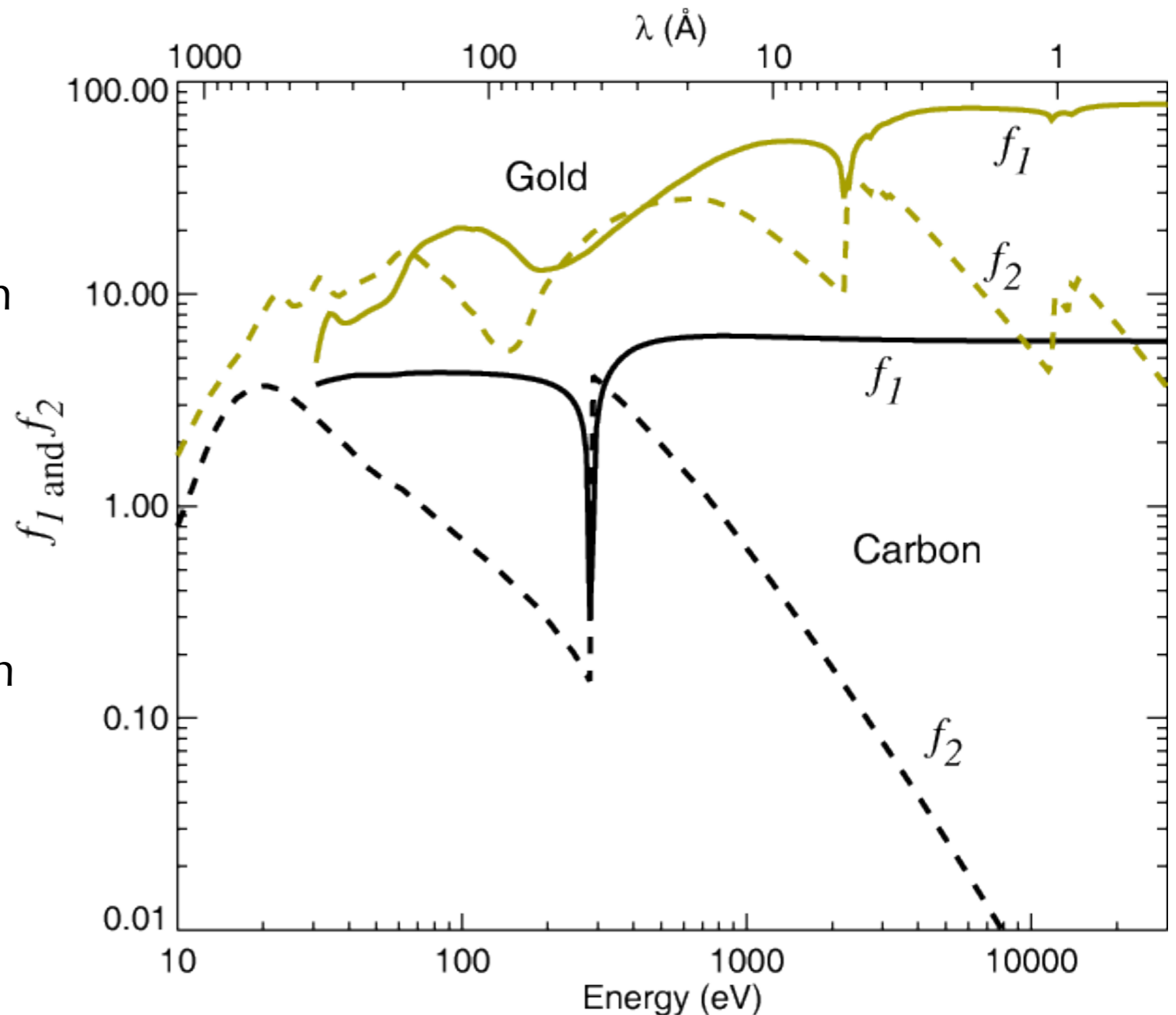
Ich möchte die Fachgenossen auf diese Erscheinung hinweisen und beifügen, daß die Erscheinung wahrscheinlich auf Totalreflexion beruht. Nach der klassischen Dispersionstheorie müssen wir erwarten, daß der Brechungsexponent  $n$  für Röntgenstrahlen nahe an 1 liegt, aber im allgemeinen doch von 1 verschieden ist.  $n$  wird kleiner bzw. größer als 1 sein, je nachdem der Einfluß derjenigen Elektronen auf die Dispersion überwiegt, deren Eigenfrequenz kleiner oder größer ist als die Frequenz der Röntgenstrahlen. Die Schwierigkeit einer Bestimmung von  $n$  liegt darin, daß  $(n - 1)$  sehr klein ist (etwa  $10^{-5}$ ). Es ist aber leicht einzusehen, daß bei nahezu streifender Inzidenz der Röntgenstrahlen im Falle  $n < 1$  eine nachweisbare Totalreflexion auftreten muß.

# X-ray refractive index

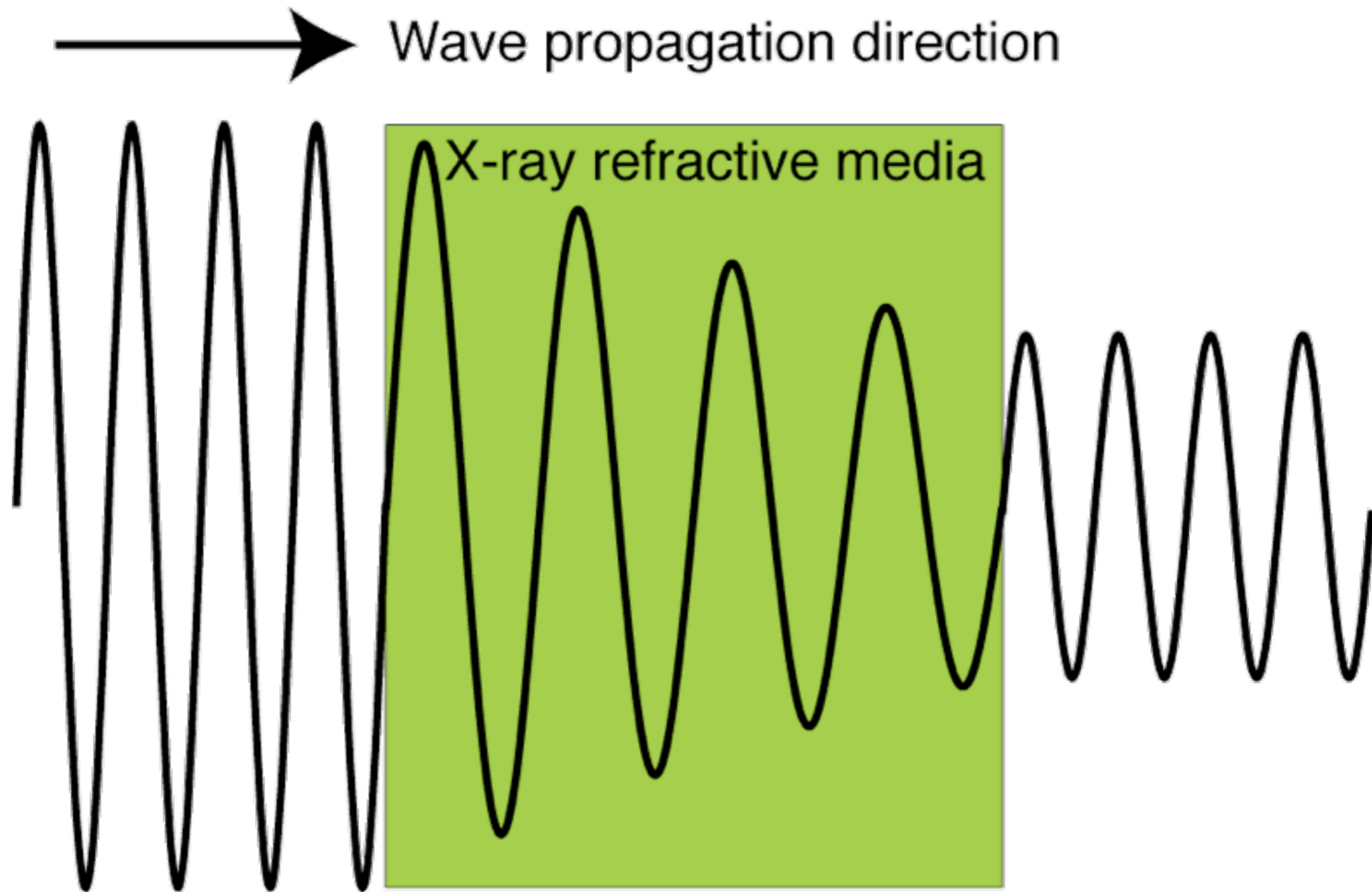
Refractive index: based on a damped, driven harmonic oscillator model in the limit of high frequency and low damping:

$$n = 1 - \frac{n_a r_e}{2\pi} \lambda^2 (f_1 + if_2)$$

where  $n_a$  gives atoms/volume,  $r_e = 2.82 \times 10^{-15}$  m is the classical radius of the electron, and  $(f_1 + if_2)$  specify the atom's oscillator strength at a given photon energy



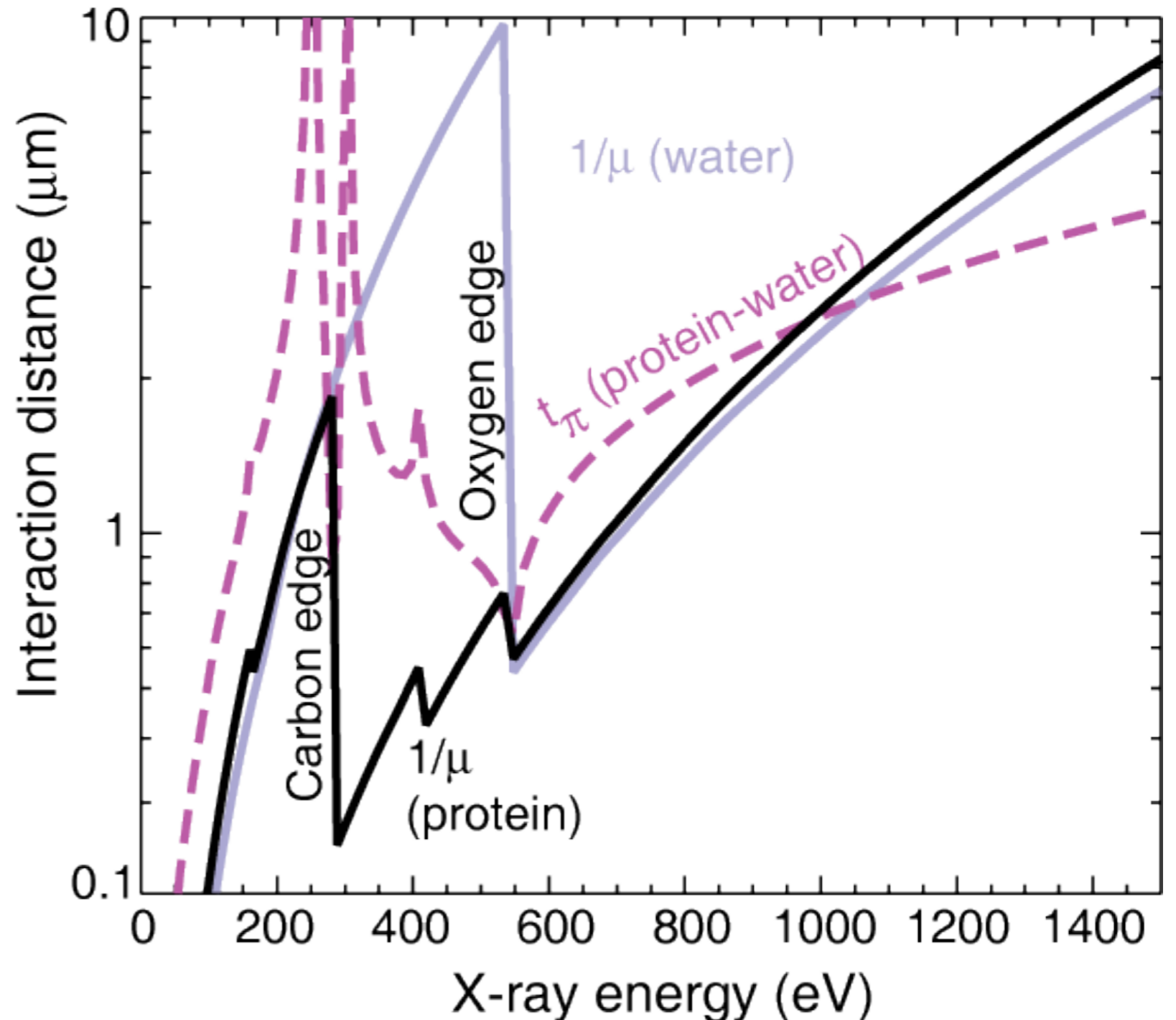
# X rays in media



# Soft and wet: water window, phase contrast

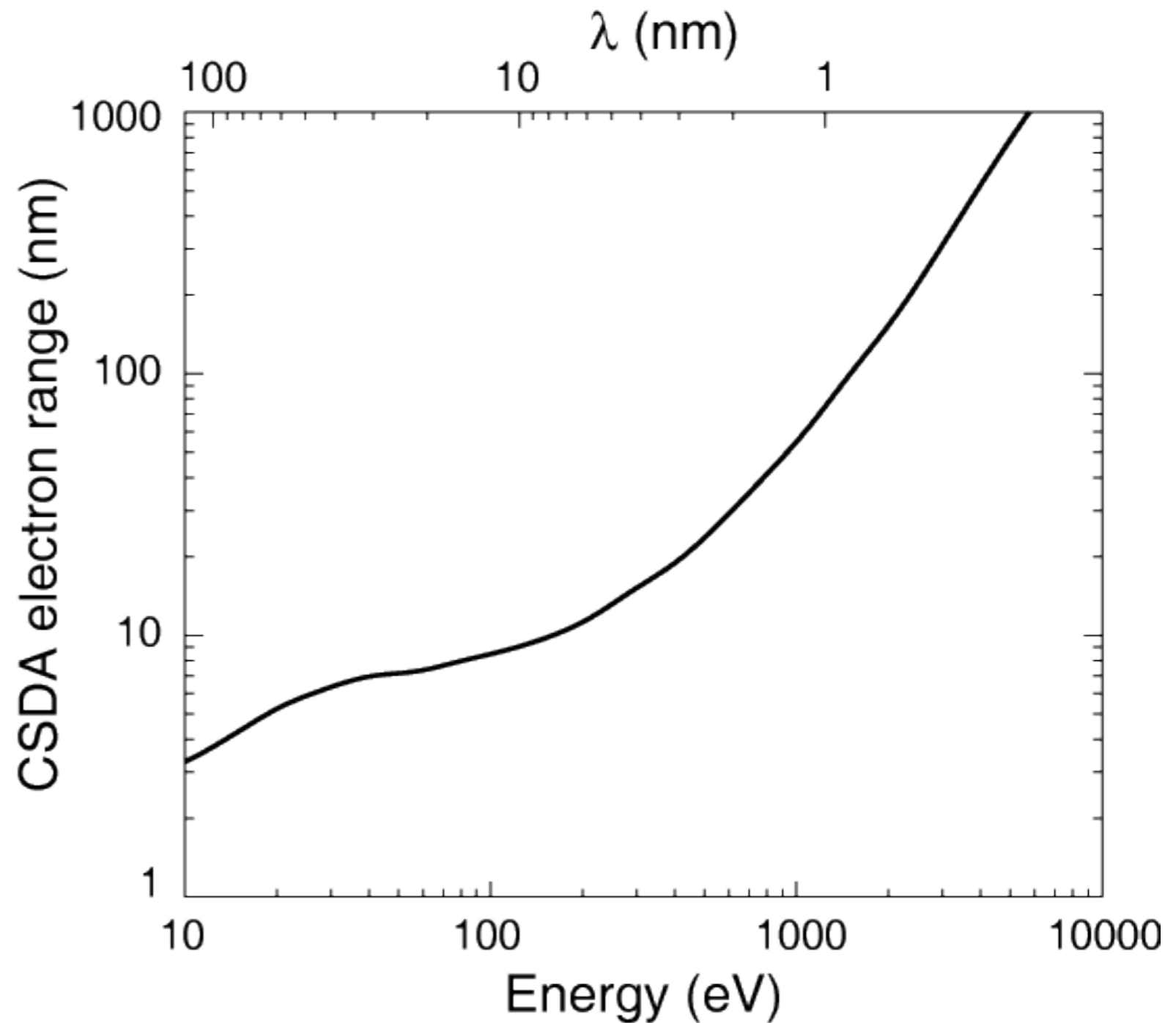
Water window: Wolter, *Ann. Phys.* **10**, 94 (1952); Sayre *et al.*, *Science* **196**, 1339 (1977).

Phase contrast: Schmahl and Rudolph, in Cheng and Jan, *X-ray Microscopy: Instrumentation and Biological Applications* (Springer, 1987).

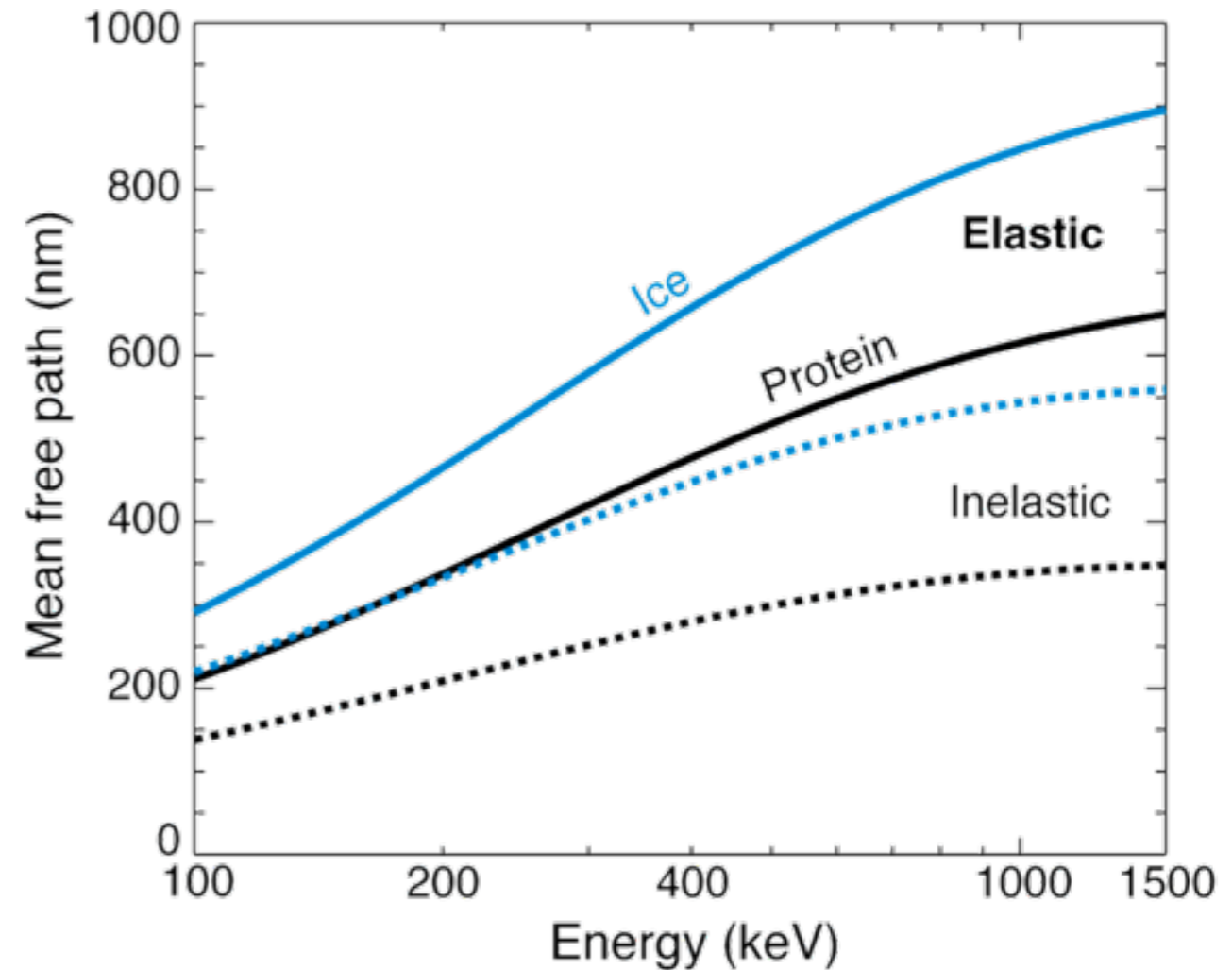
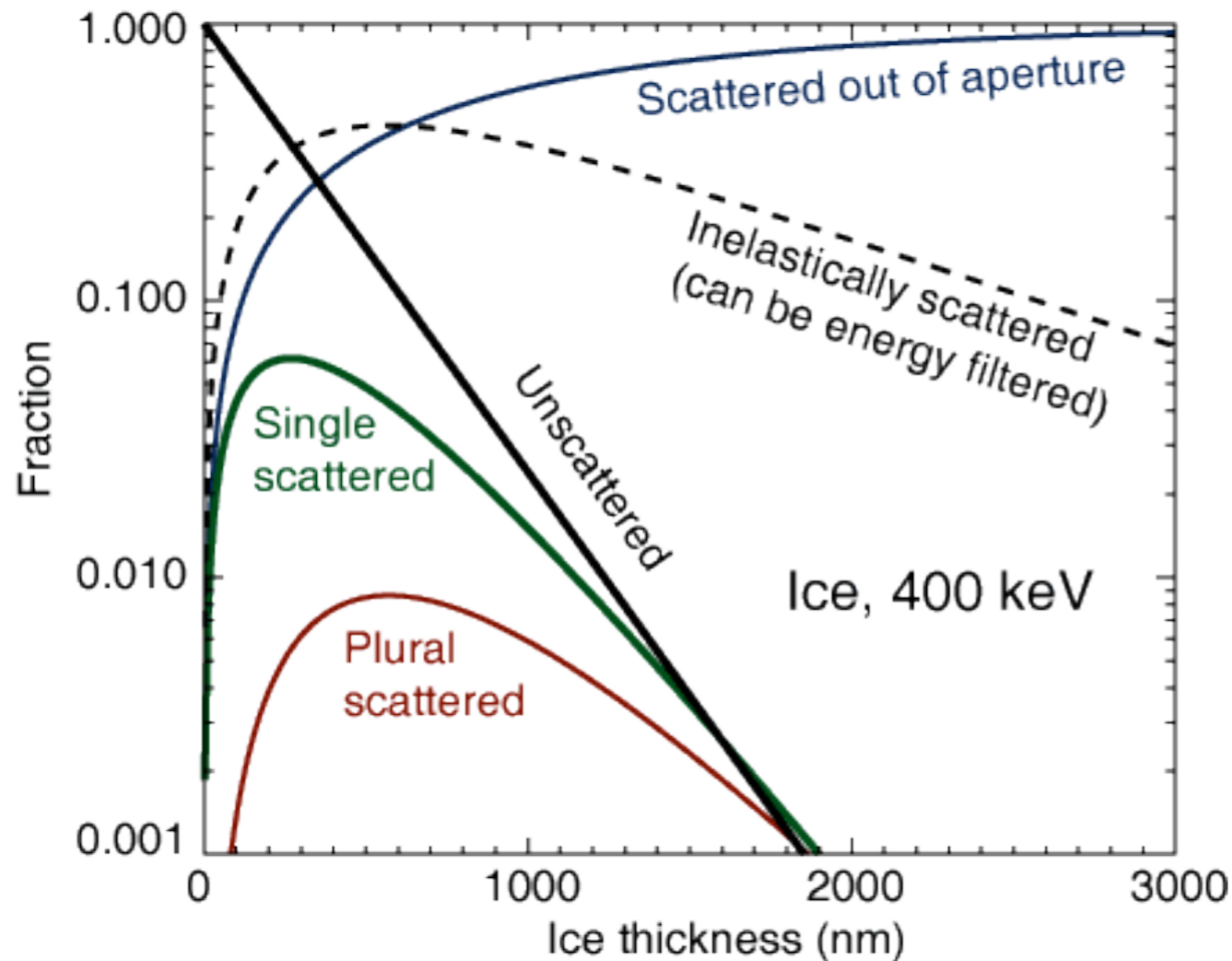


# X-ray absorption: the aftermath

Primary electrons undergo multiple inelastic collisions  
Continuous slowing down approximation (CSDA): range over which majority of energy is deposited



# Electron interactions



These plots: Jacobsen, Medenwaldt, and Williams, in **X-ray Microscopy & Spectromicroscopy** (Springer, 1998)

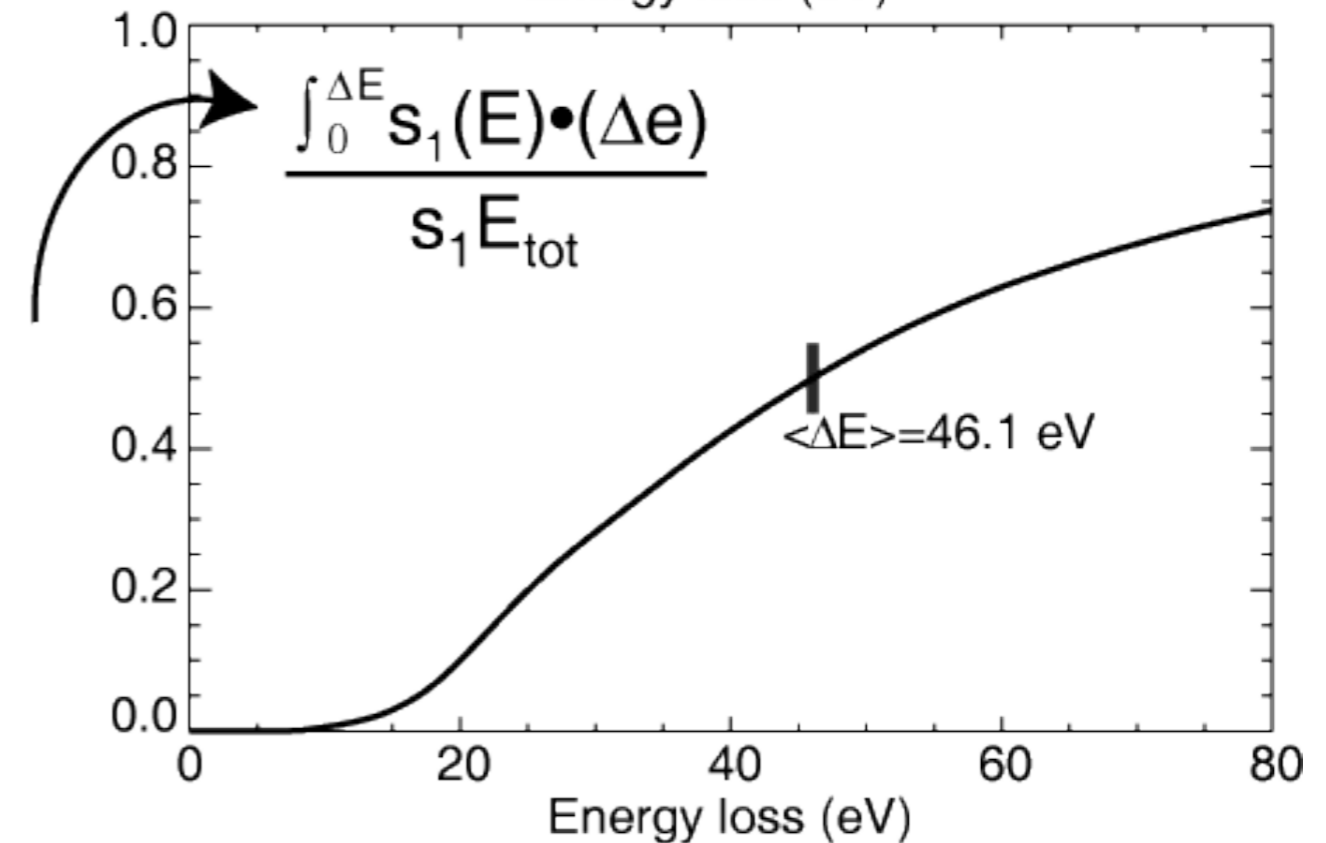
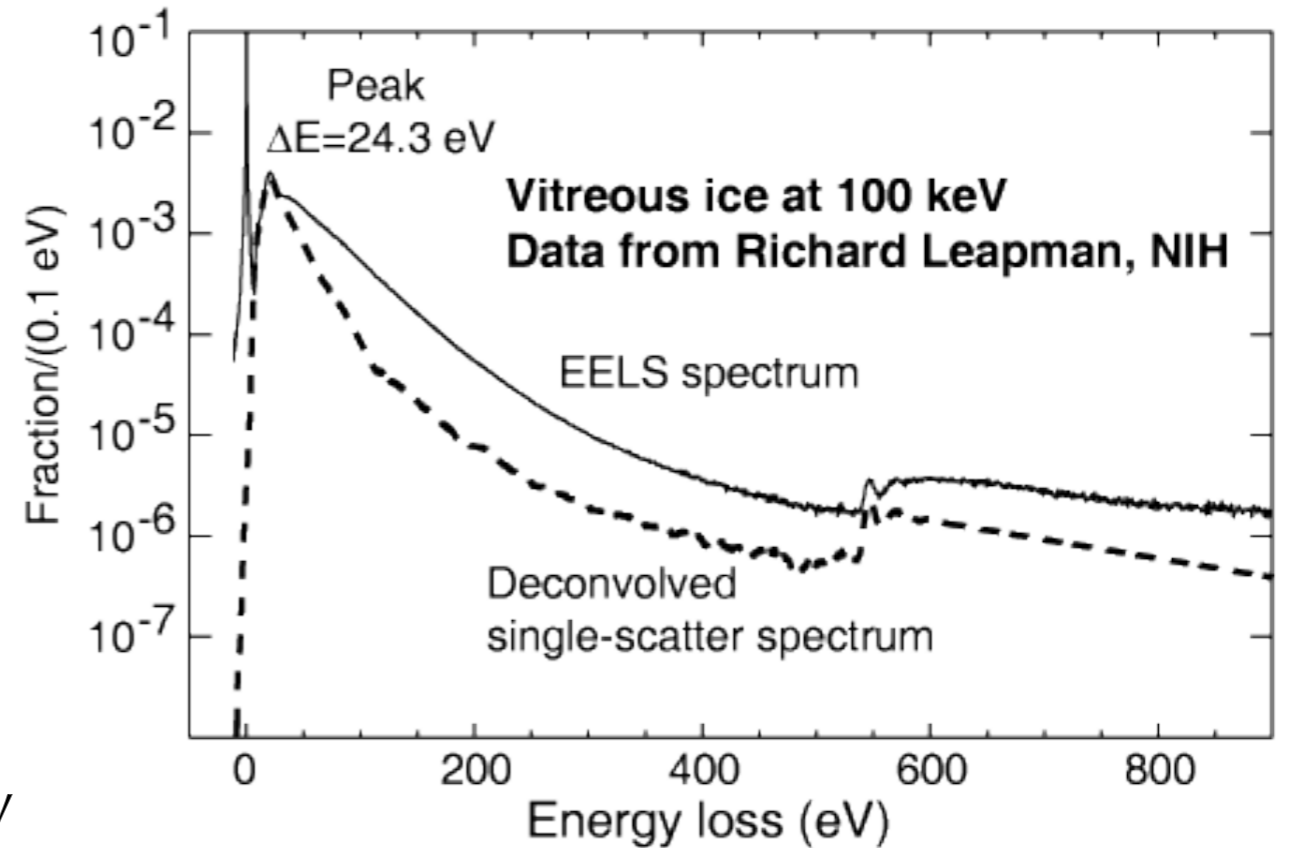


# Electrons: inelastic energy deposition

Inelastic scattering: energy transfer of 35-45 eV

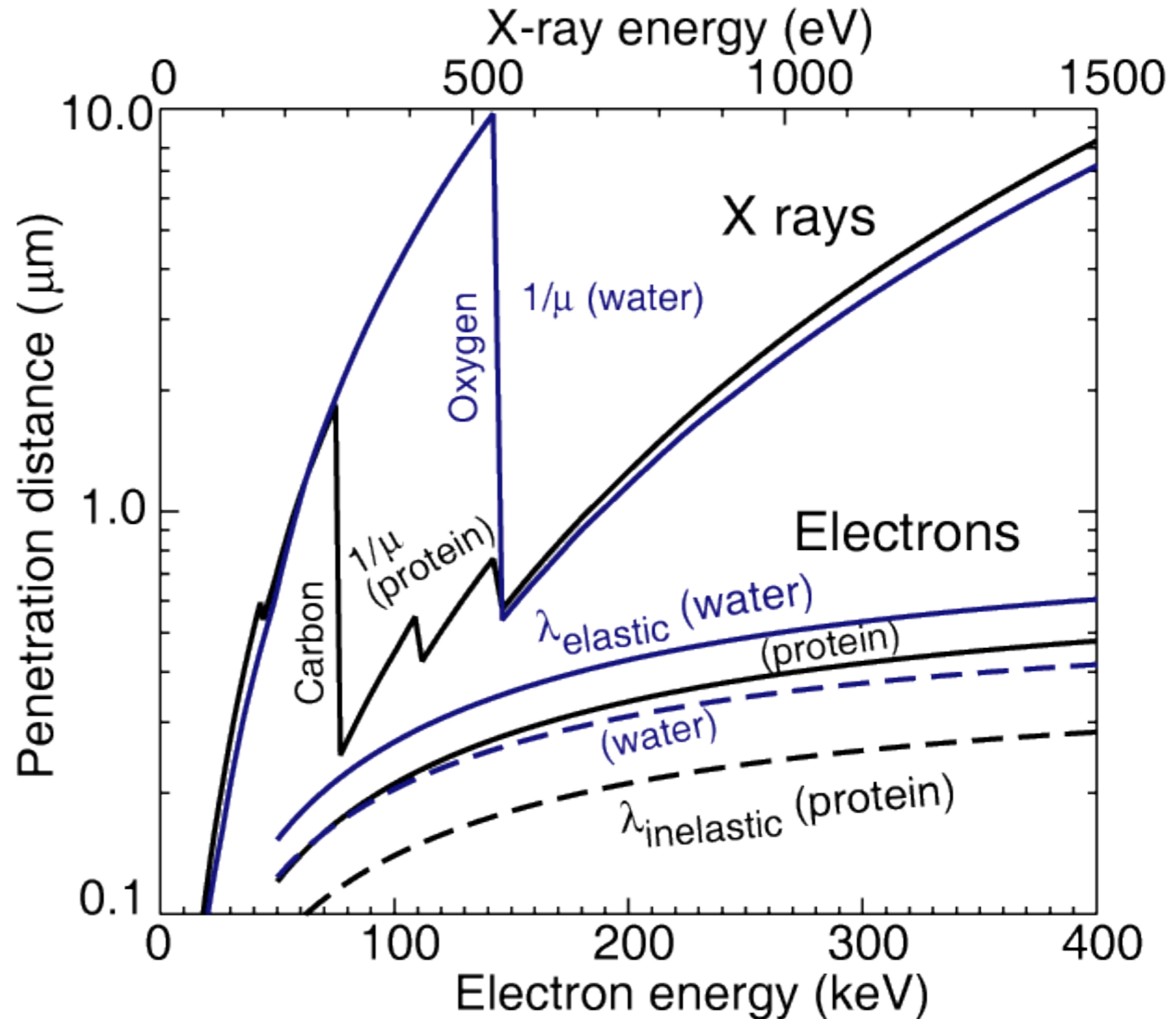
At 100 keV,  $1 \text{ e}^-/\text{nm}^2 \Rightarrow 3.2 \times 10^4 \text{ Gray}$

(1 Gray = 1 J/kg)



# X rays and electrons

Consider penetration distance:  $1/e$  absorption length for x rays, scattering mean free paths for electrons



# Atomic resolution imaging: electrons or photons?

## 10 keV photons

- About 100 absorption events per elastic scatter
- About 10 keV deposited per absorption
- Therefore about  $10^6$  eV deposited per elastic scatter
- A thousand scattered photons:  
 $10^3 \cdot 10^6$  eV into  $(2 \text{ \AA})^3$ , or  $2 \times 10^{13}$  Gray

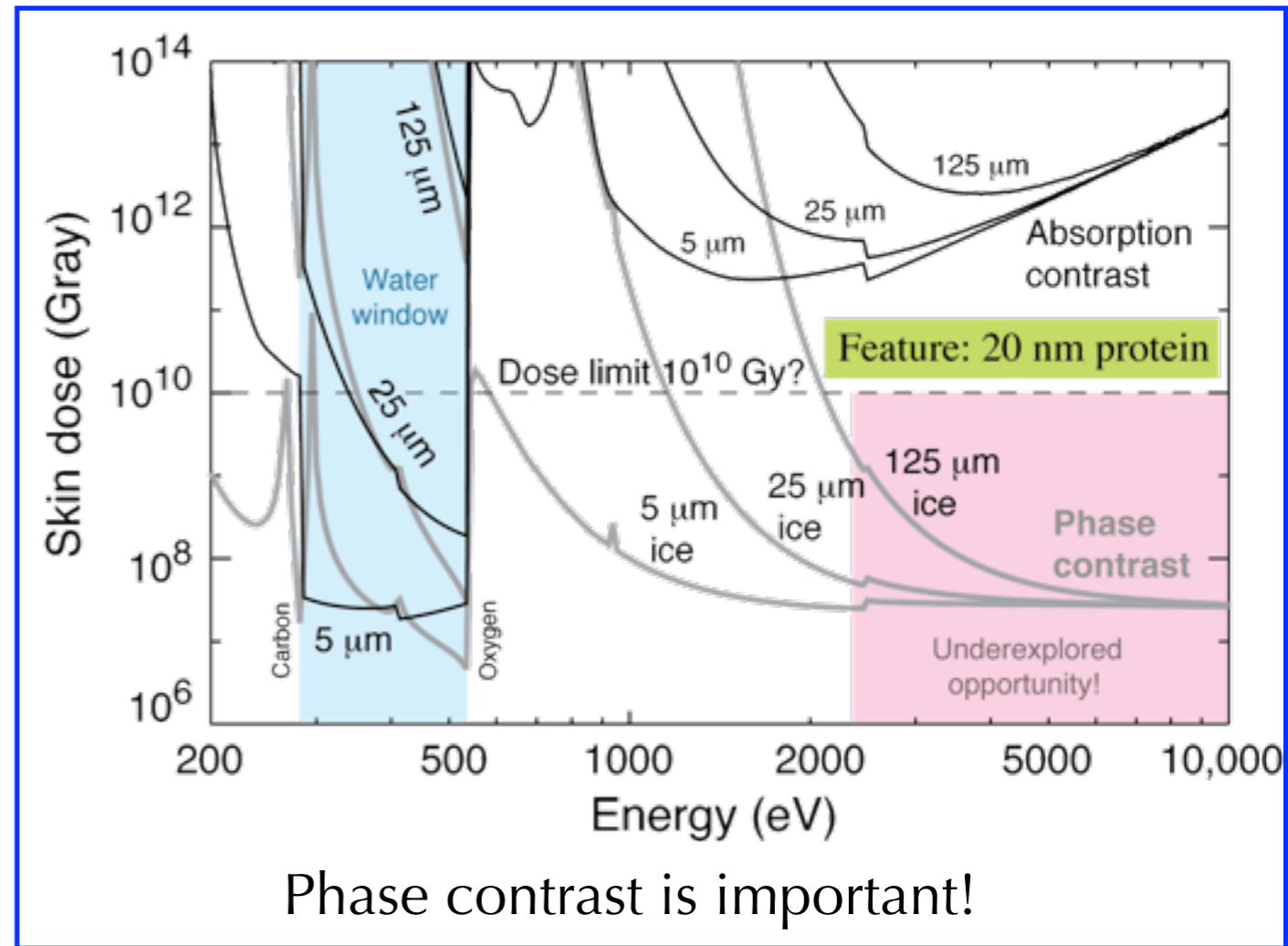
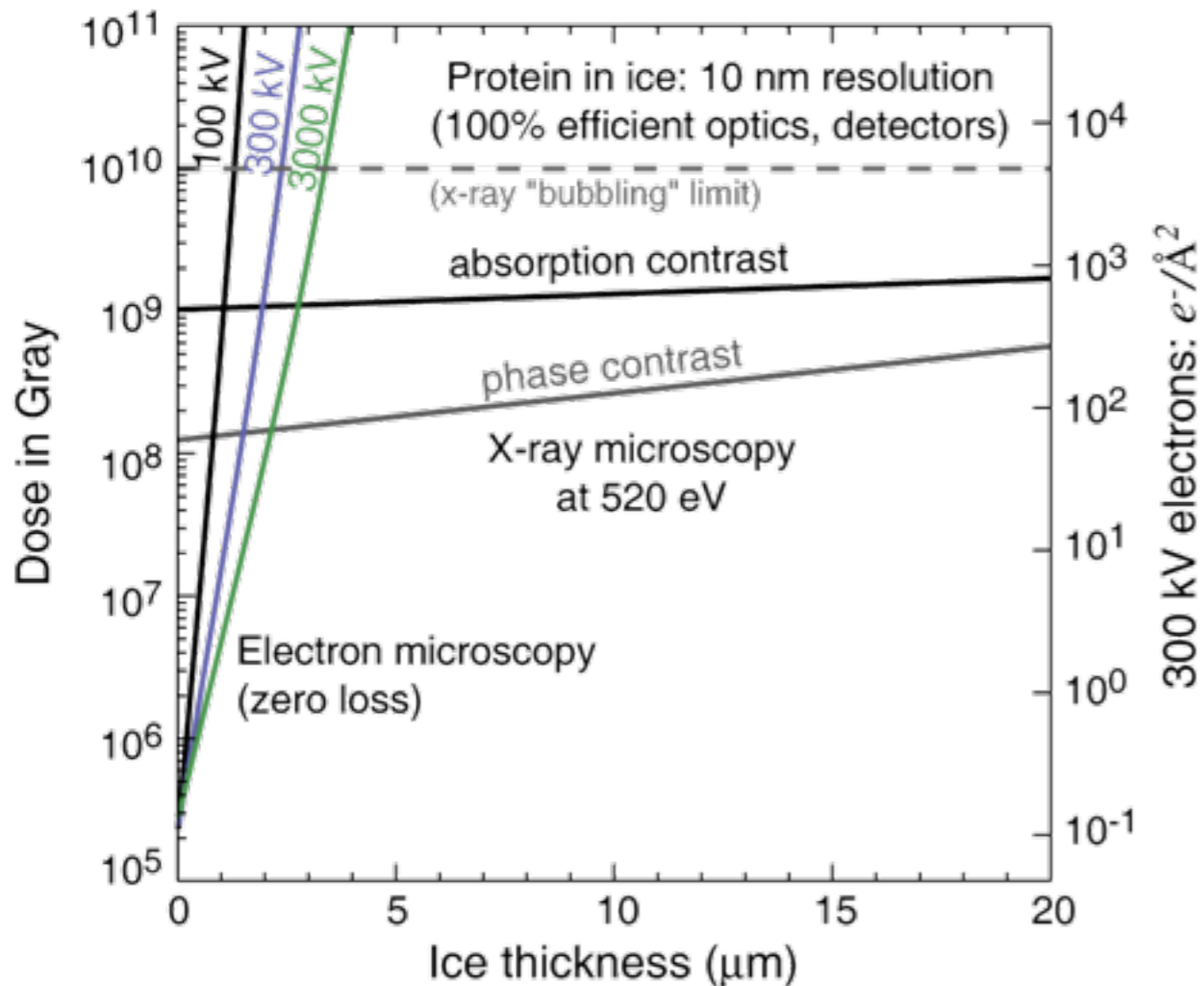
## 100 keV electrons

- About 2.5 inelastic scatters per elastic scatter
- About 45 eV deposited per inelastic scatter
- Therefore about  $10^2$  eV deposited per elastic scatter
- A thousand scattered electrons:  
 $10^3 \cdot 10^2$  eV into  $(2 \text{ \AA})^3$ , or  $2 \times 10^9$  Gray

- Electrons are better than photons for atomic resolution imaging: J. Breedlove and G. Trammell, *Science* **170**, 1310 (1970); R. Henderson, *Q. Rev. Biophys.* **28**, 171 (1995).
- X-ray crystallography's answer: spread the dose out over many identical unit cells
- X-ray Free Electron Lasers: get image in  $<100$  fsec, before damage

# X rays are better than electrons for thick specimens

- $\lambda=100\text{-}10$  nm: minimum penetration in entire electromagnetic spectrum.
- No more than 1 high-resolution image of wet, soft samples unless frozen.
- At energies  $>3$  keV, opportunities for thick specimens.

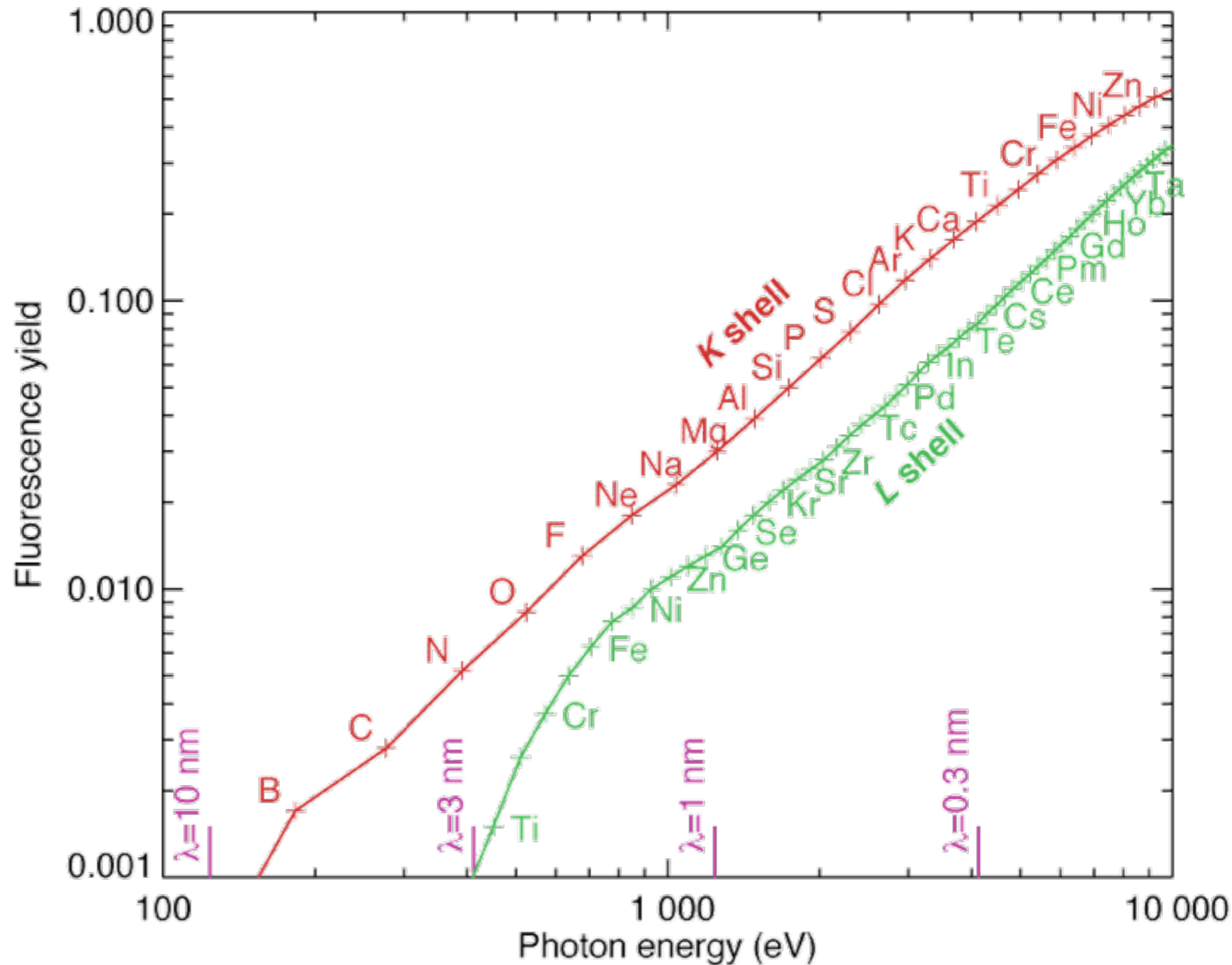


Phase contrast is important!

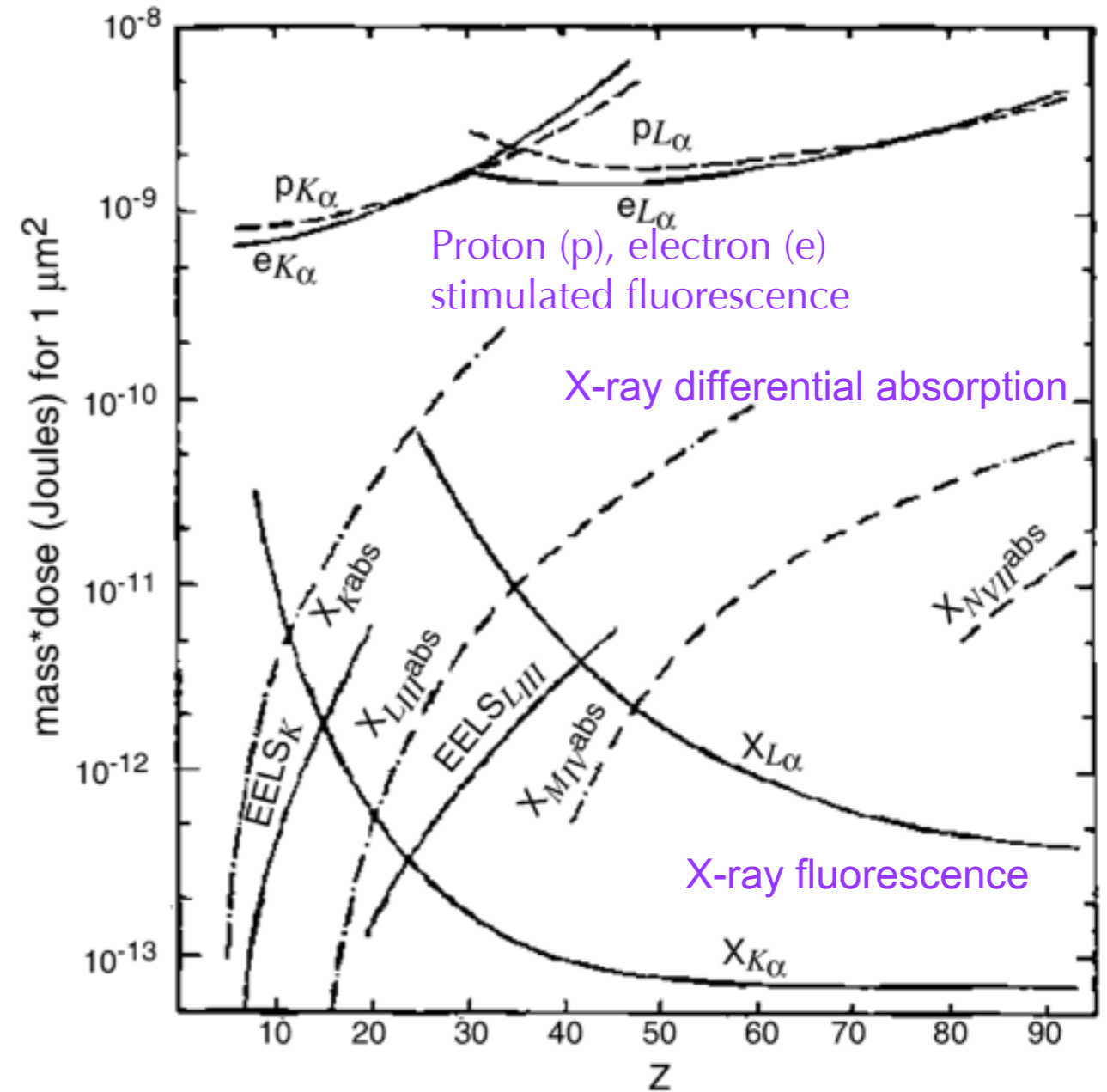
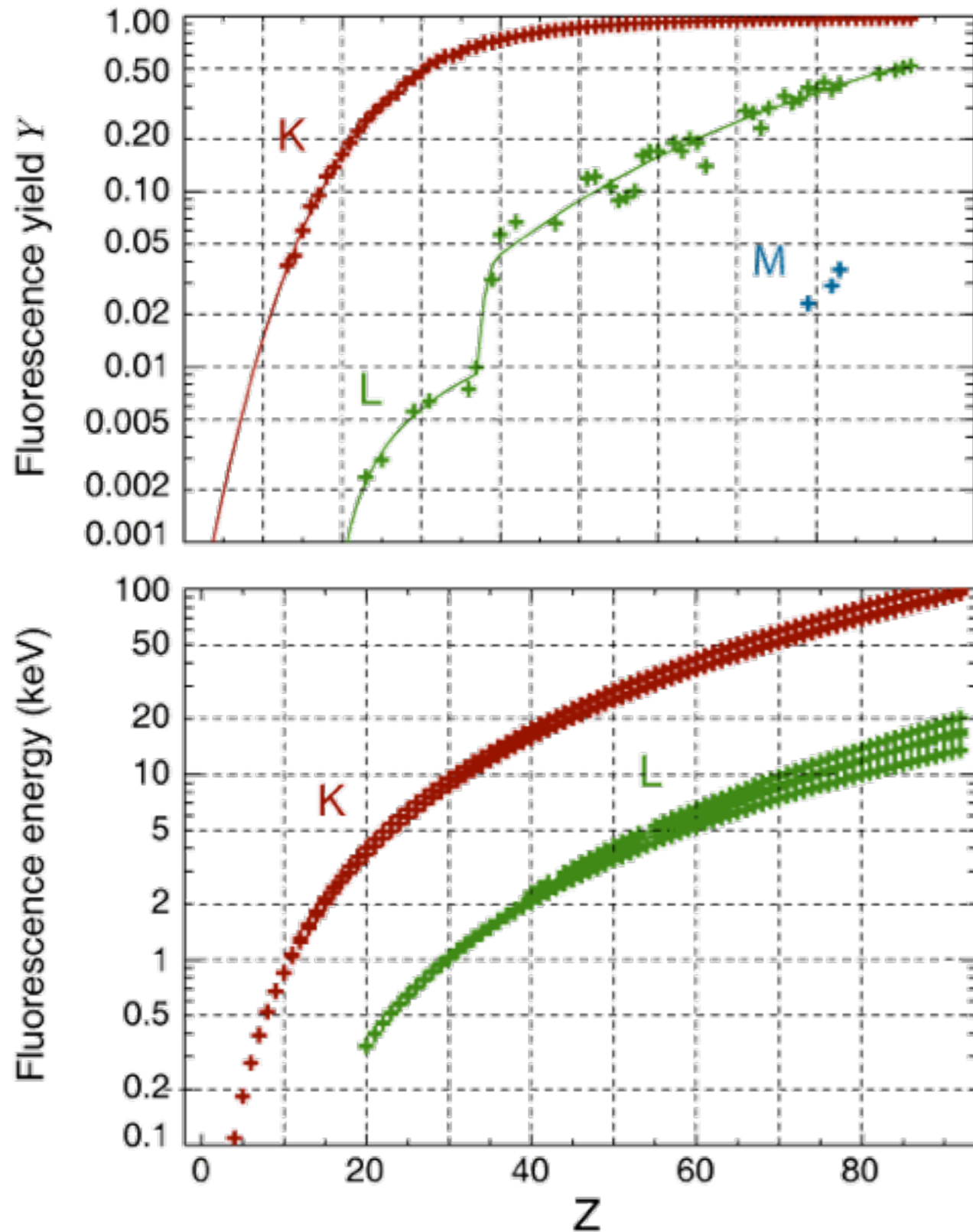
These plots: based on Jacobsen, Medenwaldt, and Williams, in **X-ray Microscopy & Spectromicroscopy** (Springer, 1998). See also Sayre *et al.*, *Science* **196**, 1339 (1977).

# Detecting trace elements

- Differential absorption is great for soft x-ray spectromicroscopy, but at  $>1\%$  concentration.
- X-ray fluorescence:  **$\sim 1000\times$  better sensitivity** than electrons for trace elemental mapping (ion concentrations etc.). Parts per billion!



# Fluorescence: trace element concentrations

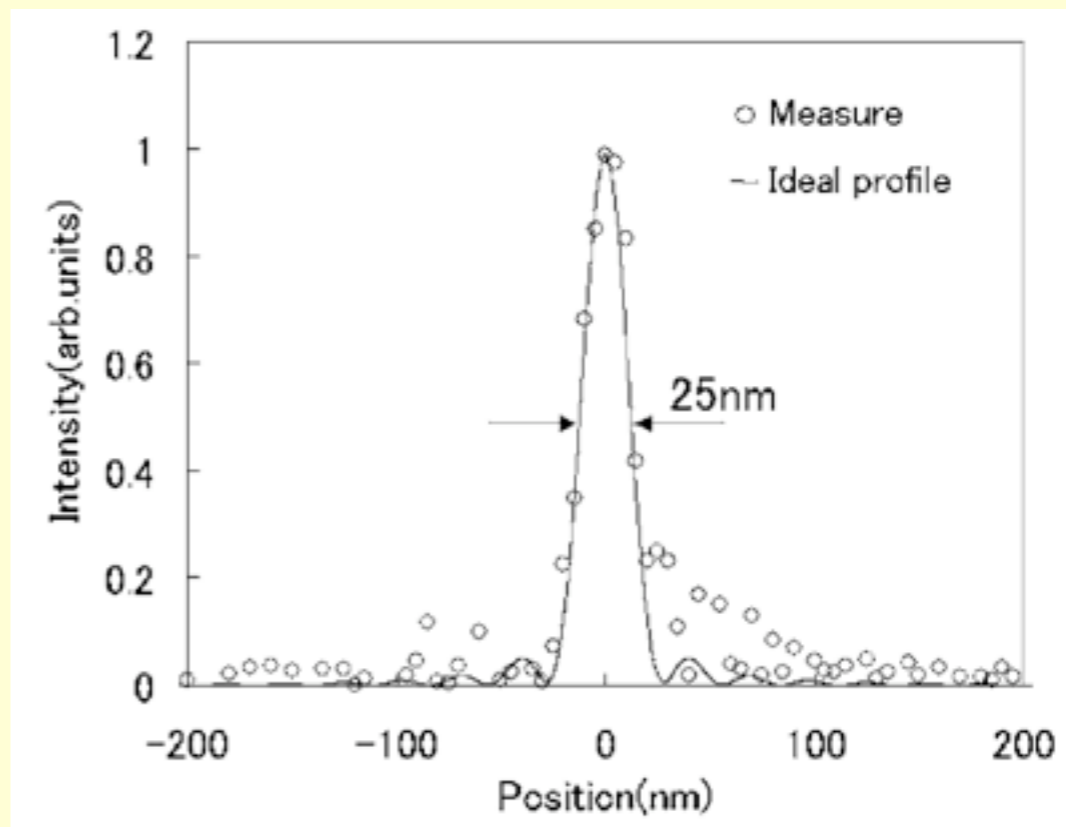
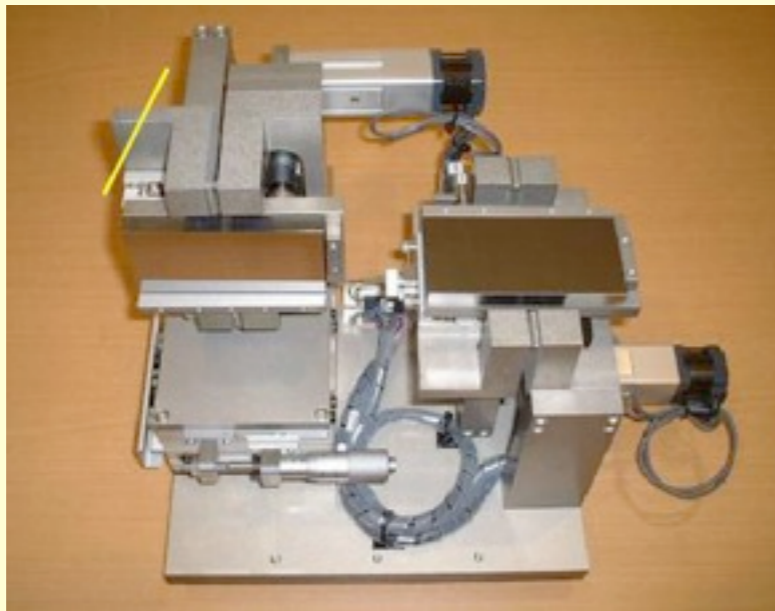


J. Kirz, in *Scanning Electron Microscopy 2*, 1980, p. 239. EELS=electron energy loss spectroscopy. Hard-to-find reprint: <http://tinyurl.com/2eu7q4>

# Reflective x-ray optics

- Grazing incidence critical angle for mirror reflection:  
$$\cos\theta_c = 1 - \alpha\lambda^2 f_1 \quad \text{or} \quad \theta_c \approx \lambda\sqrt{2\alpha f_1}$$
- Use two orthogonal cylinders for 2D focusing: Kirkpatrick and Baez, *J. Opt. Soc. Am.* **38**, 766 (1948)

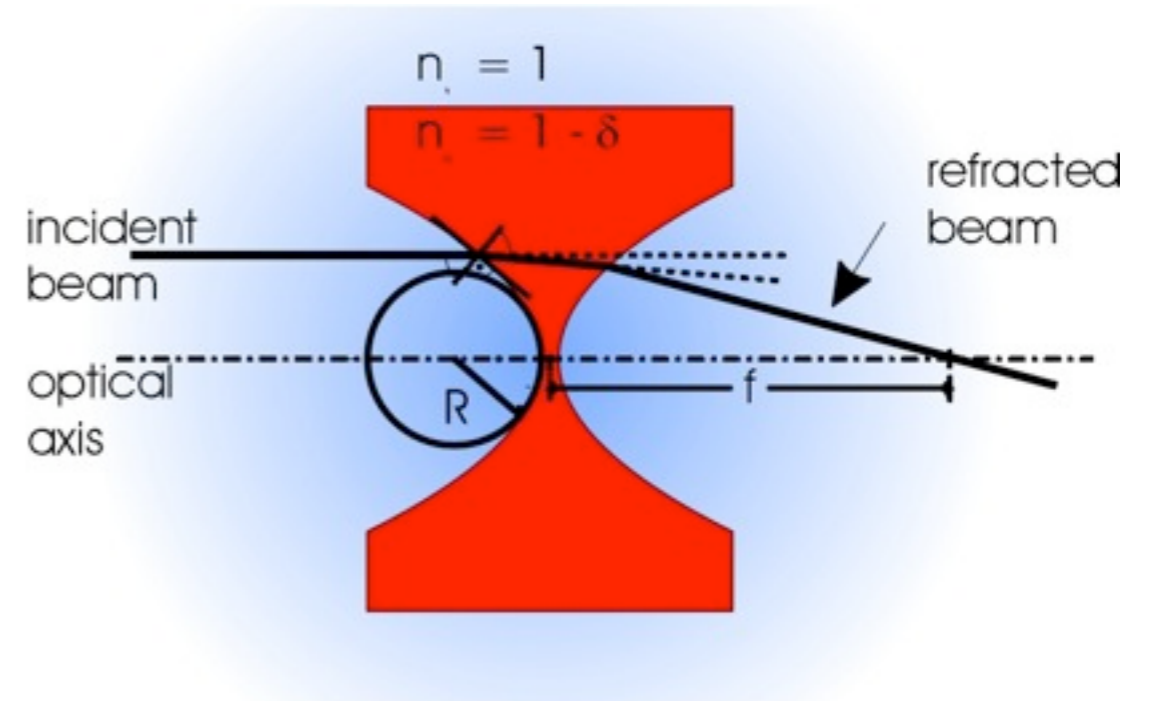
Mimura, Yamauchi *et al.*, *Appl. Phys. Lett.* **90**, 051903 (2007): 25 nm using elastic emission machining.



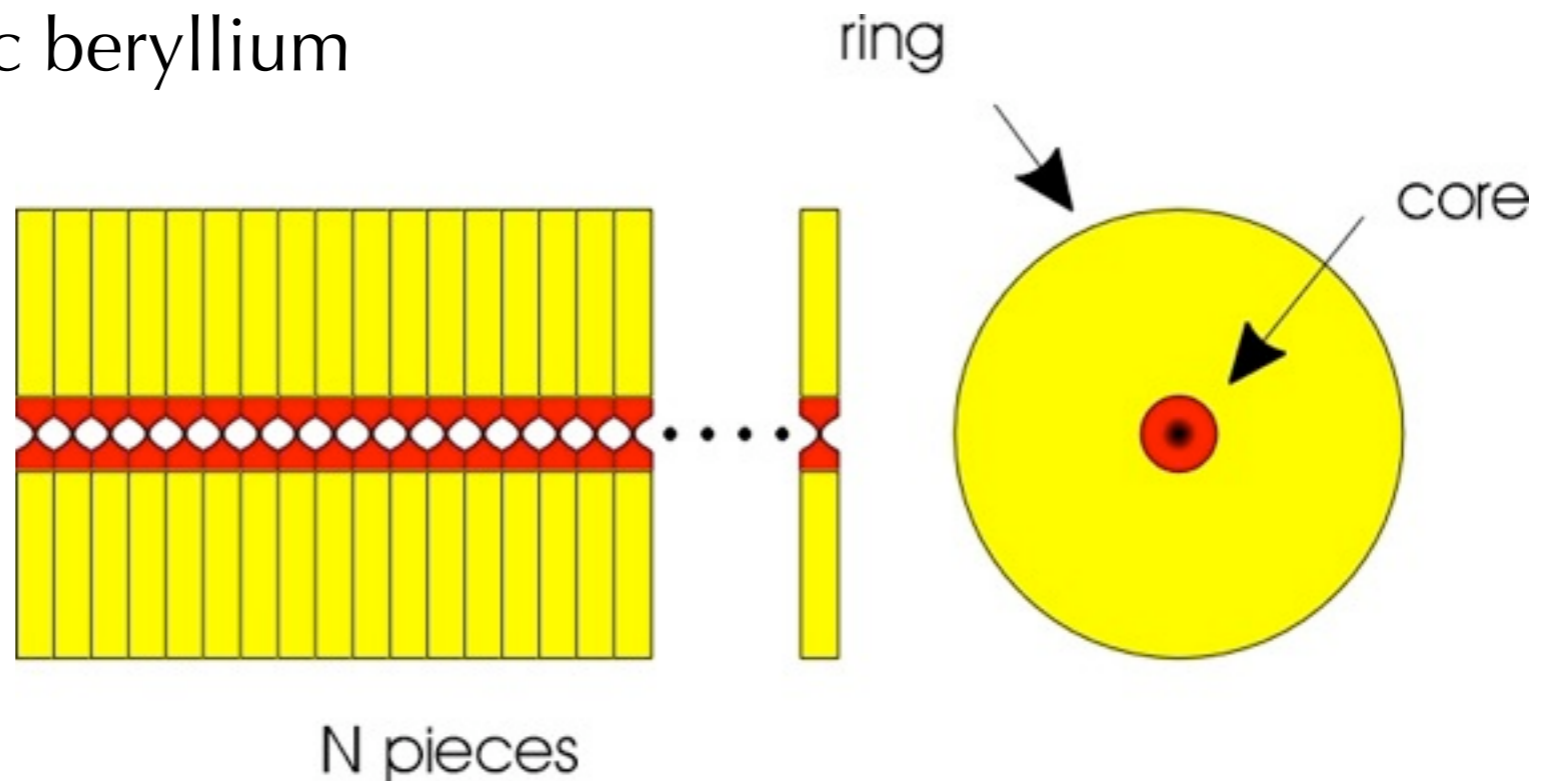
Synthetic multilayer mirrors: work well at approx.  $\lambda \geq 10$  nm

# Compound refractive lenses

- Röntgen tried to make lenses, but found no focusing.
- Focal length of one lens is long – so combine many lenses! Tomie; Snigirev *et al.*, *Nature* **384**, 49 (1996); Lengeler *et al.*, *J. Synch. Rad.* **9**, 119 (2002).
- Resolution approaching 100 nm at 5-10 keV with parabolic beryllium lenses



Compound refractive lenses at Universität Aachen



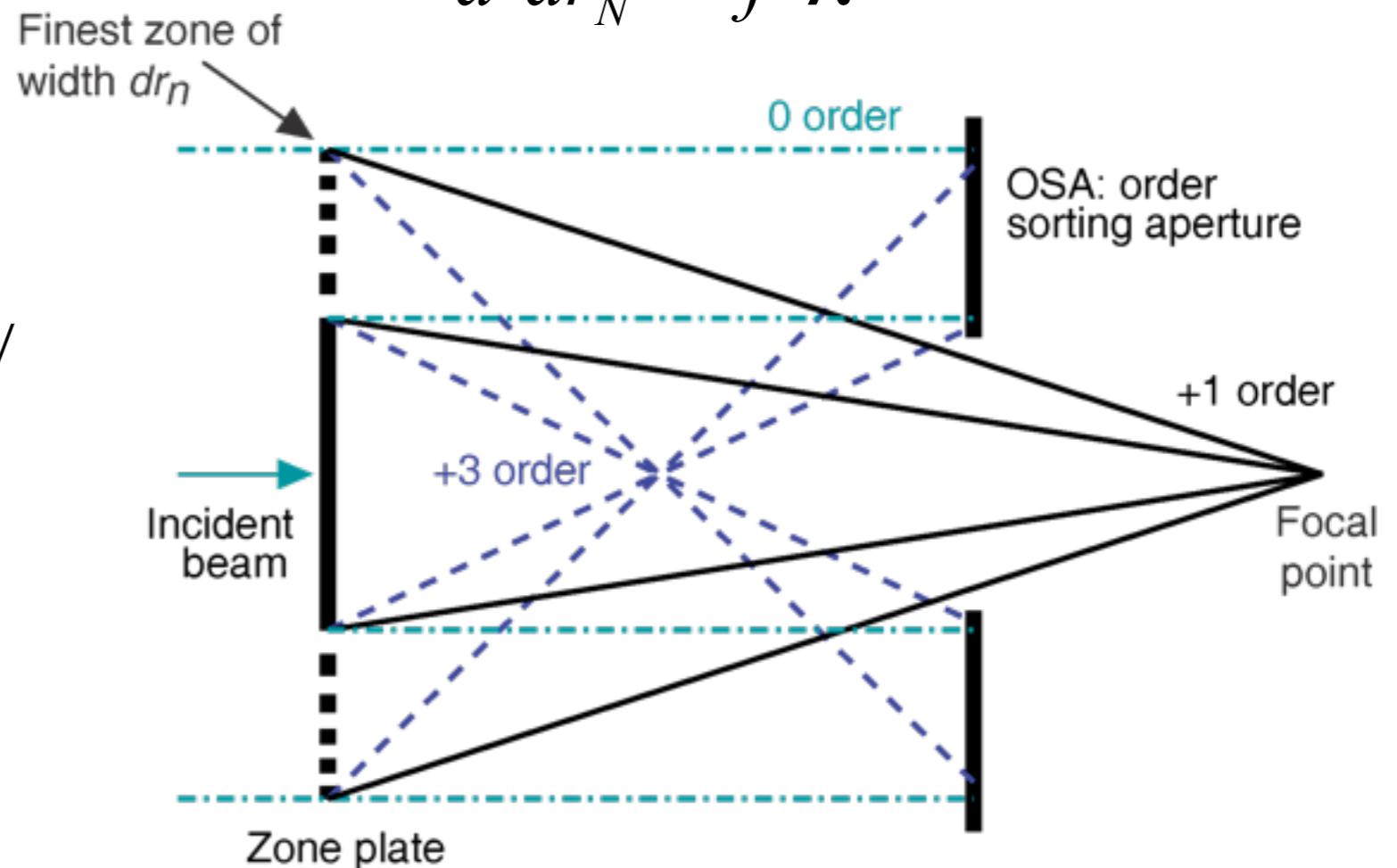


# X-ray focusing: Fresnel zone plates

- Diffractive optics: radially varied grating spacing
- Largest diffraction angle is given by outermost (finest) zone width  $dr_N$  as  $\theta = \lambda / (2 dr_N)$
- Rayleigh resolution is  $0.61 \lambda / (\theta) = 1.22 dr_N$
- Zones must be positioned to  $\sim 1/3$  width over diameter (10 nm in 100  $\mu\text{m}$ , or 1:10<sup>4</sup>)

Diameter  $d$ , outermost zone width  $dr_N$ , focal length  $f$ , wavelength  $\lambda$ :

$$d dr_N = f \lambda$$



Central stop and order sorting aperture (OSA) to isolate first order focus

# Fresnel zone plate images

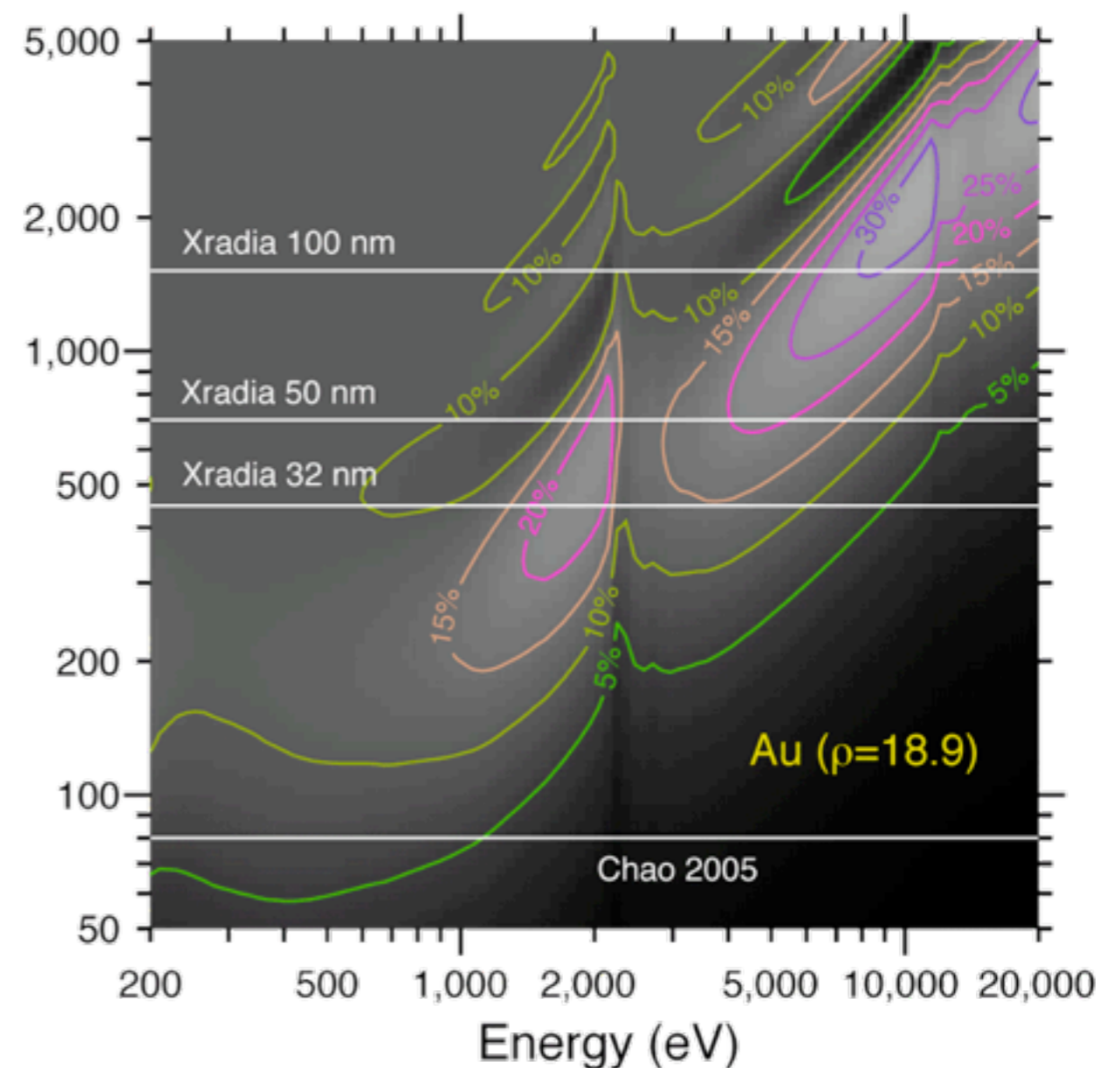
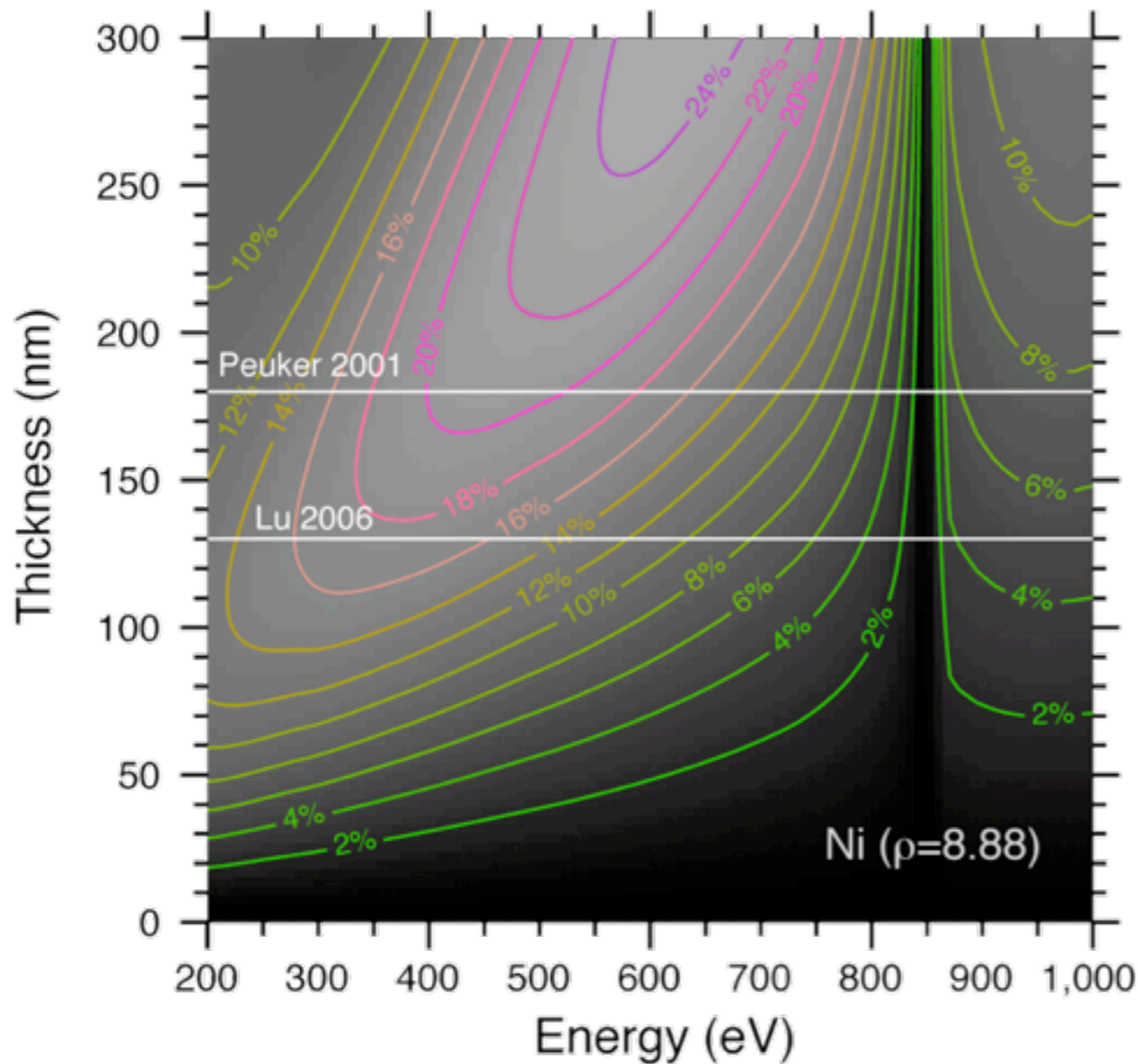
R. W. Wood (1898): zone plate figure drawn with a pen and a compass!  
Photographically reduced



PLATE 2. ZONE-PLATE, FROM A DRAWING.

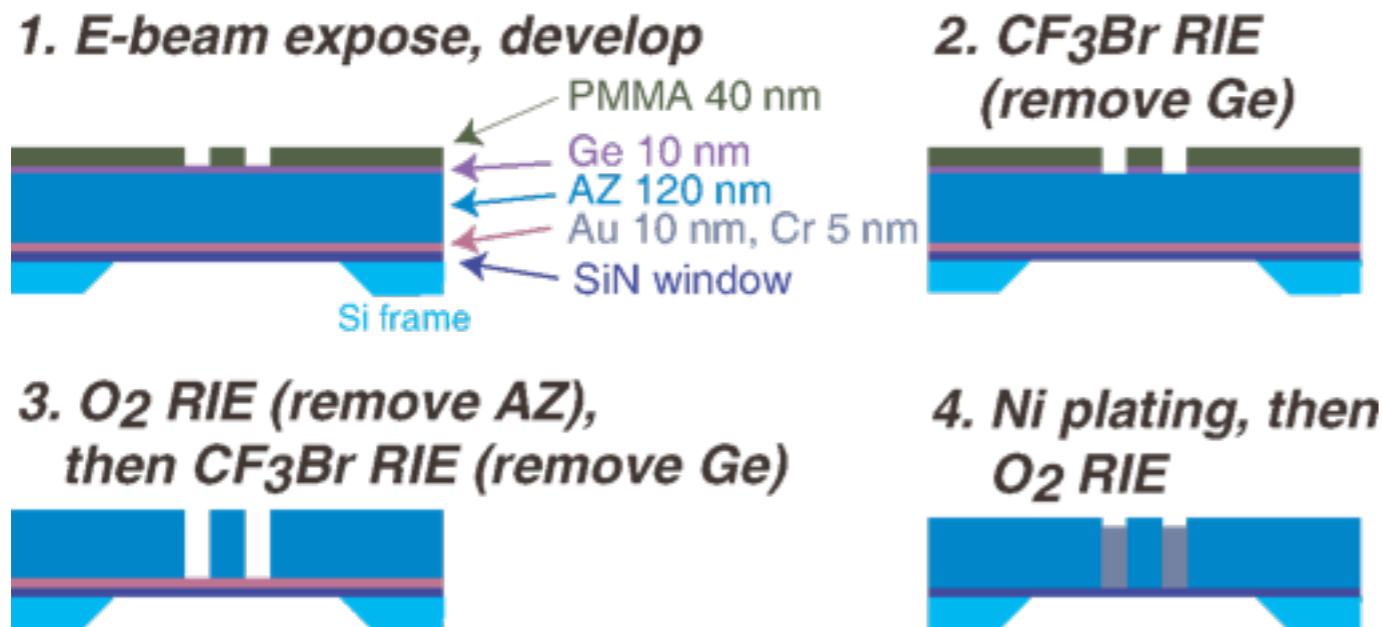
# Zone plate efficiency and thickness

For binary zones, 1:1 mark:space ratio.  
See Kirz, *J. Opt. Soc. Am.* **64**, 301 (1974)



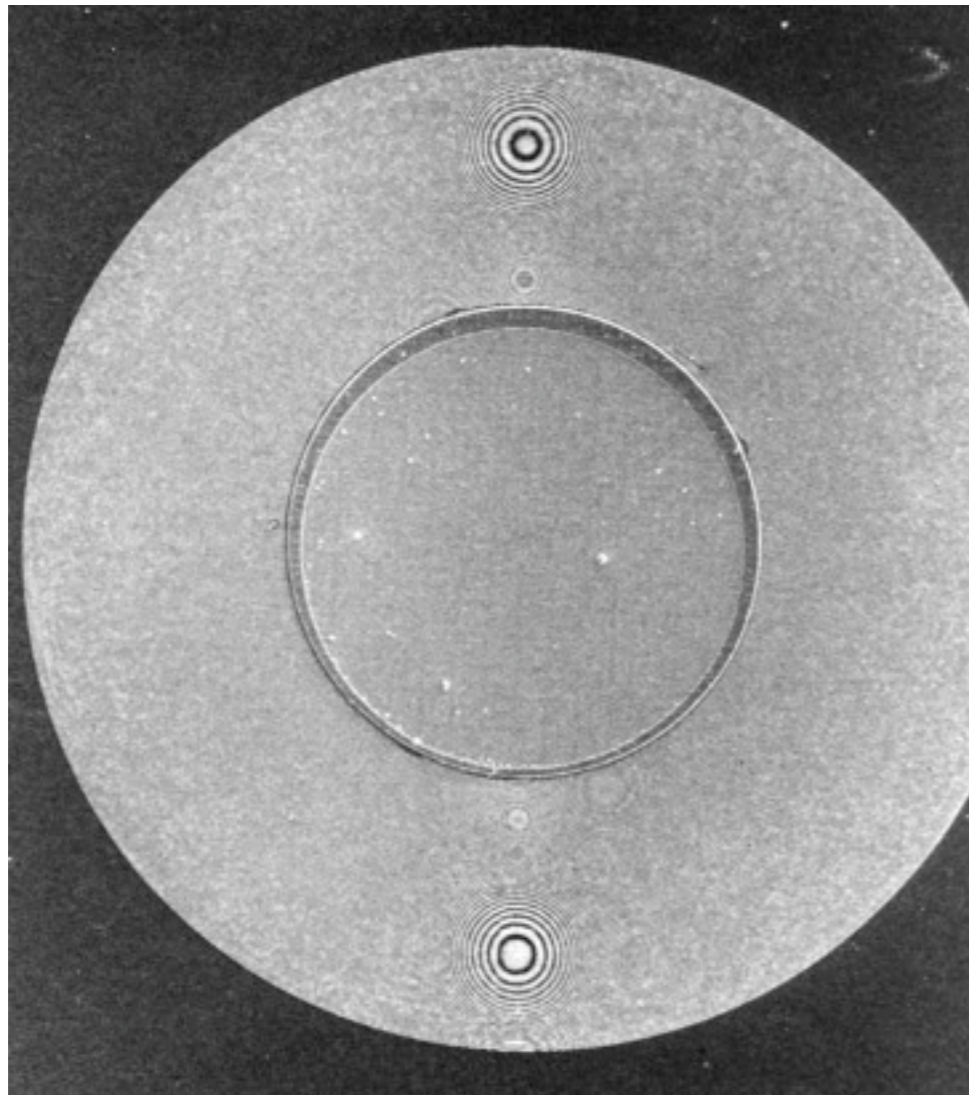
# Zone plates by electron beam lithography

- Electron beam lithography: produces the finest possible structures (other than what nature can be persuaded to make by itself)
- M. Lu, A. Stein (PhD 2002; now BNL), S. Spector (PhD 1998; now Lincoln Lab), C. Jacobsen (Stony Brook)
- D. Tennant (Lucent/New Jersey Nanotech Consortium)
- JEOL JBX-9300FS: 1 nA into 4 nm spot, 1.2 nm over 500  $\mu\text{m}$ , 100 keV

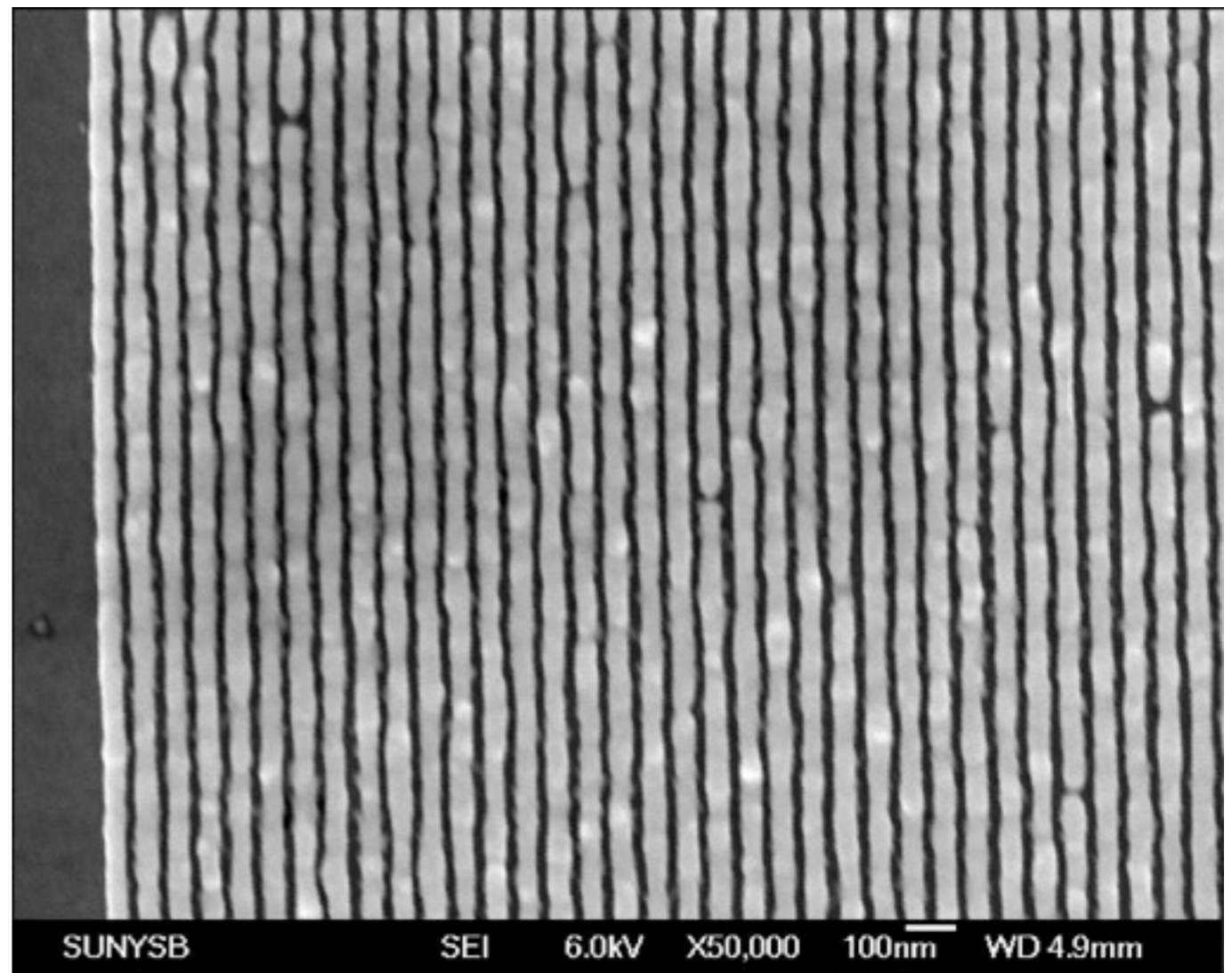


A. Stein and JBX-9300FS

# Fresnel Zone Plates in nickel

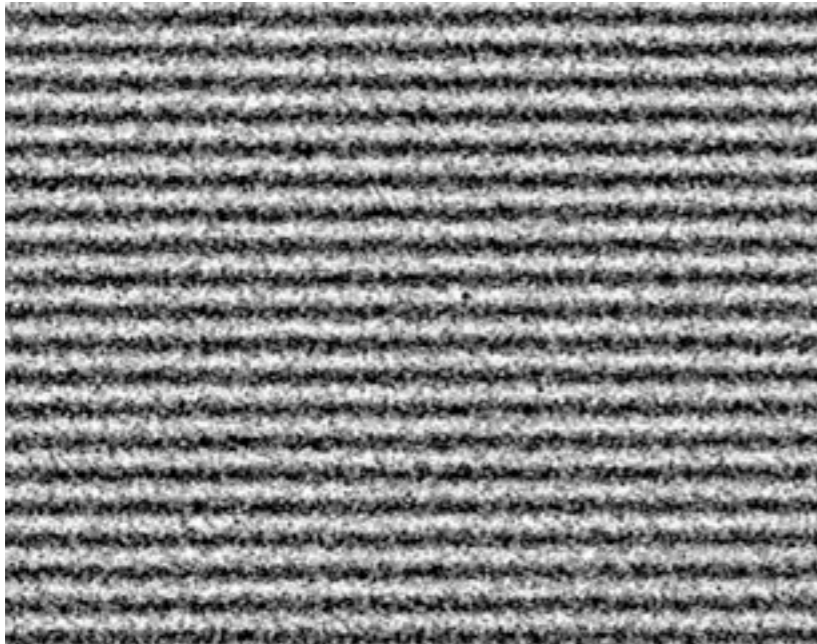


Diameter: 160  $\mu\text{m}$  or about 3x diameter of one hair (A. Stein)

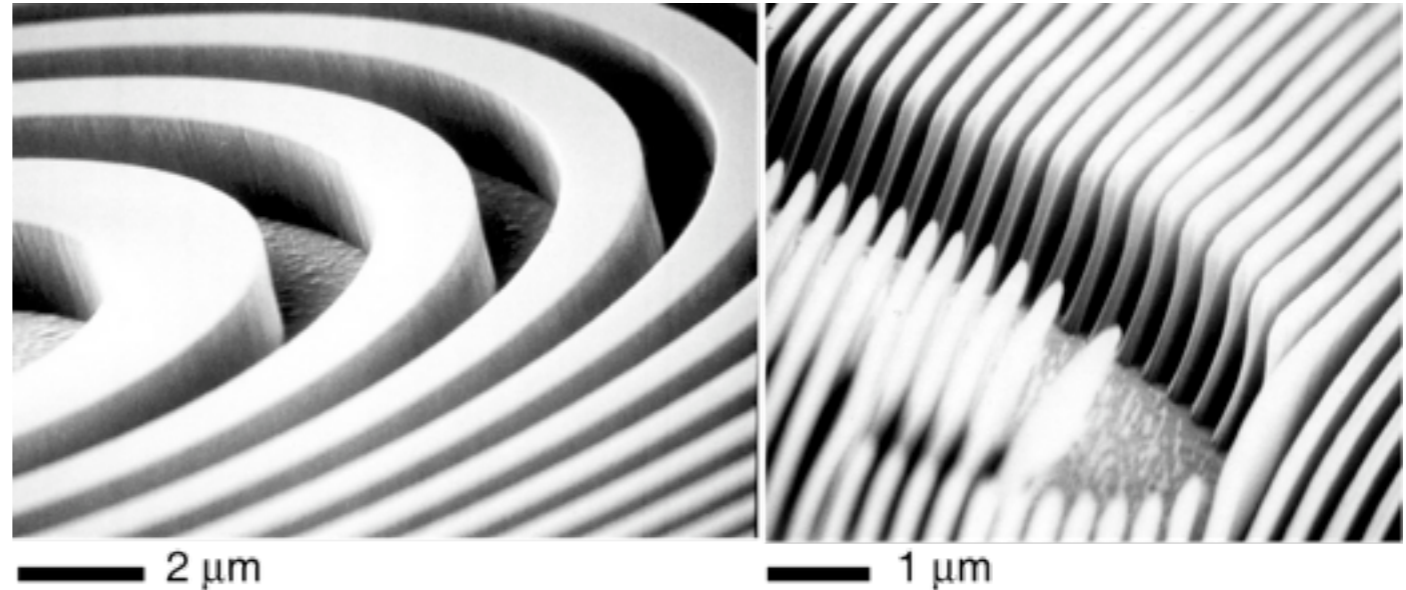


Finest linewidth: 0.030  $\mu\text{m}$  or 30 nm, or about 150 atoms across (M. Lu)

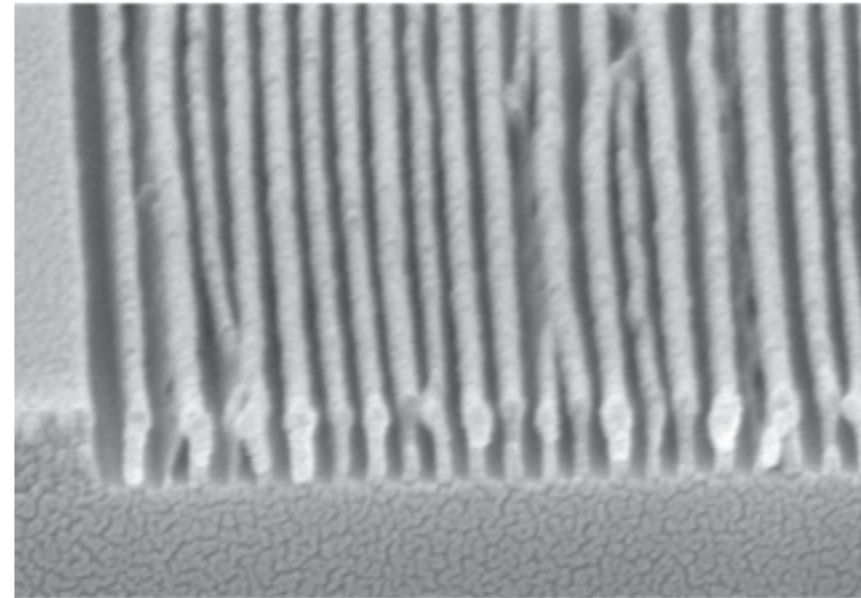
# Fabrication of zone plates



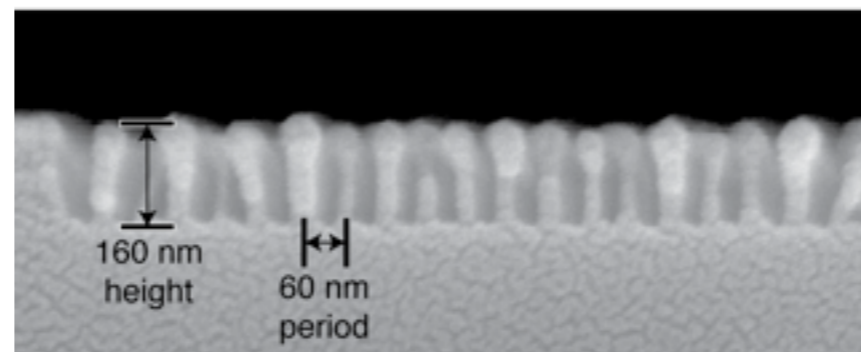
15.1 nm half-pitch multilayer slice imaged with a 15 nm outermost zone width zone plate. Chao et al., Nature **435**, 1210 (2005). But efficiency only ~3%. Other results: 9.2% at 20 nm: Peuker, Appl. Phys. Lett. **78**, 2208 (2001)



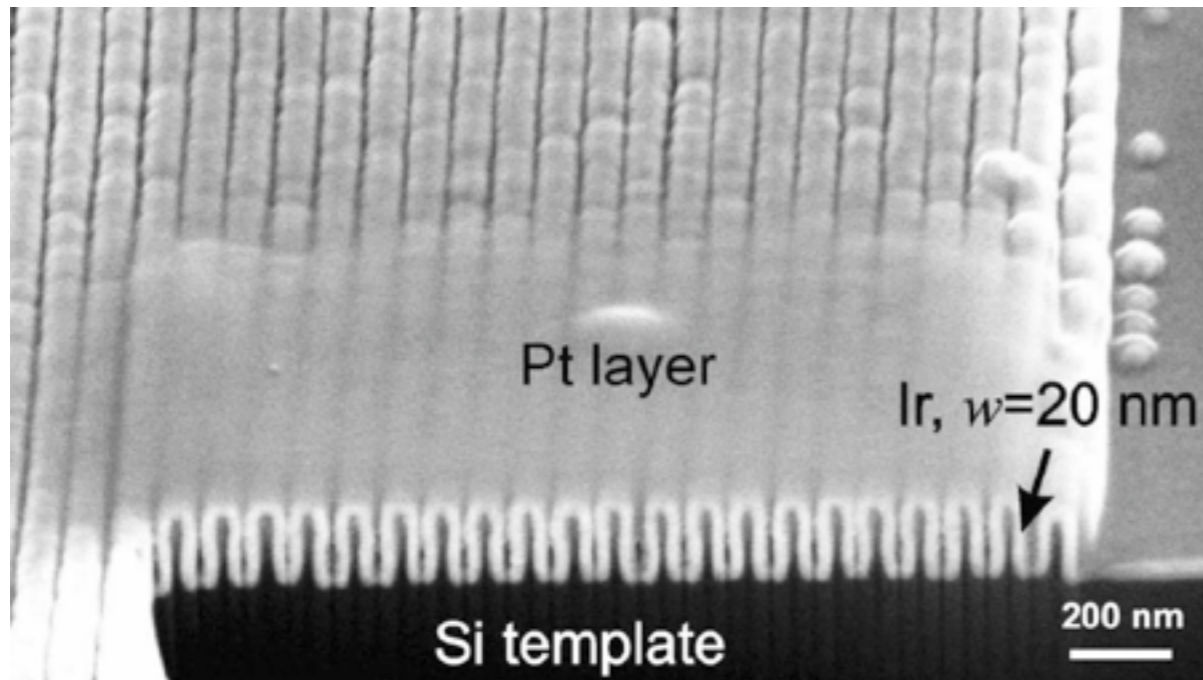
Gold zone plates, Xradia, Inc.: 70 nm outermost zones, 1 μm thick



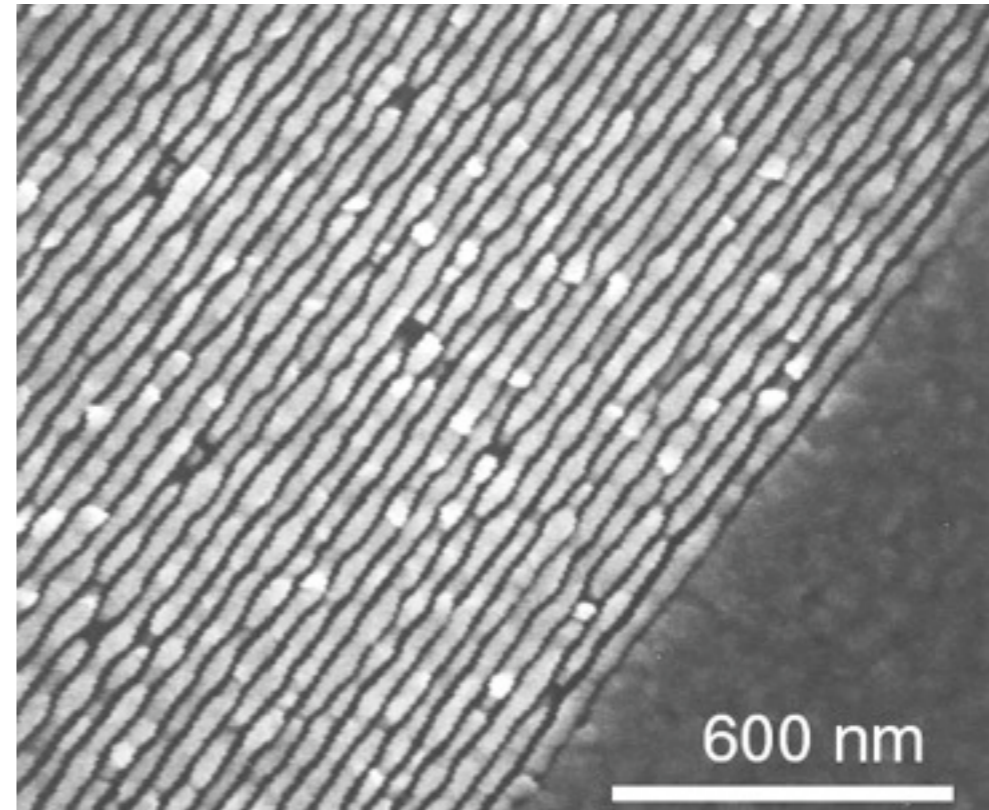
Test structures showing fabrication challenges (M. Lu)



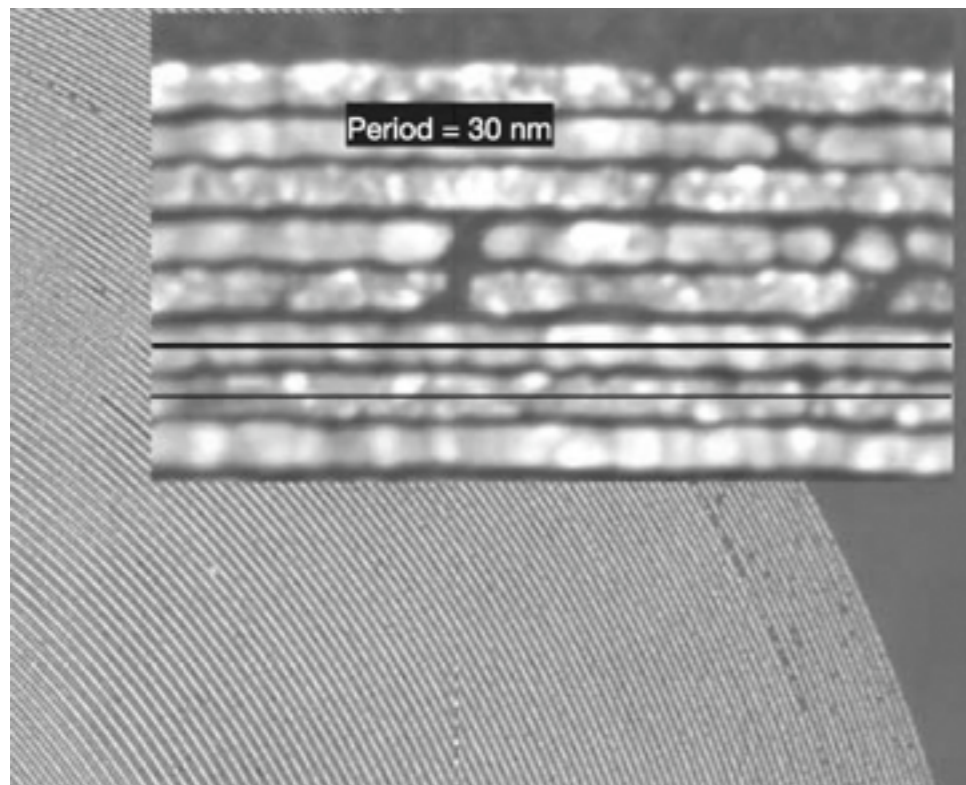
# Zone plate fabrication examples



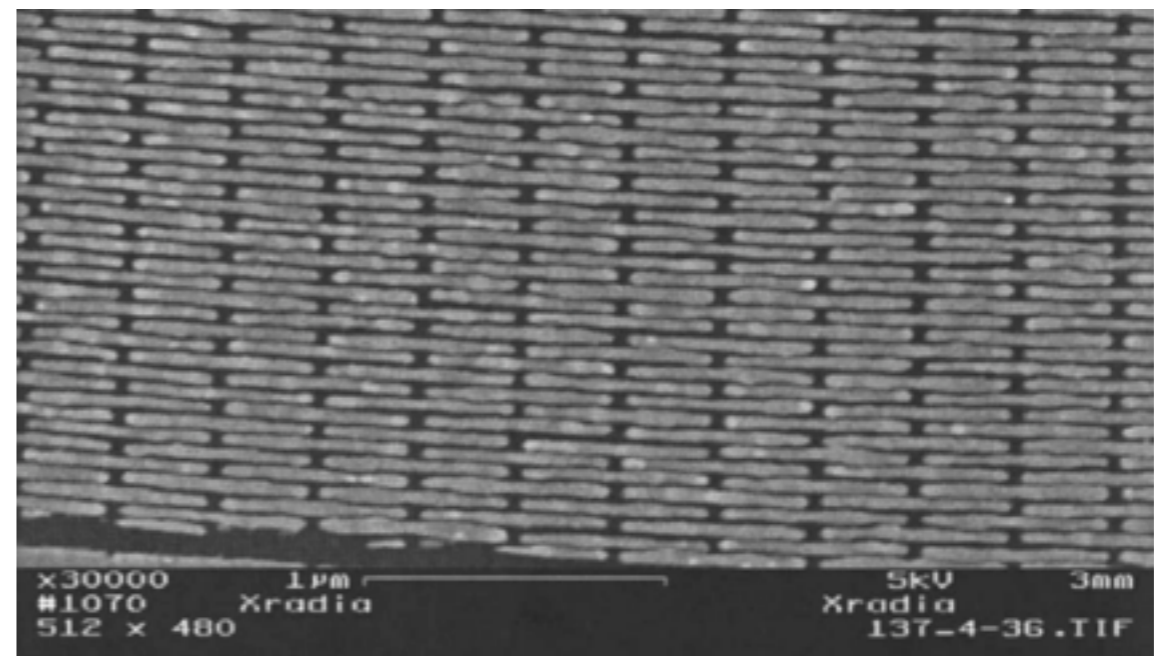
PSI, 20 nm wide, 170 nm tall Ir, 100  $\mu\text{m}$  diameter:  
Jefimovs *et al.*, *Phys. Rev. Lett.* **99**, 264801 (2007).



Stony Brook, 18 nm wide, 60 nm tall Ni, 80  $\mu\text{m}$  diameter:  
Spector *et al.*, *J. Vac. Sci. Tech. B* **15**, 2872 (1997).



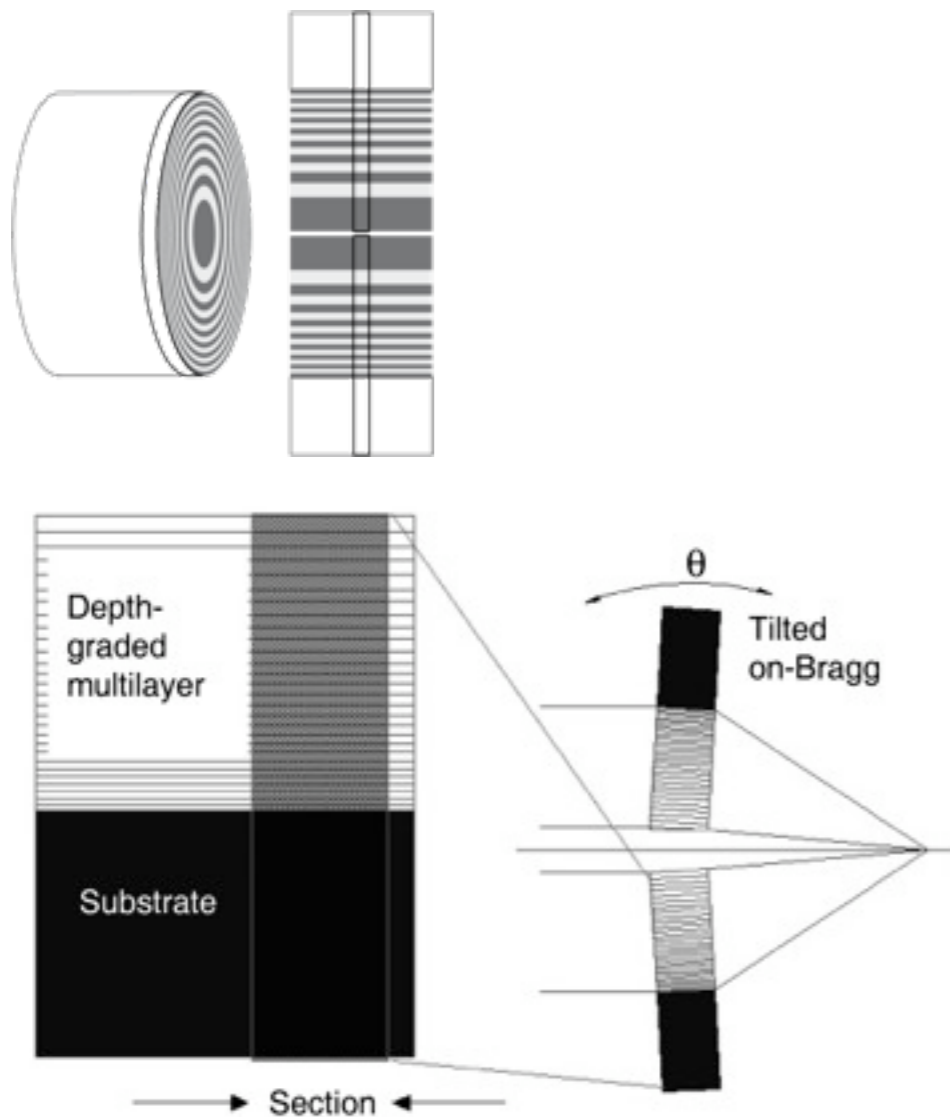
CXRO/LBL, 15 nm wide, 80 nm tall Au, 30  $\mu\text{m}$  diameter:  
Chao *et al.*, *Nature* **435**, 1210 (2005).



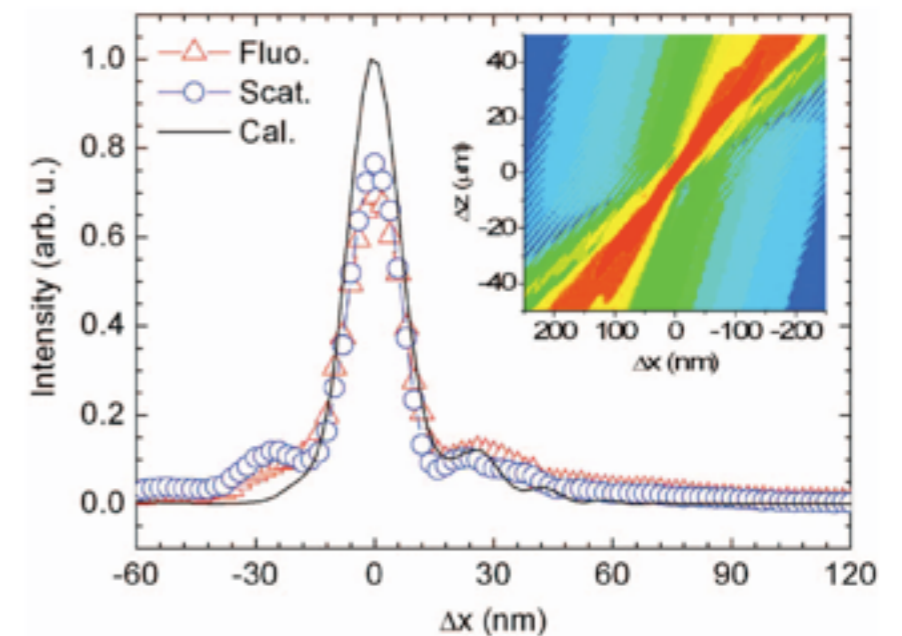
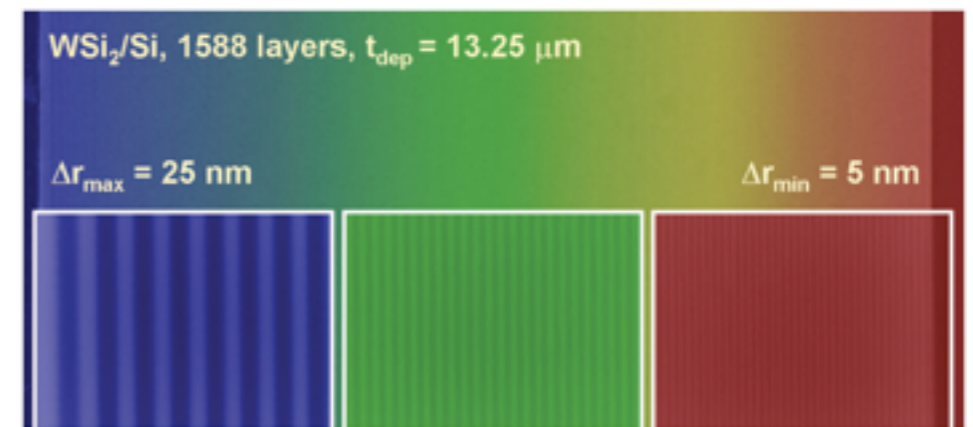
Xradia, 24 nm wide, 300 nm tall Au, 133  $\mu\text{m}$  diameter:  
Feng *et al.*, *J. Vac. Sci. Tech. B* **25**, 2004 (2007).

# Multilayer Laue lenses

- Forget top-down circles, and go sideways! Start by depositing thinnest zones first on a flat substrate, and work your way up to thicker zones. Cross two 1D lenses for 2D focusing. Maser et al., *SPIE 5539*, 185 (2004)
- For thick optics, you want to tilt to be on the Bragg condition anyway [Maser, PhD thesis; Maser and Schmahl, *Opt. Comm.* **89**, 355 (1992)]



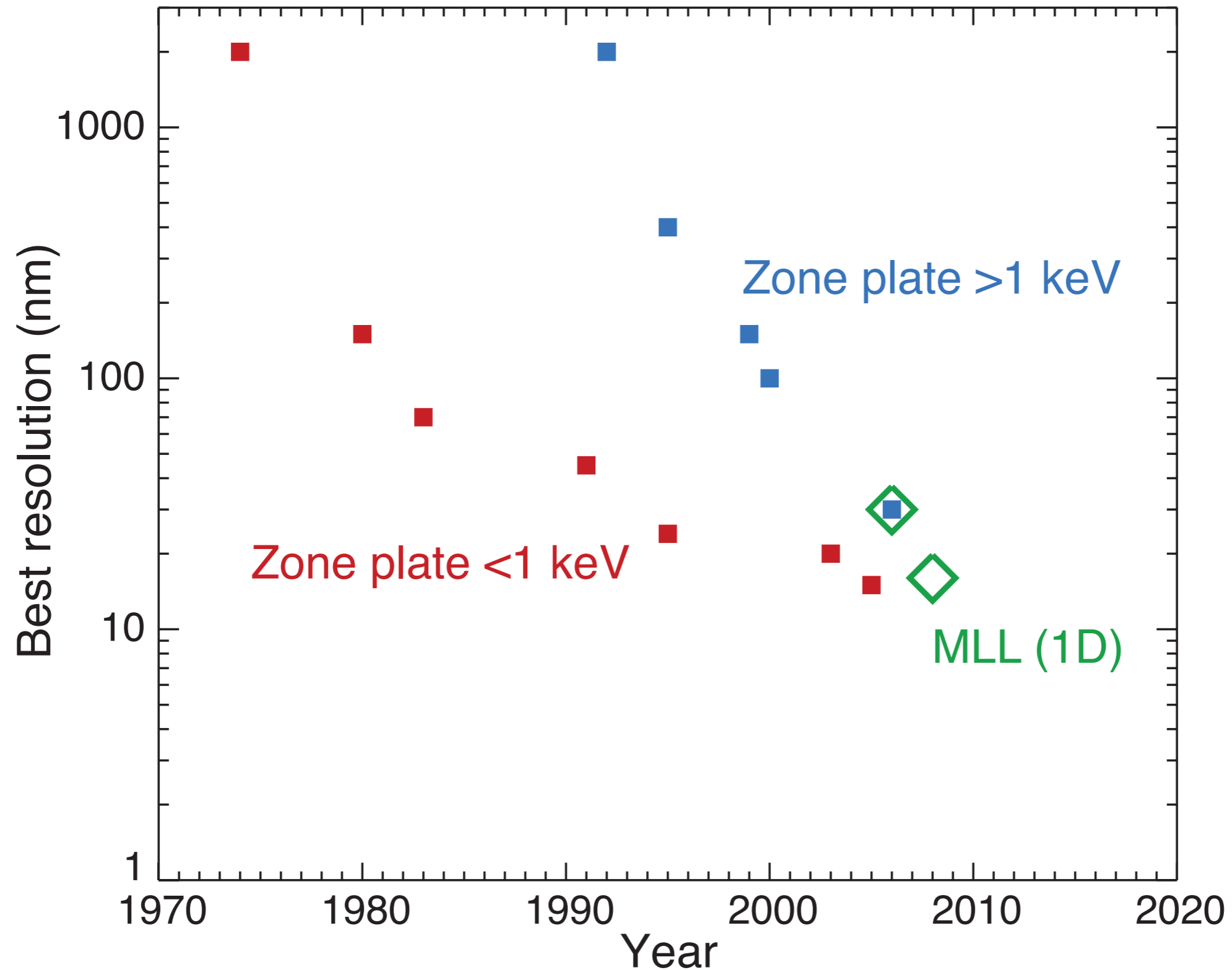
Maser et al., *SPIE 5539*, 185 (2004)



16 nm 1D focus: Kang et al., *Appl. Phys. Lett.* **92**, 21114 (2008)



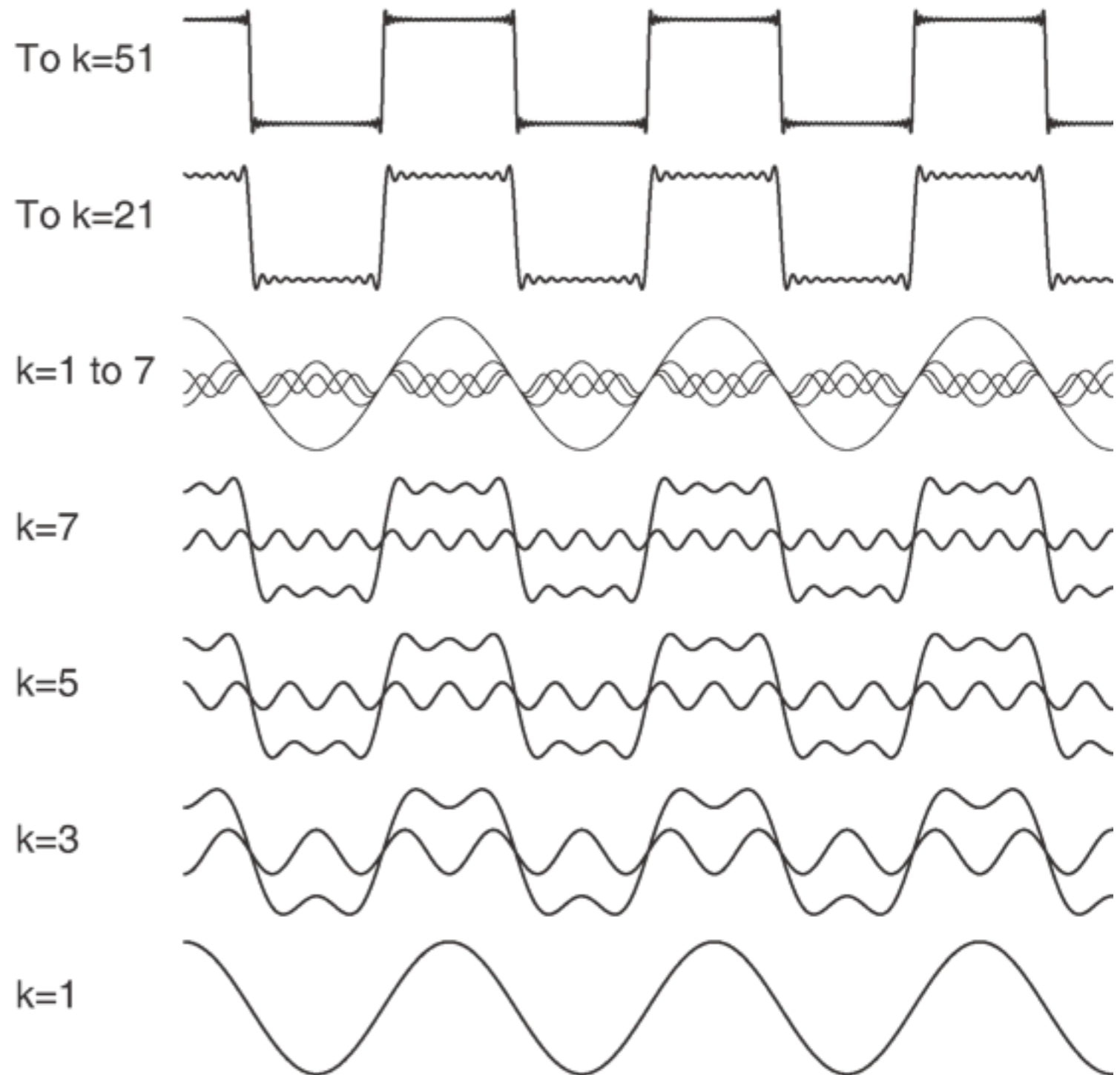
# X-ray optics: best published resolution



# How do we measure resolution?

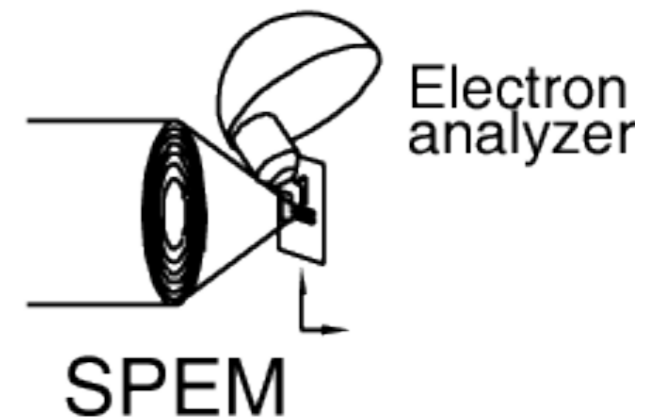
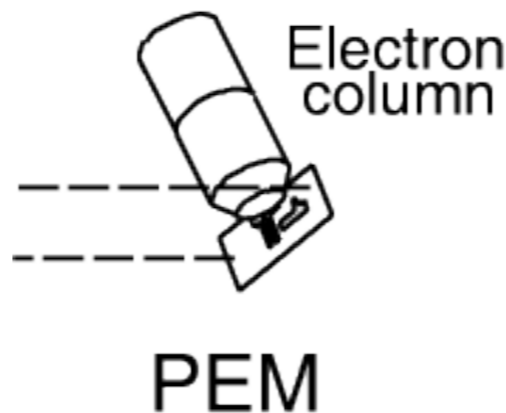
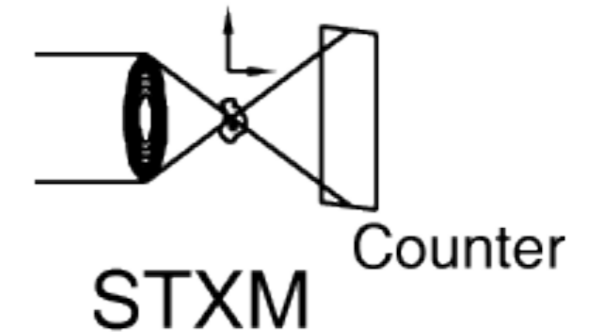
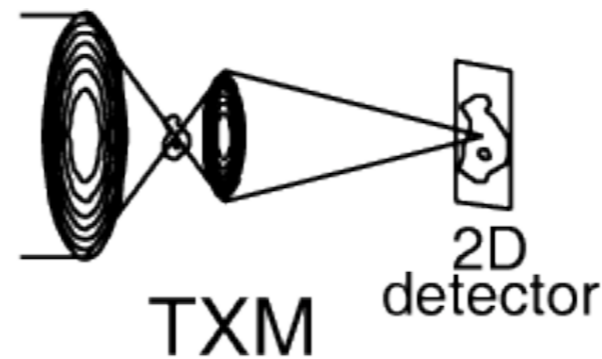
- With an audio system, you discuss the frequency response. Does it reproduce the bass notes at low frequencies? Does it reproduce the cymbal crashes at high frequencies?
- Fourier decomposition: we can treat (nearly) any function as an addition of sine waves

Jean Baptiste  
Joseph, Baron de  
Fourier  
(1768-1830)



# X-ray microscope types

- X-ray optics: zone plates, Kirkpatrick-Baez mirrors, multilayer-coated mirrors, refractive lenses...
- Electron optics: imaging, or energy filtering, or both



*Incoherent illumination*

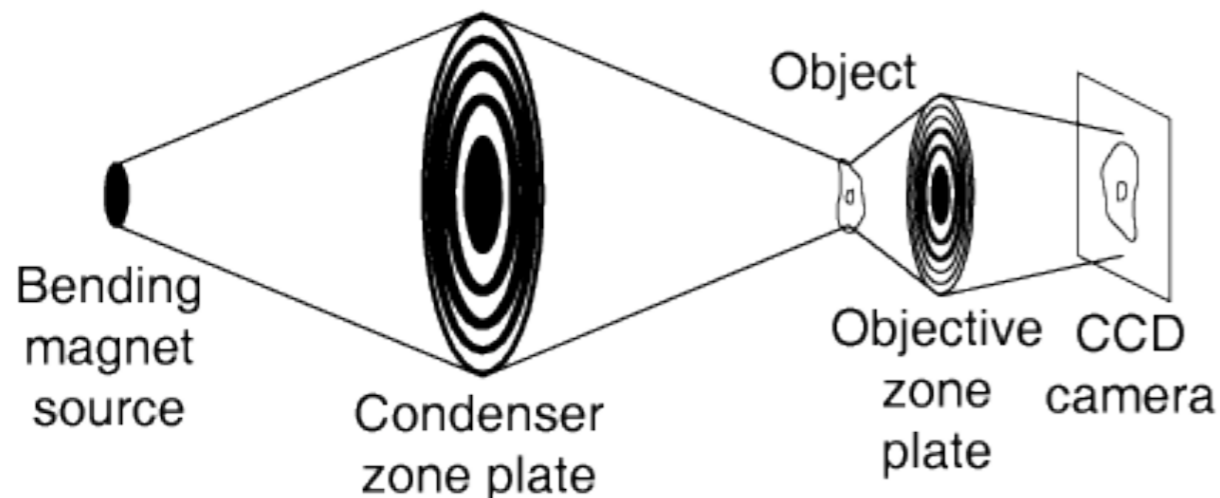
*Coherent illumination*

# Zone plate microscopes

## TXM

- Incoherent illumination; works well with a bending magnet, with fast imaging
- More pixels (e.g.,  $2048^2$ )
- Moderate spectral resolution in most cases - but new instrument at BESSY, Berlin!

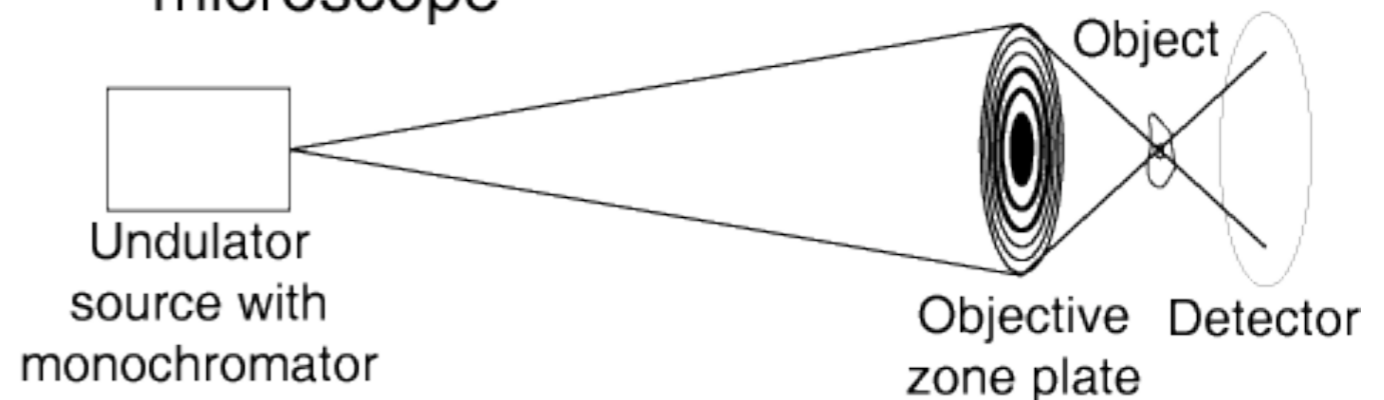
TXM: transmission x-ray microscope



## STXM

- Coherent illumination; works best with an undulator
- Less dose to sample ( $\sim 10\%$  efficient ZP)
- Better suited to conventional grating monochromator [high  $E/(\Delta E)$ ]
- Microprobes: fluorescence etc.

STXM: scanning transmission x-ray microscope



# Scanning and full-field

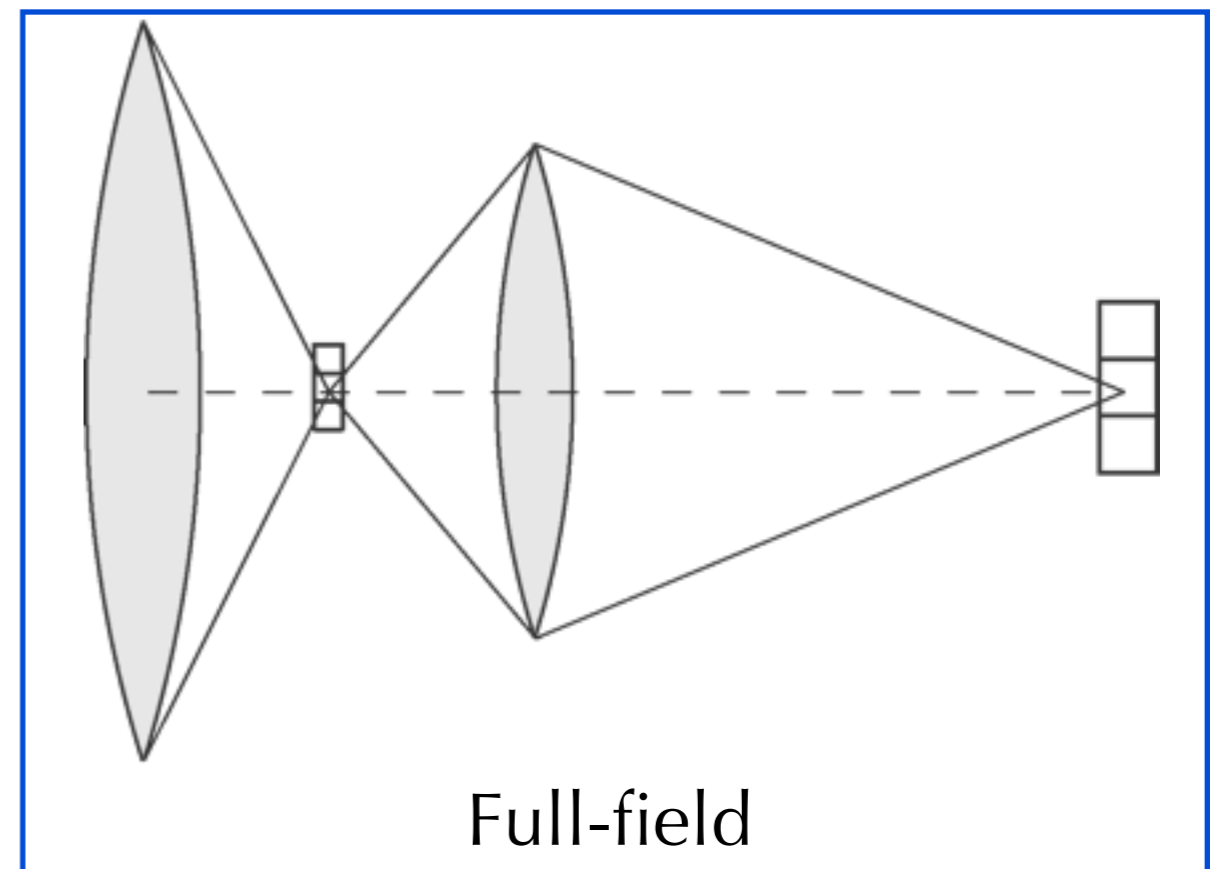
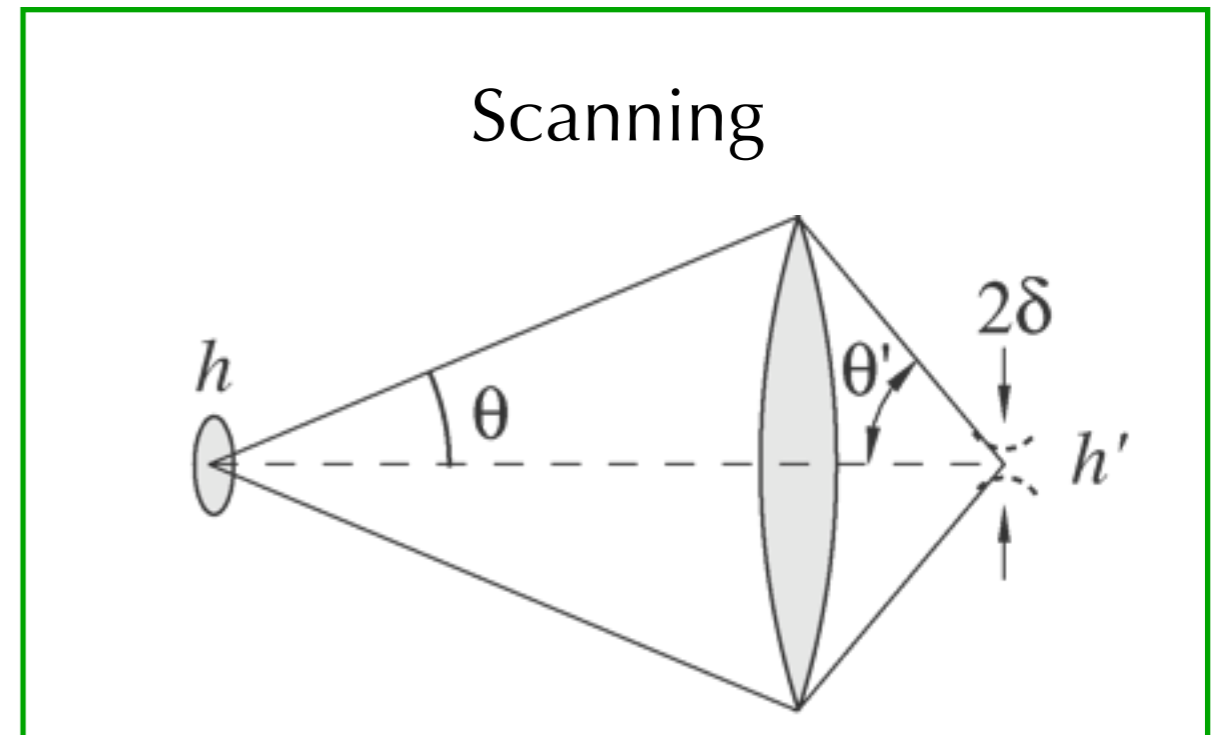
- General property of lenses: preserve size•angle product (Liouville's Theorem), so

$$h\theta = h'\theta'$$

- Microprobe/STXM: want  $h' < \delta$  so that diffraction limit of optic rather than geometrical image of source dominates spot size
- Rayleigh resolution of  $\delta = 0.61 \frac{\lambda}{\theta}$  thus gives phase space of

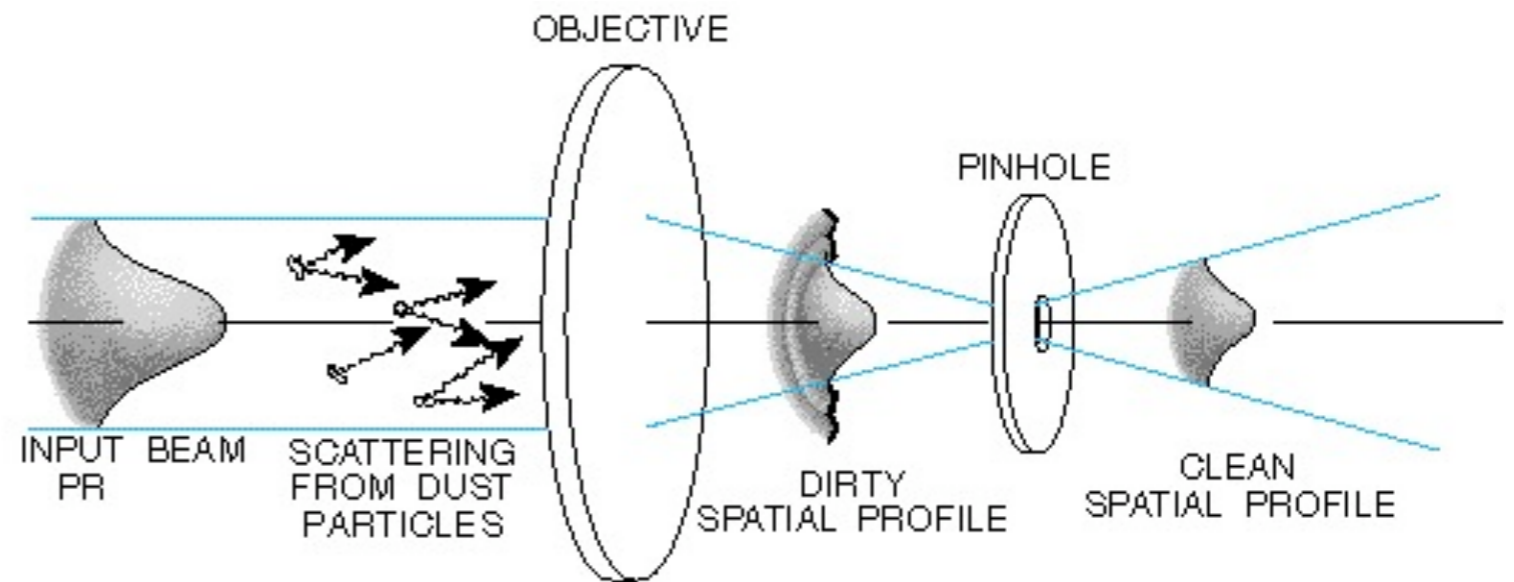
$$(2\delta)(2\theta) = 2.44\lambda$$

- Full-field: each pixel in object is diffraction limit of optic, but can have many pixels simultaneously!



# Controlling spatial coherence

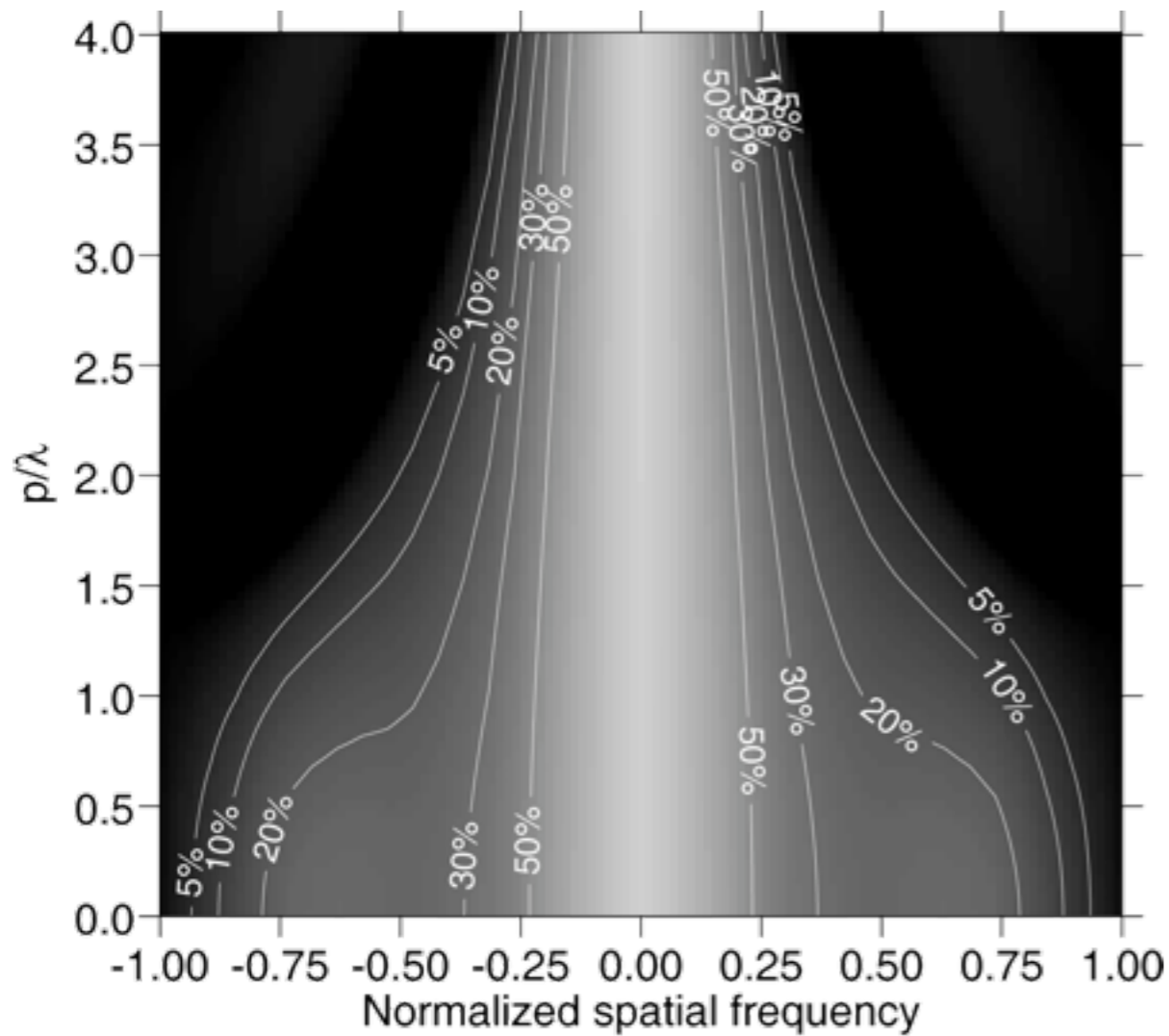
- Coherent flux: phase space area of  $\lambda$  in each dimension. Coherent flux is  $B \cdot \lambda^2$ . Green, BNL-50522 (1976); Kondratenko and Skrinsky, Opt. Spectr. **42**, 189 (1977).
- Spatial filter: pinhole at the focus of a lens. Passes only the spatially coherent fraction of an incident beam.



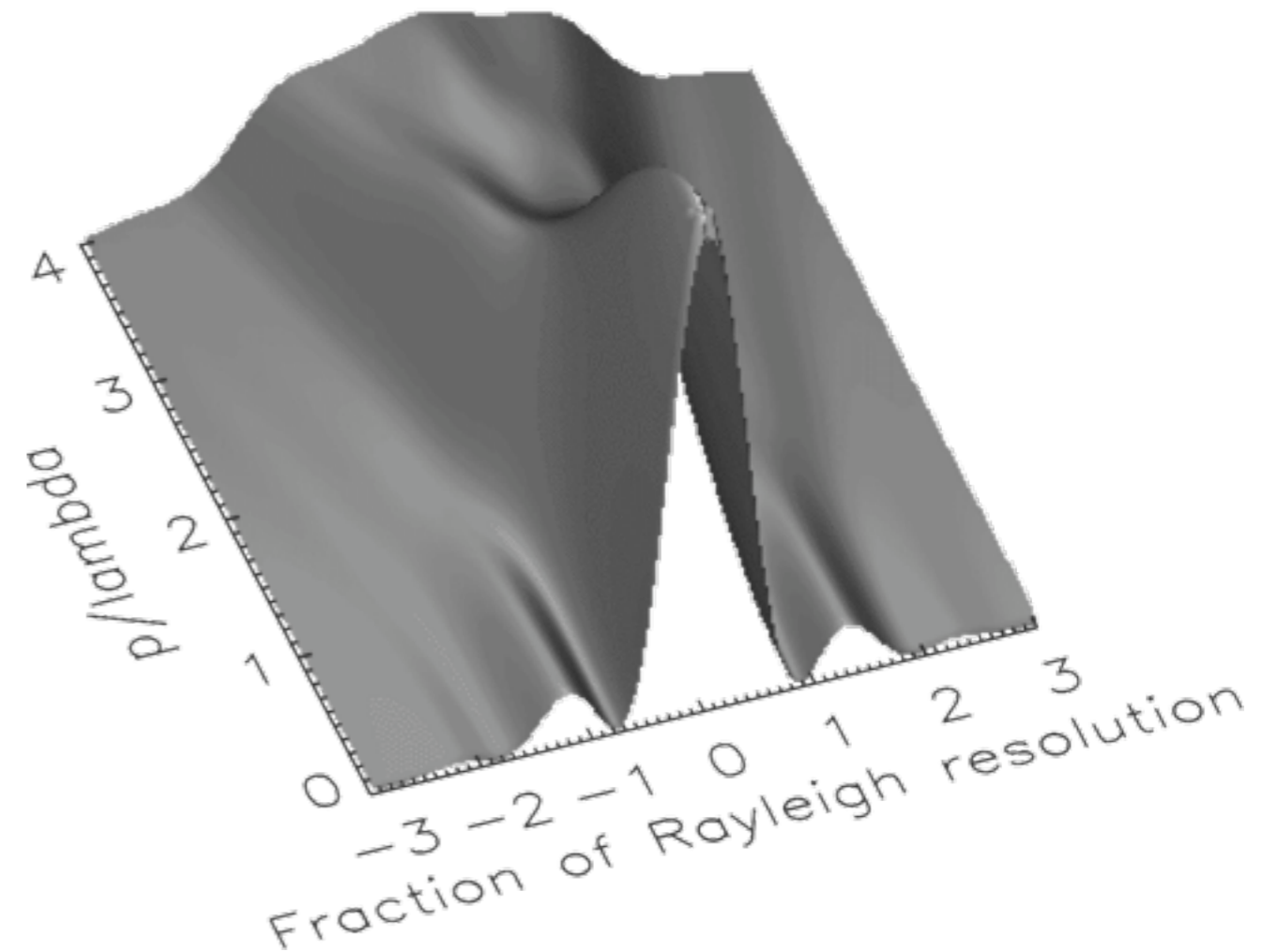
Diagram, photo from Newport catalog

# Effects of spatial incoherence on STXM

How close must  $p=h\theta$  be to  $\lambda$ ?



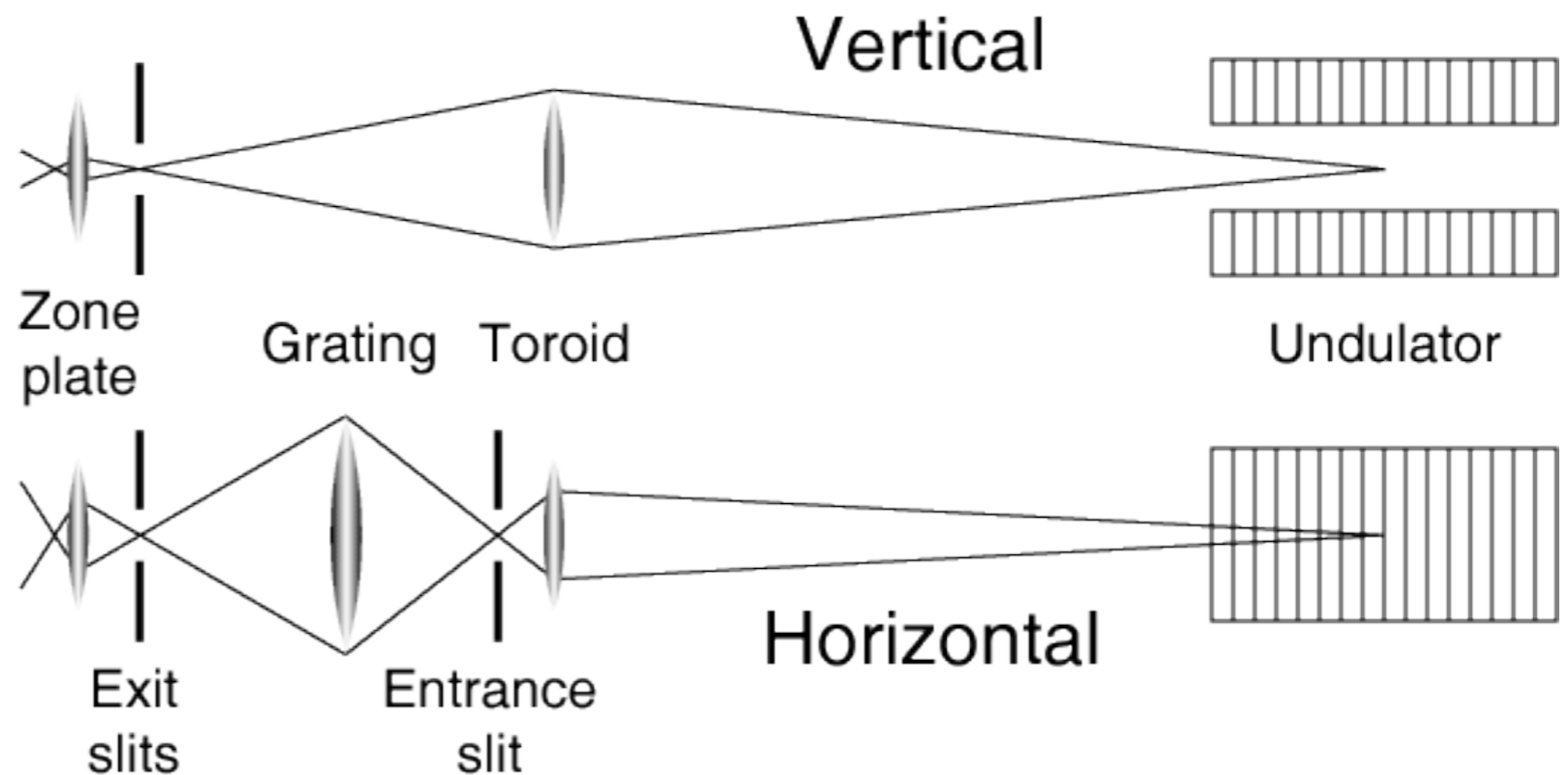
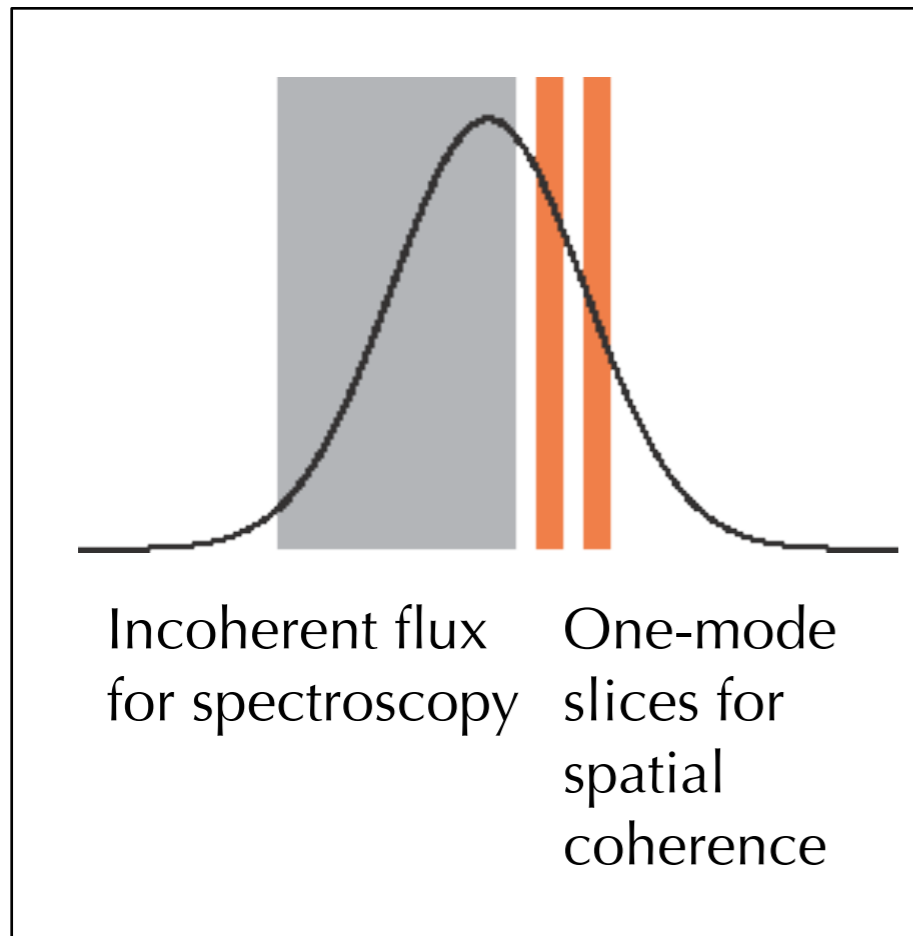
Effect on modulation transfer function MTF  
(50% central stop)



Effect on point spread function PSF  
(50% central stop)

# Soft x-ray undulator at the NSLS

- Electron beam emittance determines photon source emittance.
- Horizontal emittance is about  $100\lambda$ . Mode sharing



Slits as spatial filters;  
monochromator for temporal  
coherence



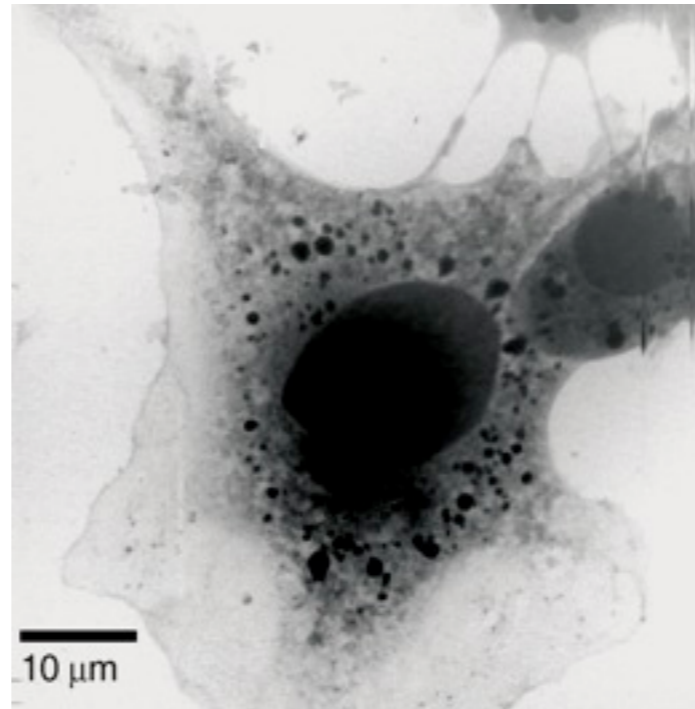
# 2D imaging with Stony Brook STXMs

Scanning zone plate microscopes  
U15 and X17t (1983-1987): Kirz  
(Stony Brook) and Rarback  
(NSLS).

X1A (since 1989): Kirz and  
Jacobsen (Stony Brook)

2D imaging is moderately  
useful but...

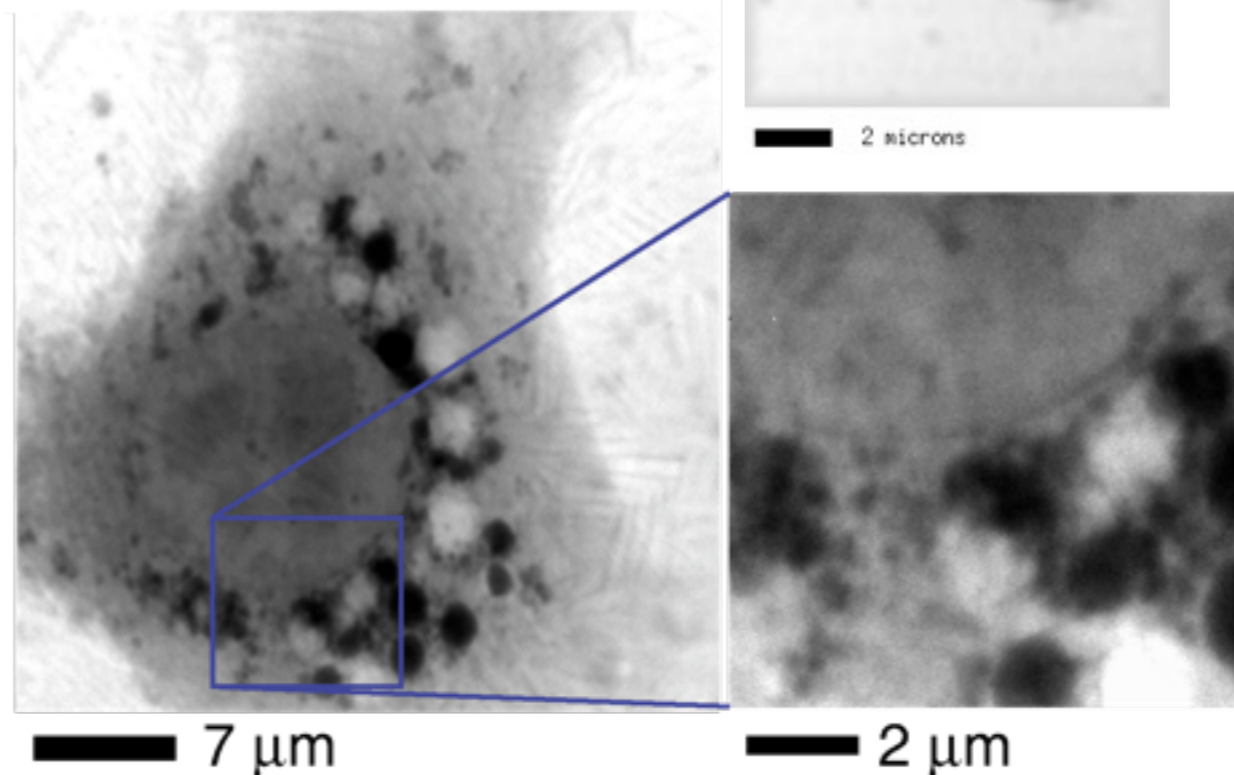
- Cannot track fluorescently-labeled proteins in living cells
- Resolution is inferior to cryoEM, though do not need to section
- Best utility may lie beyond simple 2D imaging



NIL 8 fibroblast (wet, fixed):  
Oehler *et al.*



Human sperm  
(unfixed): Wirick,  
Fleckenstein,  
Sheynkin *et al.*



Fibroblast (frozen hydrated): Maser *et al.*, *J. Microsc.* **197**, 68 (2000)

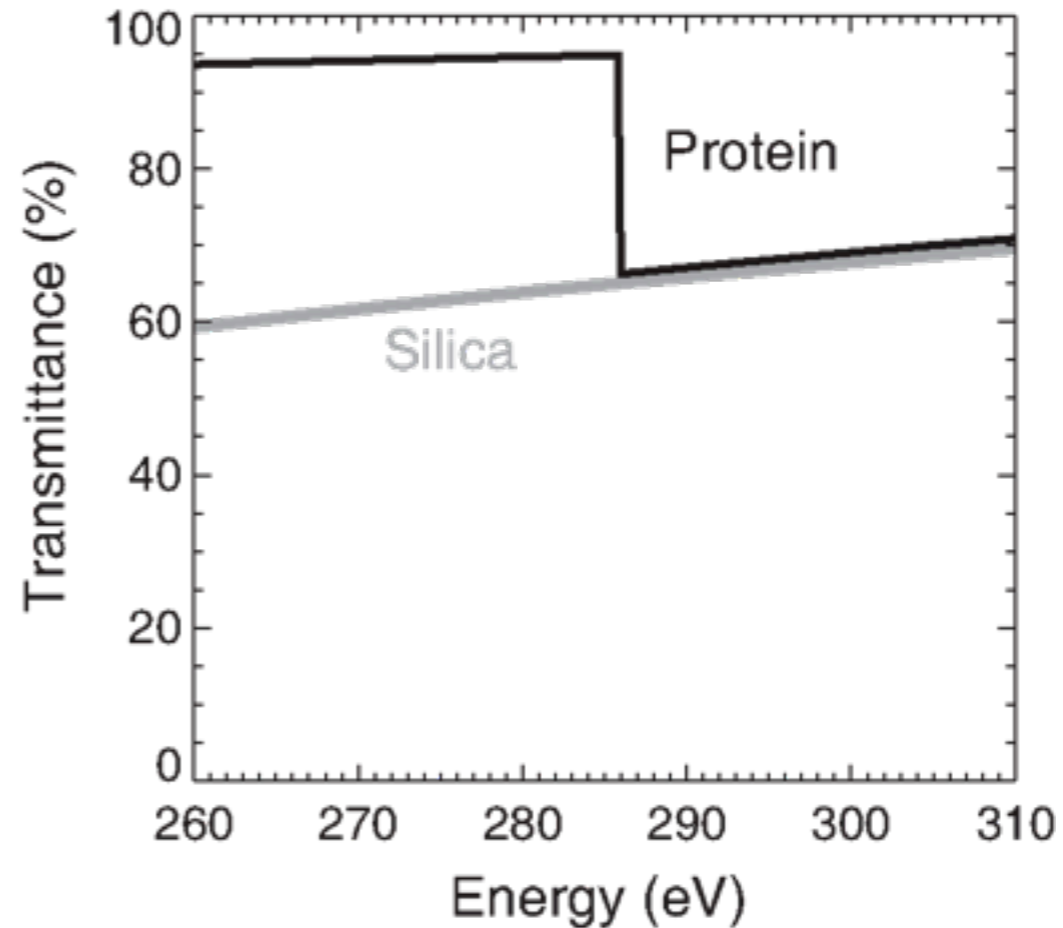
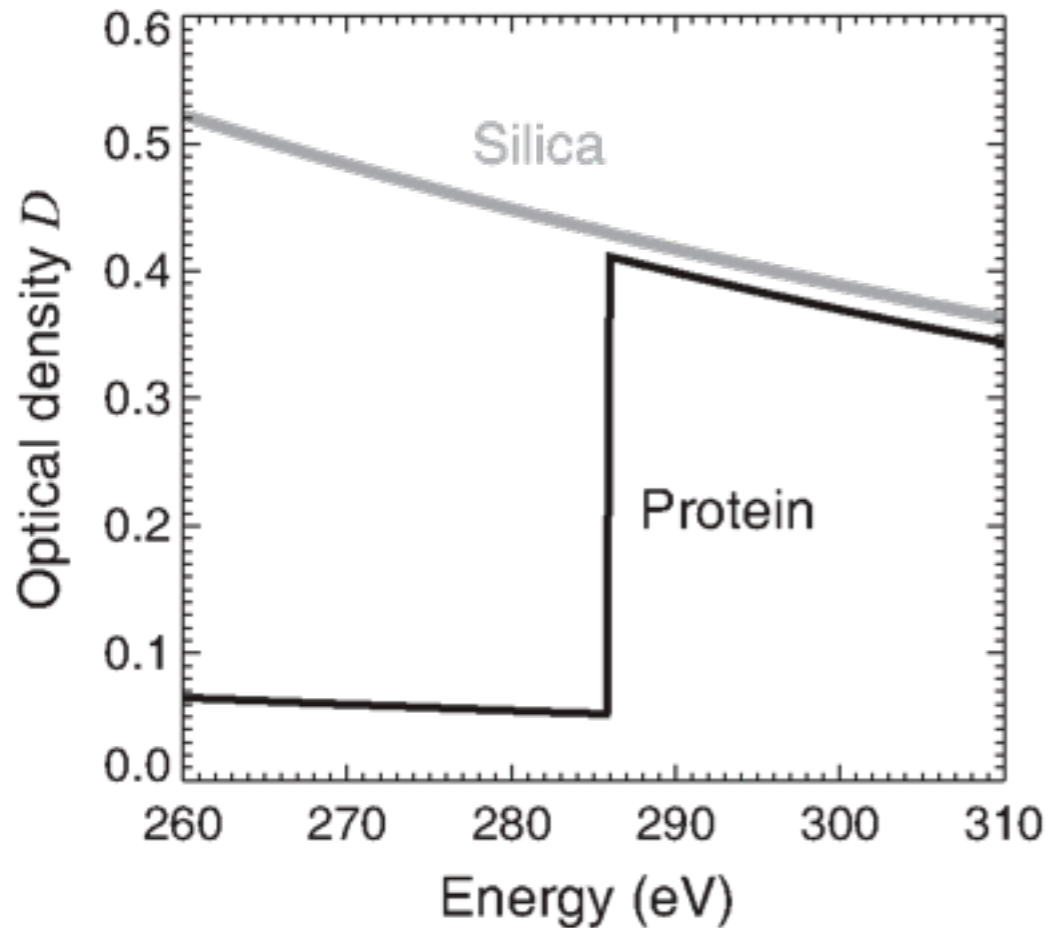
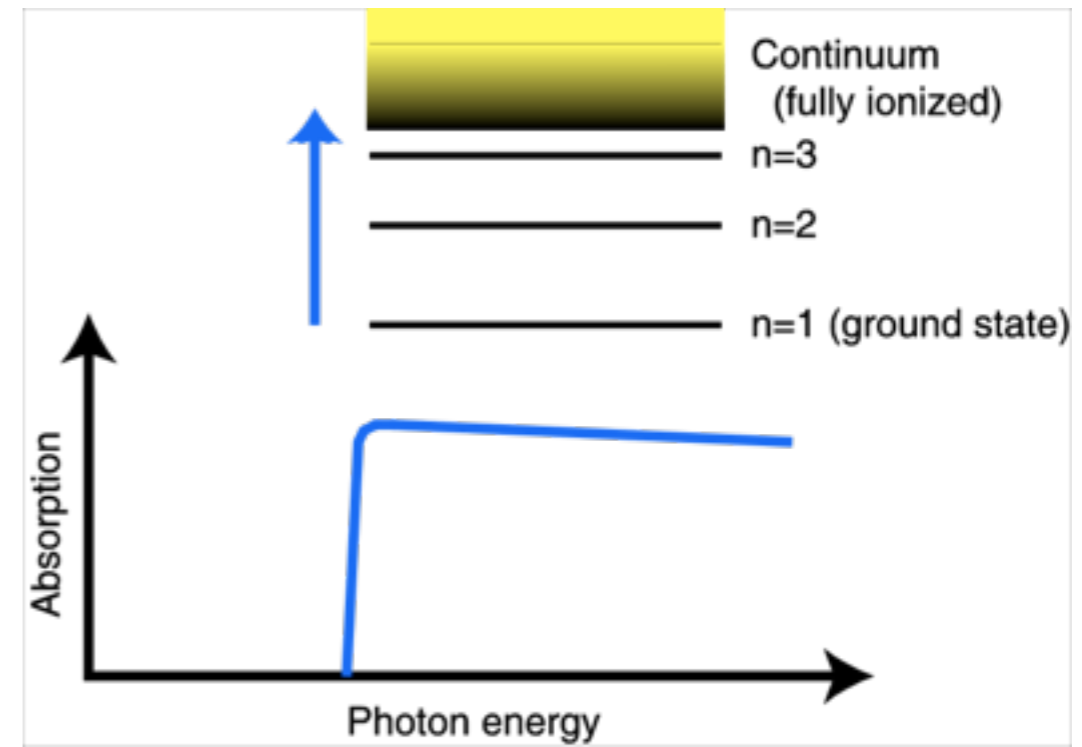
# Absorption edges

Lambert-Beer law: linear absorption coefficient  $\mu$

$$I = I_0 \exp[-\mu(E) \cdot t] = I_0 \exp[-D(E)]$$

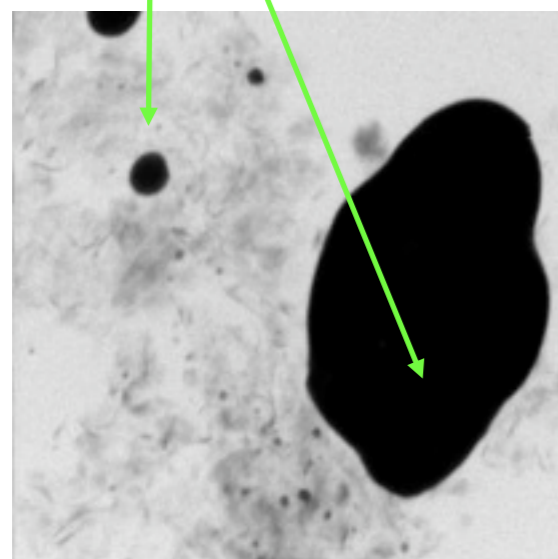
This coefficient makes a jump at specific elemental absorption edges!

This example: 0.1  $\mu\text{m}$  protein, silica

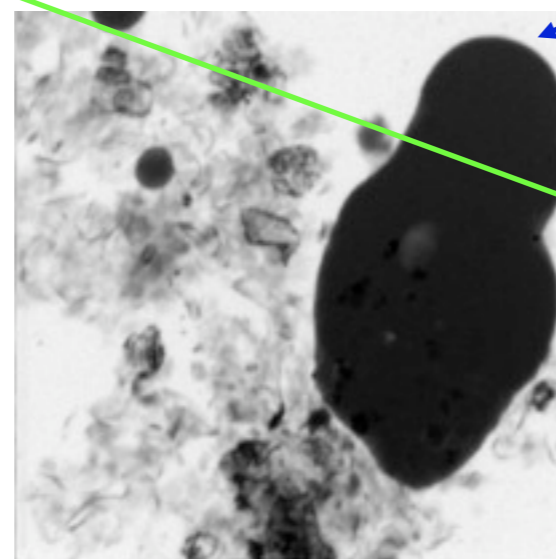


# X-ray microscopy of colloids

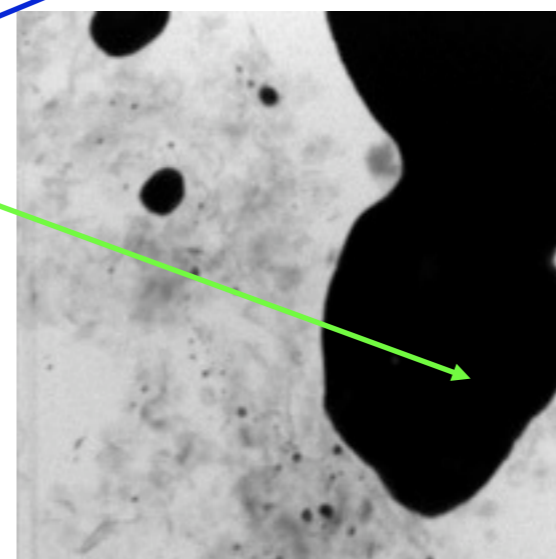
- U. Neuhäusler (Stony Brook/Göttingen), S. Abend (Kiel), G. Lagaly (Kiel), C. Jacobsen (Stony Brook), Colloid and Polymer Science **277**, 719 (1999)
- Emulsion: water, oil droplets, clay, and layered double hydroxides (LDH)
- “Caged” part of oil droplet remains fixed; “uncaged” part can disperse



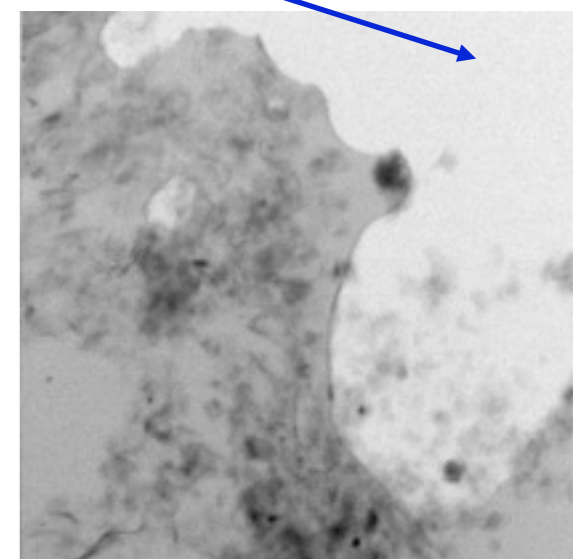
346 eV: calcium weakly absorbing. Clays and LDHs absorb equally



352.3 eV: calcium strongly absorbing. Calcium-rich LDHs are highlighted.



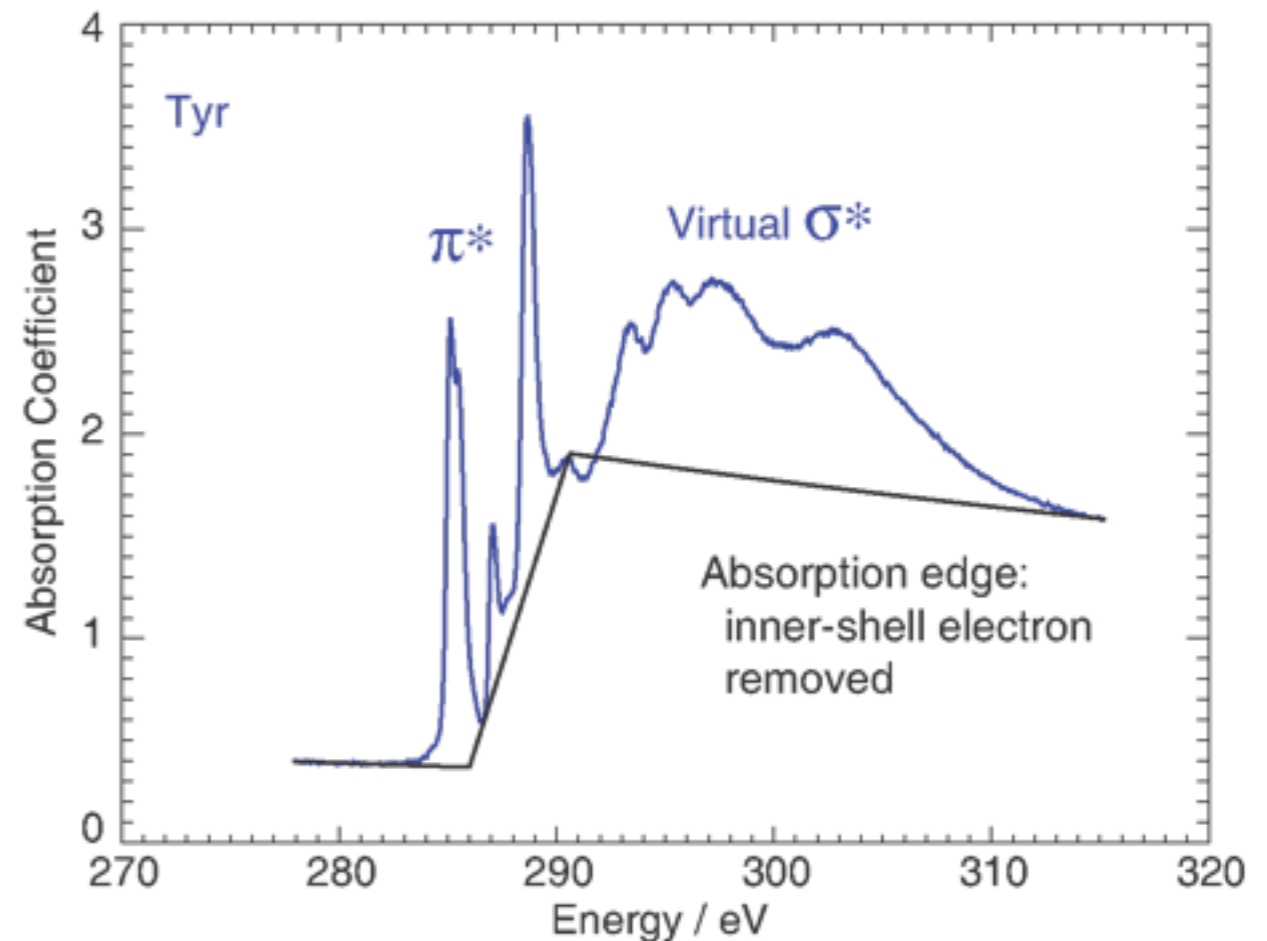
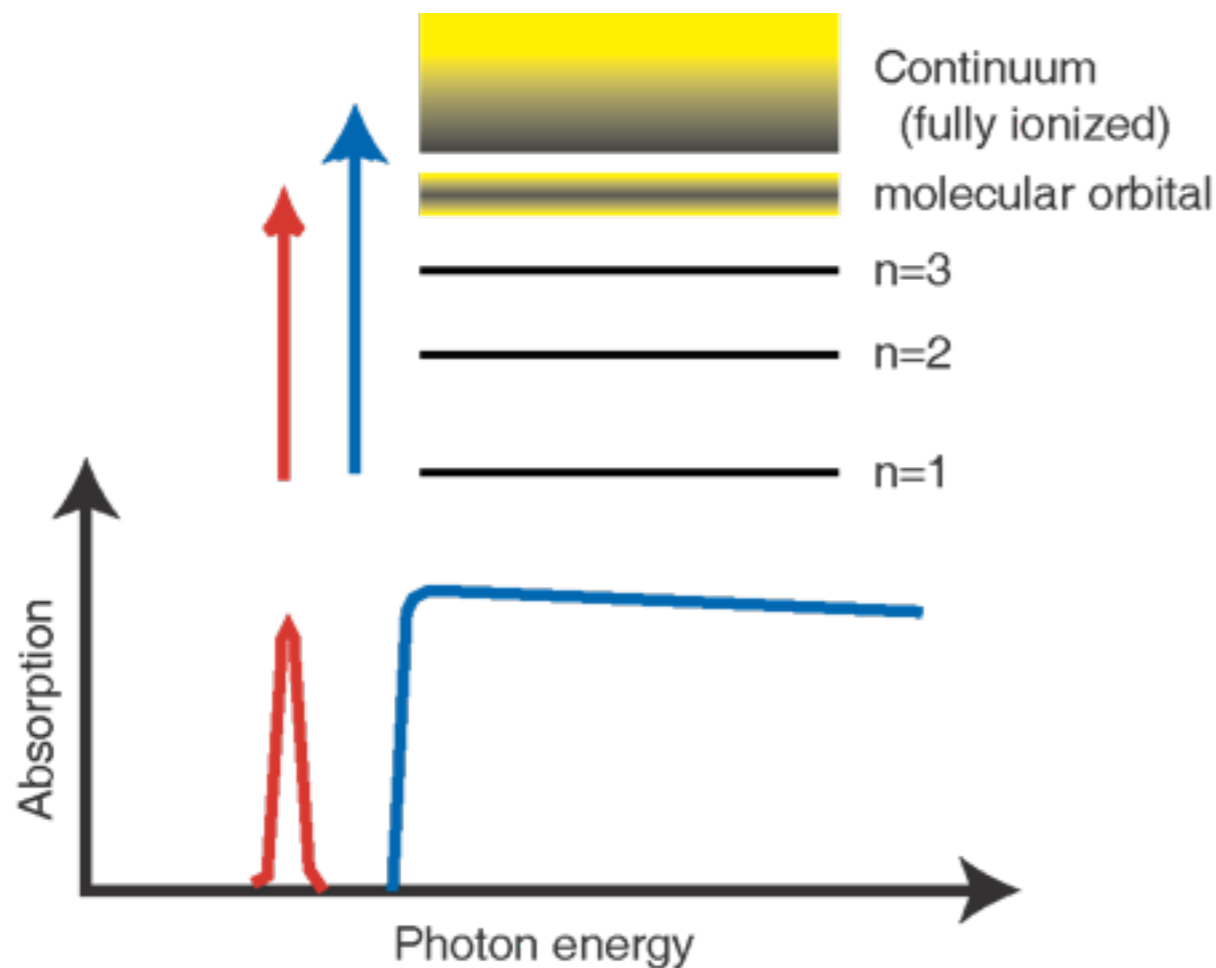
290 eV: carbon strongly absorbing



284 eV: carbon (oil drop) weakly absorbing

# Near-edge absorption fine structure (NEXAFS) or X-ray absorption near-edge structure (XANES)

- Fine-tuning of the x-ray energy near an atom's edge gives sensitivity to the chemical bonding state of atoms of that type
- First exploitation for chemical state transmission imaging: Ade, Zhang *et al.*, *Science* **258**, 972 (1992) – Stony Brook/X1A



Compared with UV “tickling” of molecular orbitals, core-level electrons come from a single, well-defined state!

# Near-edge spectroscopy: ELNES and XANES

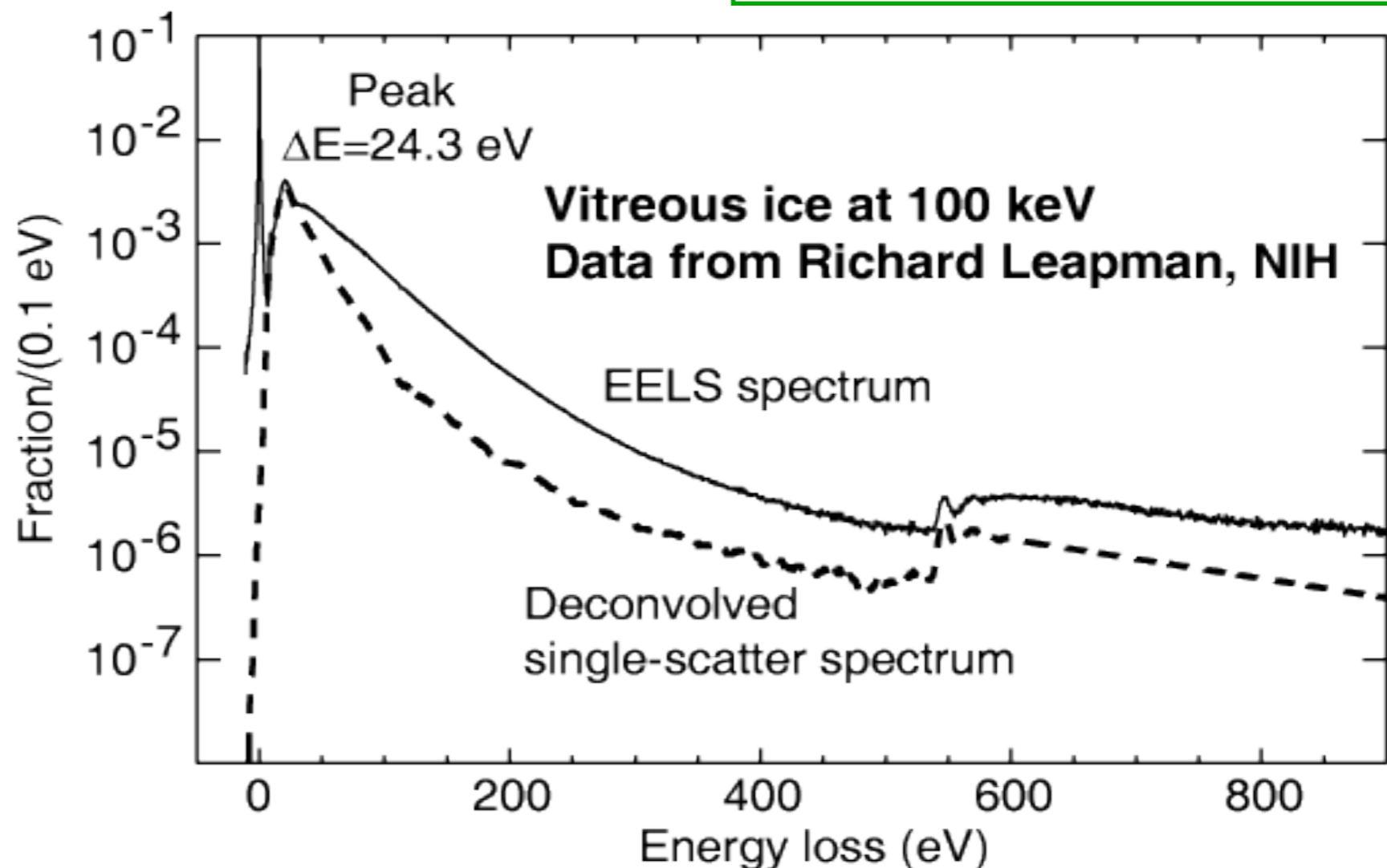
## ELNES (electron Energy Loss)

- Plural inelastic scattering
- Many elements at once - but plasmon modes are always excited (damage)
- $\Delta E$  was  $\sim 0.6$  eV, but now  $< 0.1$  eV in some cases

## XANES (X-ray Absorption)

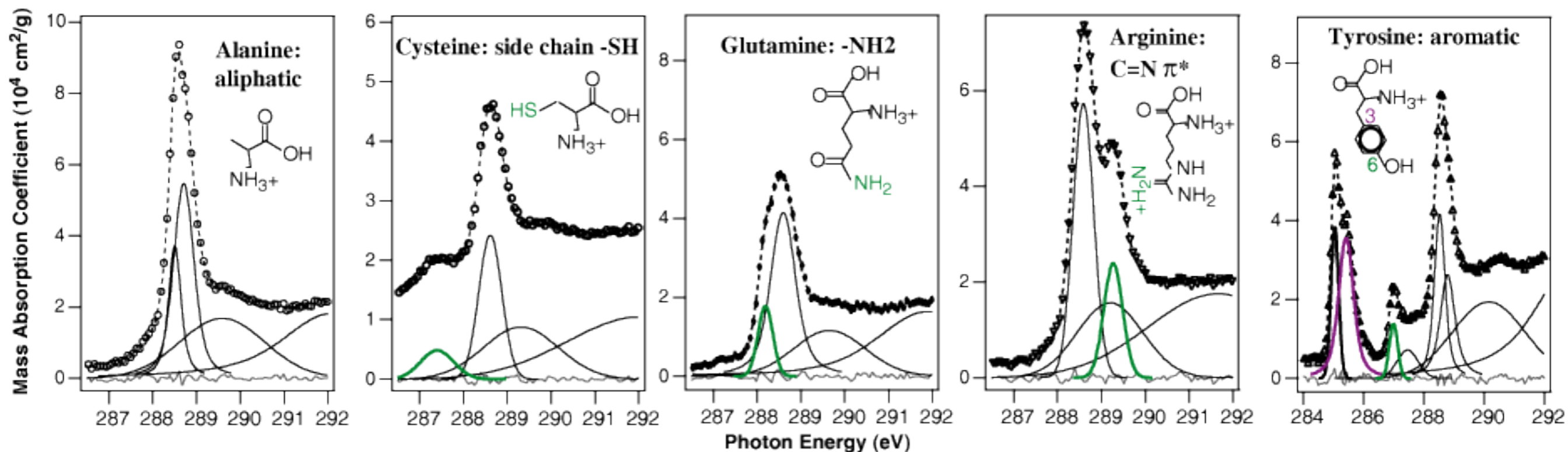
- No plural scattering
- One element at a time - slow but less damage
- $\Delta E$  of 0.05-0.1 eV is common

- Electrons  $\sim 1000\times$  more damaging:
- Isaacson and Utlaut, *Optik* **50**, 213 (1978)
  - Rightor *et al.*, *J. Phys. Chem. B* **101**, 1950 (1997).



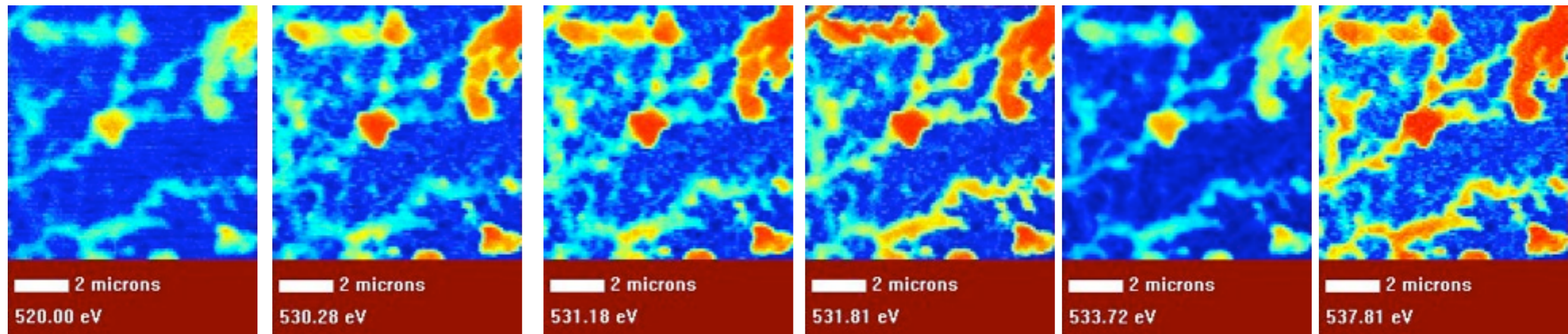
# C-XANES of amino acids

- K. Kaznatcheyev *et al.*, *J. Phys. Chem. A* **106**, 3153 (2002)
- Experiment: K. Kaznatcheyev *et al.*, Stony Brook (now CLS)
- Theory: O. Plashkevych, H. Ågren *et al.*, KTH Stockholm; A. Hitchcock, McMaster

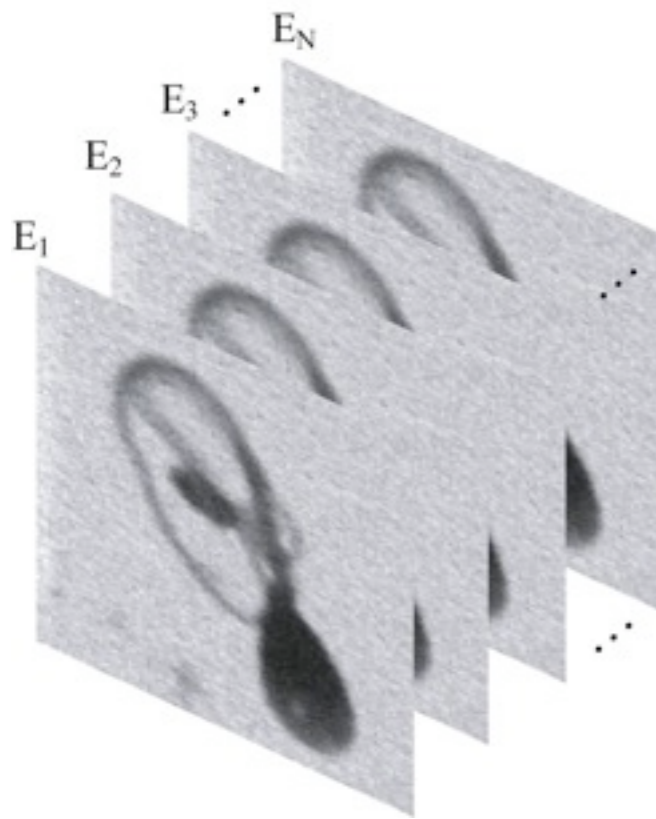


Polymers: see e.g., Dhez, Ade, and Urquhart, *JESRP* **128**, 85 (2003)

# Spectromicroscopy from image sequences



Lu in hematite (T. Schäfer)



Aligned spectral image sequences:  
Jacobsen *et al.*, *J. Microscopy* **197**,  
173 (2000)

**$10^4$ - $10^5$  spectra!** Too many to analyze “by hand.”  
Complex mixtures *etc.*; life is not made up of uniform thin films.  
How to deal with the complexity?  
1. PCA for noise reduction, orthogonalization.  
2. Cluster analysis to find patterns.  
3. Non-negative matrix factorization for final analysis.

# Spectromicroscopy analysis

We measure the optical density  $D=\mu t$  from  $I=I_0\exp[-\mu t]$ , which gives us a matrix over  $n=1..N$  energies and  $p=1..P$  pixels of the **data**:

$$D_{N \times P} = \begin{bmatrix} D_{11} & \text{pixels} & D_{1P} \\ \text{spectra} & & \vdots \\ D_{N1} & \dots & D_{NP} \end{bmatrix}$$

We wish we could interpret this in terms of a set of  $s=1..S$  components. We would then have a matrix of their **spectra**

$$\mu_{N \times S} = \begin{bmatrix} \mu_{11} & \text{components} & \mu_{1S} \\ \text{spectra} & & \vdots \\ \mu_{N1} & \dots & \mu_{NS} \end{bmatrix}$$

We would also have a matrix of their **thicknesses**

$$t_{S \times P} = \begin{bmatrix} t_{11} & \text{pixels} & t_{1P} \\ \text{components} & & \vdots \\ t_{S1} & \dots & t_{SP} \end{bmatrix}$$

What we have

What we wish we had



# Doing the math

- We measure the **data** but want to interpret it as **spectra** times **thicknesses**:

$$\begin{bmatrix} D_{11} & \text{pixels} & D_{1P} \\ \text{spectra} & & \vdots \\ D_{N1} & \dots & D_{NP} \end{bmatrix} = \begin{bmatrix} \mu_{11} & \text{components} & \mu_{1S} \\ \text{spectra} & & \vdots \\ \mu_{N1} & \dots & \mu_{NS} \end{bmatrix} \cdot \begin{bmatrix} t_{11} & \text{pixels} & t_{1P} \\ \text{components} & & \vdots \\ t_{S1} & \dots & t_{SP} \end{bmatrix}$$

or  $D_{N \times P} = \mu_{N \times S} \cdot t_{S \times P}$

- If we know all  $S$  components and their **spectra**  $\mu_{N \times S}$ , we can obtain thickness **maps**:

$$t_{S \times P} = \mu_{S \times N}^{-1} \cdot D_{N \times P}$$

- Matrix  $\mu_{N \times S}$  of all spectra can be inverted using singular matrix decomposition (SVD). See e.g., Zhang *et al.*, *J. Struct. Biol.* **116**, 335 (1996); Koprinarov *et al.*, *J. Phys. Chem. B* **106**, 5358 (2002).

# What if we don't know the components or their spectra $\mu_{N \times S}$ ?

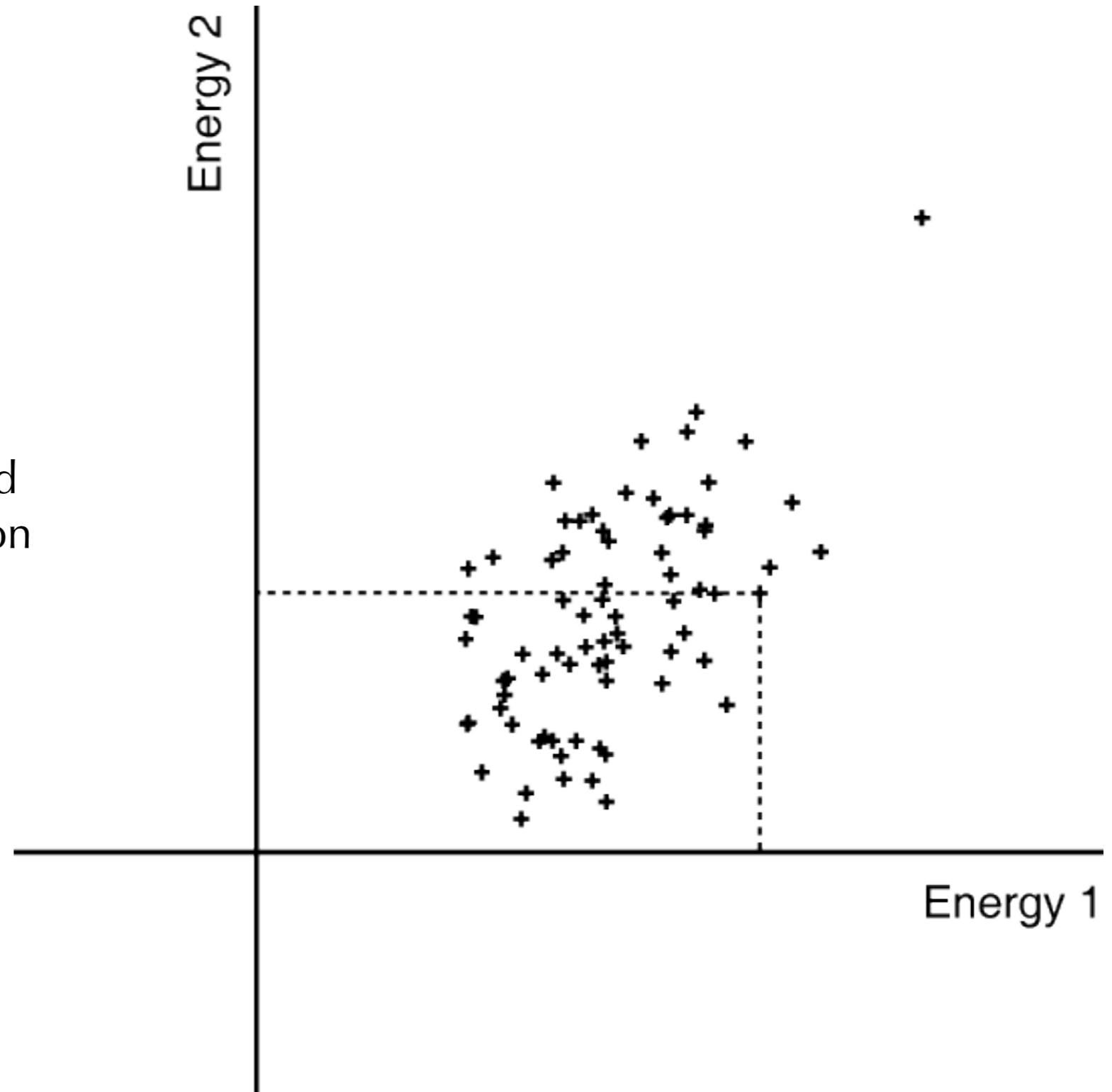
- “Natural” specimens, such as in biology or environmental science
- Reactive phases, rather than simple mixing
- Complexity! 300x300 pixel image contains  $10^5$  spectra!
- Let's reduce the complexity using principal component analysis or PCA

PCA in spectromicroscopy: King *et al.*, *J. Vac. Sci. Tech. A* **7**, 3301 (1989); A. Osanna & C. Jacobsen, XRM99 proceedings; Bonnet *et al.*, *Ultramicroscopy* **77**, 97 (1999).

# Principal component analysis (PCA)

Can we find new orthogonal coordinates that better represent the data?

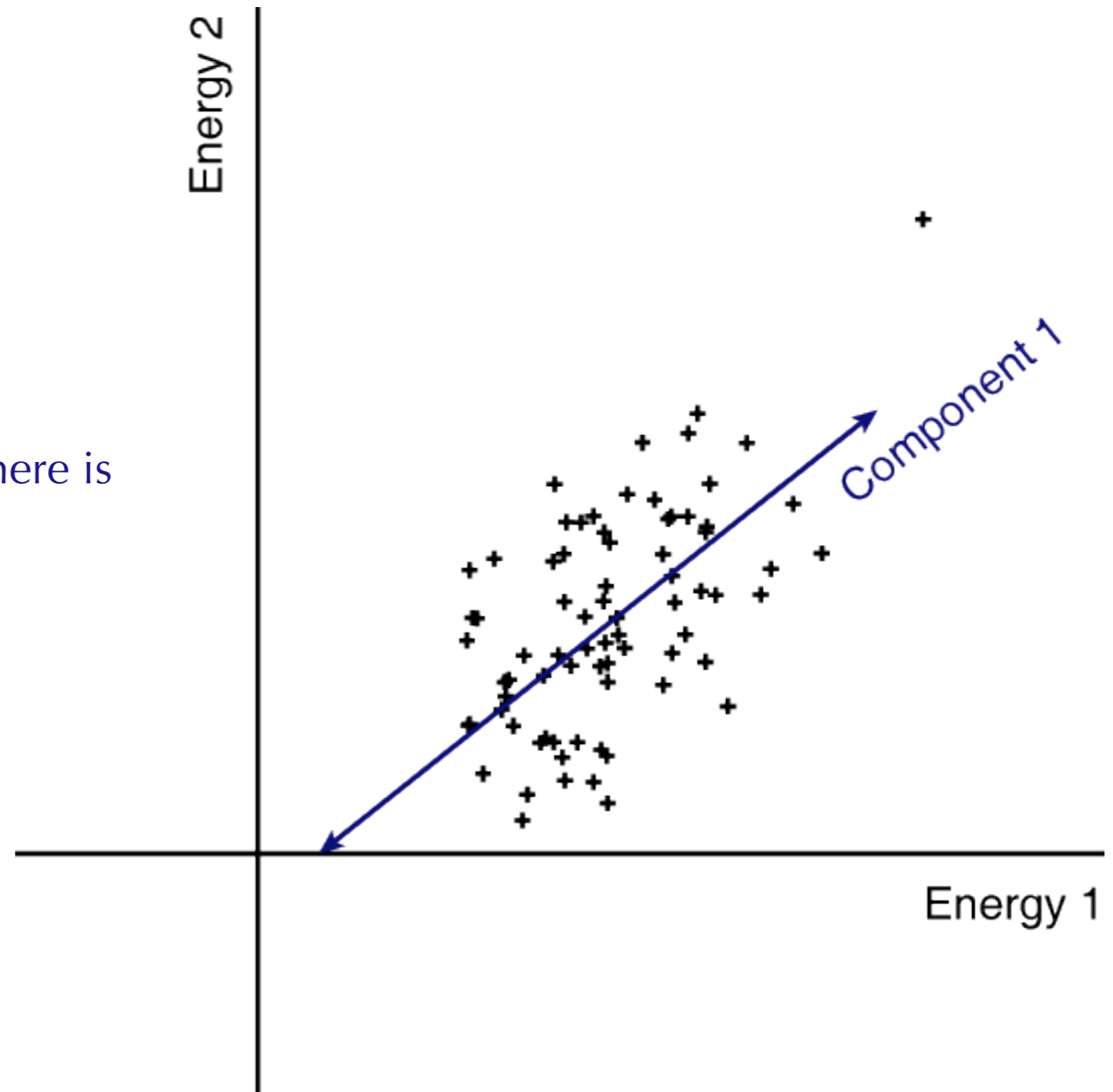
Scatterplot: pixels plotted based on signal at two different photon energies



# Principal component analysis (PCA)

Can we find new orthogonal coordinates that better represent the data?

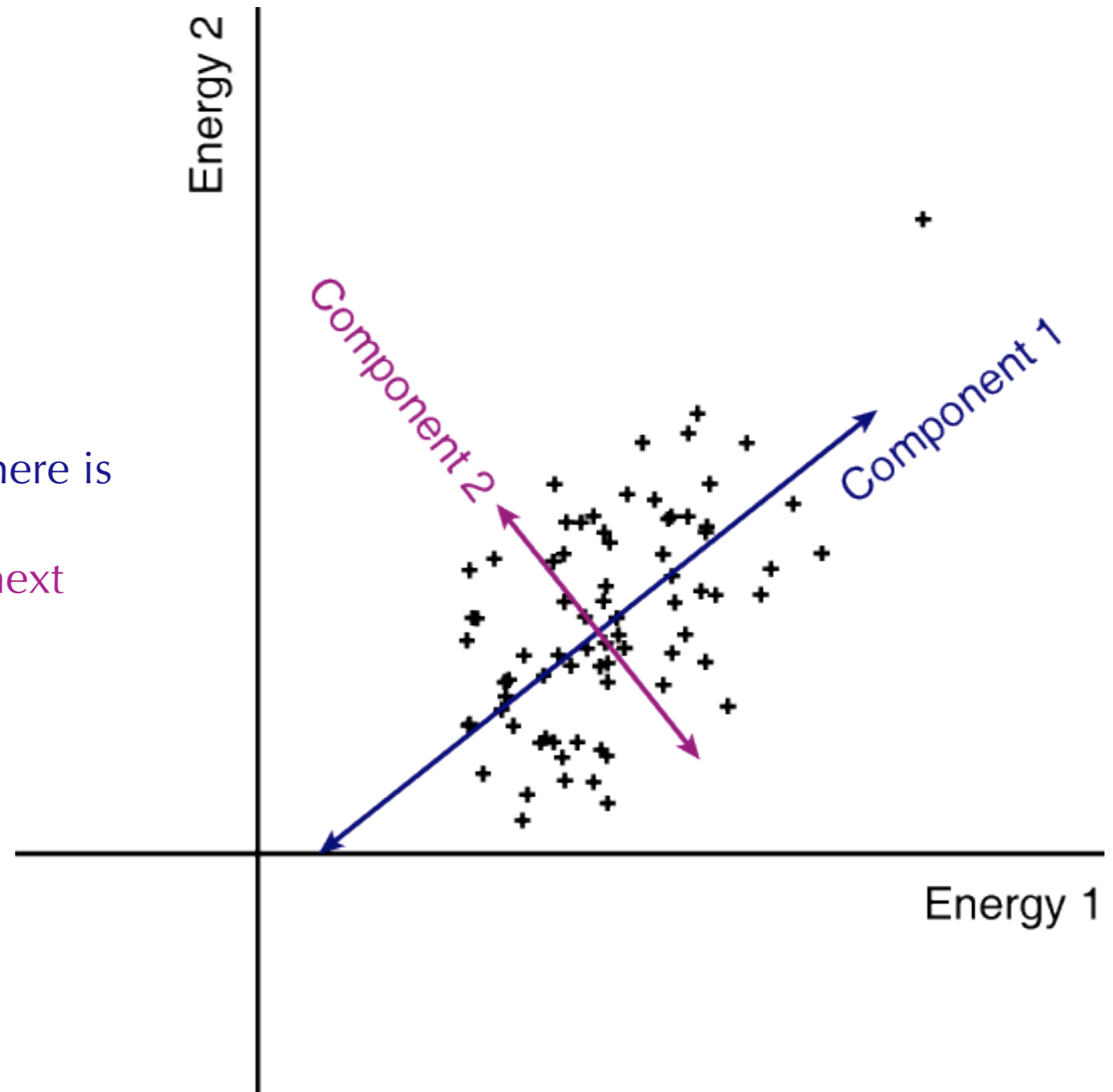
1. Find the axis along which there is the greatest variance



# Principal component analysis (PCA)

Can we find new orthogonal coordinates that better represent the data?

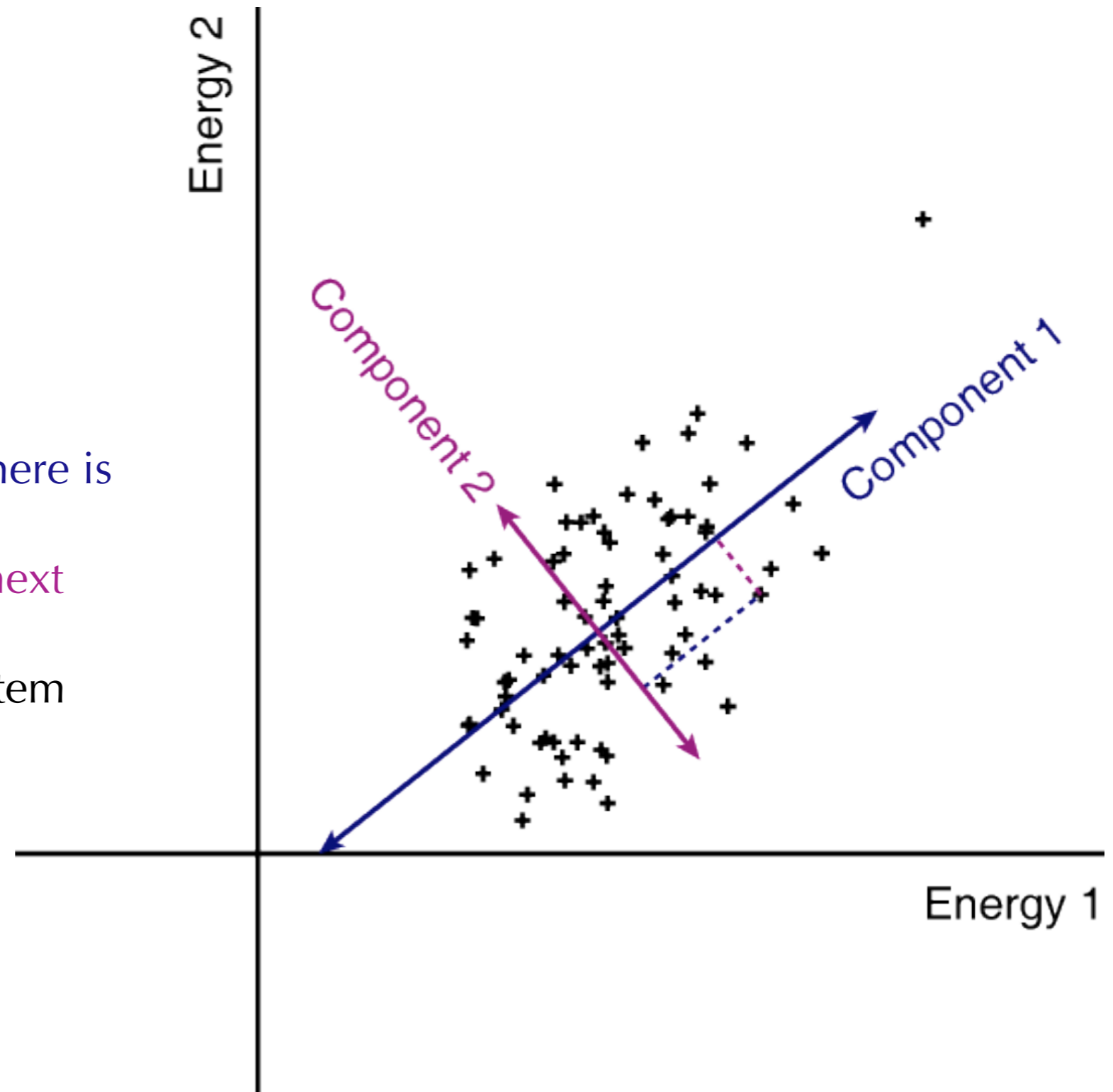
1. Find the axis along which there is the greatest variance
2. Find an orthogonal axis of next greatest variance



# Principal component analysis (PCA)

Can we find new orthogonal coordinates that better represent the data?

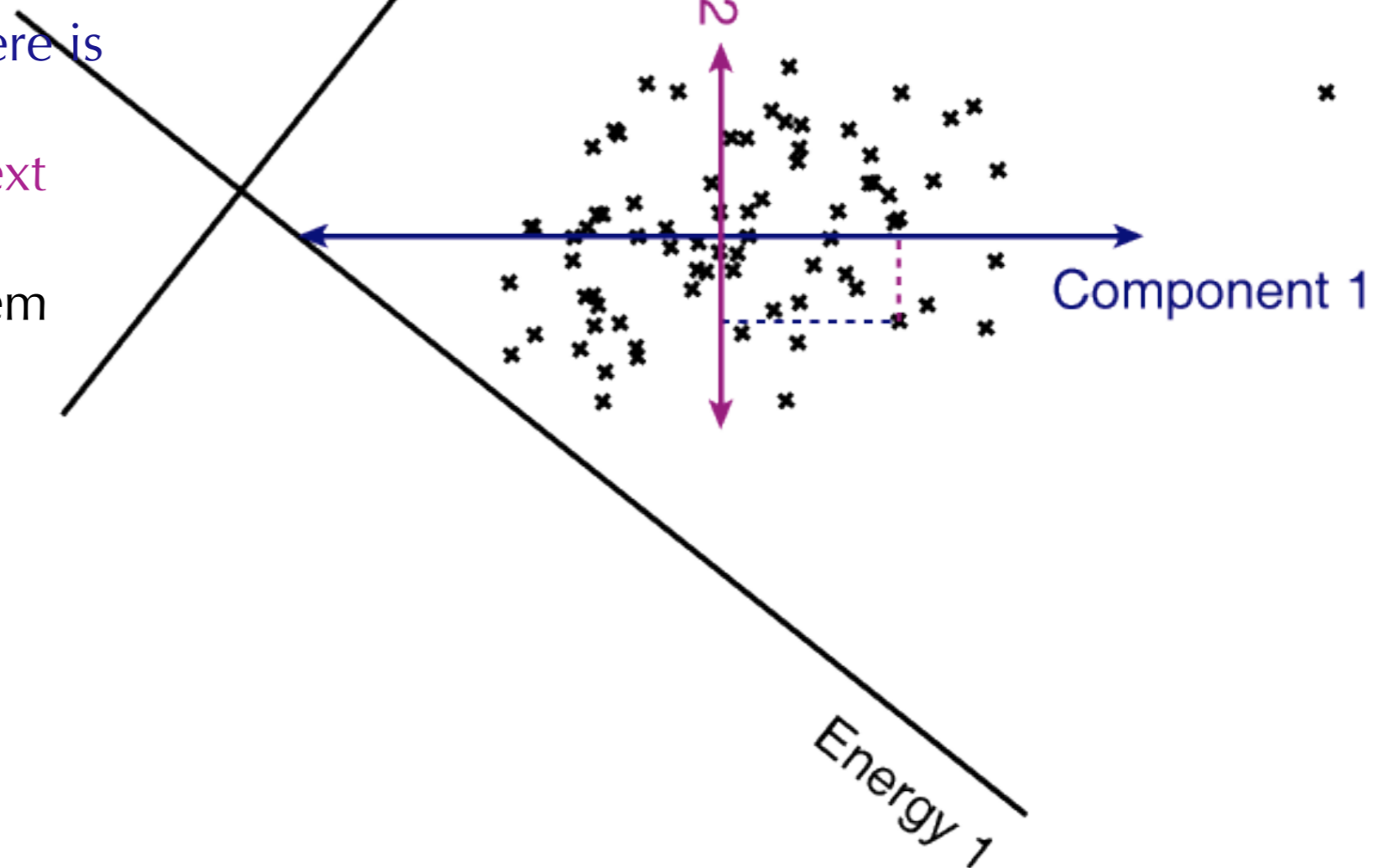
1. Find the axis along which there is the greatest variance
2. Find an orthogonal axis of next greatest variance
3. Gives a new coordinate system



# Principal component analysis (PCA)

Can we find new orthogonal coordinates that better represent the data?

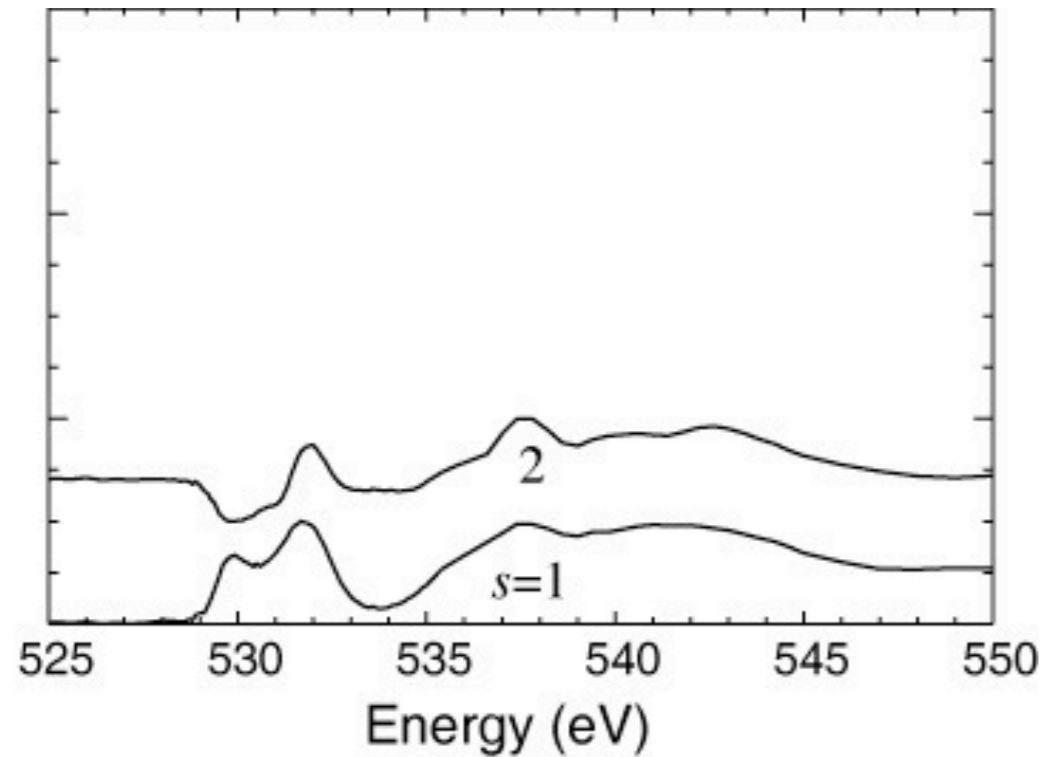
1. Find the axis along which there is the greatest variance
2. Find an orthogonal axis of next greatest variance
3. Gives a new coordinate system
4. Rotate onto new, orthogonal coordinate system



# PCA and factor compression

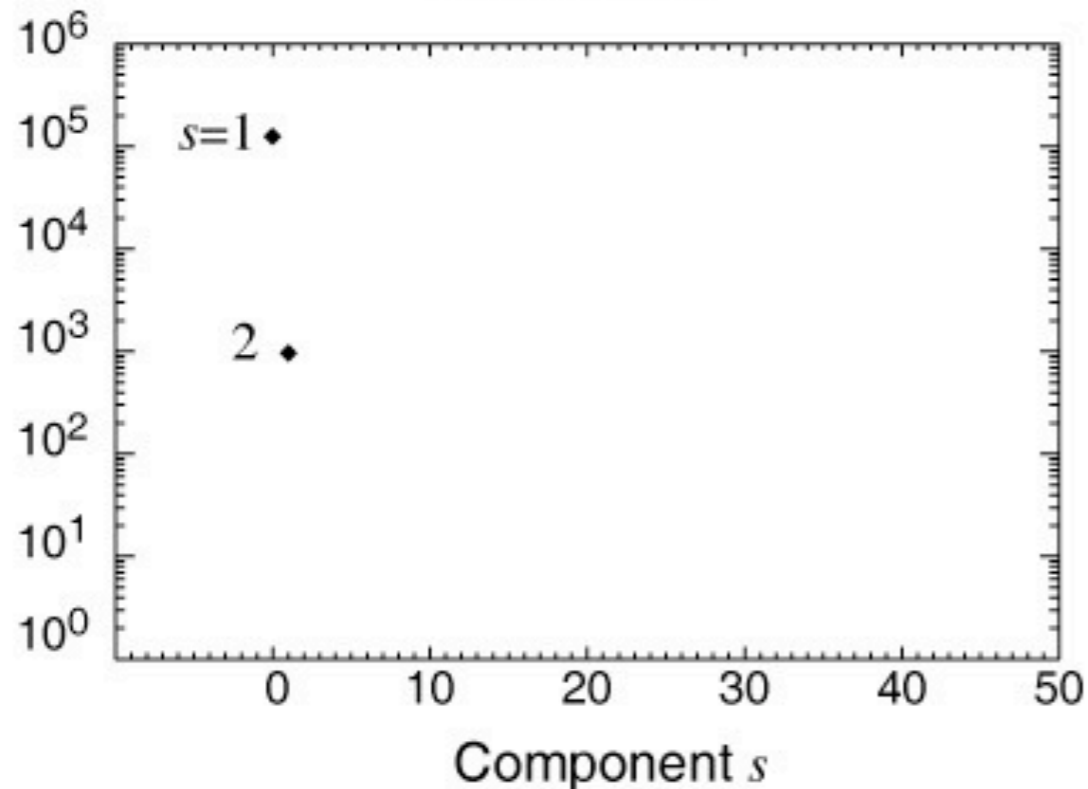
For an abstract component: contribution is singular value times singular spectrum

A) Eigenspectra

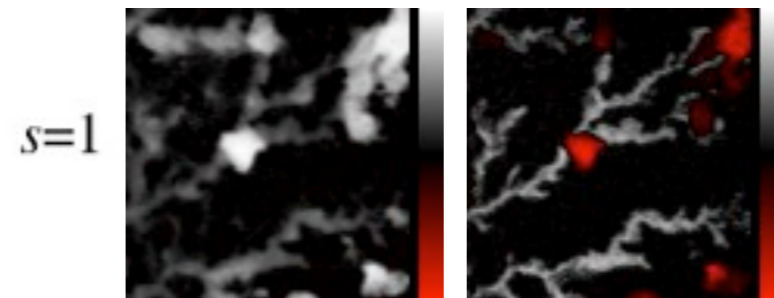


Find reduced number of **significant** components  $\bar{S}_{abstract}$

B) Eigenvalues  $\lambda(s)$



C) Eigenimages

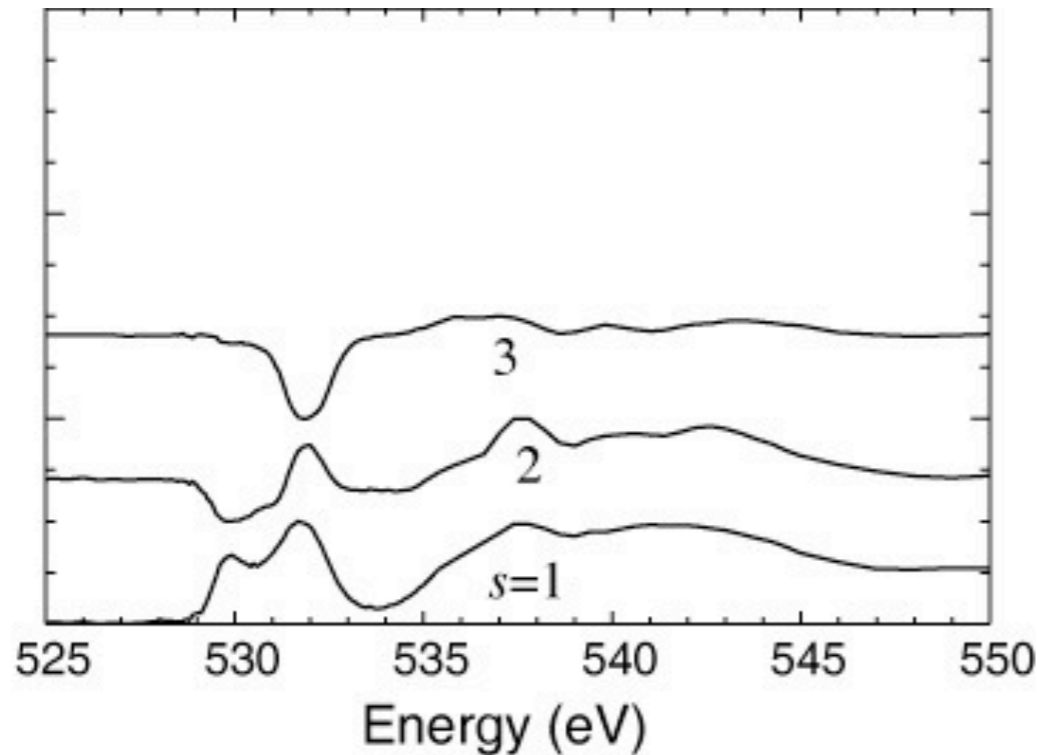




# PCA and factor compression

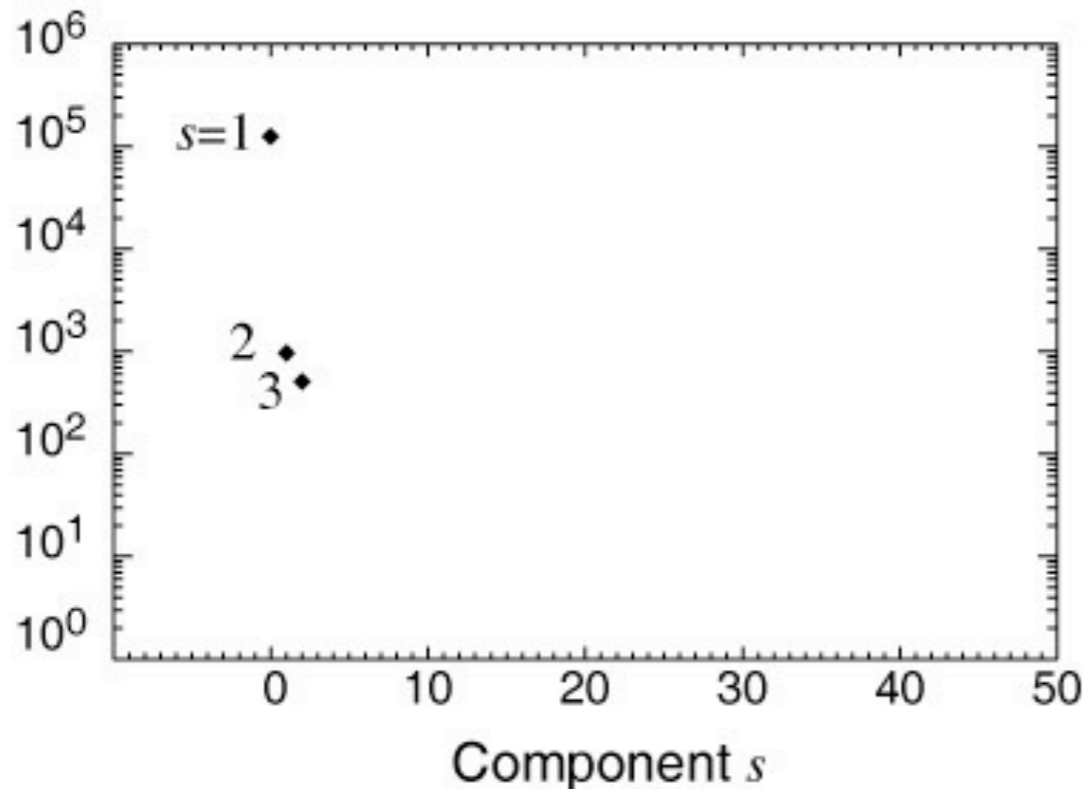
For an abstract component: contribution is singular value times singular spectrum

A) Eigenspectra

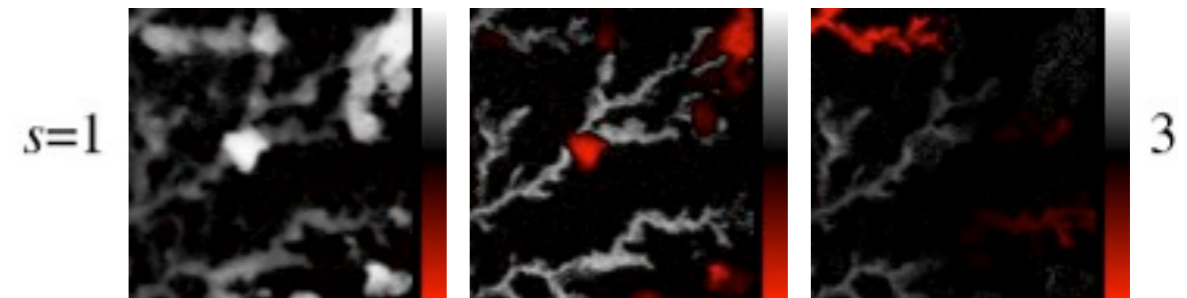


Find reduced number of **significant** components  $\bar{S}_{abstract}$

B) Eigenvalues  $\lambda(s)$



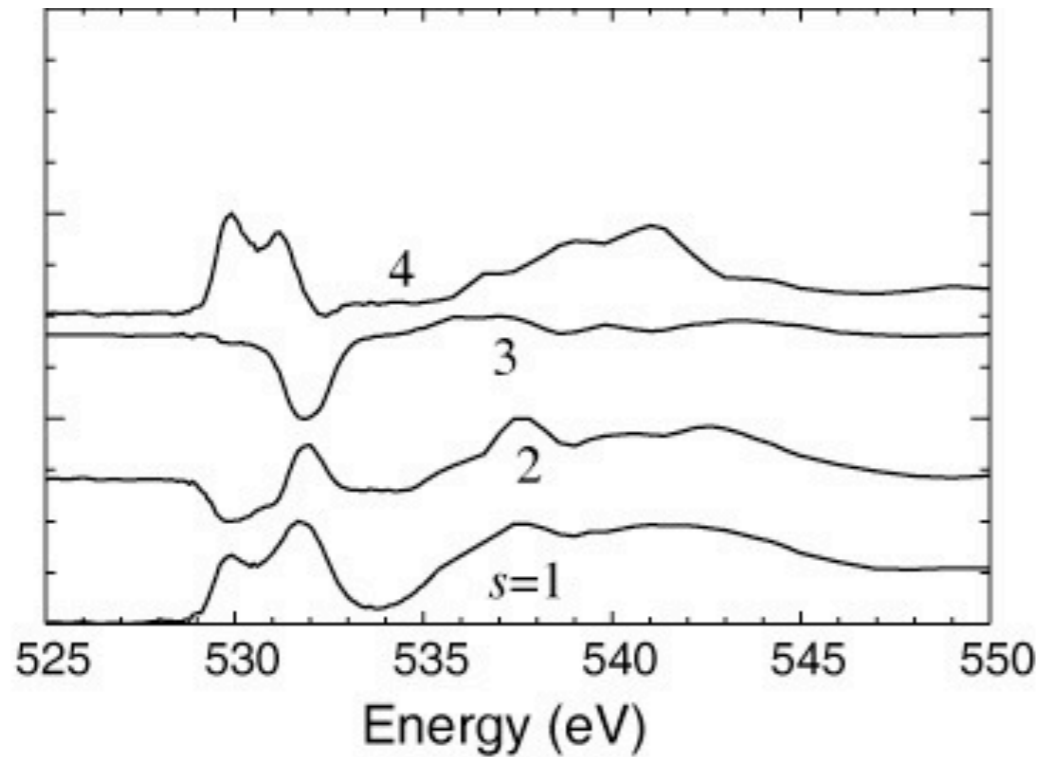
C) Eigenimages



# PCA and factor compression

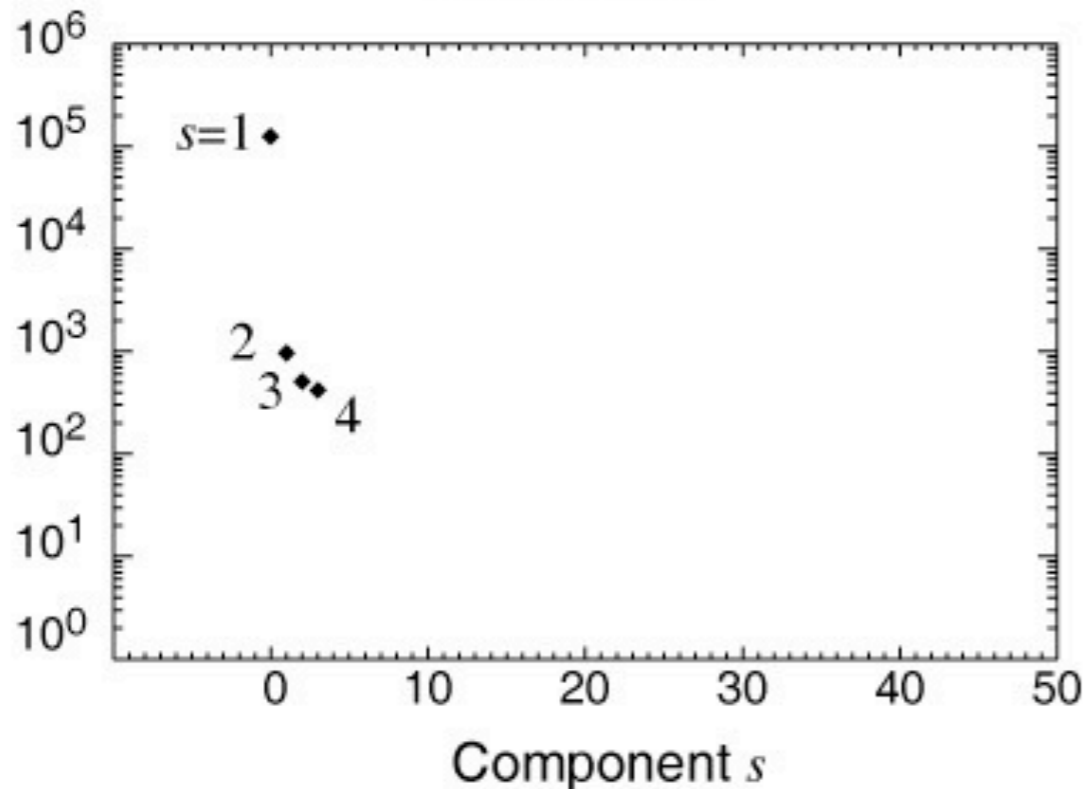
For an abstract component: contribution is singular value times singular spectrum

A) Eigenspectra

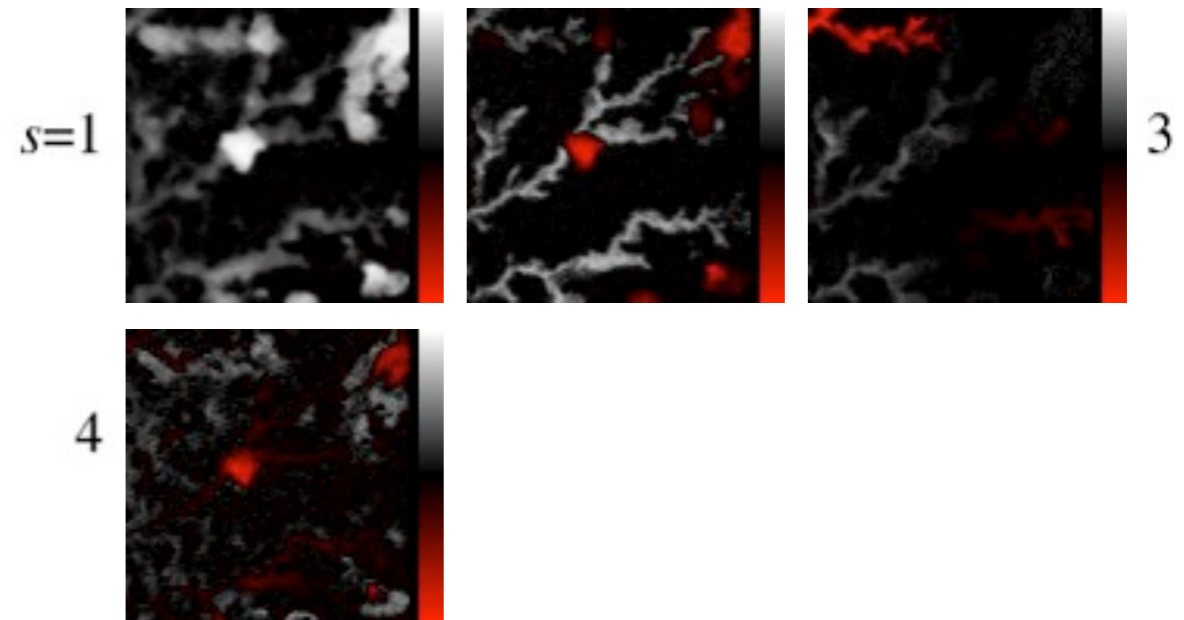


Find reduced number of **significant** components  $\bar{S}_{abstract}$

B) Eigenvalues  $\lambda(s)$



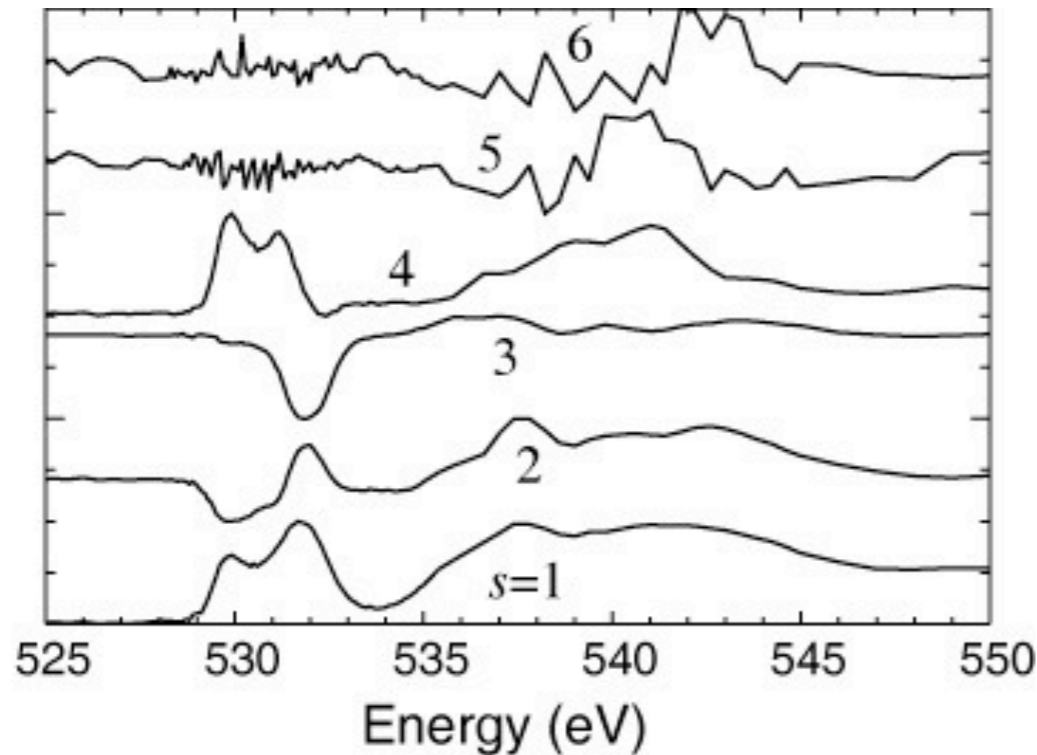
C) Eigenimages



# PCA and factor compression

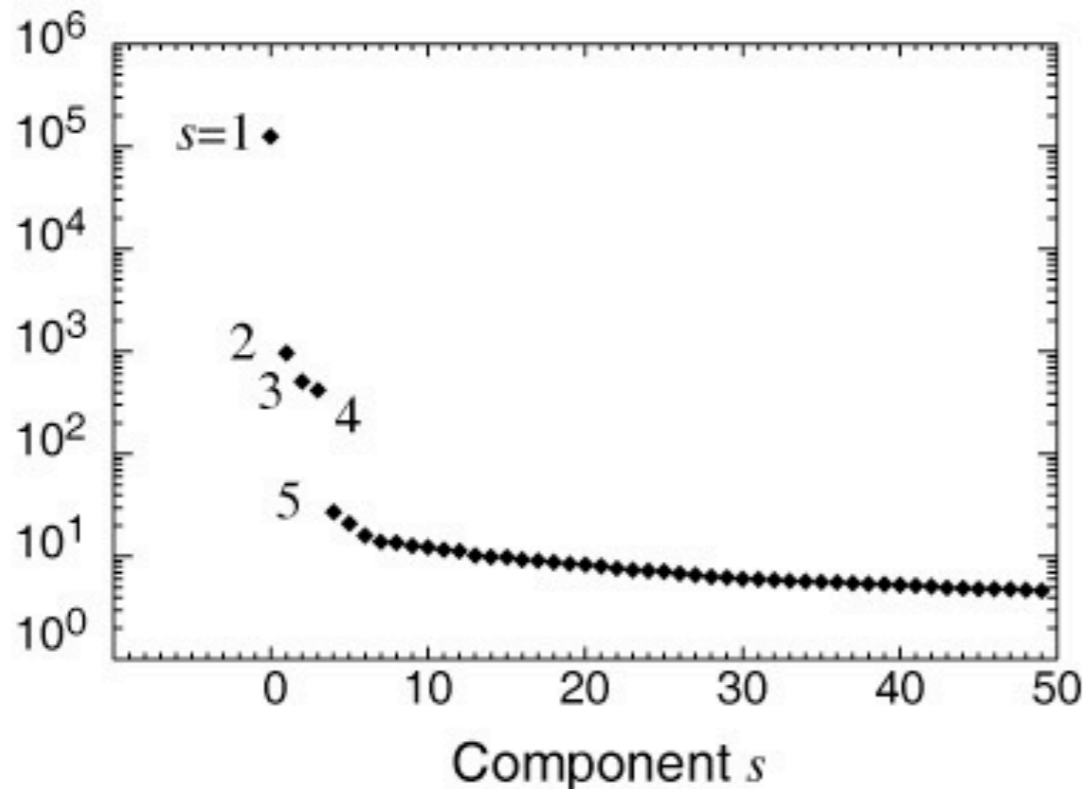
For an abstract component: contribution is singular value times singular spectrum

A) Eigenspectra

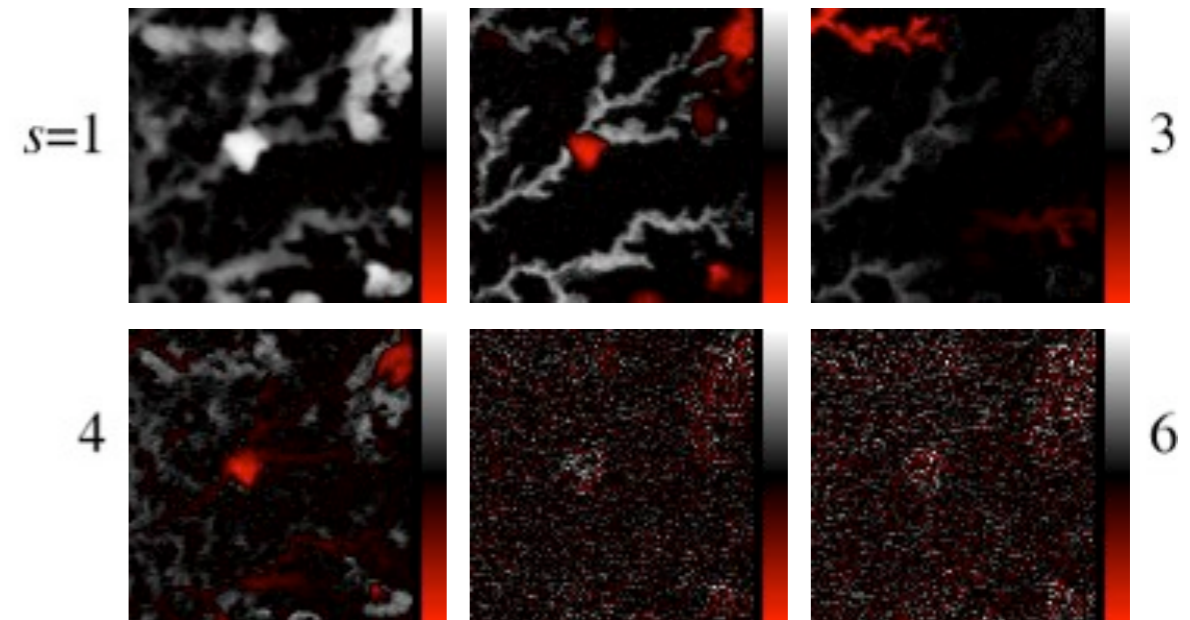


Find reduced number of **significant** components  $\bar{S}_{abstract}$

B) Eigenvalues  $\lambda(s)$

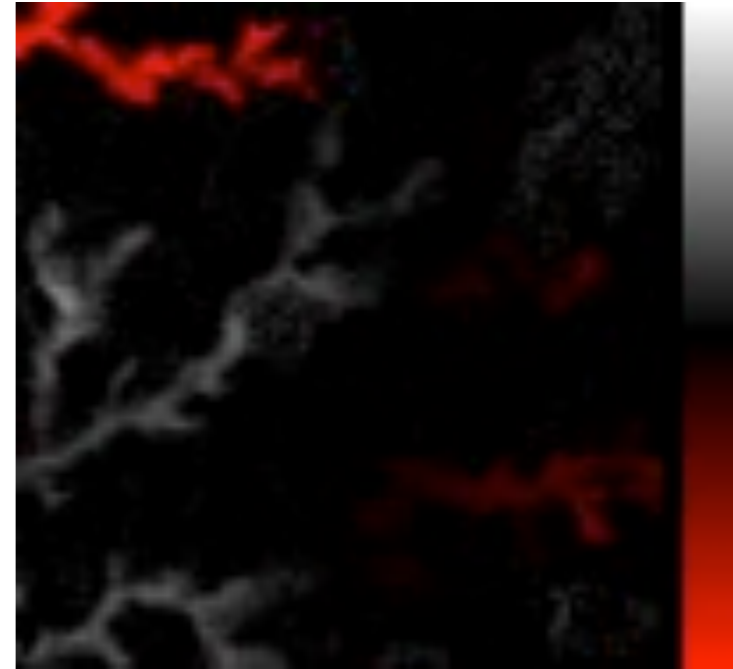
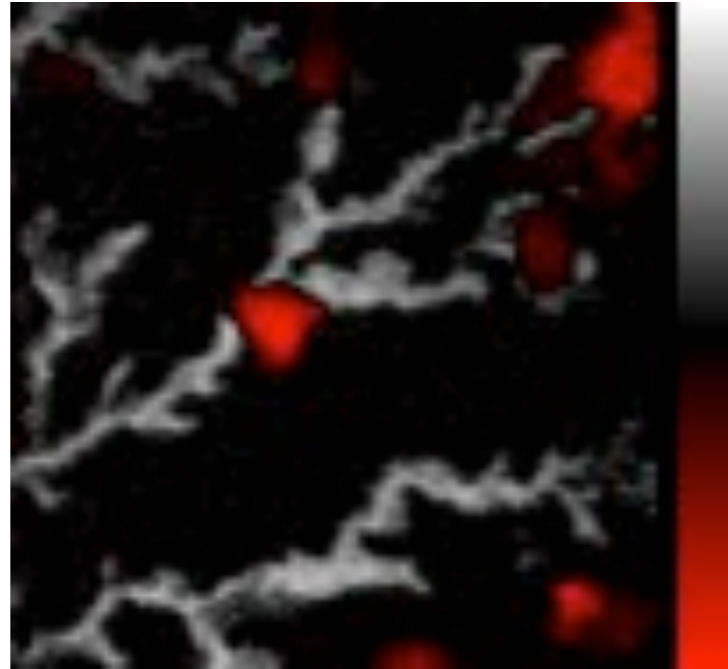
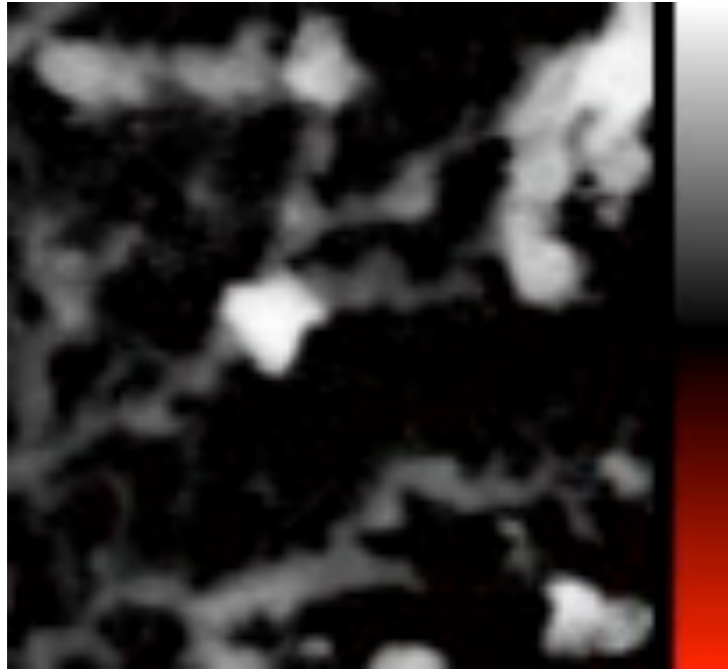


C) Eigenimages



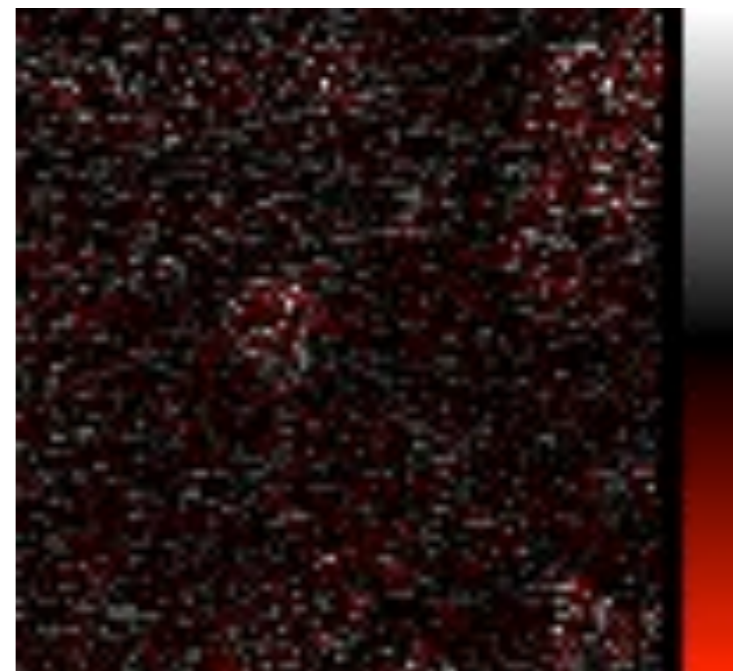
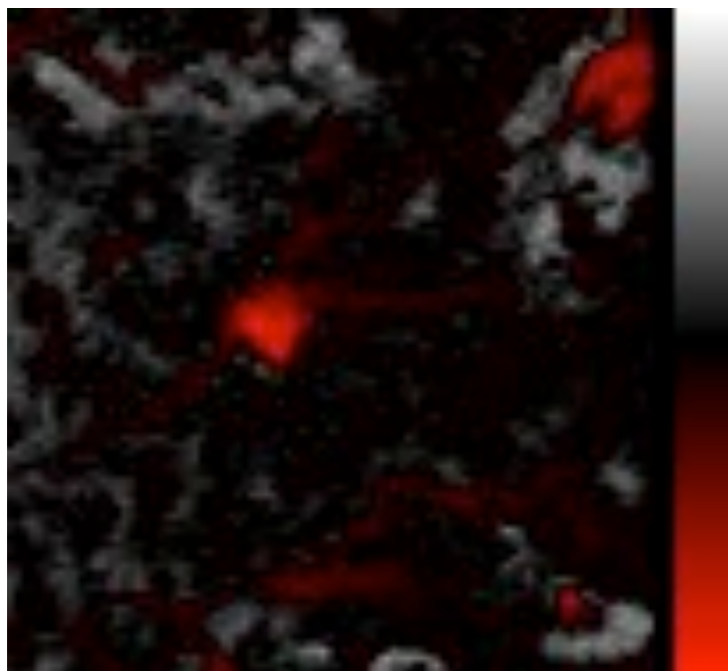
# Eigenimages

1



3

4



6

# PCA gets us *something*...

- Principal component analysis lets you **reduce** and **orthogonalize** the data set!
- **Reduction**: filter out spectral variations that are poorly correlated throughout the dataset (smells like photon noise!). We went from  $N=140$  energies to  $\bar{S}_{\text{abstract}}=4$  components
- **Orthogonality** might have nice consequences

But we have a problem...

- Eigenspectra  $> 1$  are abstract. They have negative optical densities, so they are not readily interpretable.
- “Rotating” eigenspectra to make them positive is not always sufficient; can have more distinct mixtures than eigenspectra.

# A well-known problem

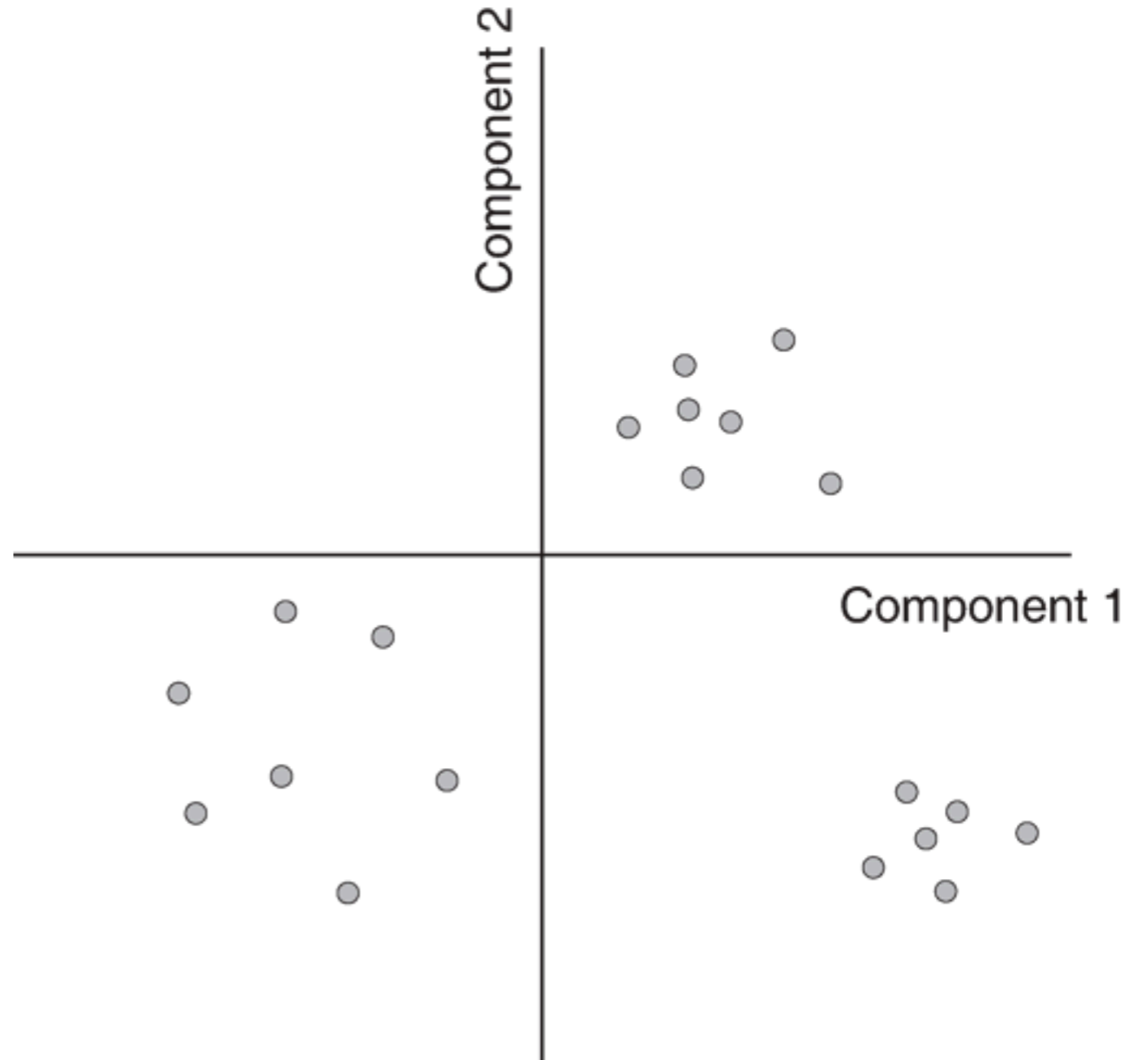
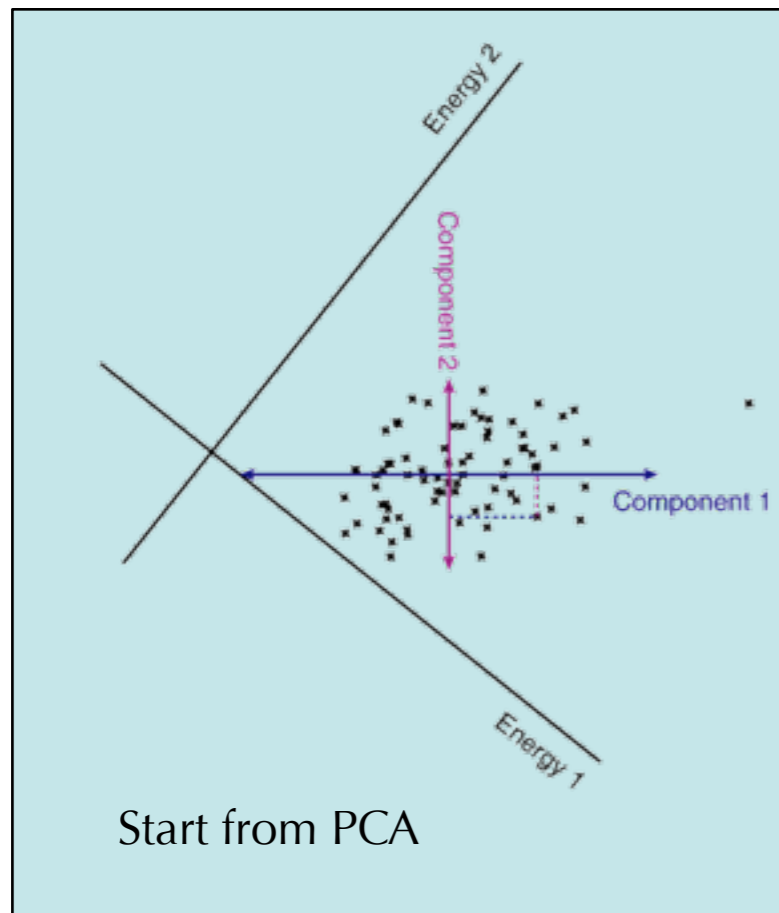
We chose to follow an approach which is well known in the literature:

“You can’t always get what you want; but if you try sometimes, well you just might find you get what you need”

M. Jagger, K. Richards *et al.*, *Let it Bleed* **1**, 1 (1969)

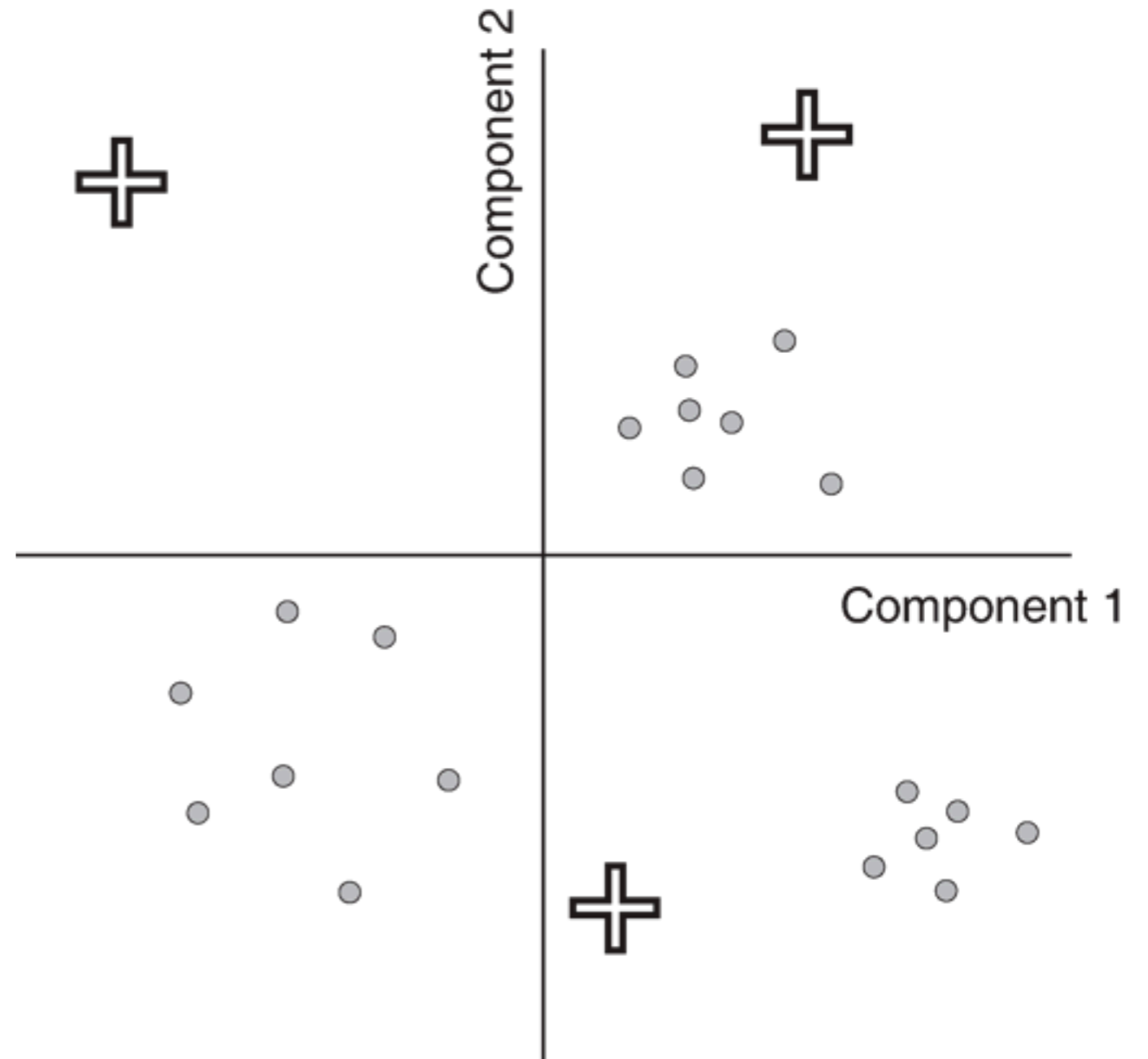
# Cluster analysis: Euclidian distance learning algorithm

- Kohonen, *Proc. IEEE* **78**, 1464 (1990)
- Pixels are scattered according to weighting of each component



# Cluster analysis: Euclidian distance learning algorithm

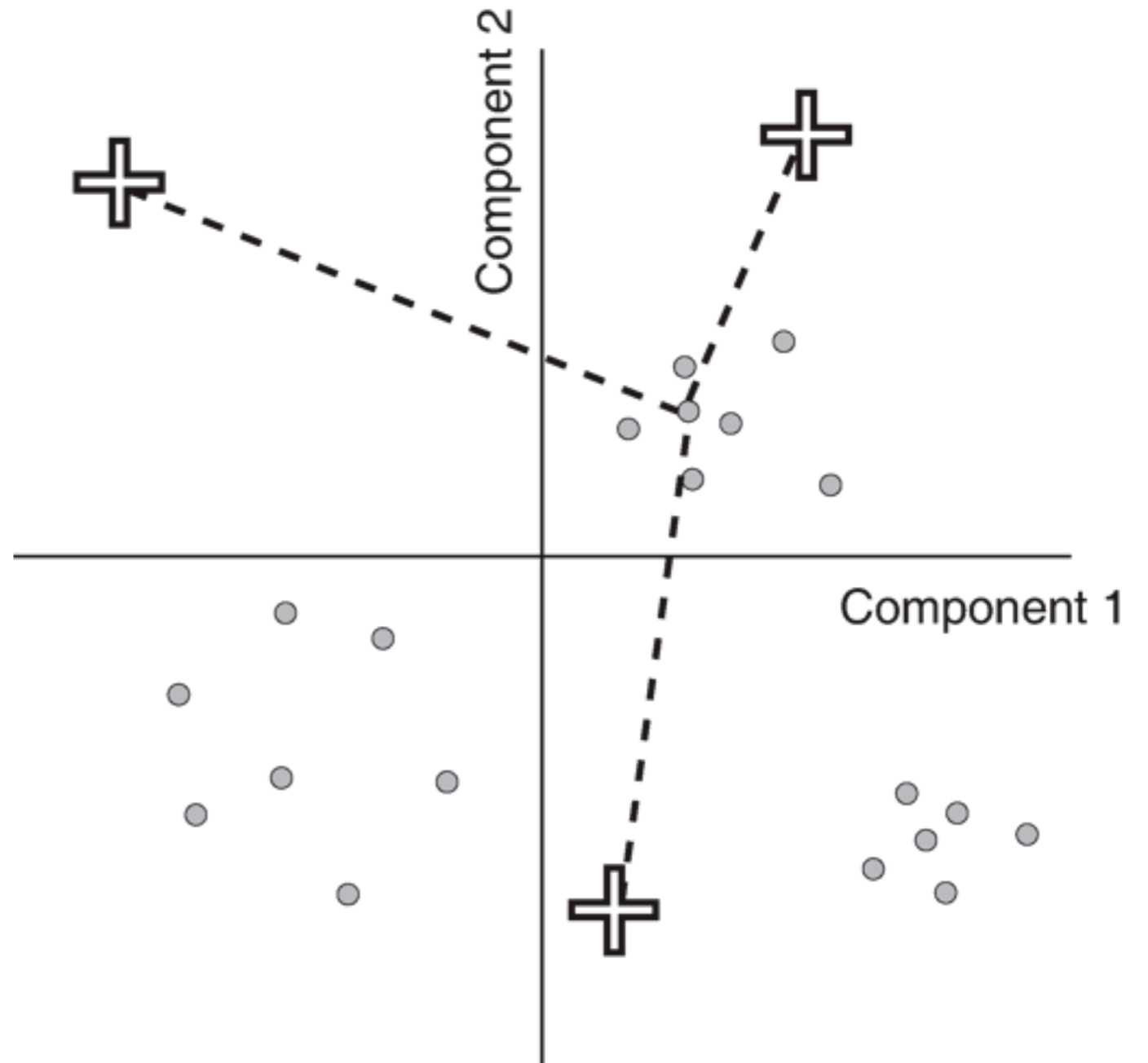
- Kohonen, *Proc. IEEE* **78**, 1464 (1990)
- Pixels are scattered according to weighting of each component
- Put down cluster centers at random positions.





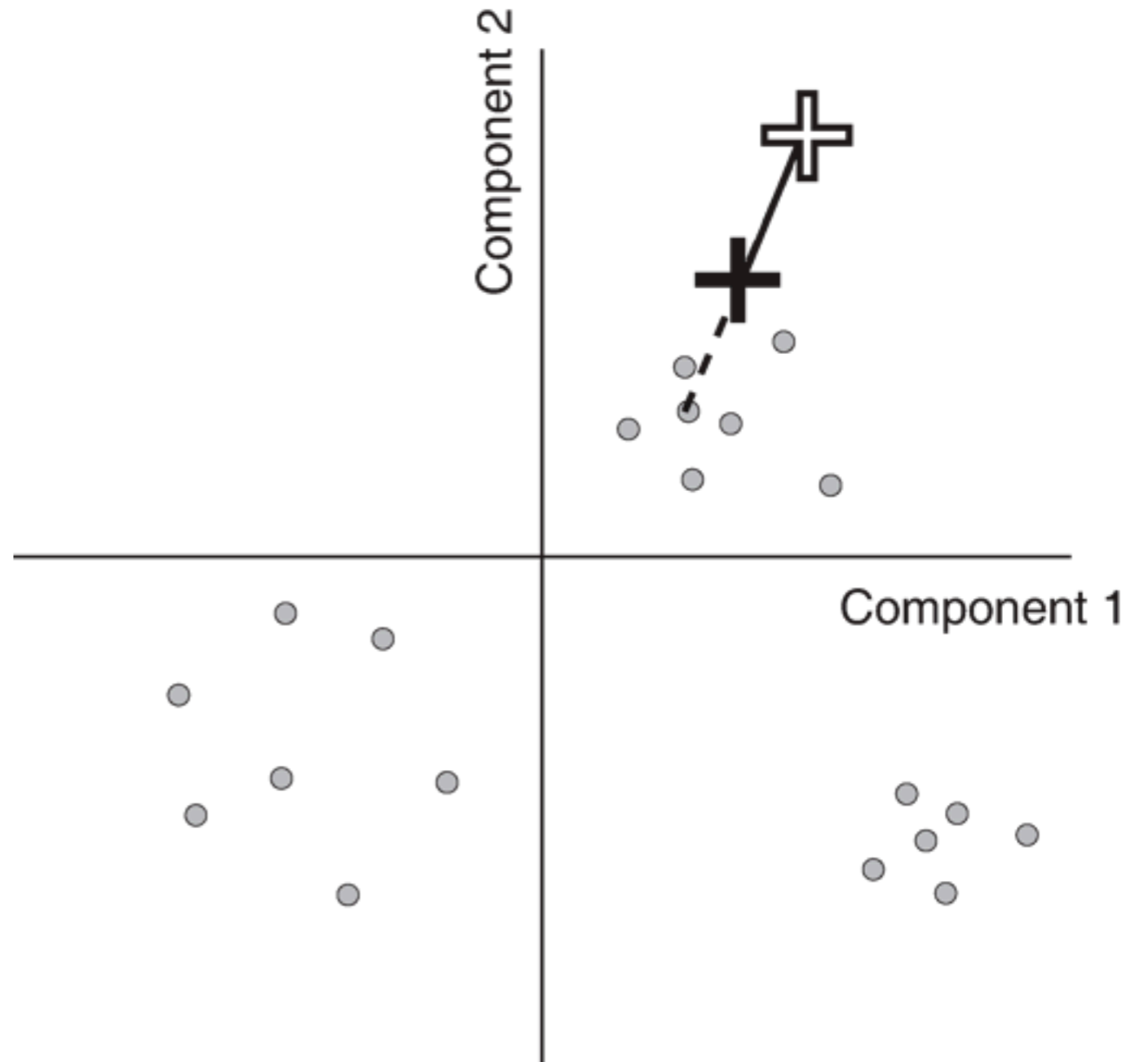
# Cluster analysis: Euclidian distance learning algorithm

- Kohonen, *Proc. IEEE* **78**, 1464 (1990)
- Pixels are scattered according to weighting of each component
- Put down cluster centers at random positions.
- Iterate through all pixels, several times:
  - Calculate distances from one pixel to all cluster centers.



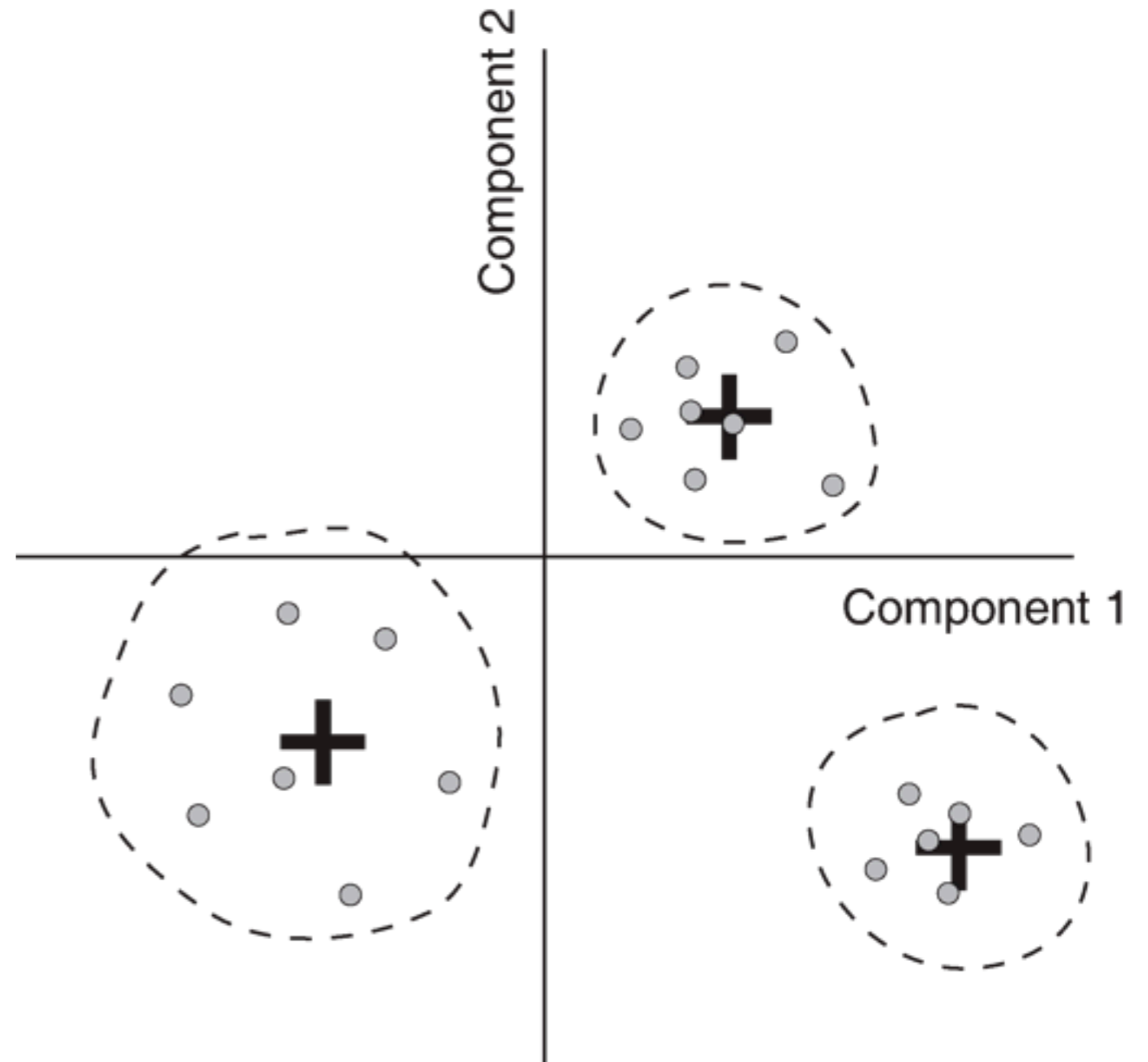
# Cluster analysis: Euclidian distance learning algorithm

- Kohonen, *Proc. IEEE* **78**, 1464 (1990)
- Pixels are scattered according to weighting of each component
- Put down cluster centers at random positions.
- Iterate through all pixels, several times:
  - Calculate distances from one pixel to all cluster centers.
  - Pick shortest distance.
  - Move cluster center partway to pixel.



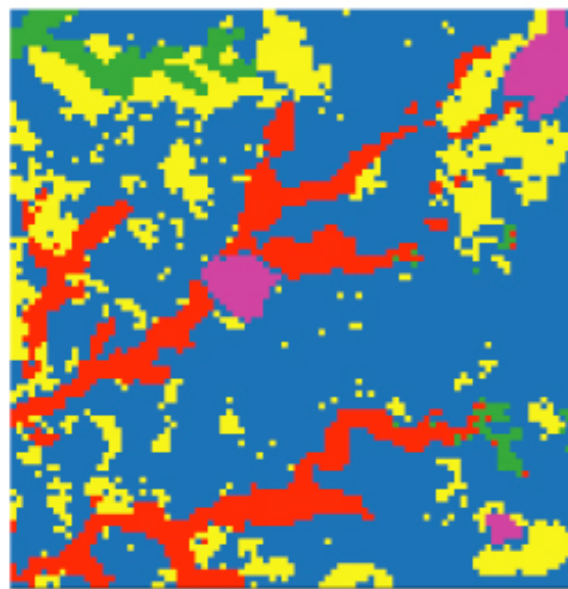
# Cluster analysis: Euclidian distance learning algorithm

- Kohonen, *Proc. IEEE* **78**, 1464 (1990)
- Pixels are scattered according to weighting of each component
- Put down cluster centers at random positions.
- Iterate through all pixels, several times:
  - Calculate distances from one pixel to all cluster centers.
  - Pick shortest distance.
  - Move cluster center partway to pixel.
- Cluster pixels with their nearest cluster center

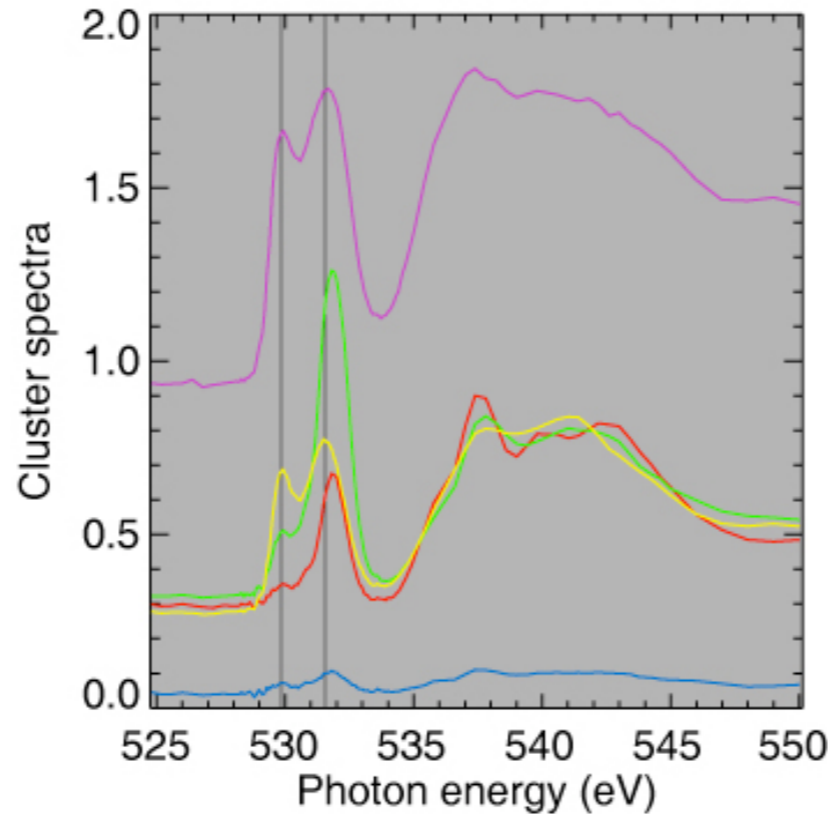


# Cluster analysis: Lu in hæmatite

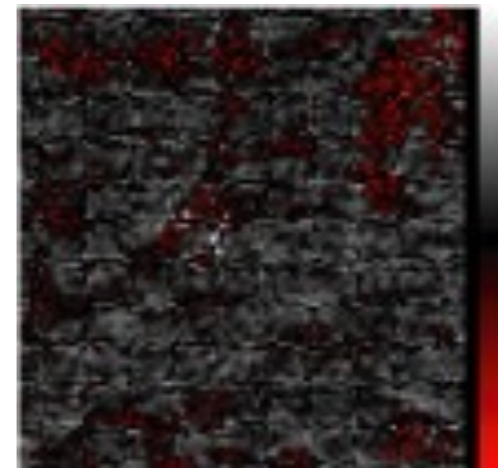
A) Cluster indices



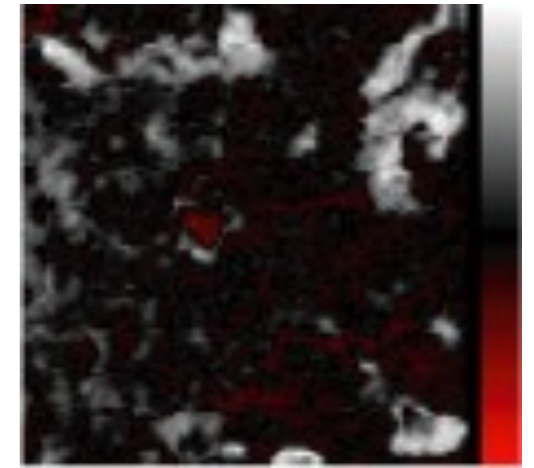
2  $\mu\text{m}$



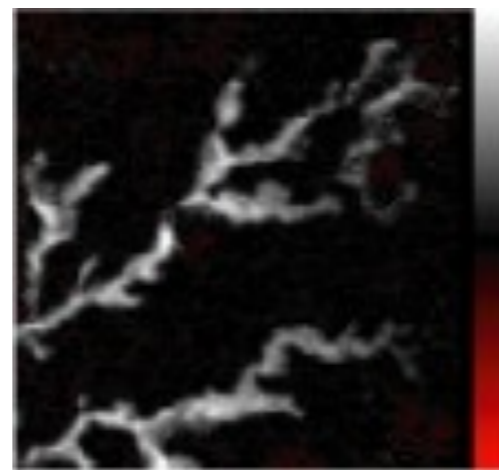
cluster 1



cluster 2



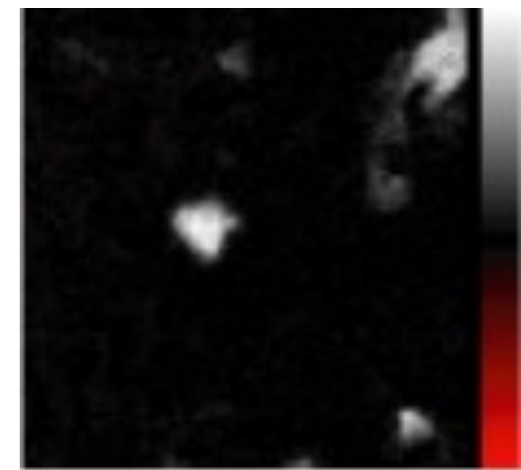
cluster 3



cluster 4



cluster 5

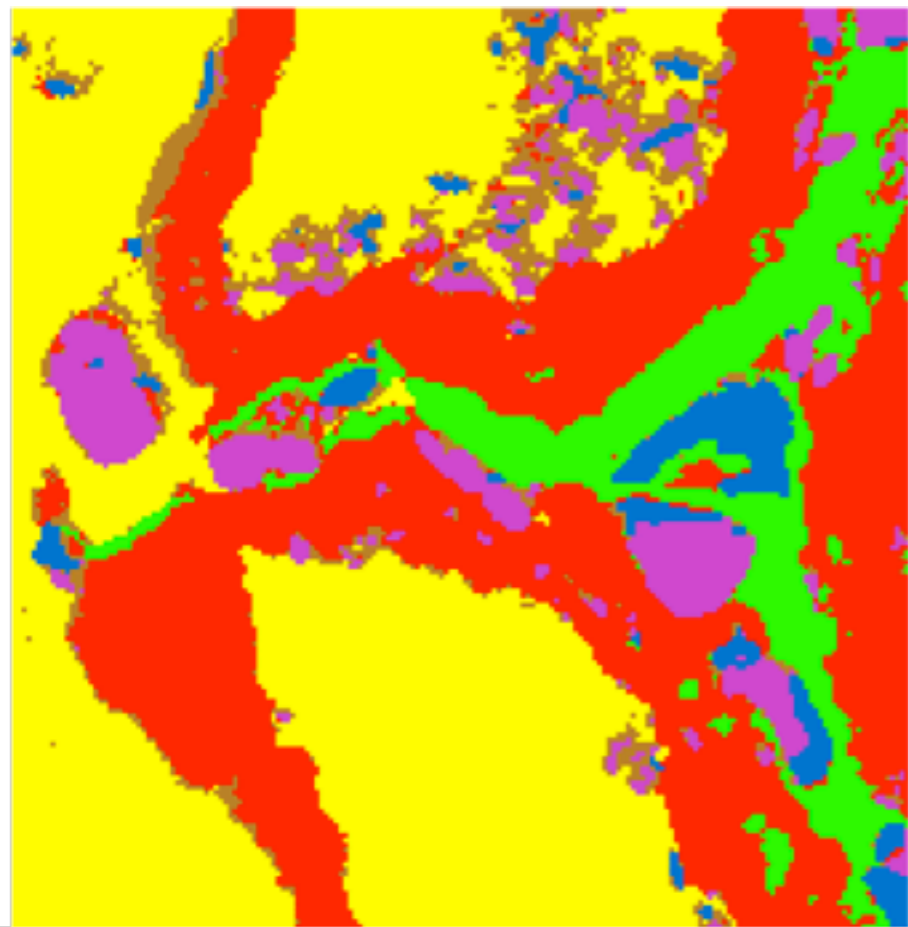


- Lu as a stand-in for Am in nuclear wastes; hæmatite can be a groundwater colloid that increases transport rate 1000x
- Oxygen XANES shows two different incorporation phases of Lu in hæmatite (clusters 2 and 5)
- Lerotic, Jacobsen, Schäfer, Vogt, *Ultramic.* **100**, 35 (2004)

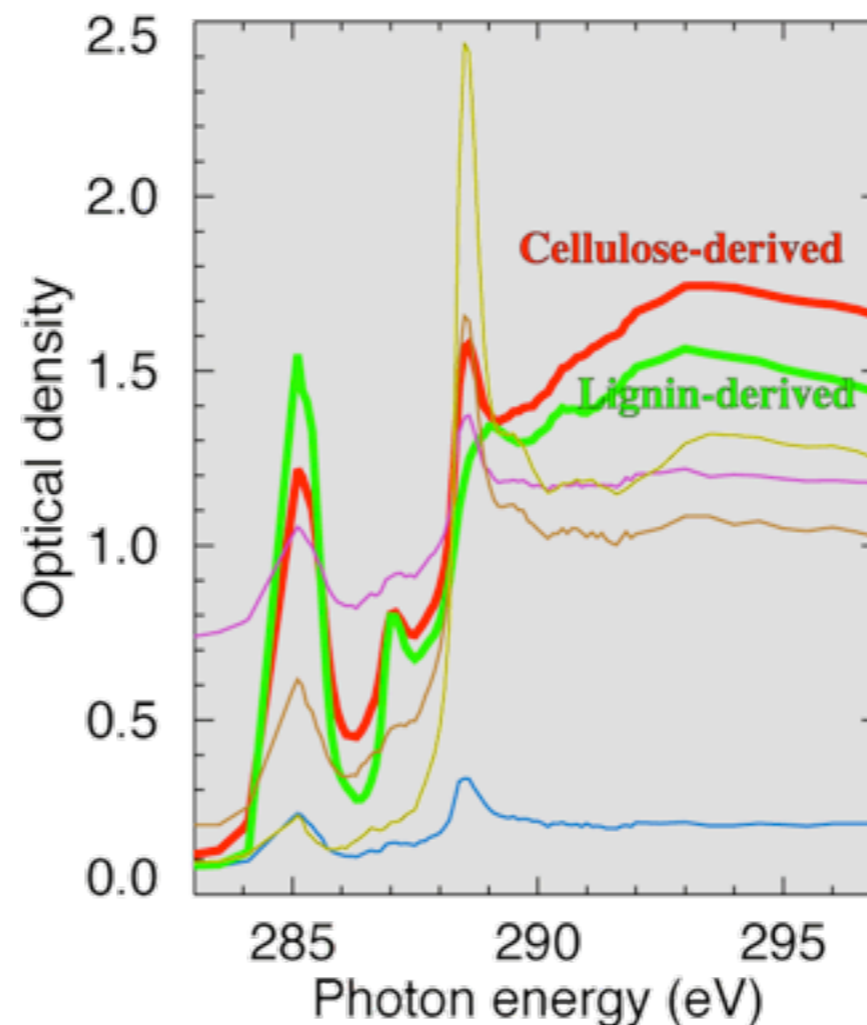
Red spots: negative values, because cluster spectra are not guaranteed to “span the set”

# Cluster analysis: simplifying complexity

- Ethanol from lignocellulose materials is promising: large fraction of total biomass, easier cultivation.
- But there are great challenges in economically separating cellulose from lignin!
- Soft x-ray spectromicroscopy can map cellulose and lignin so that one can see the effects of various enzymes.



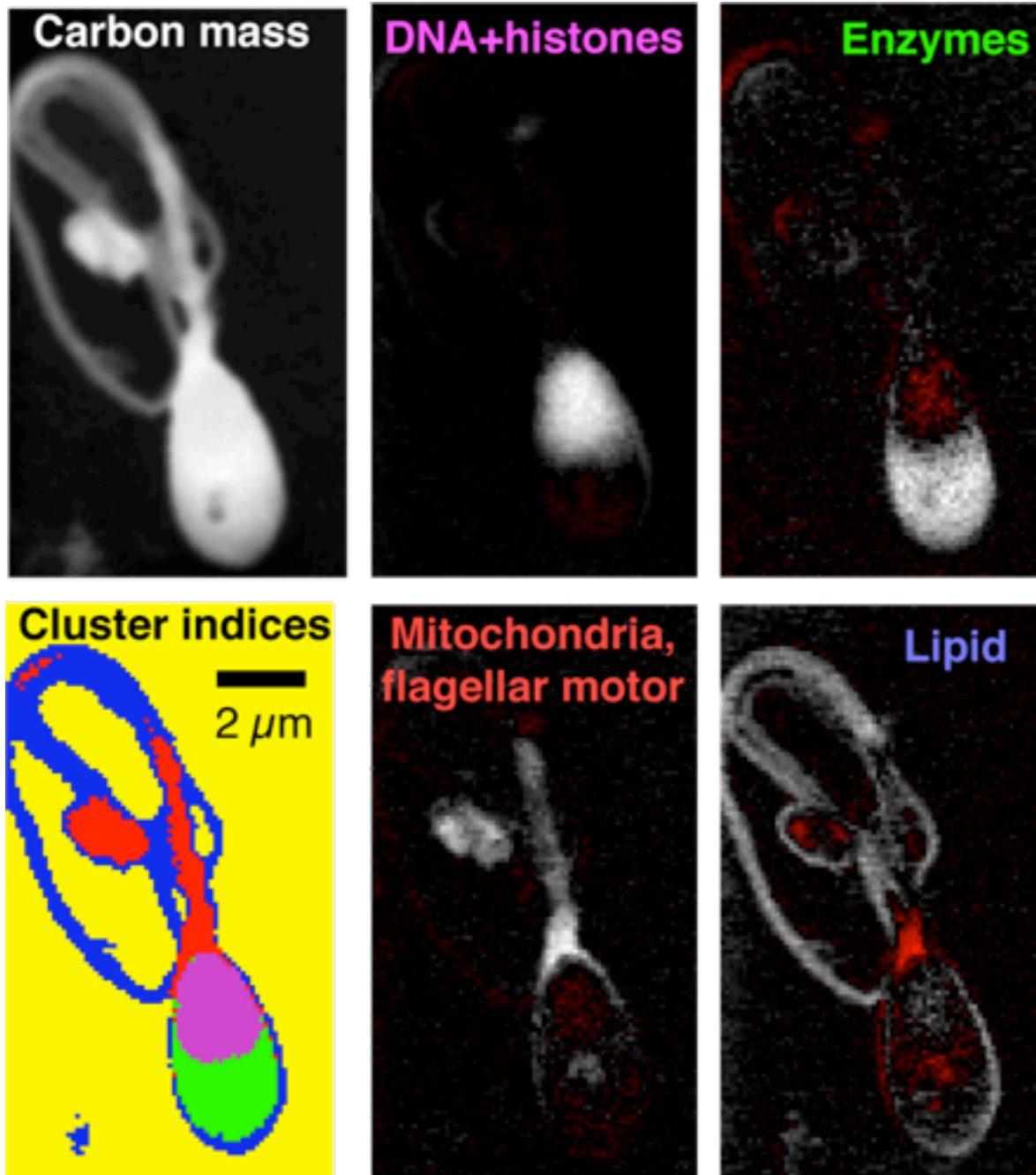
4  $\mu\text{m}$



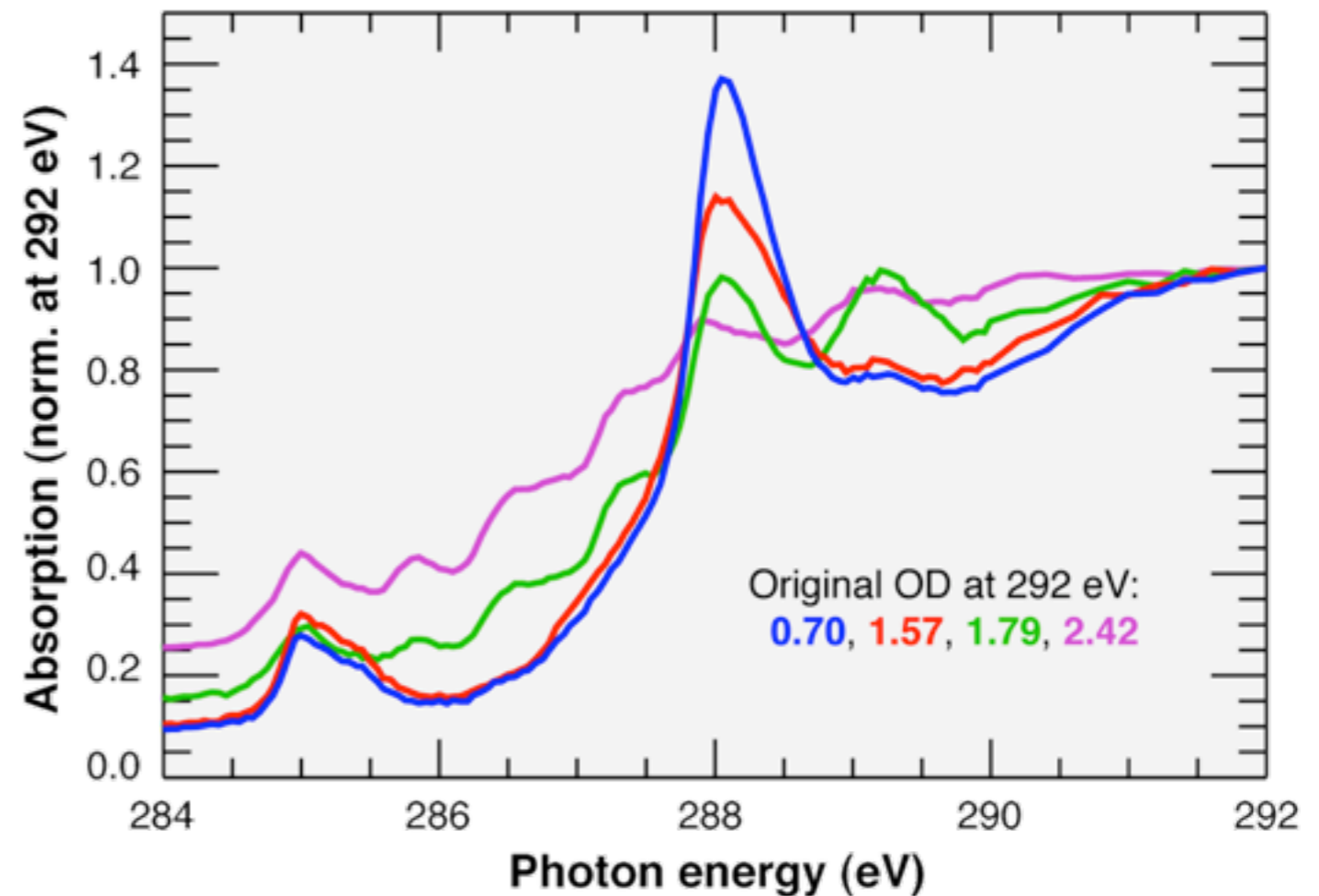
Lignin and cellulose in 400 million year old chert: Boyce *et al.*, *Proc. Nat. Acad. Sci.* **101**, 17555 (2004), with subsequent pattern recognition analysis by Lerotic *et al.*, *Ultramicroscopy* **100**, 35 (2004).

# Cluster analysis: human sperm

Biochemical organization of sperm revealed directly from data: enzyme-rich region, DNA+histones, mitochondria and flagellar motor, lipid



H. Fleckenstein, M. Lerotic, Y. Sheynkin *et al.*, Stony Brook. Human sperm, air-dried.

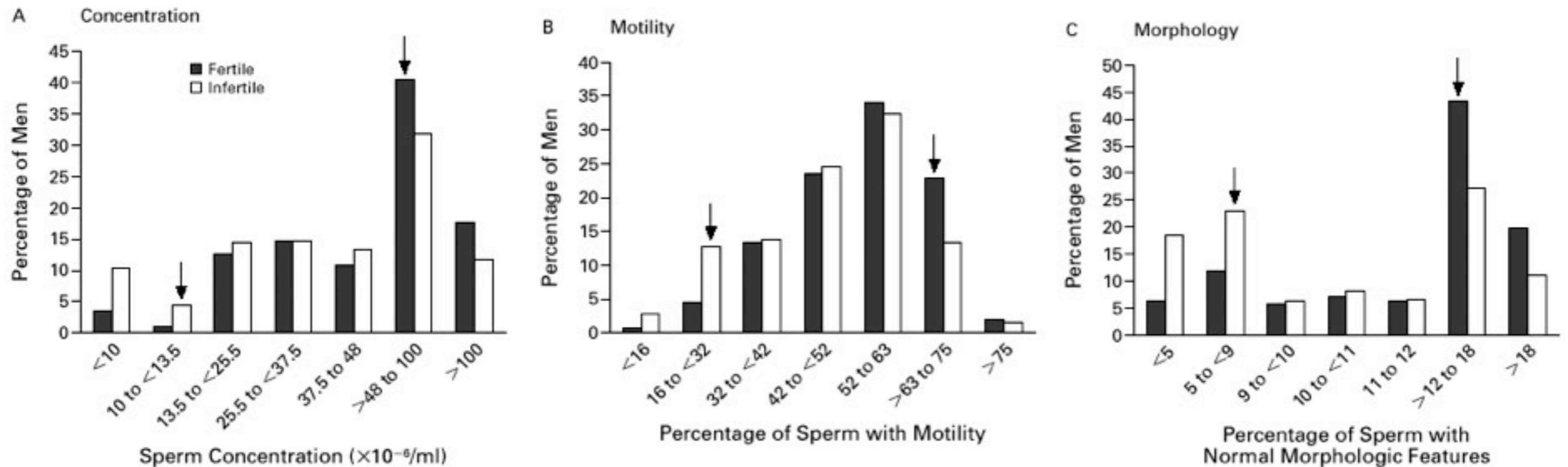


Red spots: negative values, because cluster spectra are not guaranteed to “span the set”

# “Sperm morphology, motility, and concentration in fertile and infertile men”

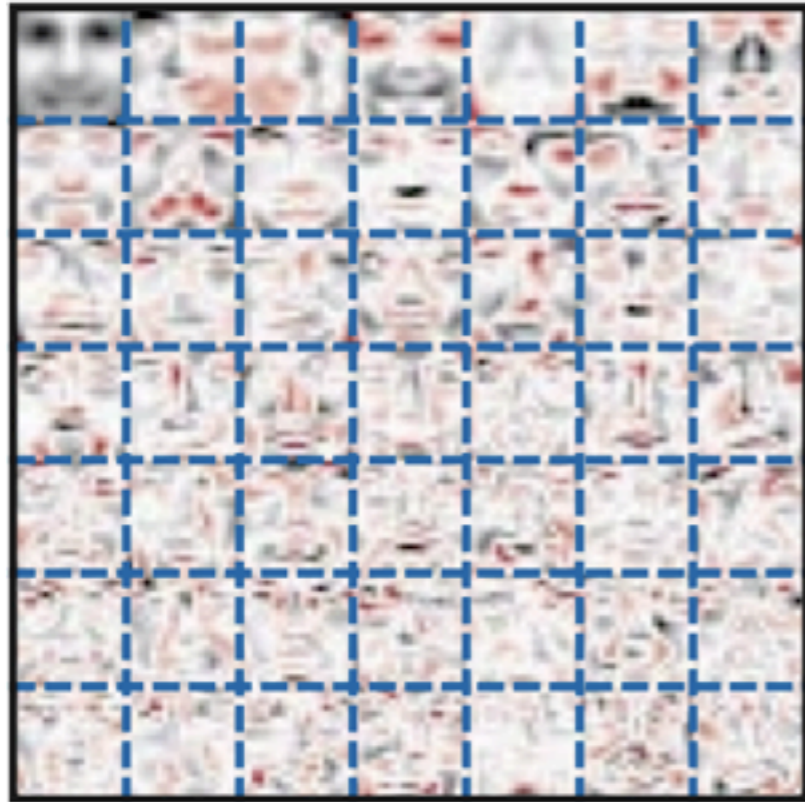
Guzick *et al.*, *New England Journal of Medicine* **345**, 1388 (2001)

“Although semen analysis is routinely used to evaluate the male partner in infertile couples, sperm measurements that discriminate between fertile and infertile men are not well defined... Threshold values for sperm concentration, motility, and morphology can be used to classify men as subfertile, of indeterminate fertility, or fertile. None of the measures, however, are diagnostic of infertility.”

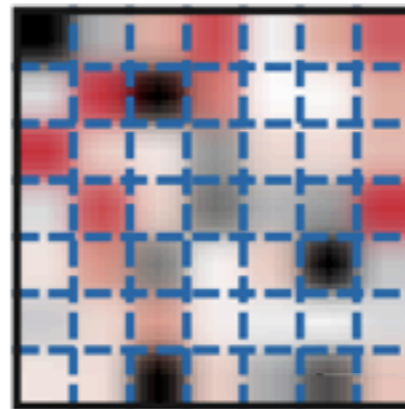


# Avoiding negativity: non-negative matrix factorization

PCA



x



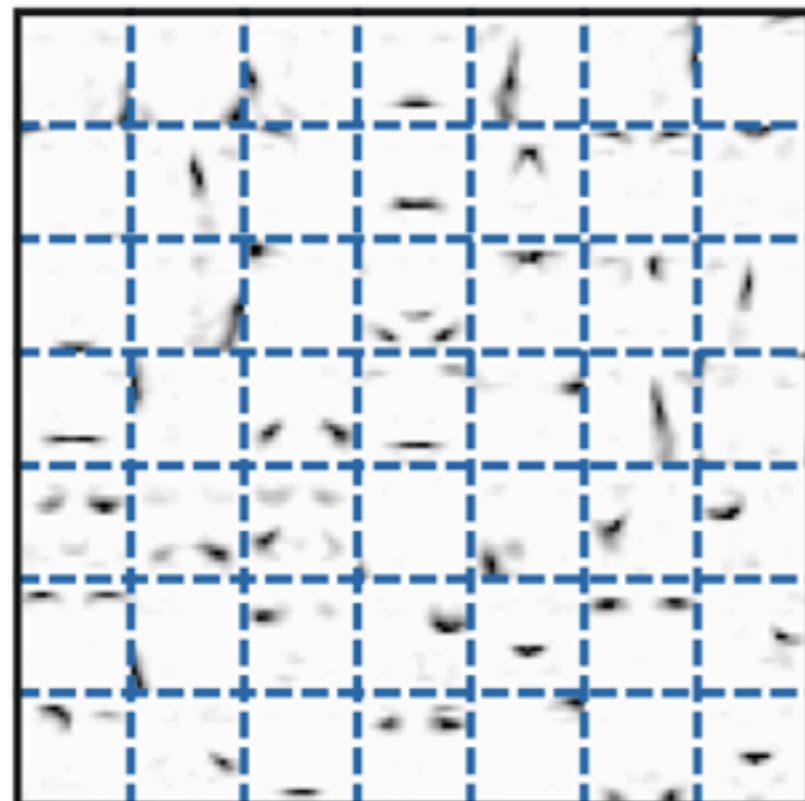
=



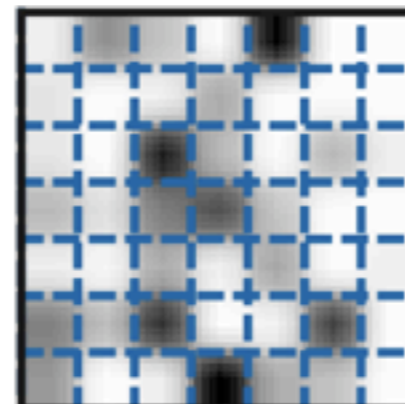
Lee and Seung, *Nature* **401**, 788 (1999)

Principal component analysis

NMF



x



=



Non-negative matrix factorization



# Non-negative matrix factorization

- Iterative procedure:

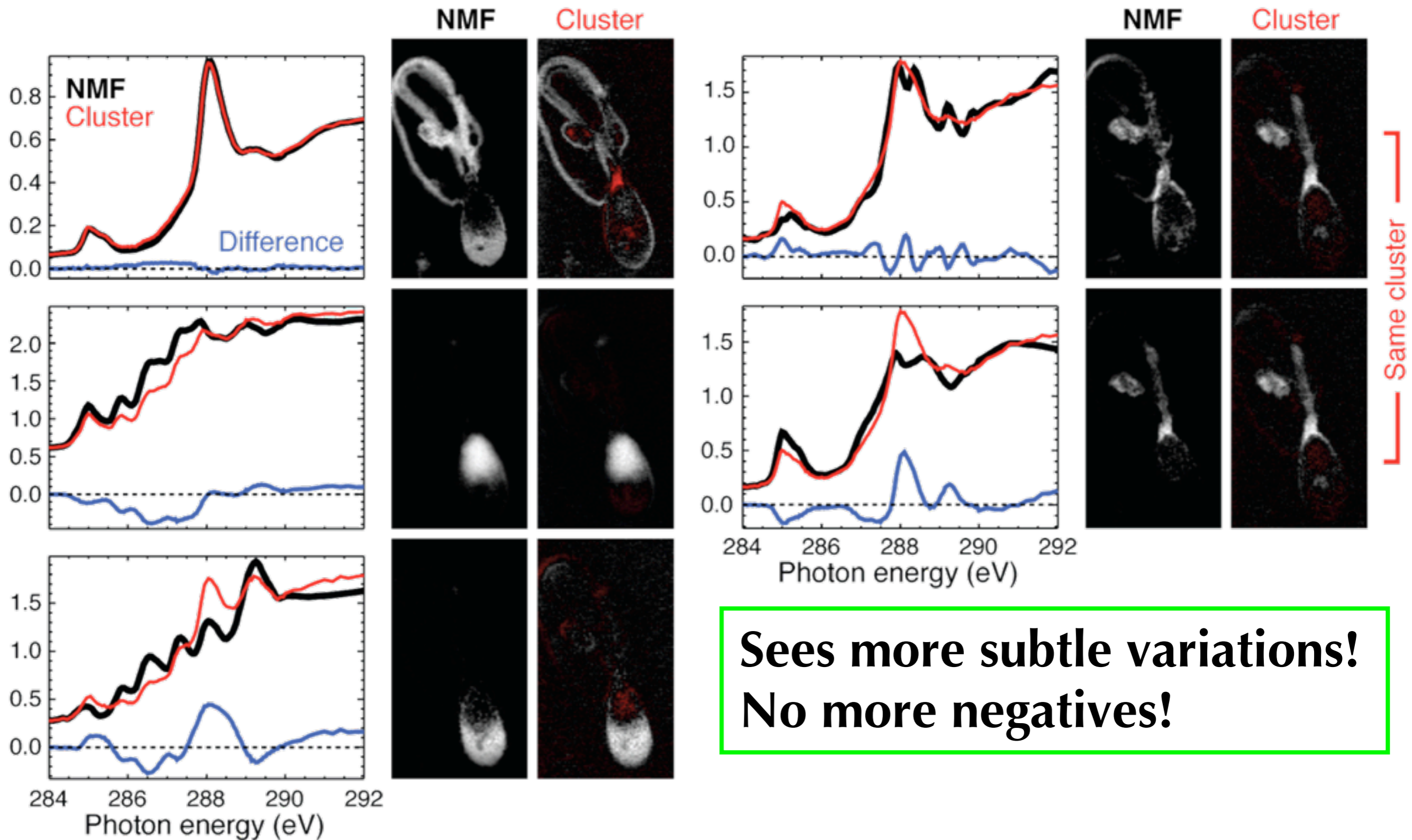
$$\mu_{N \times S} := \mu_{N \times S} \cdot \left( \frac{D_{N \times P}}{\mu_{N \times S} \times t_{S \times P}} \times t_{P \times S}^T \right)$$

For those pixels where  $\mu_{N \times S} \times t_{S \times P}$  gives larger values than those present in the data  $D_{N \times P}$ , this estimate update will drive  $\mu_{N \times S}$  towards smaller values and vice versa.

$$t_{S \times P} := t_{S \times P} \cdot \left( \mu_{S \times N}^T \times \frac{D_{N \times P}}{\mu_{N \times S} \times t_{S \times P}} \right)$$

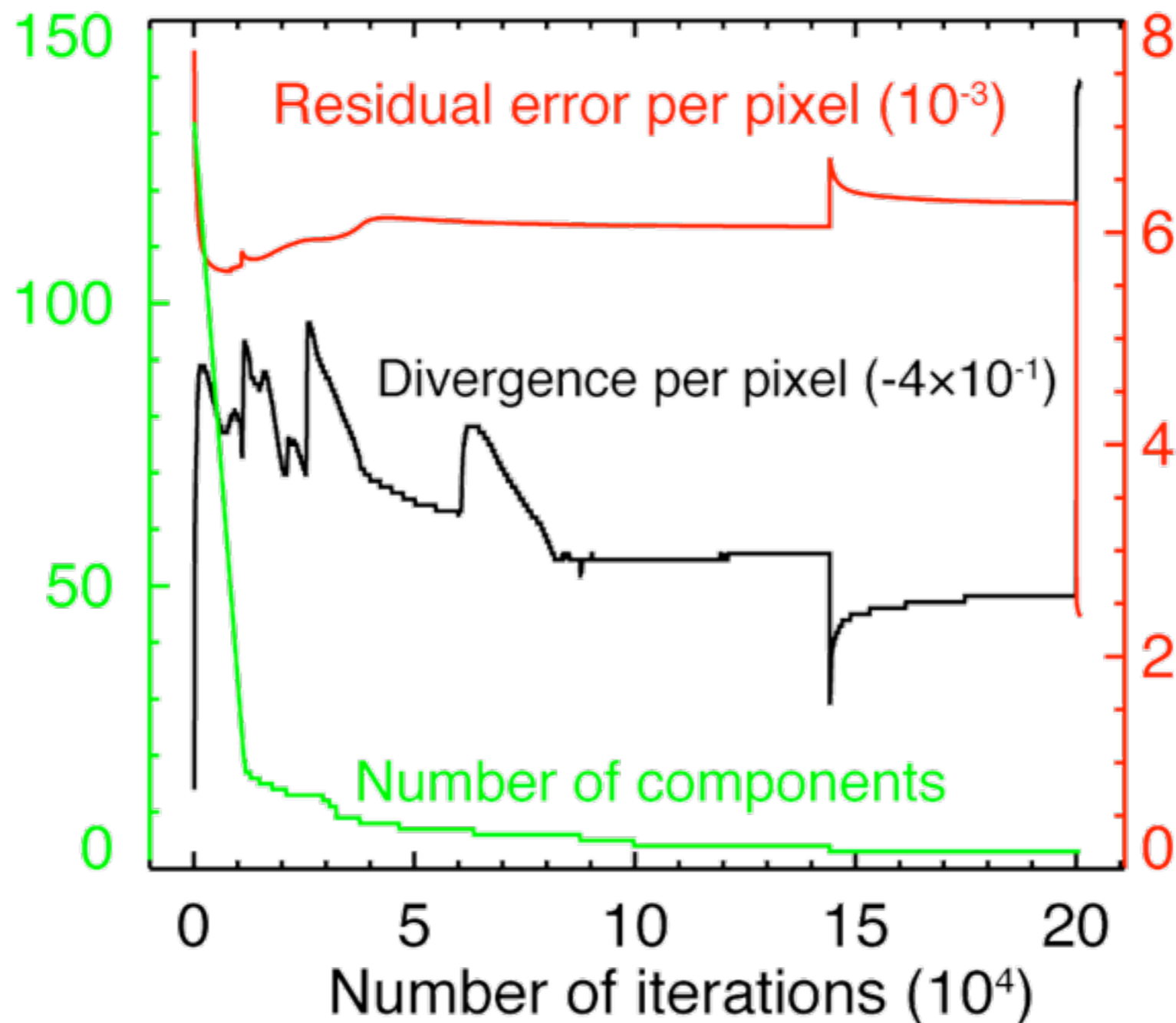
- Fleckenstein and Jacobsen (unpublished),  
after Lee and Seung (1999)

# NMF analysis of sperm



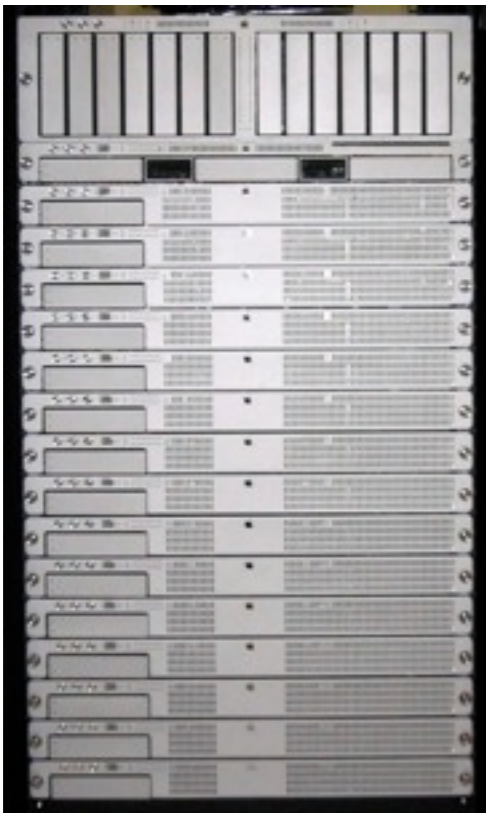
# NMF: many, many iterations

- We've been trying to speed it up...
- Bigger hammer: computation on graphics processors



# Matrix math summary

- There are good methods for factoring  $D_{N \times P} = C_{N \times S} \cdot R_{S \times P}$
- One winds up with eigenvectors in both  $R$  and  $C$ , and eigenvalues.
- Covariance approach is usually faster.
- Parallel computing (clusters, NVidia CUDA) can be very effective because
  - Most calculations are matrix multiplications
  - In multiplication, each resultant matrix element involves a product of two vectors (“trivially parallelizable”).



- We have  $N$  shoppers, and  $P$  items for purchase
- We want to find  $S$  customer types:  $D_{N \times P} = C_{N \times S} \cdot R_{S \times P}$
- You, as customer  $n$ , match customer types given in  $C_{N \times S}$
- Customer types  $S$  like to purchase items  $P$  as given by  $R_{S \times P}$

## Customers Who Bought This Item Also Bought



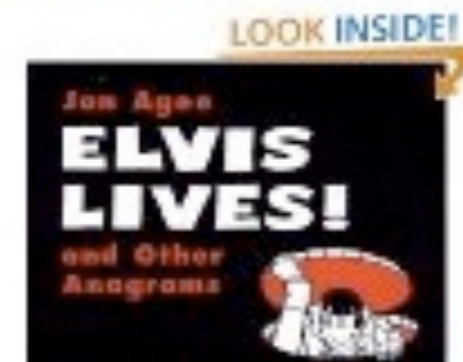
[Go Hang a Salami! I'm a Lasagna Hog!: and Other P...](#)  
by Jon Agee

★★★★★ (7) \$6.96



[Sit on a Potato Pan, Otis!: More Palindromes](#) by Jon Agee

★★★★★ (2)

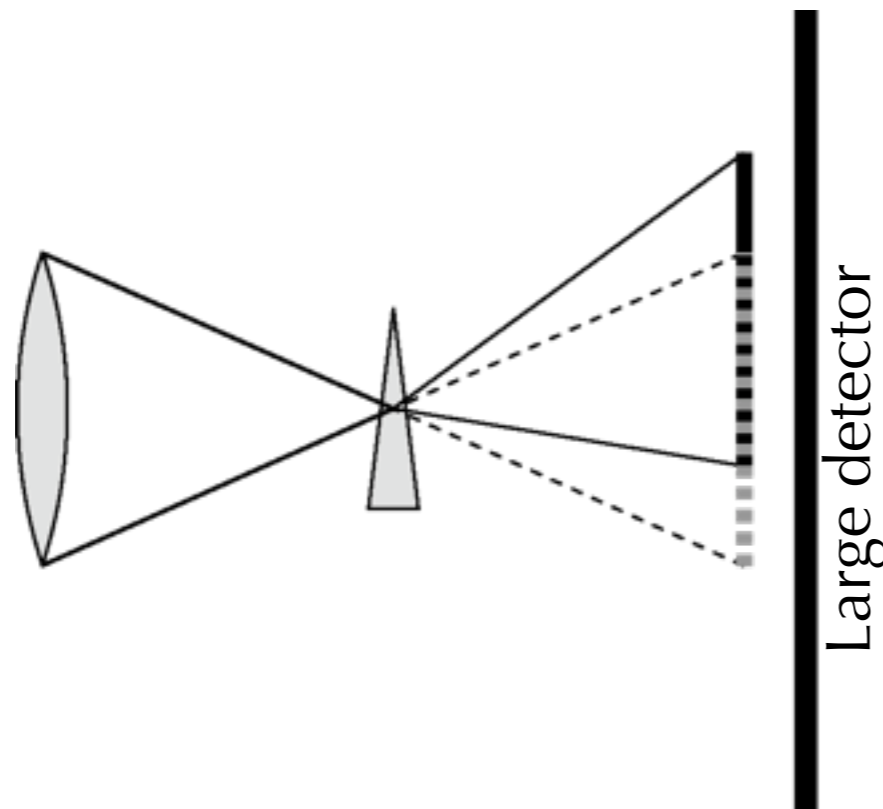


[Elvis Lives!: and Other Anagrams \(Sunburst Book\)](#)  
by Jon Agee

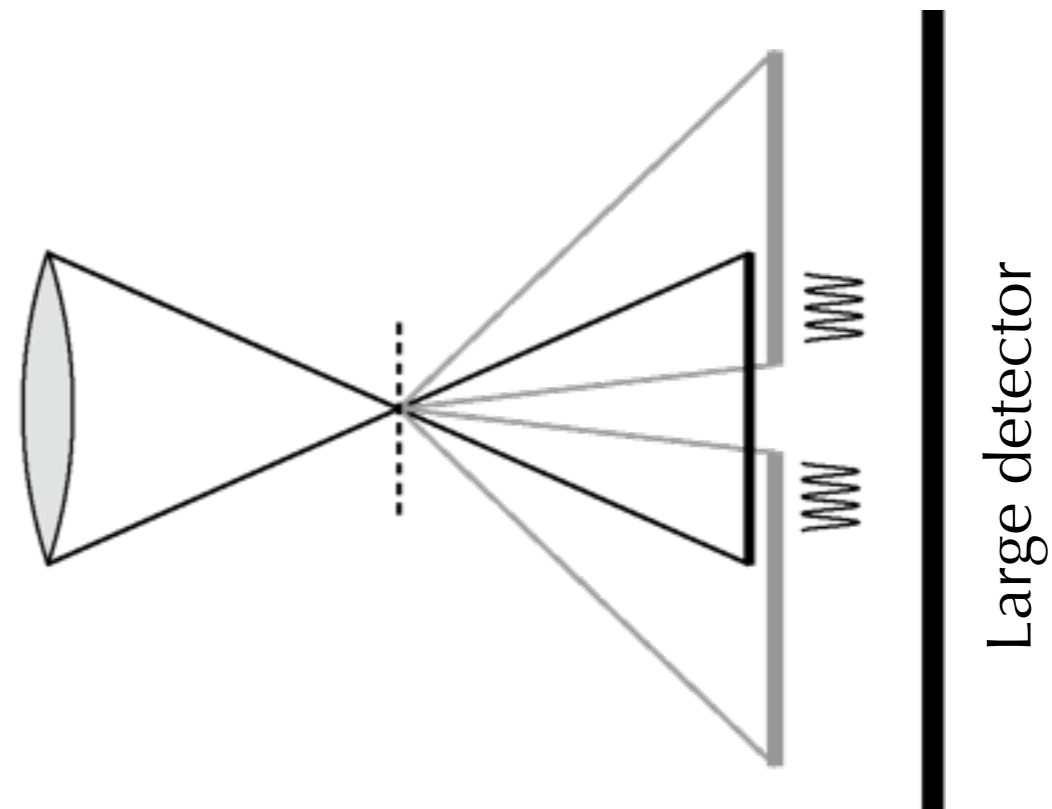
★★★★☆ (1) \$8.95

# STXM: contrast depends on detector

- Large area detector: sensitive only to absorption
- Point detector on-axis: coherent imaging
- Detector with restricted or segmented spatial response: some degree of phase contrast



Phase gradient (prism)

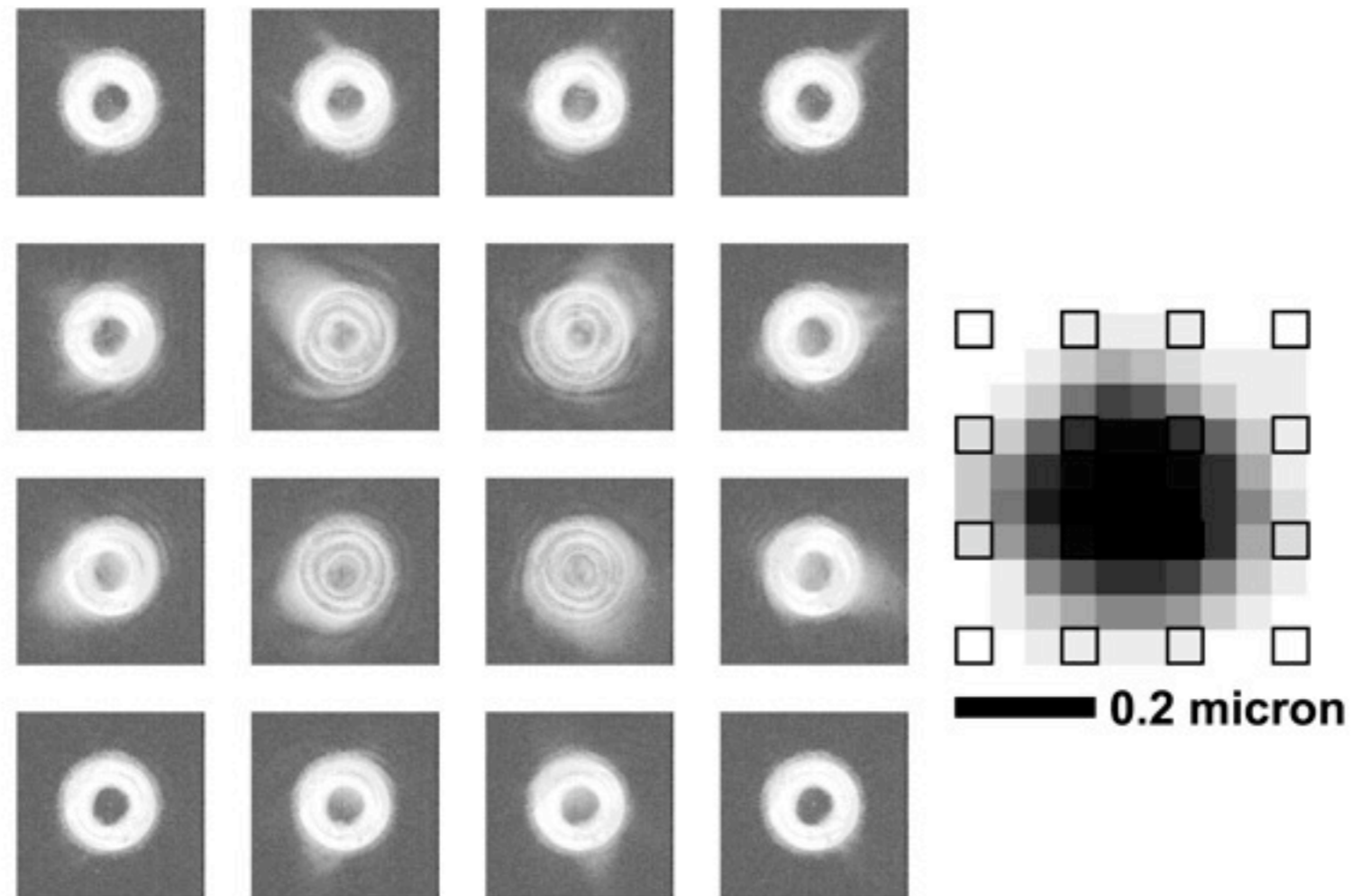


Spatial frequency in object

See e.g., Spence and Cowley, *Optik* **50**, 129 (1978); Nellist *et al.*, *Nature* **374**, 630 (1995).

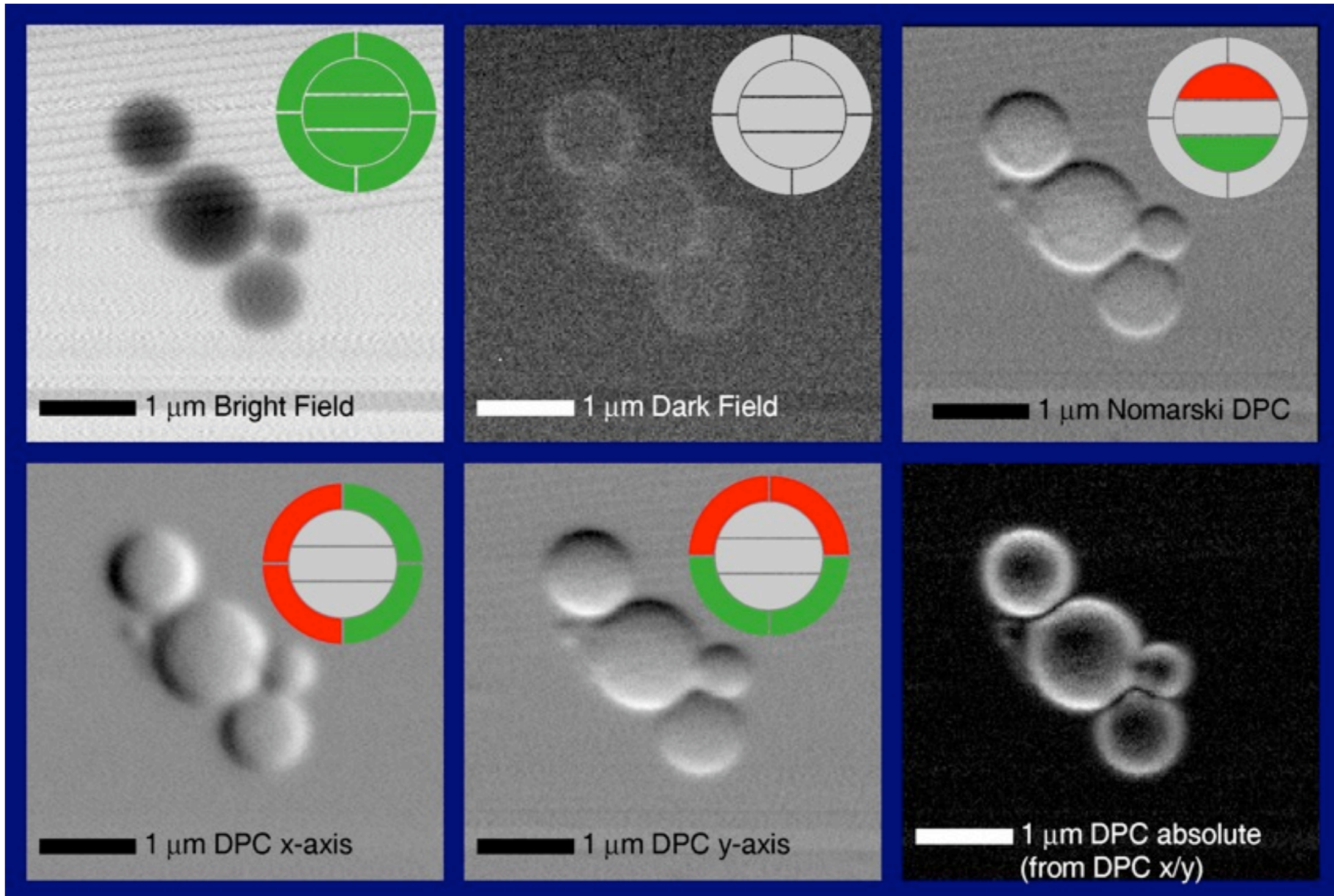
# STXM: CCD as the ultimate detector

- Record microdiffraction pattern per pixel; Wigner phase reconstruction. Chapman, *Ultramicroscopy* **66**, 153 (1996). Shown below: polystyrene sphere raw data (which was reconstructed to give amplitude and phase)



# Simultaneous Availability Of Contrast Modes

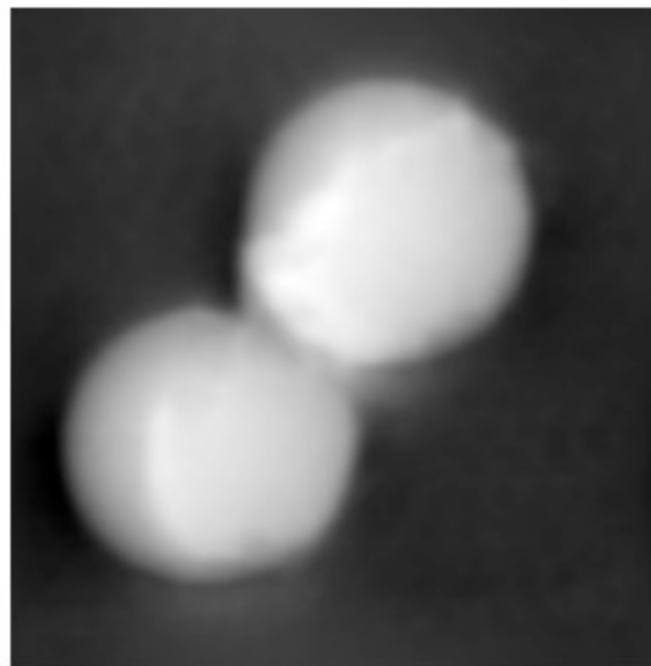
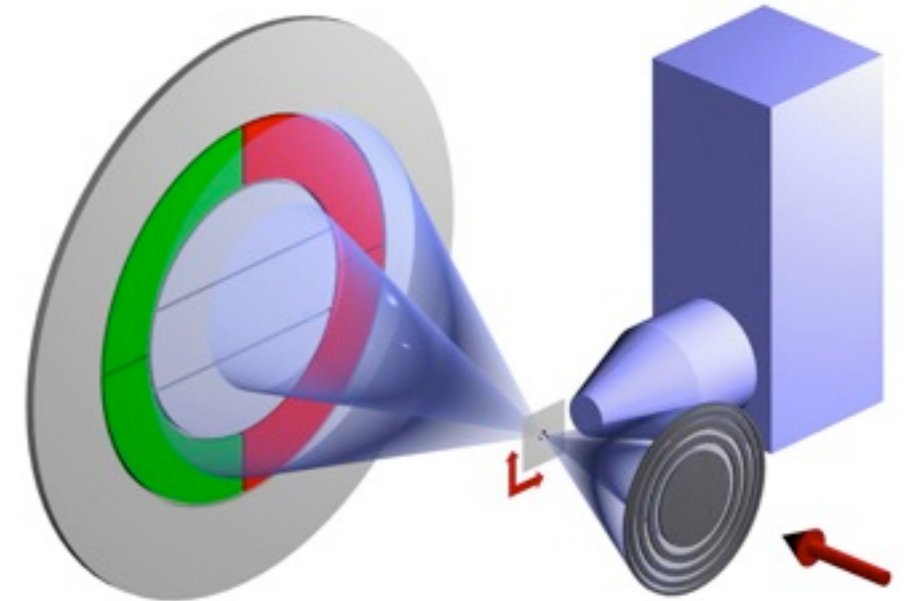
- Silica spheres 1  $\mu\text{m}$  diameter or less
- Differential phase contrast filters out intensity fluctuations of the source!





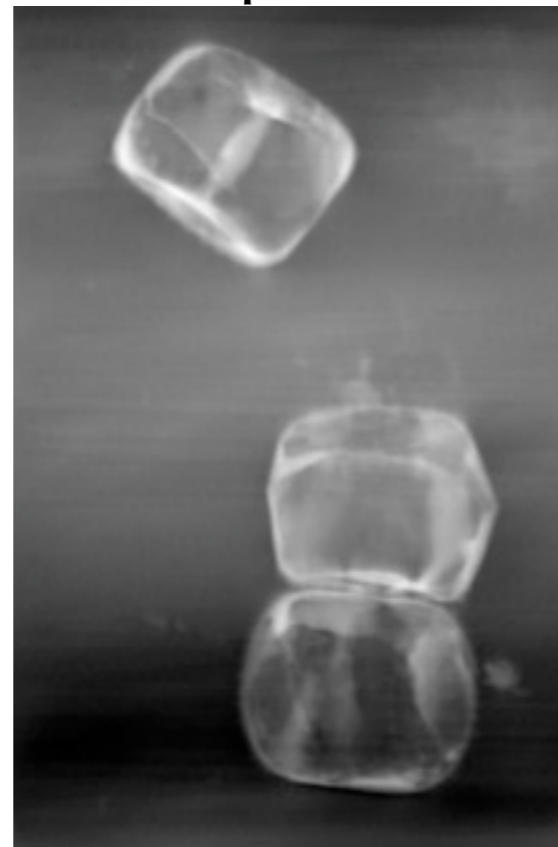
# Phase contrast in microprobes

- Place elemental maps in ultrastructural context; provide quantitative concentration.
- Segmented x-ray detector (with BNL, Max Planck silicon lab)
- Fourier optics reconstruction filters, and data fusion with elemental map data



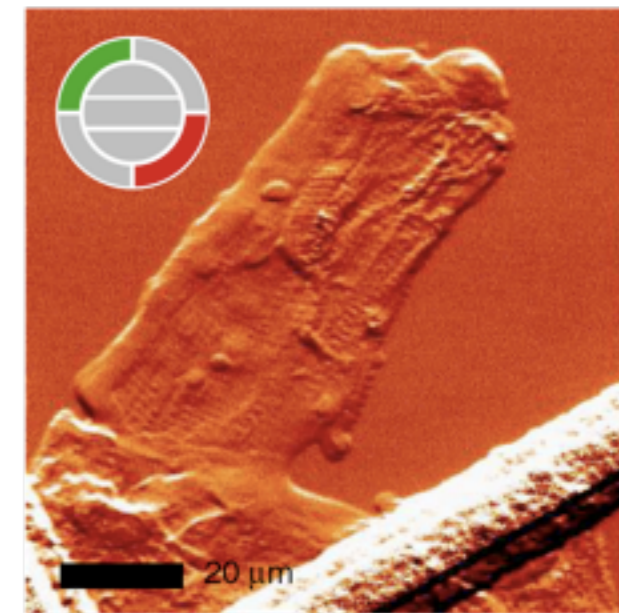
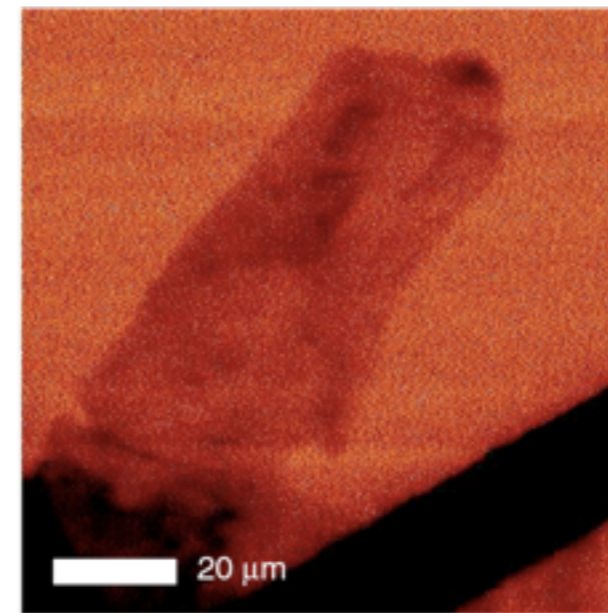
0.0 0.2 0.4 0.6

Reconstructed phase in radians of 5  $\mu\text{m}$  silica sphere: CXRO data predicts 0.60, experiment gives 0.58



5  $\mu\text{m}$

Diatom: phase corresponds to max thickness of 2.8  $\mu\text{m}$

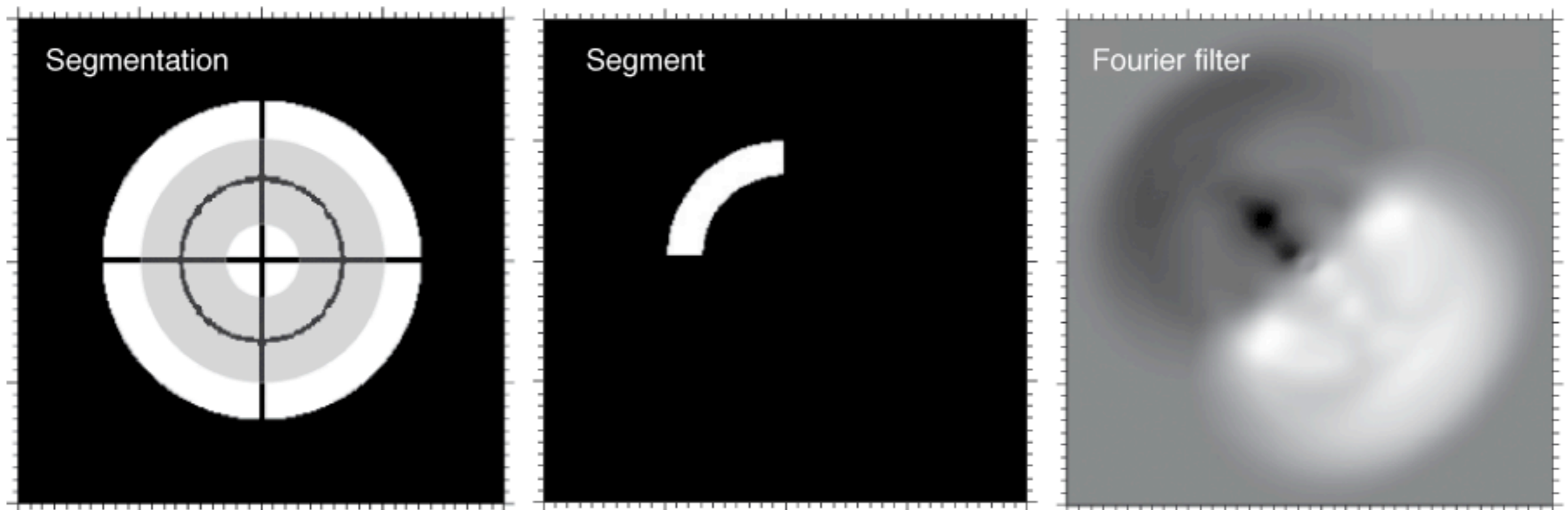


Cardiac muscle (w/Palmer, Vogt *et al.*: absorption (left) and differential phase (right) images.

Hornberger *et al.*, *Ultramic.* **107**, 644 (2007);  
Feser *et al.*, *Nucl. Inst. Meth. A* **565**, 841 (2006)

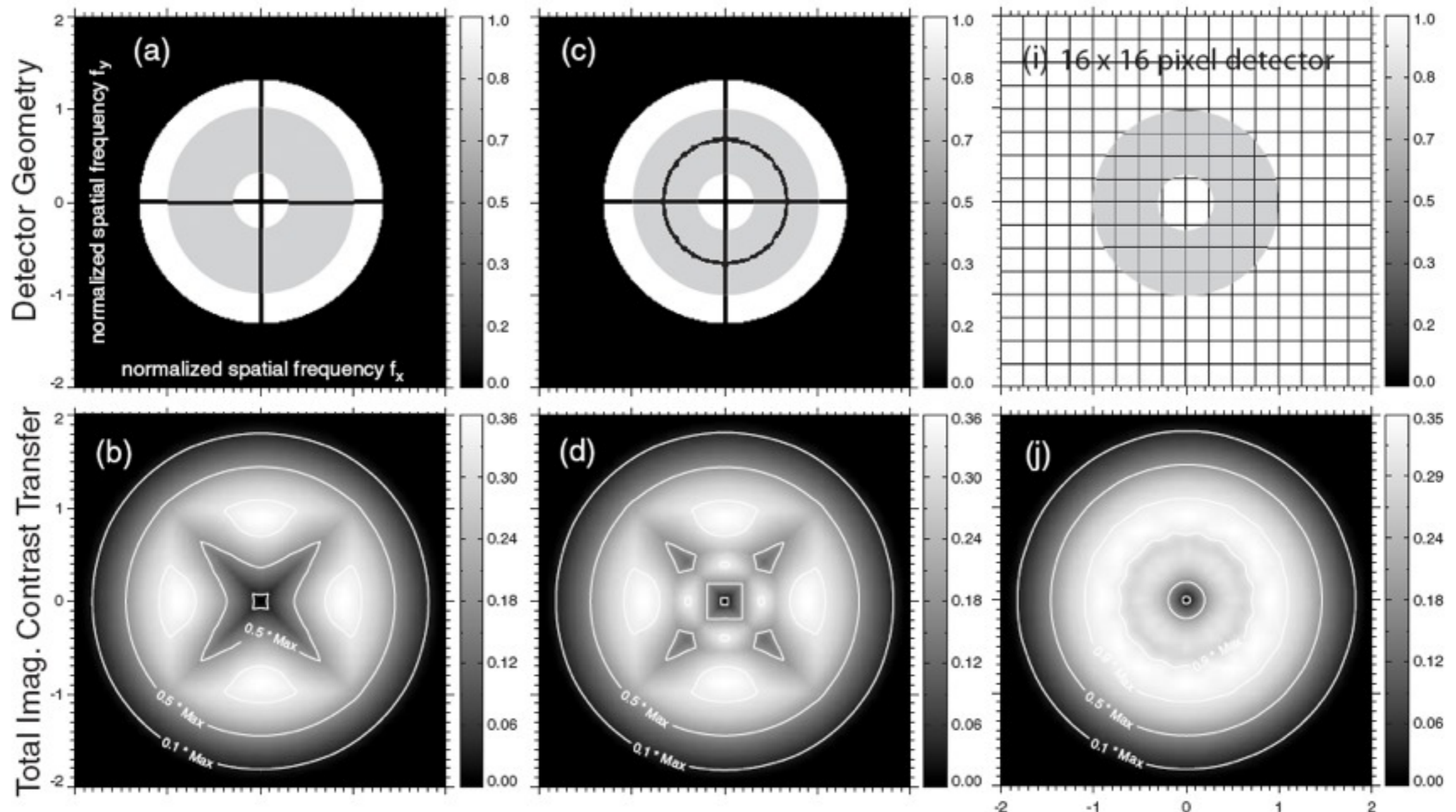
# Segmented detector and Fourier filter reconstruction

- Limited number of segments means fast readout in scanning microprobe, and fast reconstruction.
- Fourier filtering approach: inspired by STEM work of McCallum, Landauer, and Rodenburg, *Optik* **103**, 131 (1996).
- Extended and implemented by Hornberger, Feser, and Jacobsen, *Ultramic.* **107**, 644 (2007).



# Fewer segments=fast readout

Fourier plane coverage of various detector schemes  
(B. Hornberger PhD dissertation, 2007)



# Analyzing full spectra

- Peaks from trace elements can be on shoulders of strong peaks from common elements.
- Setting simple energy windows can give poor quantitation. Record full spectrum and do curve-fitting!
- Wavelength dispersive detectors can help – but often with lower collection solid angle
- This example: Twining *et al.*, *Anal. Chem.* **75**, 3806 (2003). Also ESRF, elsewhere.
- Analysis approach: Vogt, Maser, and Jacobsen, *J. Phys. IV* **104**, 617 (2003).

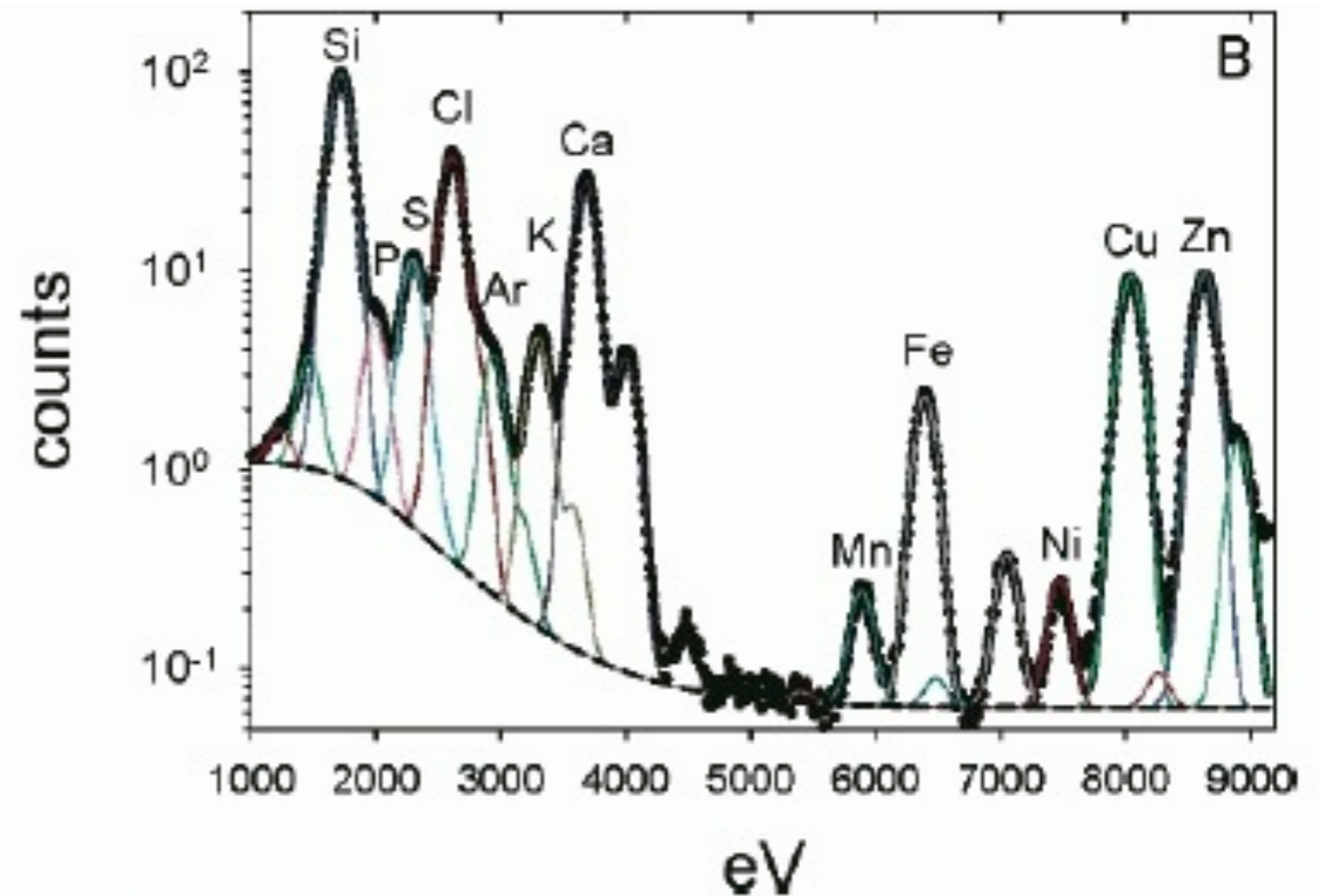
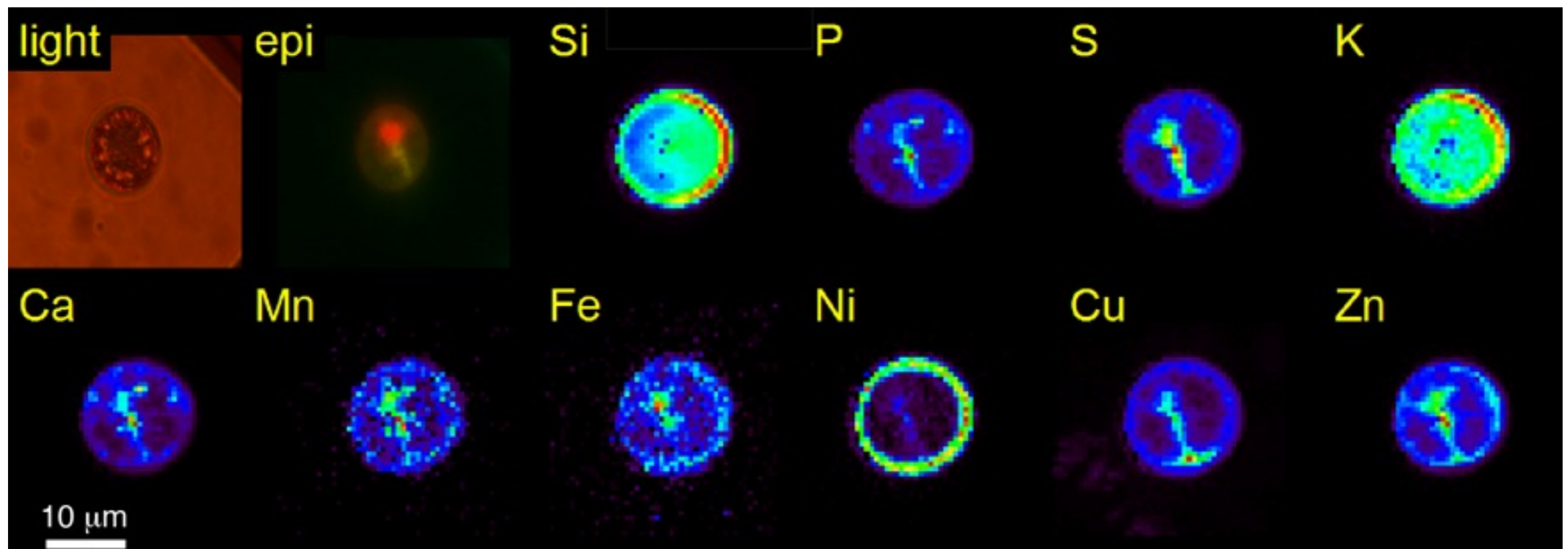


**Figure 1.** Fluorescence spectra for the marine diatom *T. weissflogii*. Pixel-averaged spectra for the target cell and a neighboring background region are plotted in (A). The  $K\alpha$  peaks of the major bioactive elements are indicated above the peaks. (B) displays the fit of the EMG model to the cell spectrum. The sigmoidal baseline is shown as a dotted line, the overall model is black, and the  $K\alpha$  and  $K\beta$  peaks for each element are displayed in various other colors.

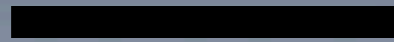
# X-ray fluorescence microprobe: trace metal studies

- Seed Southern Pacific with bioavailable iron to increase CO<sub>2</sub> uptake?
- Requires understanding of iron *and* carbon uptake in phytoplankton; combine fluorescence with phase contrast.
- Collaboration with N. Fischer, S. Baines (Stony Brook), B. Twining (South Carolina)



Twining *et al.*, *Anal. Chem.* **75**, 3806 (2003)

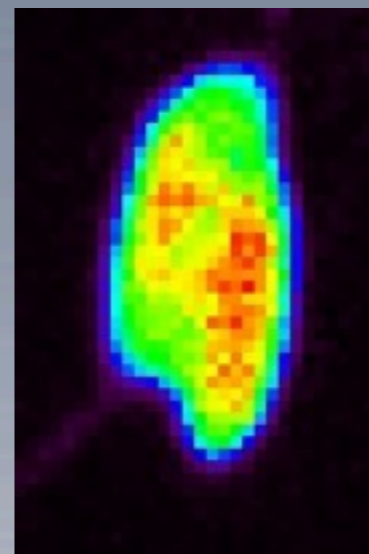
# Phosphorous, Sulfur, Silicon



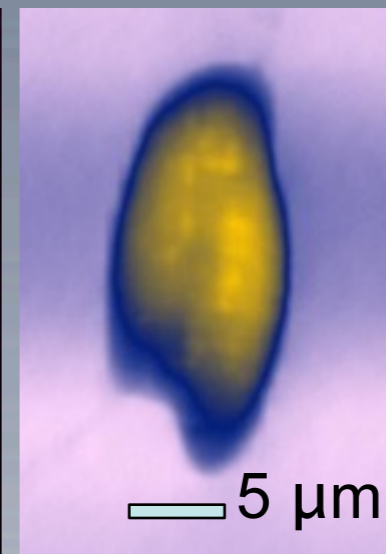
2  $\mu\text{m}$

Phase contrast needed to align low-statistics fluorescence tilt series. de Jonge *et al.*, APS; Holzner *et al.*, Stony Brook

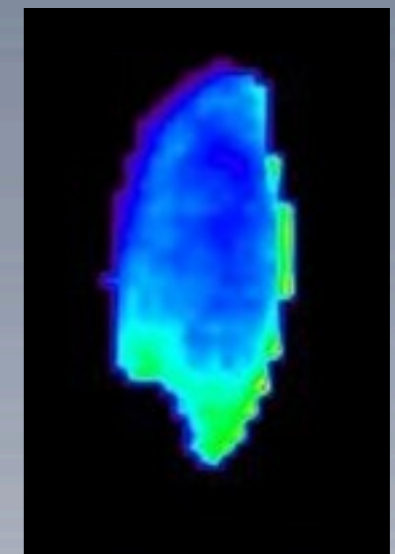
## Phase contrast tomography of cyclotella (marine protist)



Sulfur content



Protist mass



Sulfur concentration

# Scanning and full-field

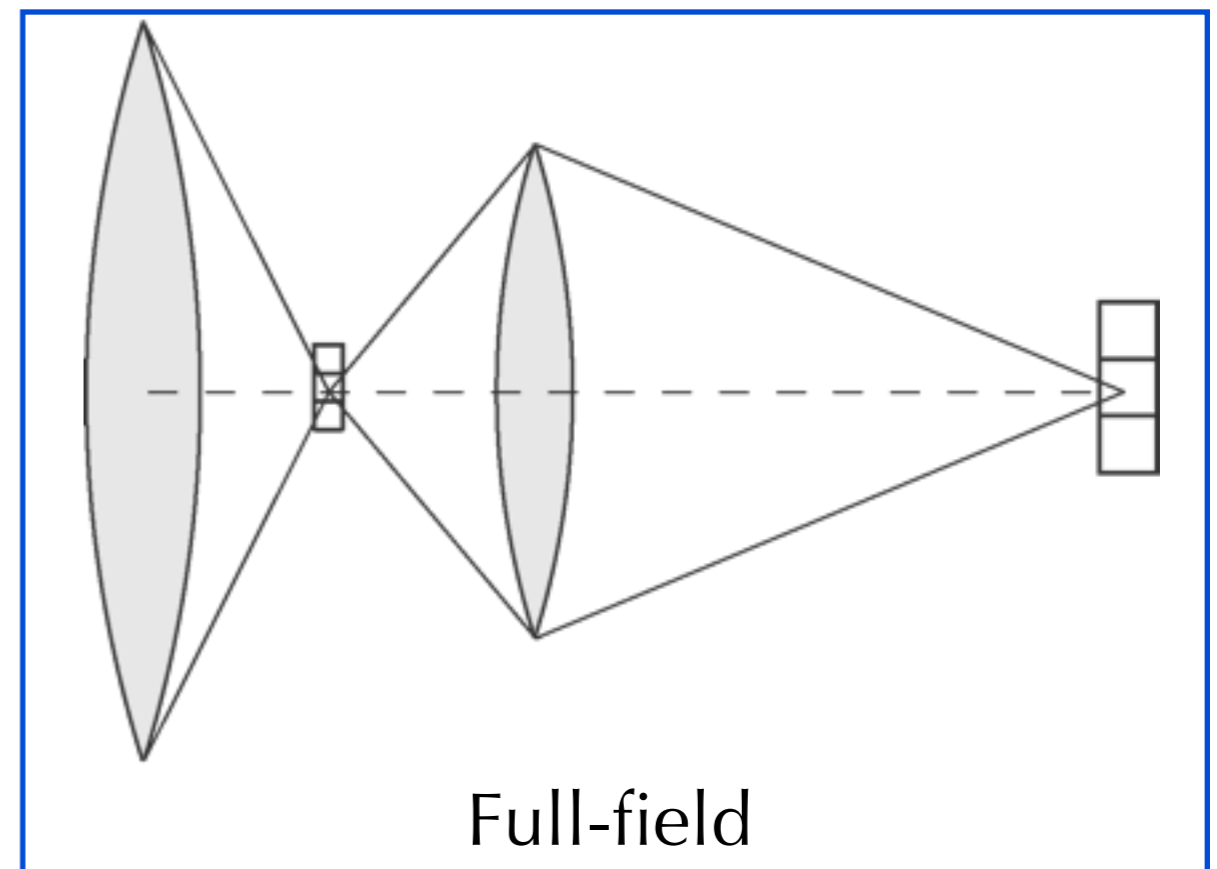
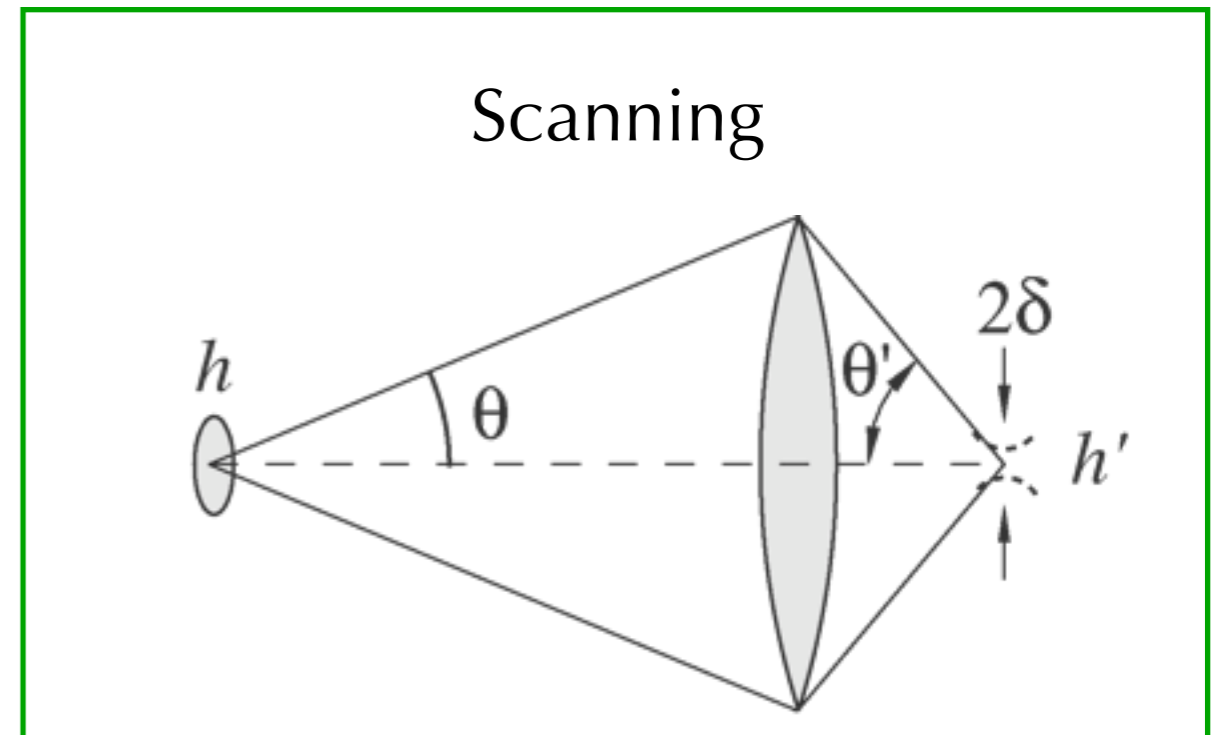
- General property of lenses: preserve size•angle product (Liouville's Theorem), so

$$h\theta = h'\theta'$$

- Microprobe/STXM: want  $h' < \delta$  so that diffraction limit of optic rather than geometrical image of source dominates spot size
- Rayleigh resolution of  $\delta = 0.61 \frac{\lambda}{\theta}$  thus gives phase space of

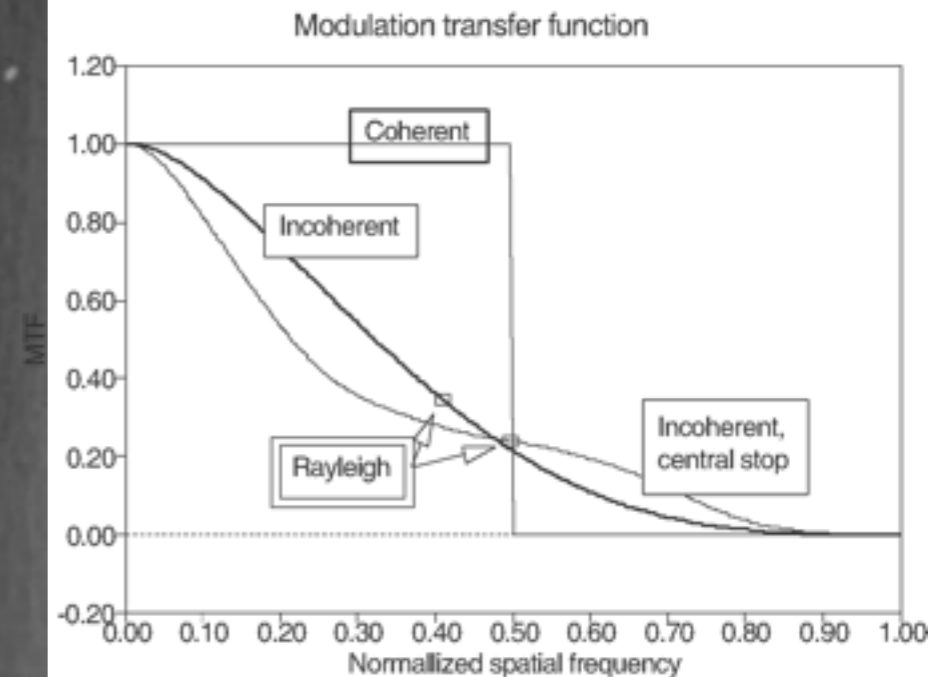
$$(2\delta)(2\theta) = 2.44\lambda$$

- Full-field: each pixel in object is diffraction limit of optic, but can have many pixels simultaneously!



# Coherence $\neq$ phase contrast!

- Incoherent illumination in TXM: Zernike phase contrast [Nobel Prize 1953; x-ray version: Schmahl *et al.*, *Optik* **97**, 181 (1994)]
- Coherent illumination in STXM: large area detector delivers incoherent imaging
- Incoherent imaging often preferred



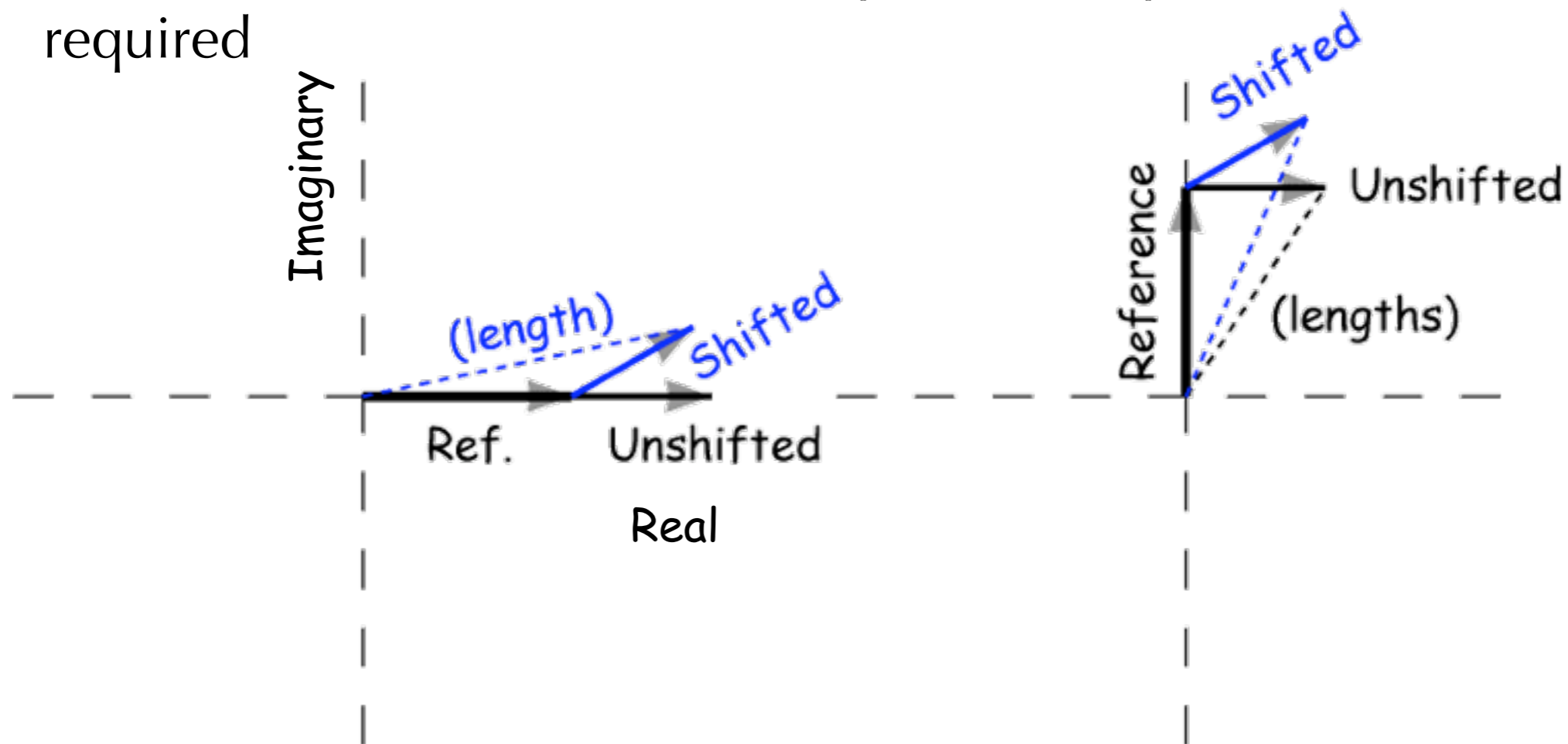
Jacobsen *et al.*,  
*Ultramicroscopy* **47**, 55 (1992)

Fig. 6-14 of Goodman, *Introduction to Fourier Optics*  
(McGraw Hill, 1968)



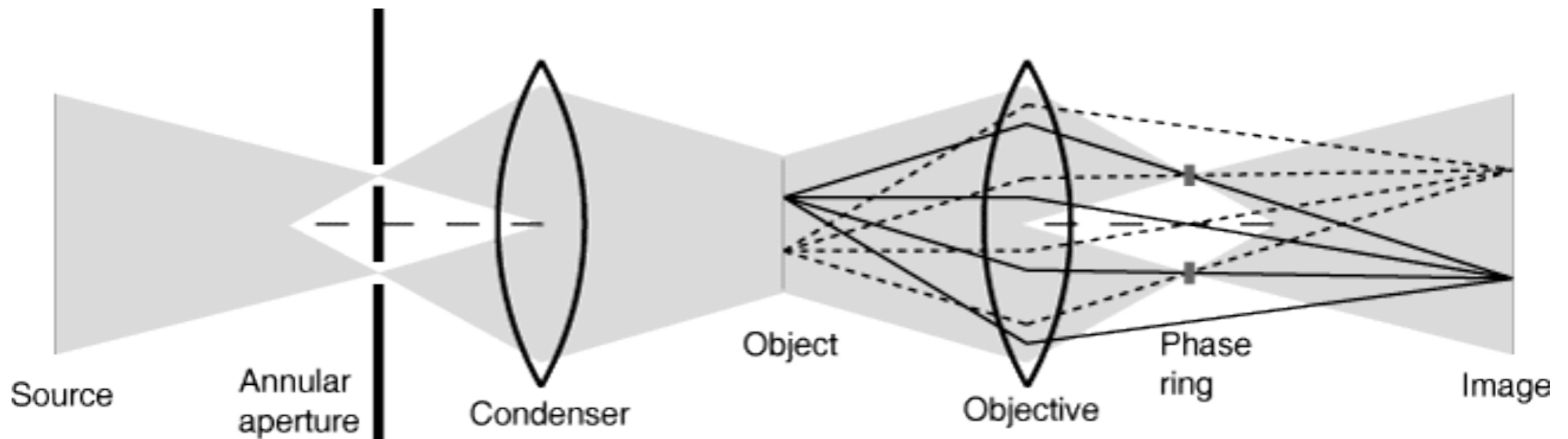
# Zernike phase contrast

- Intensity recording: phase is lost
- But phase has the information! Compare objects which are **Shifted** in phase with those that are **Unshifted**
- Must “interfere” against a **Reference** to see changes in intensity (changes in phaser length)
- Interference is done within each pixel; intra-pixel coherence not required

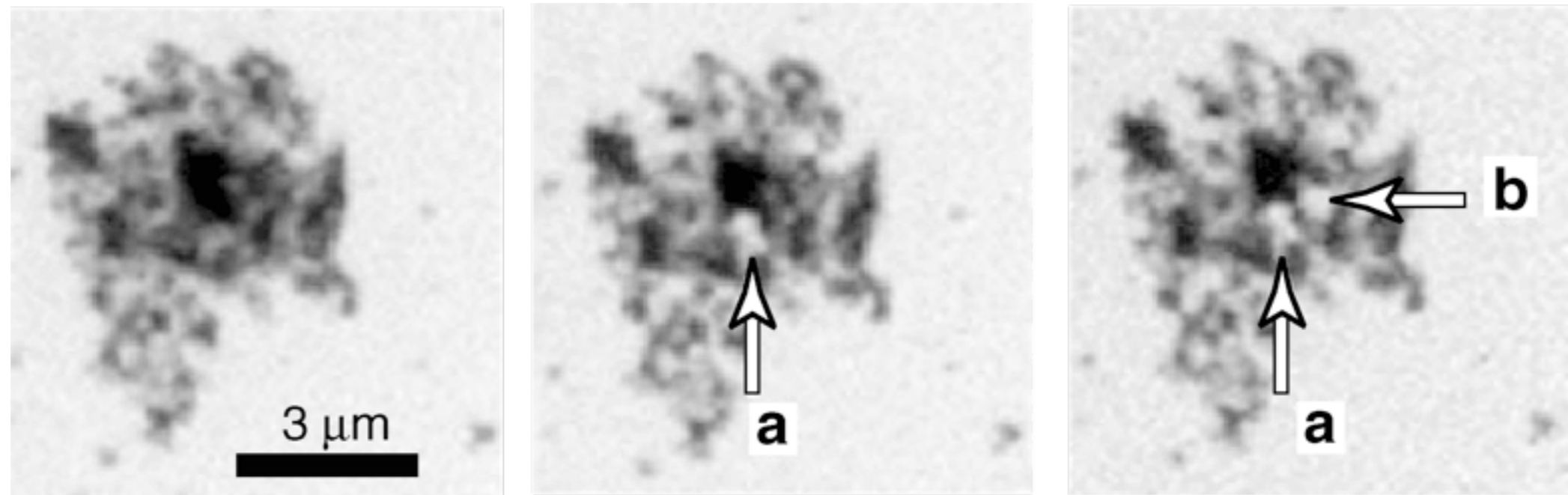


# Zernike phase contrast: ring illumination

- Annular stop, annular phase ring at respective back focal planes
- “Reference” wave (illumination) is phase shifted
- Object scatters waves, most of which then miss the phase ring



# Spectromicroscopy can be damaging!



- Study: polyacrilimide-induced flocculation of clays (irrigation of loamy soils)
- Mass loss is visible after acquiring spectra with focused beam (wet sample at room temperature)
- U. Neuhaeusler, PhD Thesis (Stony Brook/Göttingen)

# Calculating dose

- SI units for ionizing radiation: 1 Gray=1 J/kg=100 rad
- Lambert-Beer law with inverse absorption length  $\mu$ (=1.3 mm for protein at 8.98 keV):

$$I = I_0 e^{-\mu x} \quad \text{with} \quad \mu = 2 \frac{\rho N_A}{A} r_e \lambda f_2$$

- Energy per thickness:

$$\frac{dE}{dx} = h\nu \frac{dI}{dx} = h\nu \mu I_0 e^{-\mu \cdot 0} = I_0 h\nu \mu$$

- Energy per mass:

$$\frac{dE}{dm} = \frac{dE}{dx} \frac{1}{\text{Area} \cdot \rho} = h\nu \mu I_0 \frac{1}{\text{Area} \cdot \rho} = h\nu \frac{I_0 \mu}{\text{Area} \cdot \rho}$$

# Dose numbers

- G factor: number of bonds broken per 100 eV.  $G \sim 5$  for many organic molecules (room temp.)
- Break 1 bond per atom:

$$\frac{(20 \text{ eV/atom}) \cdot (N_A \text{ atoms/mol}) \cdot (1.6 \times 10^{-19} \text{ J/eV})}{(12 \text{ g/mol}) \cdot (10^{-3} \text{ kg/g})} = 1.6 \times 10^8 \text{ Gray}$$

- Representative dose in crystallography:

$$\frac{10^{14} \text{ photons}}{(50 \mu\text{m})^2} \frac{(8979 \text{ eV/photon}) \cdot (1.6 \times 10^{-19} \text{ J/eV})}{(1300 \mu\text{m}) \cdot (1.35 \text{ g/cm}^3) \cdot (10^{-4} \text{ cm}/\mu\text{m})^3 \cdot (10^{-3} \text{ kg/g})} = 3.3 \times 10^7 \text{ Gray}$$

- X-ray microscopy: doses of  $10^6$ - $10^8$  Gray are common, depending on resolution

# Effects of dose on us

- Hiroshima survivors
  - Large database, though considerable uncertainties on dose
- Chernobyl firefighters
  - 6-16 Gray: 20 of 21 died
  - 4-6 Gray: 7 of 21 died
  - 2-4 Gray: 1 of 55 died
  - 1-2 Gray: 0 of 140 died



- A solar flare event in August 1972, between Apollo 16 and 17, would have delivered a dose of 40 Gray to moonwalking astronauts.
- Space shuttle at altitude of Hubble Space Telescope for a week: about  $10^{-2}$  Gray
- Flight from New York to Tokyo: about  $5 \times 10^{-4}$  Gray
- Dose "at the fence" of Three Mile Island: about  $10^{-3}$  Gray

# The Bystander effect

When your neighbor gets killed, you might get splattered

- Single alpha particles directed on single cells; measure mutation rate.
- Addition of 1 mM octanol strongly suppresses the effect; inhibits gap-junction-mediated intercellular communication
- Implications for linear extrapolation of dose to low values

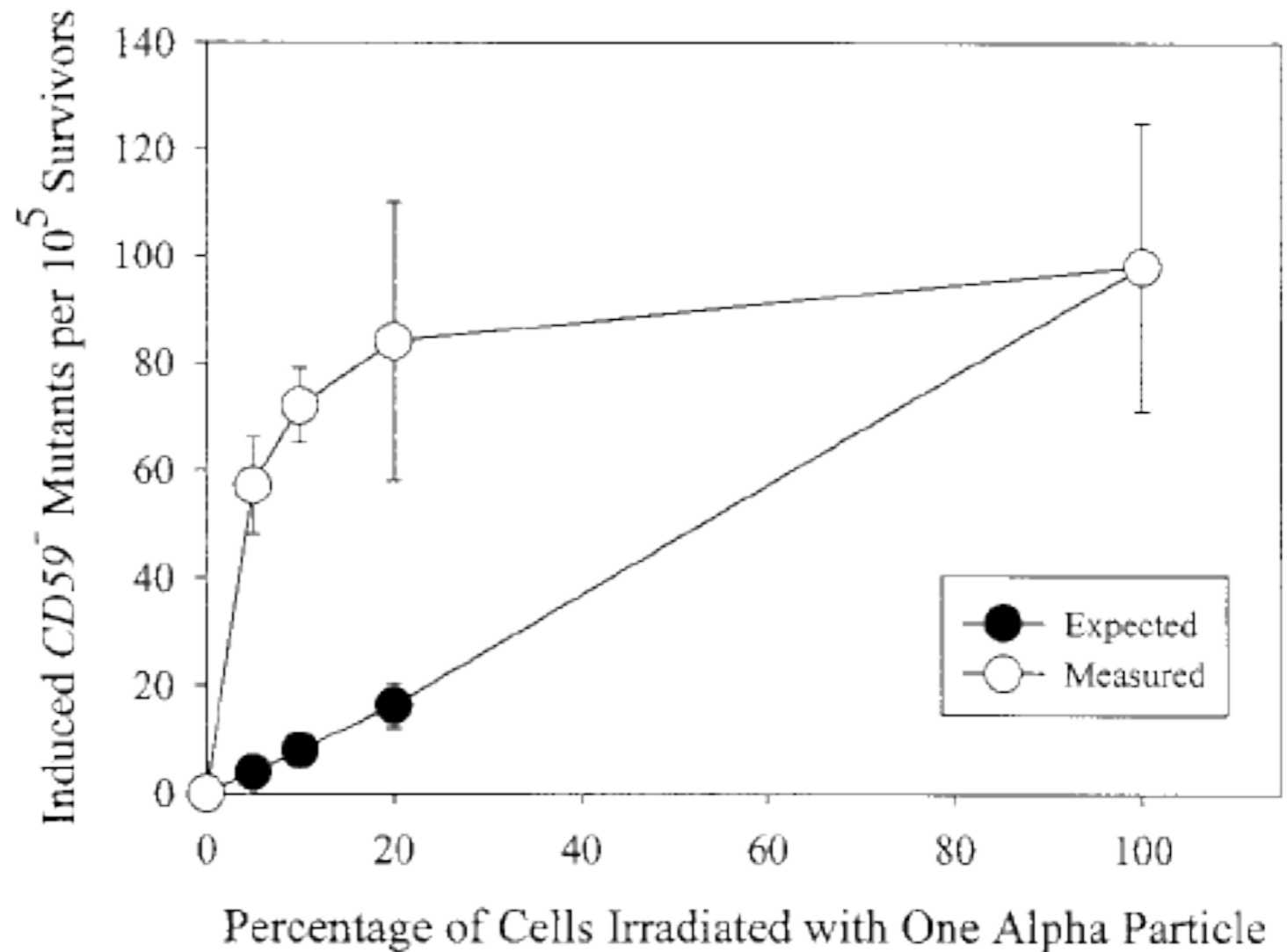
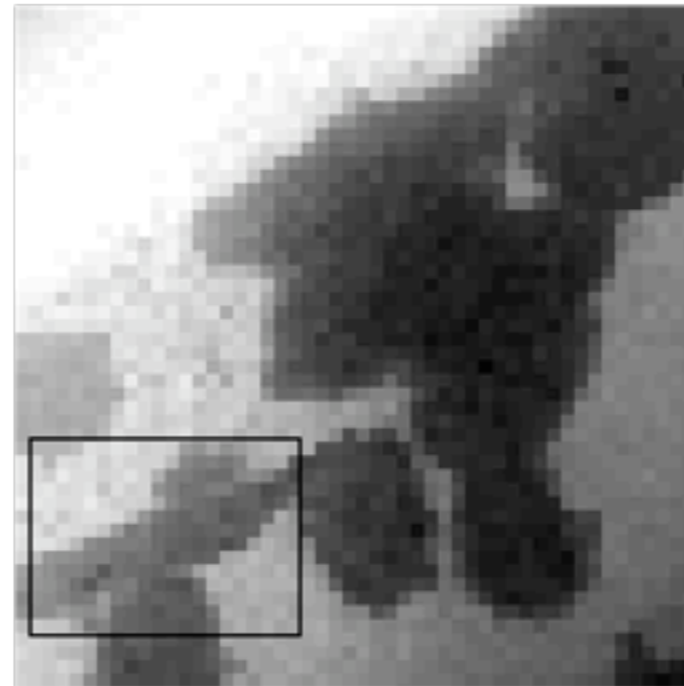


**Fig. 1.** Induced  $CD59^-$  mutant fractions per  $10^5$  survivors obtained from populations of  $A_L$  cells in which 0, 5, 10, 20, or 100% had been irradiated with exactly one  $\alpha$  particle through its nucleus. Induced mutant fraction = total mutant fraction minus background incidence, which was  $46 \pm 10$  mutants per  $10^5$  clonogenic survivors in  $A_L$  cells used in these experiments.

Zhou et al., Proc. Nat. Acad. Sci. **98**, 14410 (2001)

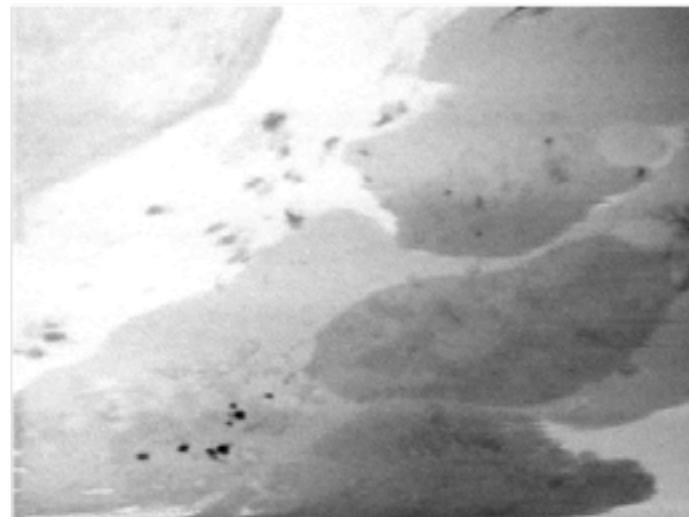
# Radiation damage on (initially) living cells

- X-rays are ionizing radiation. The dose per high resolution image is about 100,000 times what is required to kill a person
- Makes it hard to view living cells!

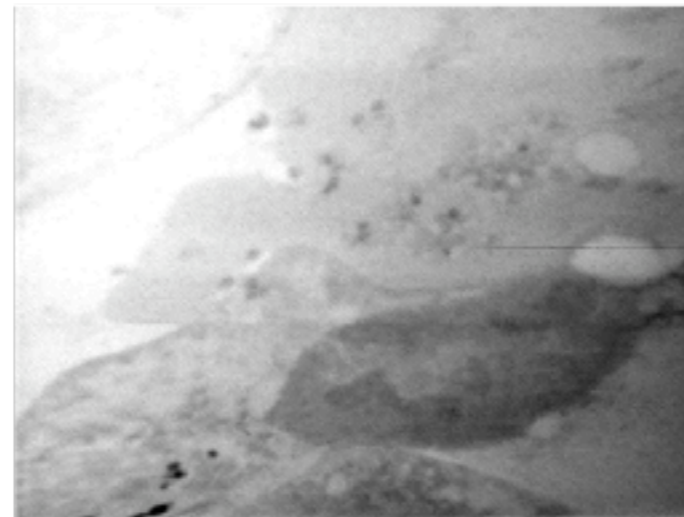


10 μm  
 $6.0 \cdot 10^2$  Gray, ET=2 min.

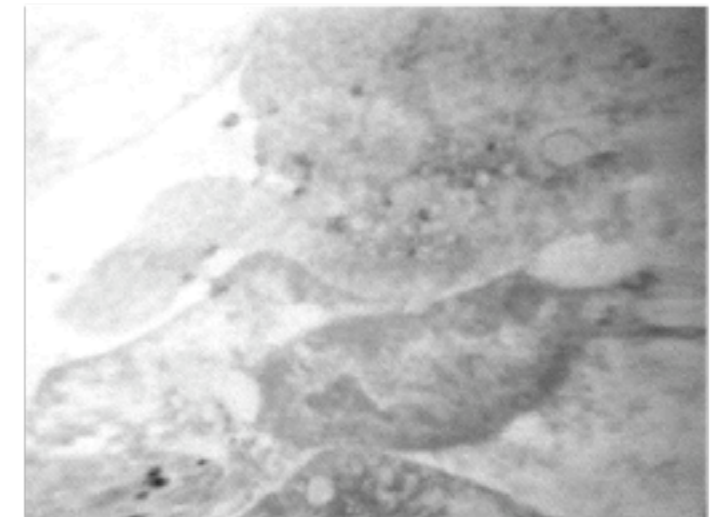
Experiment by V. Oehler, J. Fu, S. Williams, and C. Jacobsen, Stony Brook using specimen holder developed by Jerry Pine and John Gilbert, CalTech



5 μm  
 $1.2 \cdot 10^5$  Gray, ET=9.5 min.



5 μm  
 $2.4 \cdot 10^5$  Gray, ET=17 min.

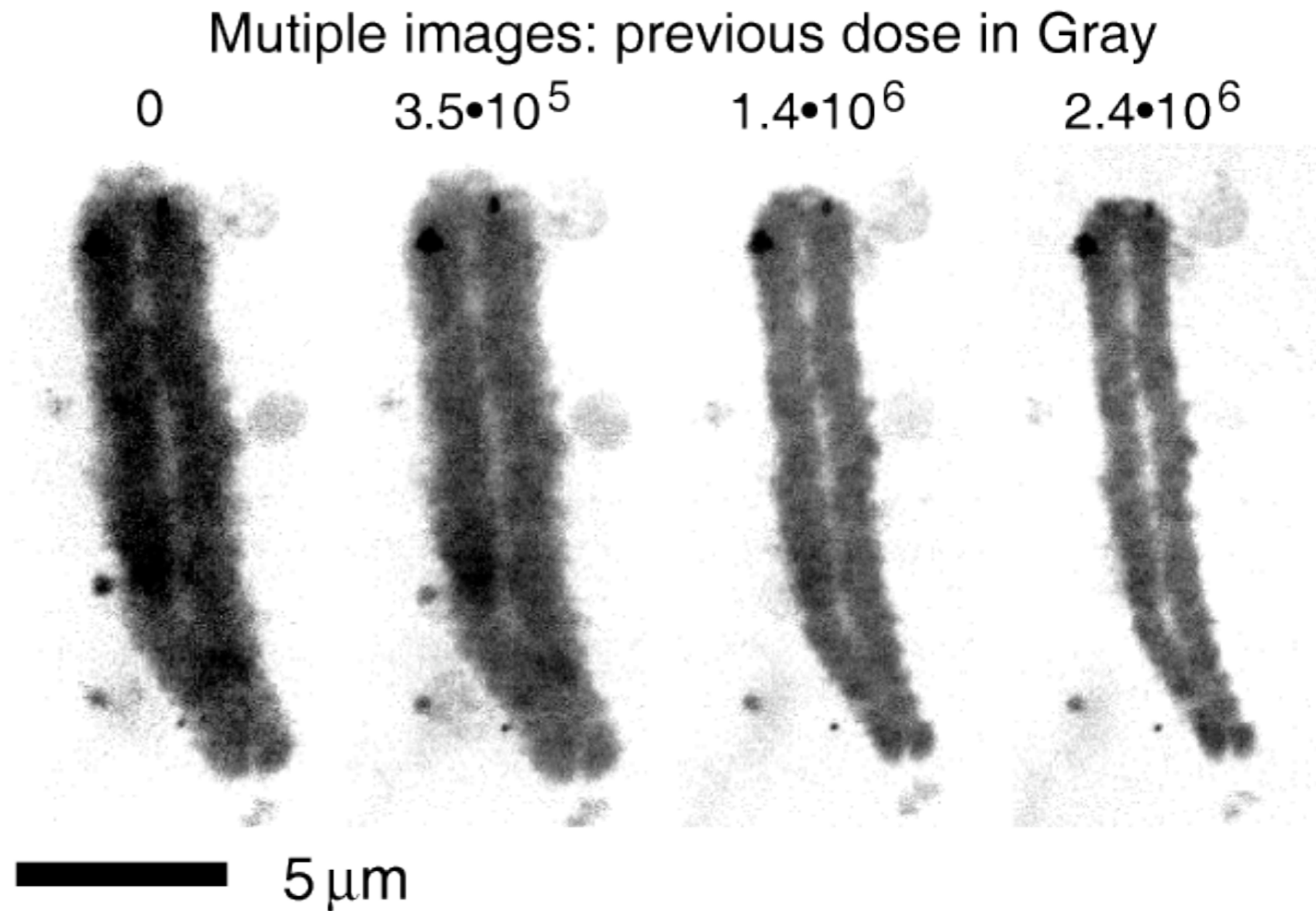


5 μm  
 $3.7 \cdot 10^5$  Gray, ET=24.5 min.



# Wet, fixed samples: one image is OK

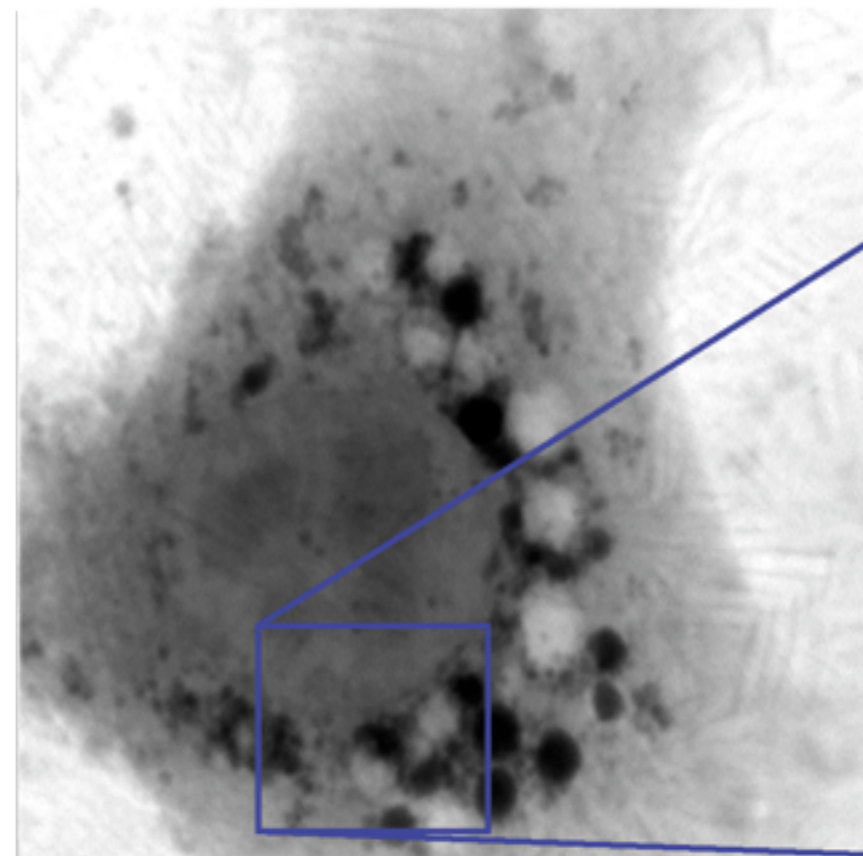
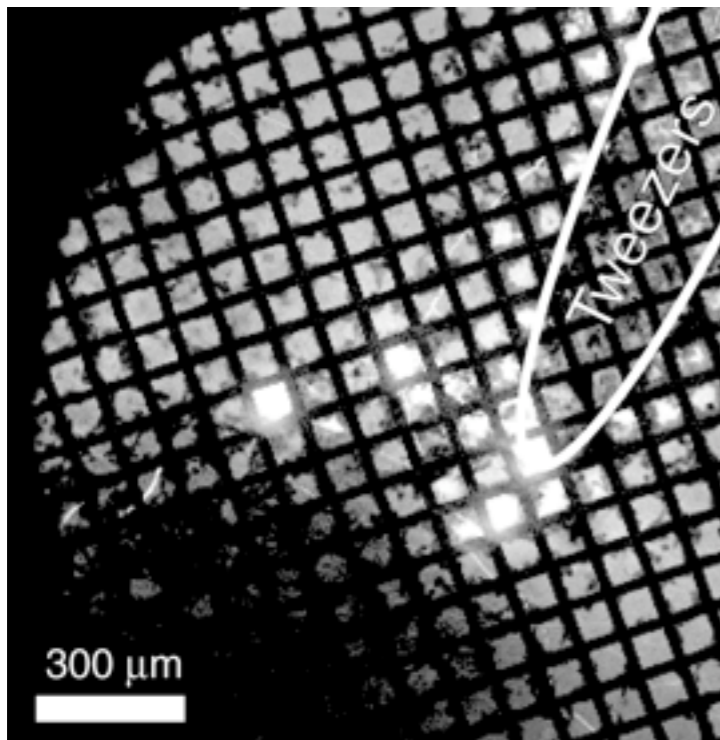
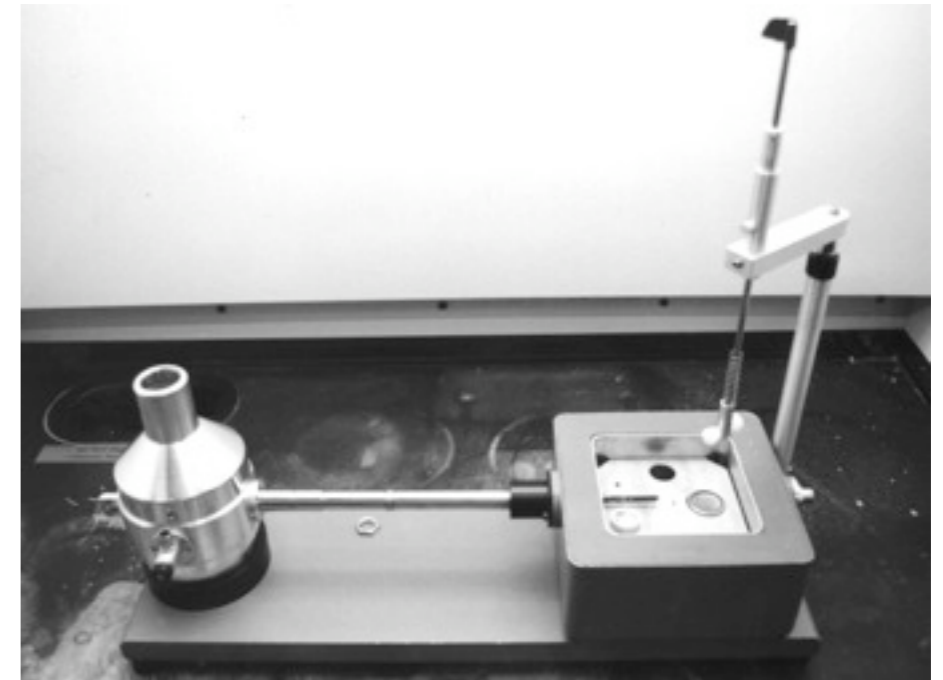
- Chromosomes are among the most sensitive specimens.
- *V. faba* chromosomes fixed in 2% glutaraldehyde. S. Williams et al., J. Microscopy **170**, 155 (1993)
- Repeated imaging of one chromosome shows mass loss, shrinkage



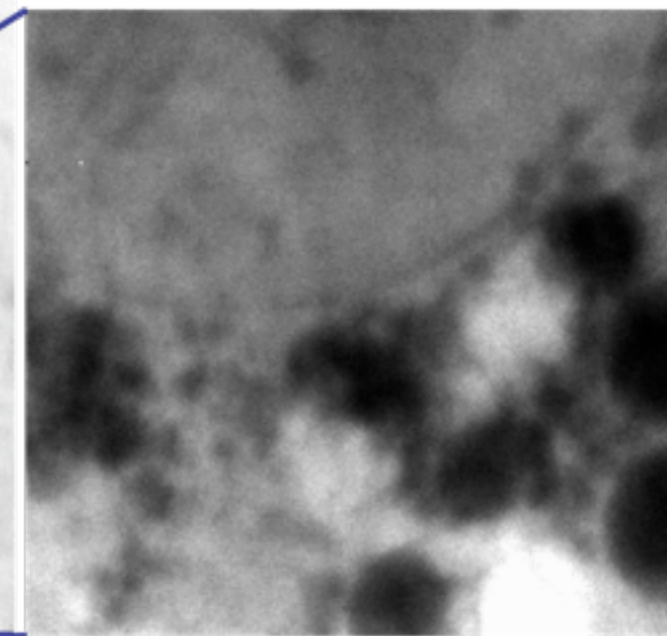
# Frozen hydrated specimens

Grids with live cells are

- Taken from culture medium and blotted
- Plunged into liquid ethane (cooled by liquid nitrogen)



Maser et al., *J. Microsc.* **197**,  
68 (2000)



7 μm

2 μm



[www.alcor.org](http://www.alcor.org)

“Cryonics is a speculative life support technology that seeks to preserve human life in a state that will be viable and treatable by future medicine [which] will include mature nanotechnology”



“Following vitrification, neuropatients are placed in individual aluminum containers”



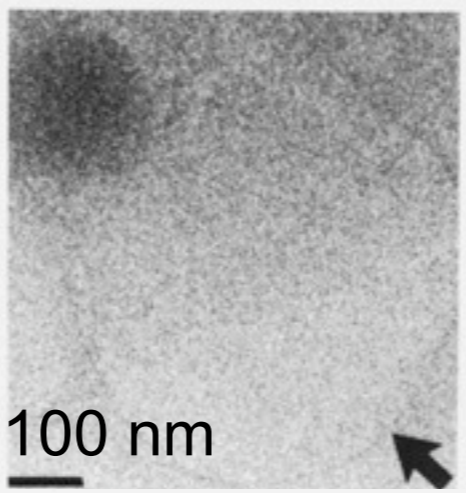
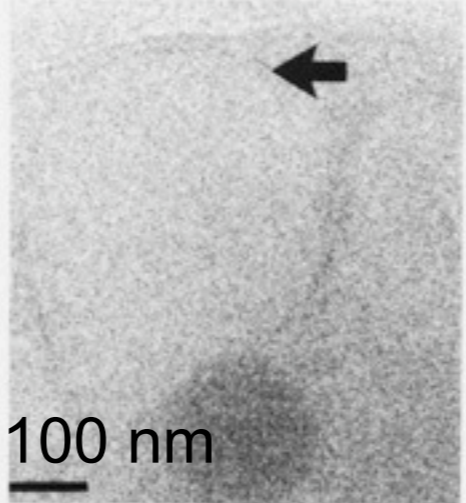
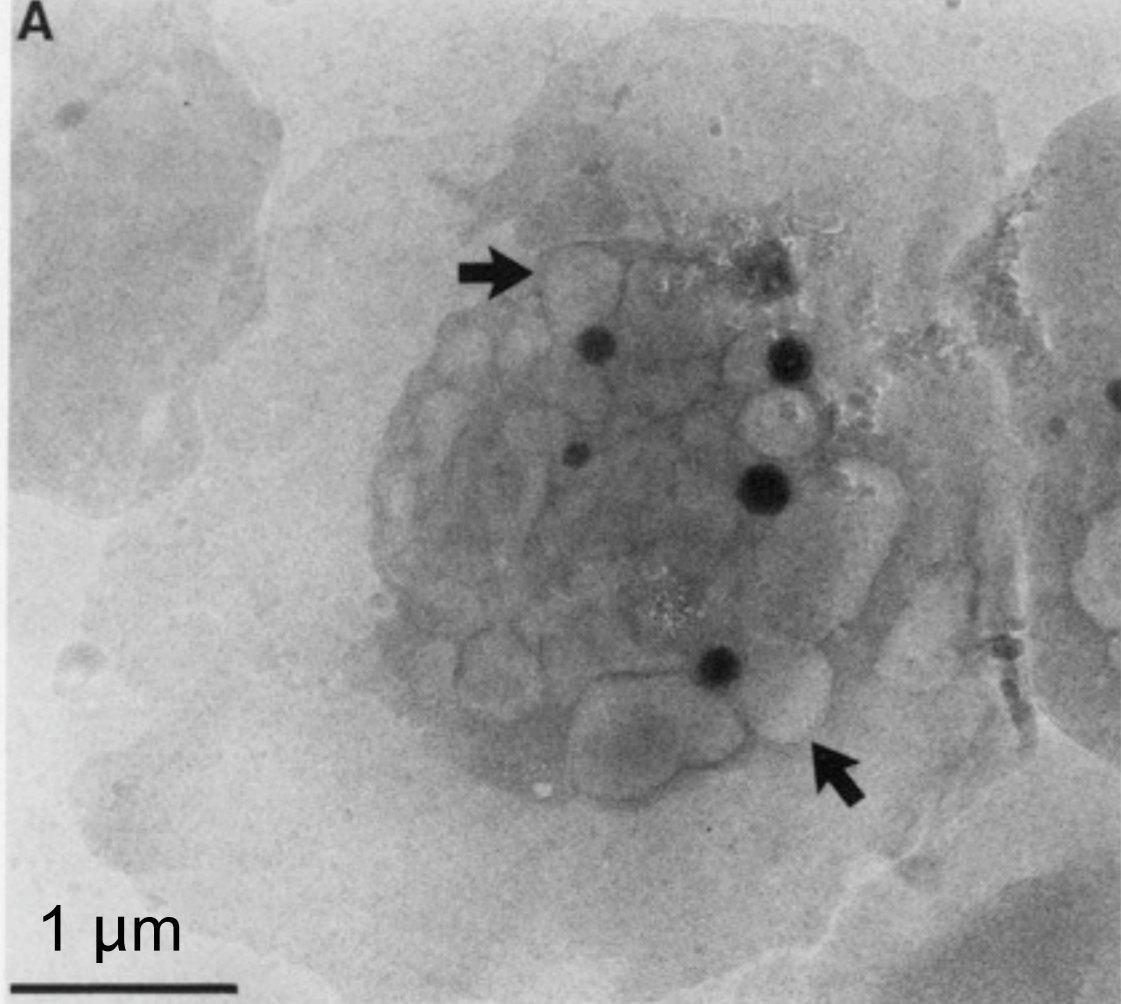
**“Cryonics cannot work for anyone who is truly brain dead”**



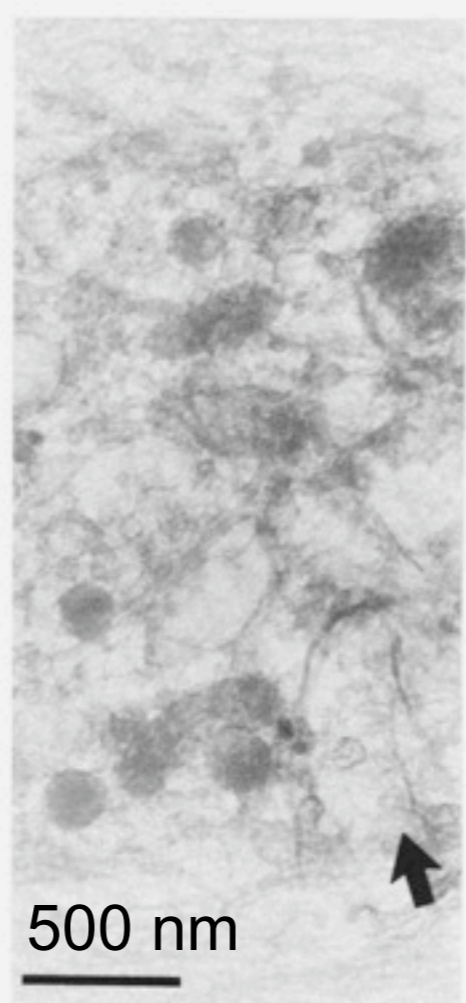
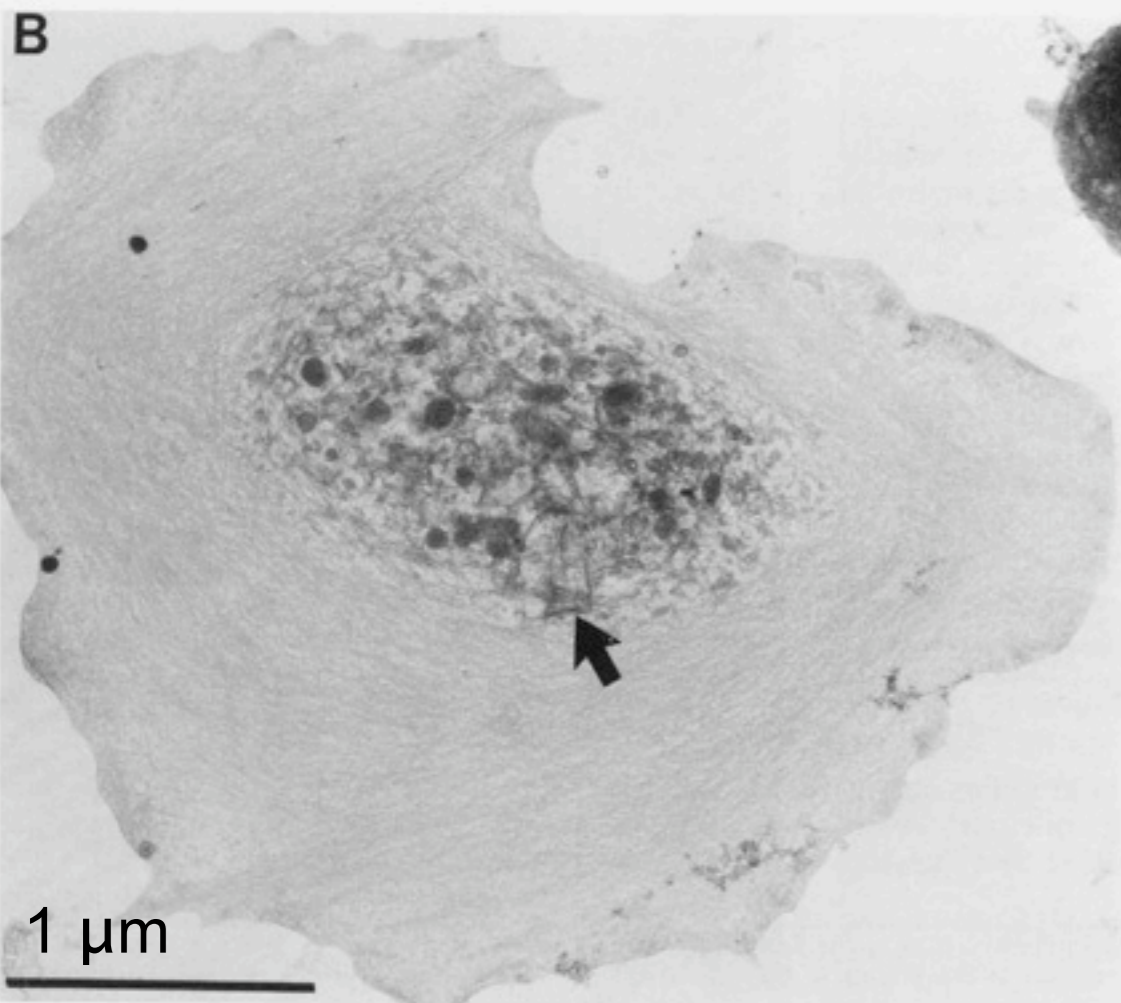
The Frozen Dead (1966)



*Futurama's*  
producer and  
lead writer



Frozen hydrated



2% glutaraldehyde fix  
1% OsO<sub>4</sub> postfix  
critical-point dry

- Human blood platelets
- 1 MeV transmission electron microscope (JEOL-1000)
- O'Toole, Wray, Kremer, and McIntosh, *J. Struct. Bio.* **110**, 55 (1993)

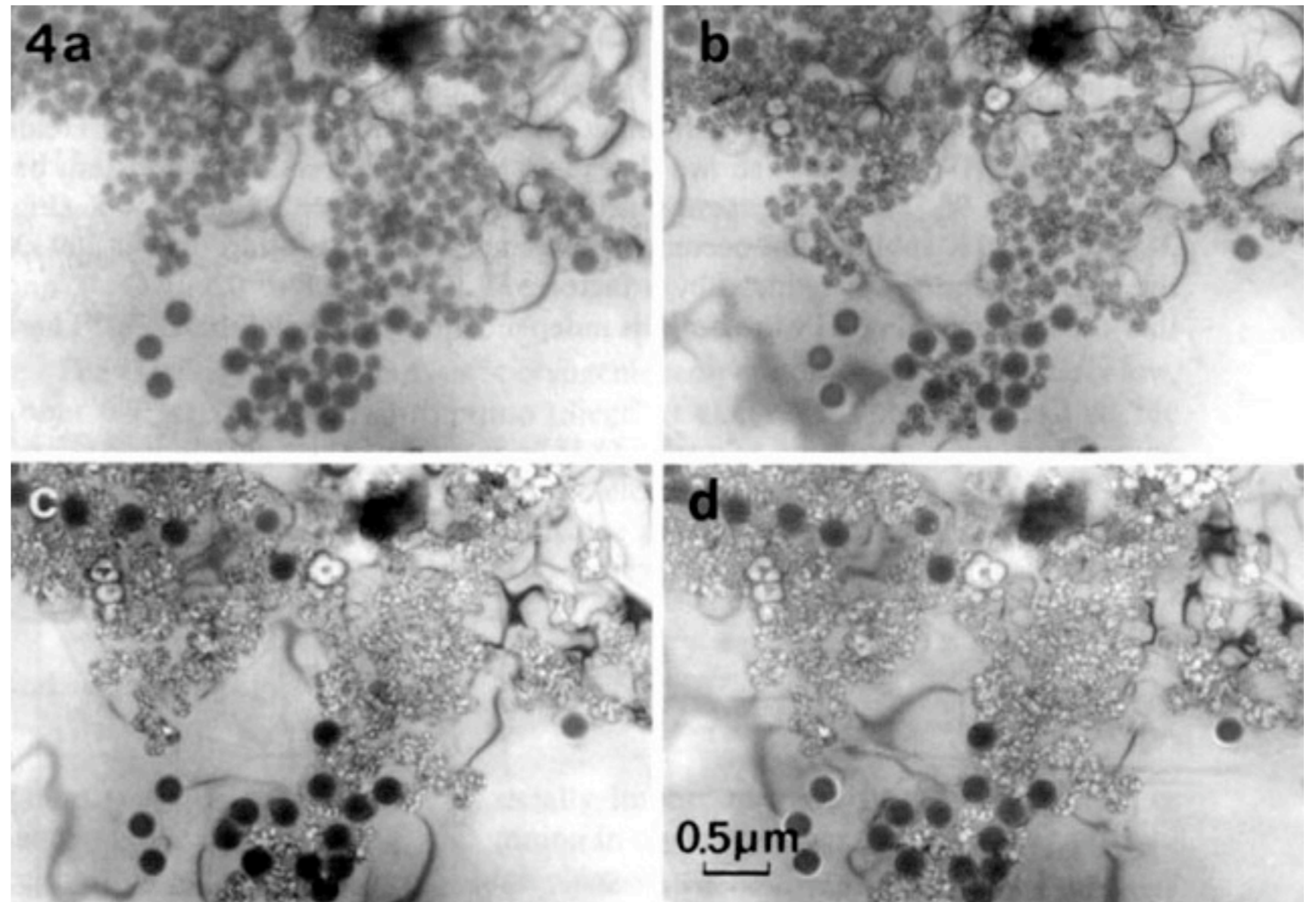
# Electrons: frozen hydrated

Polymer spheres in amorphous ice viewed with low dose rate at 100 keV

Smaller spheres: PMMA

Larger spheres: PS  
Doses are in Gray

From Y. Talmon, in Steinrecht and Zierold, **Cryotechniques in Biological Electron Microscopy** (Springer, 1987)

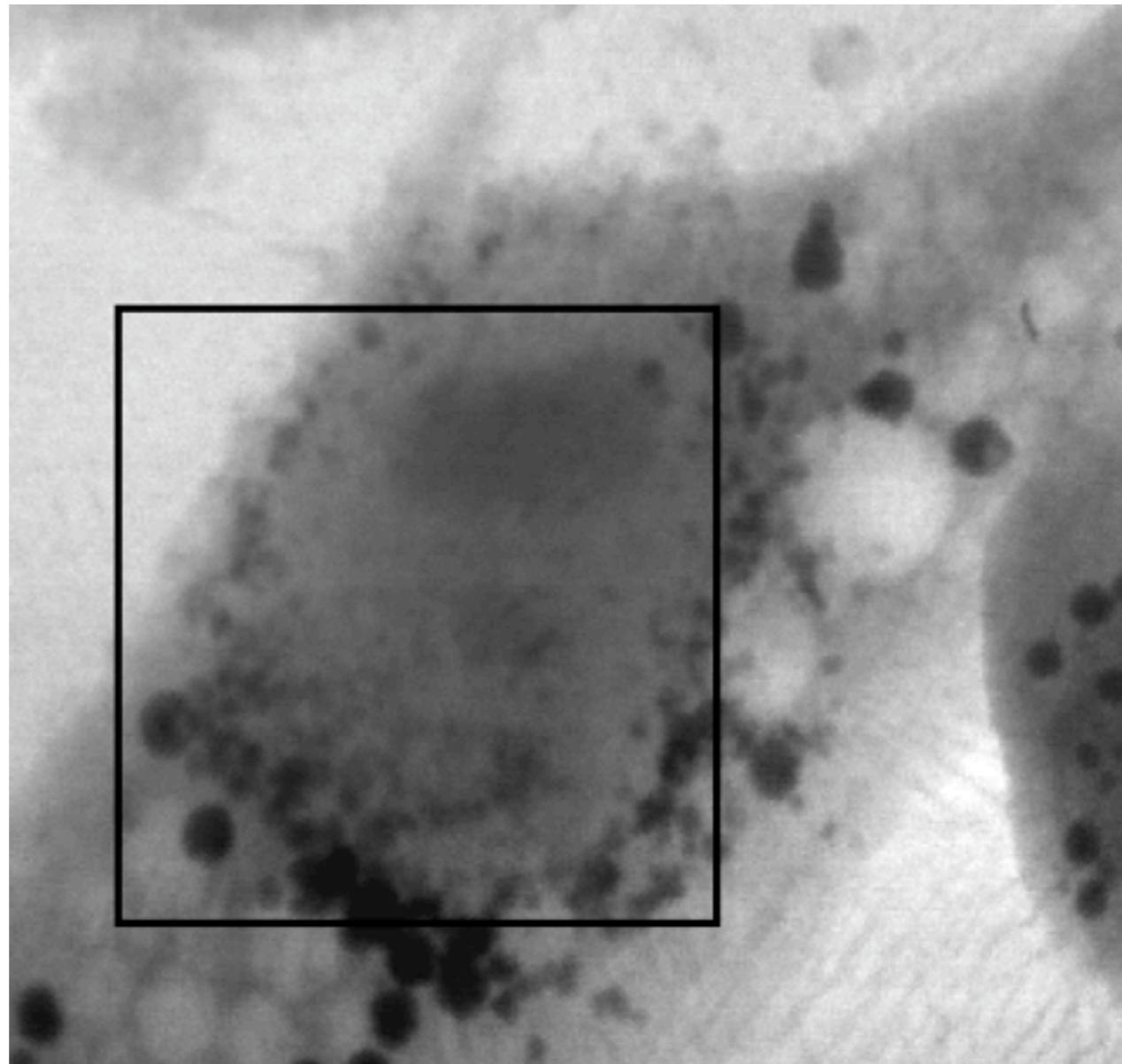


“Bubbling” dose in cryo electron microscopy:  $\sim 1000 \text{ e}^-/\text{nm}^2$  or about  $3 \times 10^7$  Gray. Bubbles: hydrogen gas [Leapman, Ultramic. **59**, 71 (1995); Sun et al., J. Mic. **177**, 18 (1995)]

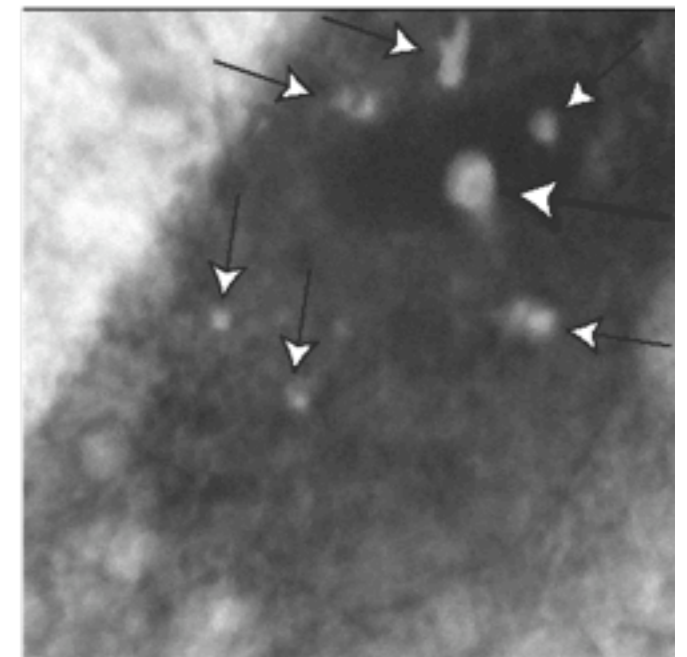
# Radiation damage resistance in cryo

Left: frozen hydrated image **after** exposing several regions to  $\sim 10^{10}$  Gray

Right: after warmup in microscope (eventually freeze-dried): holes indicate irradiated regions!

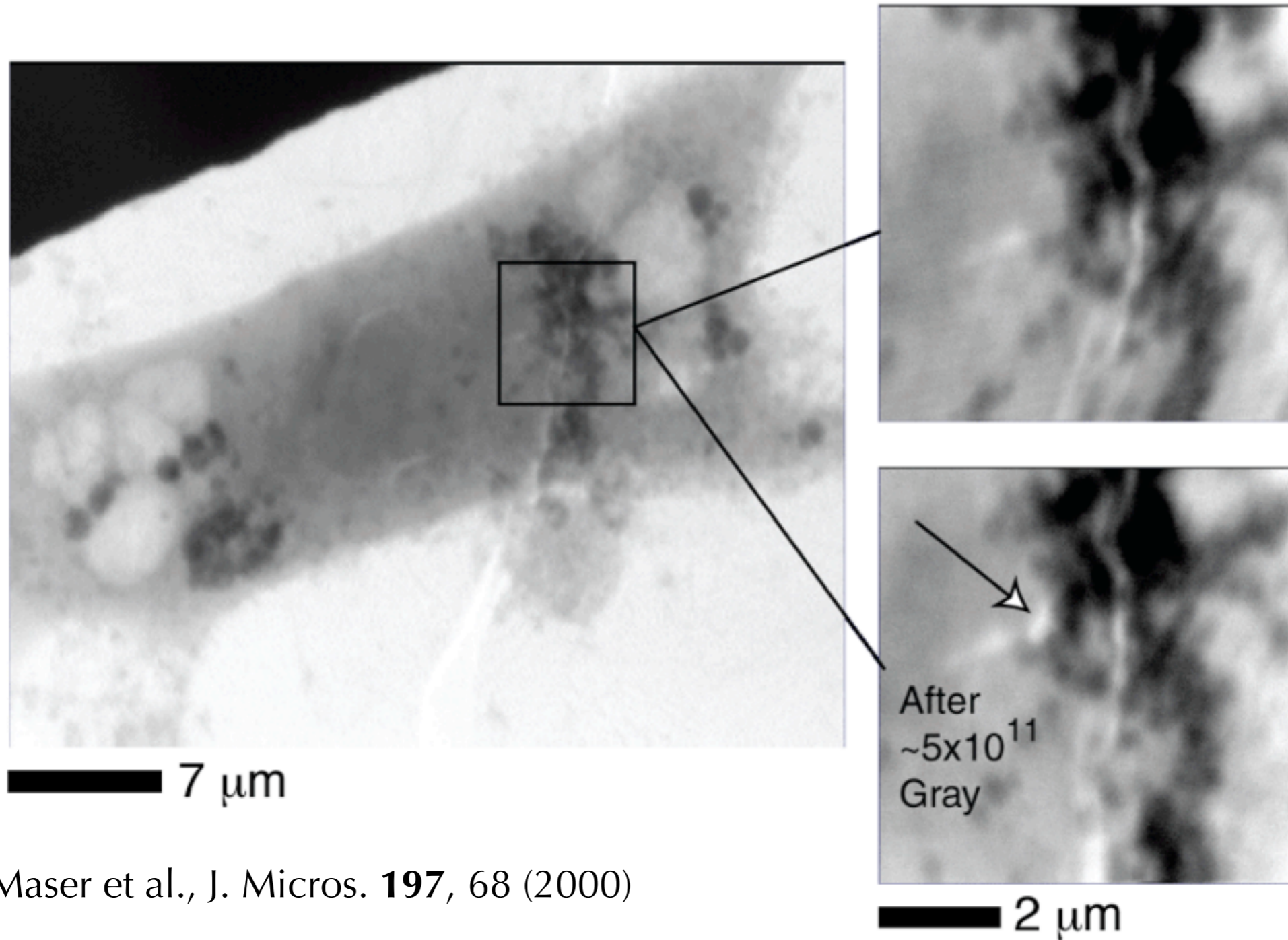


Maser et al., J. Microsc. **197**, 68 (2000)



— 7  $\mu\text{m}$

# Hints of damage?



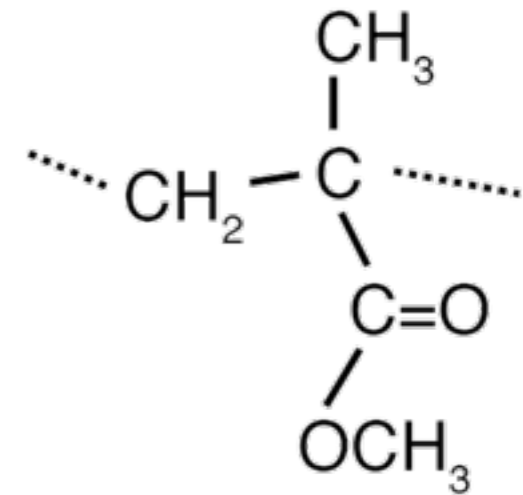
Maser et al., J. Micros. **197**, 68 (2000)

Note: we have never seen “bubbling” with soft x-rays. Lower relative dose in water, plus lower dose rate to allow for gas diffusion?

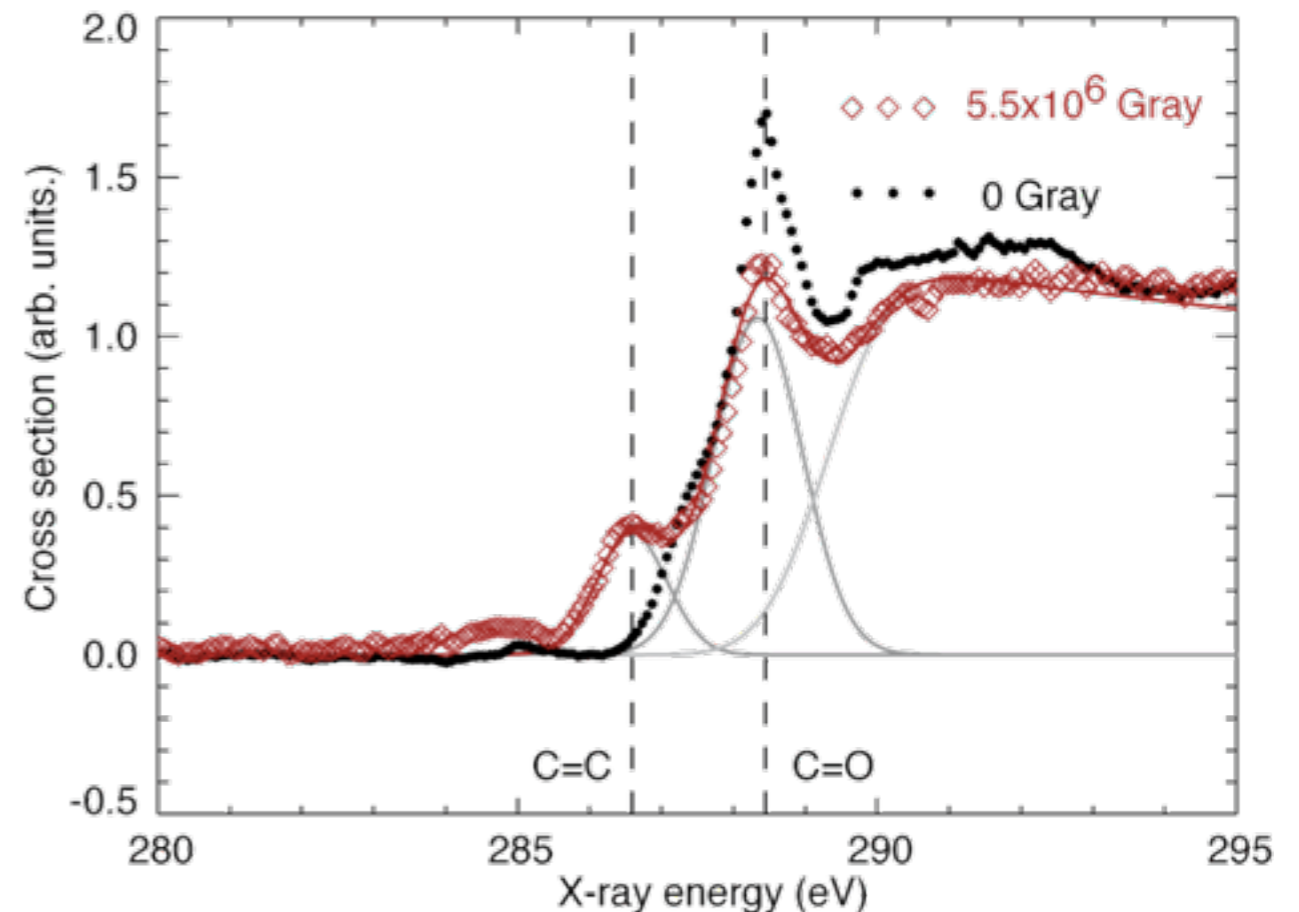
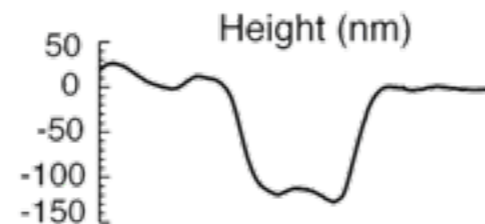
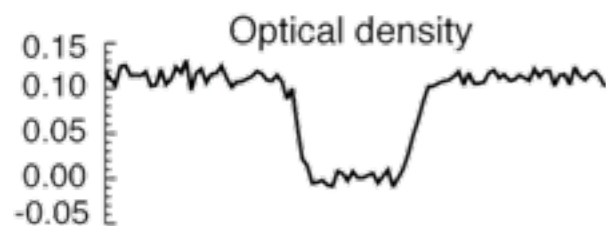
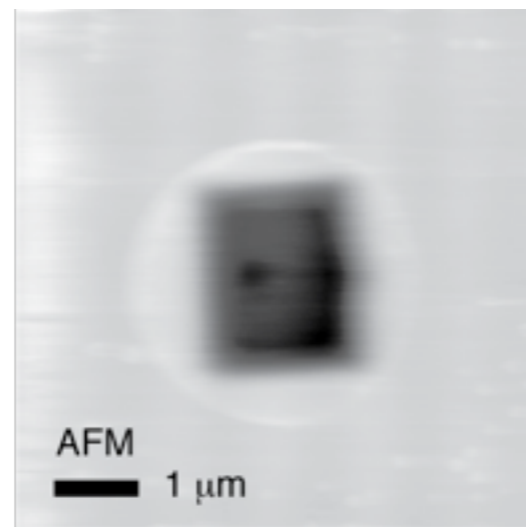
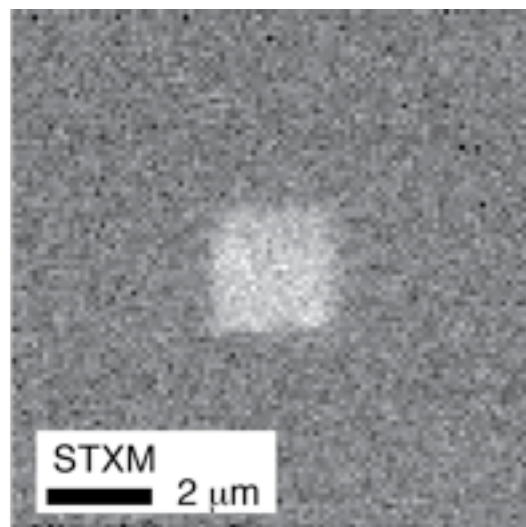


# X-ray irradiation: poly(methyl methacrylate) (PMMA)

- PMMA: poly methyl methacrylate (plexiglass!) which is especially radiation sensitive – it's used as a resist for electron beam lithography
- X. Zhang et al., J. Vac. Sci. Tech. B **13**, 1477 (1995)
- Fine step size, high flux image for dose
- Slightly defocused beam for low dose image off XANES peaks
- At end, AFM for thickness



- Defocused beam for spectrum
- Gaussian fit to measure peak strengths at XANES resonances

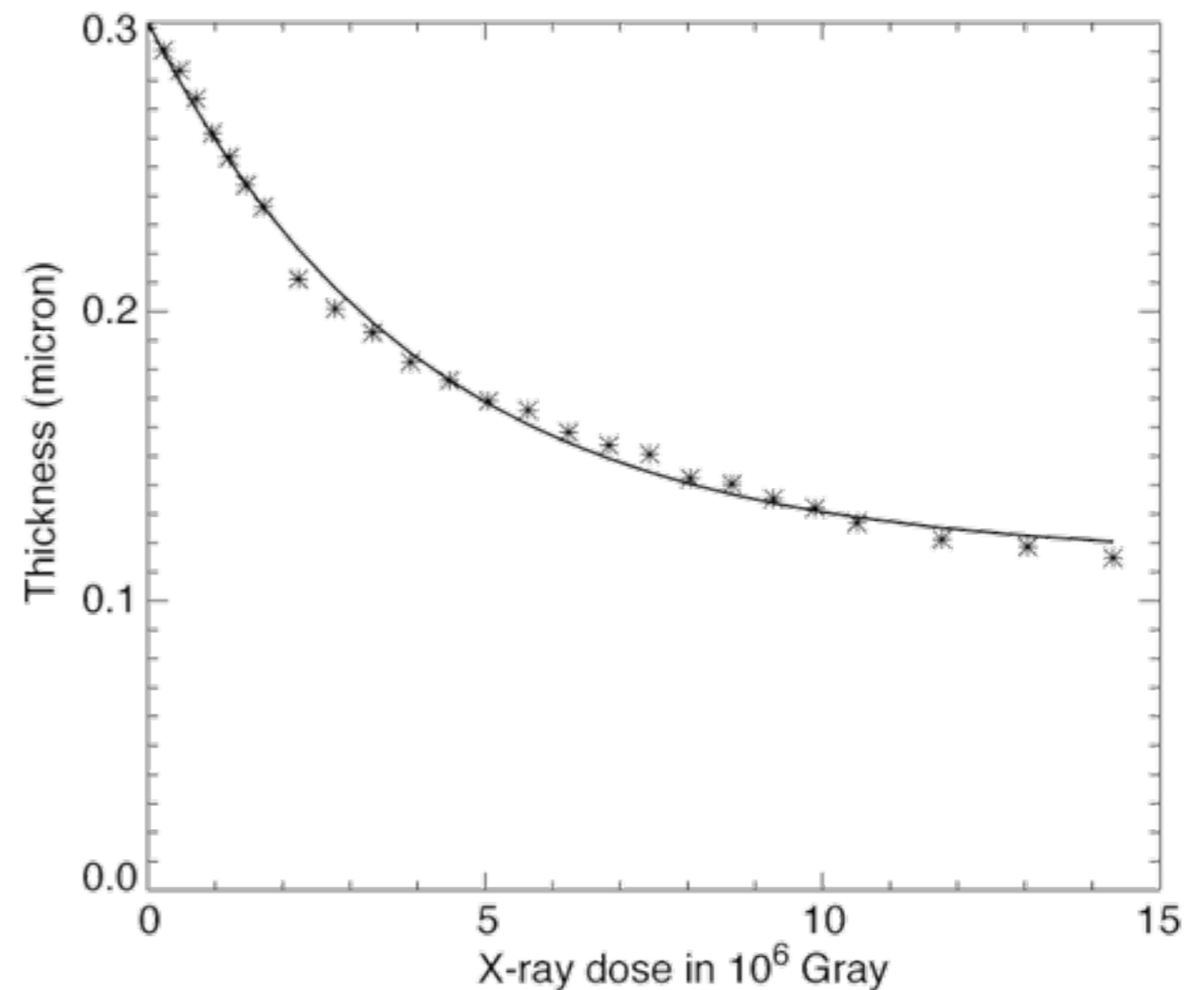
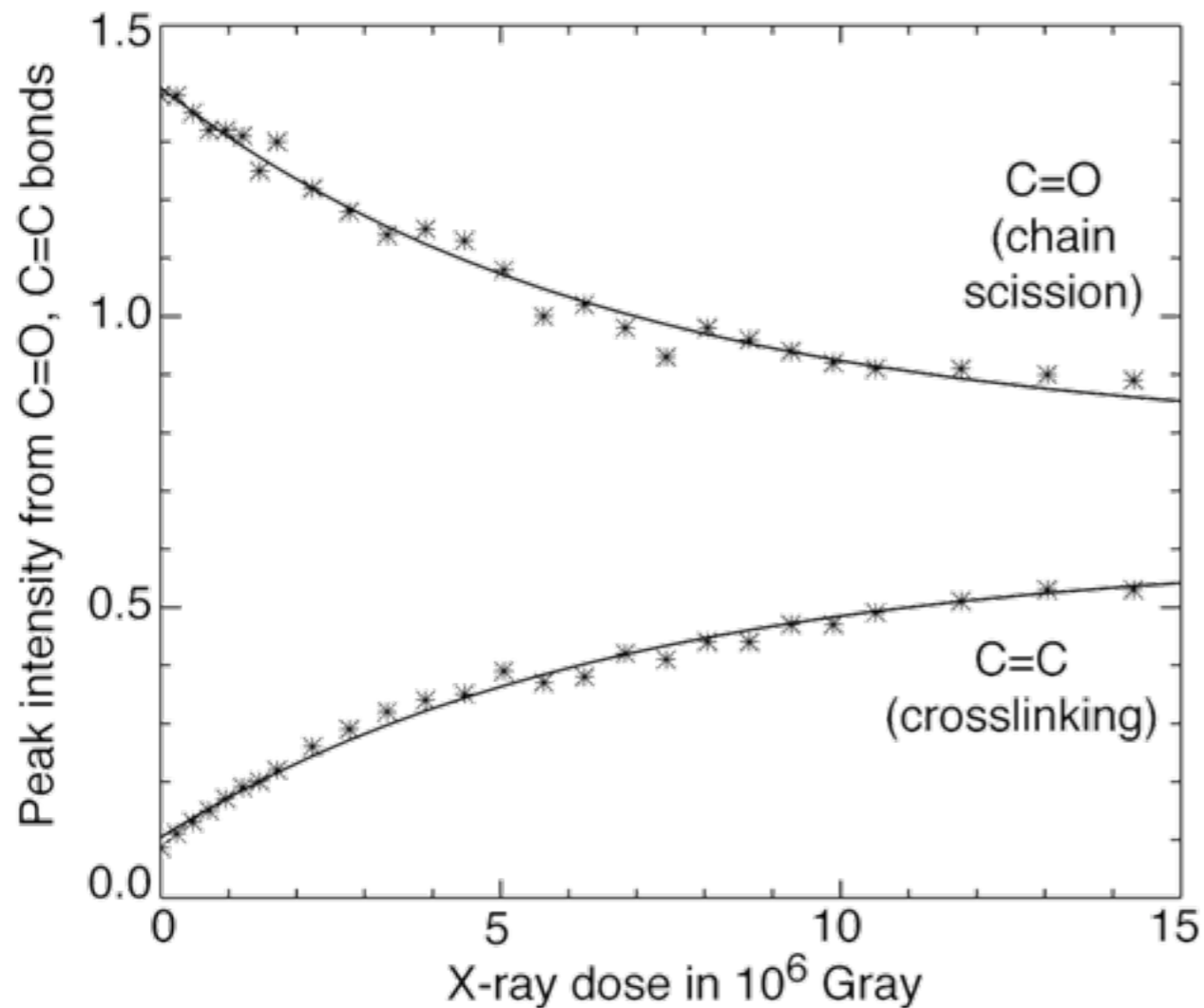


# Mass loss: small pieces fly away

X. Zhang, C. Jacobsen, S. Lindaas, S. Williams, J. Vac. Sci. Tech. B **13**, 1477 (1995)

- Chain scission: C=O peak decrease
- Crosslinking: C=C peak increase

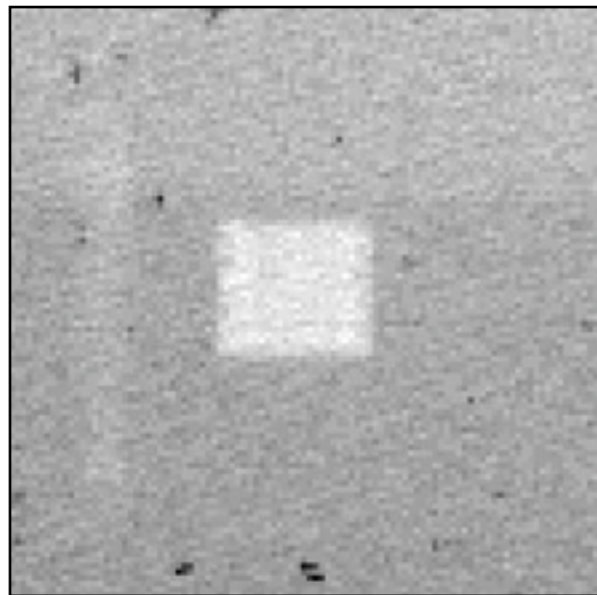
- Mass loss: optical density, AFM verification



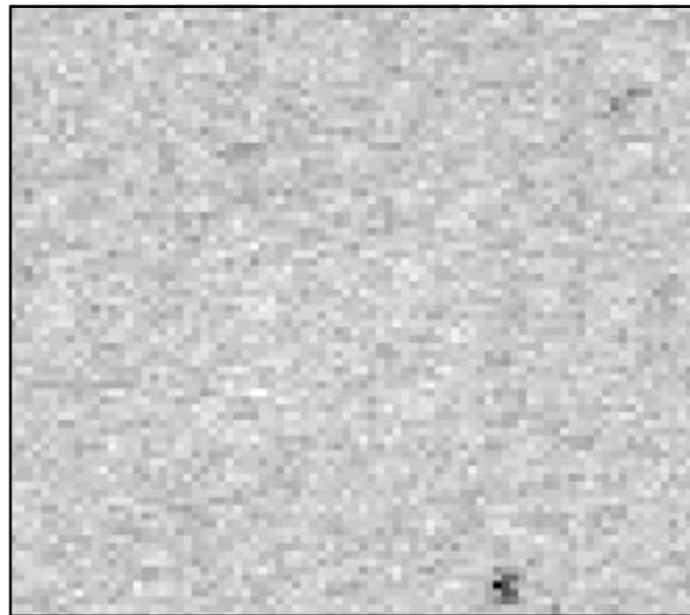
Mass spectroscopy of fragments: see Tinone et al., J. Vac. Sci. Tech. **A 13**, 1885 (1995)

# PMMA at room, LN2 temperature

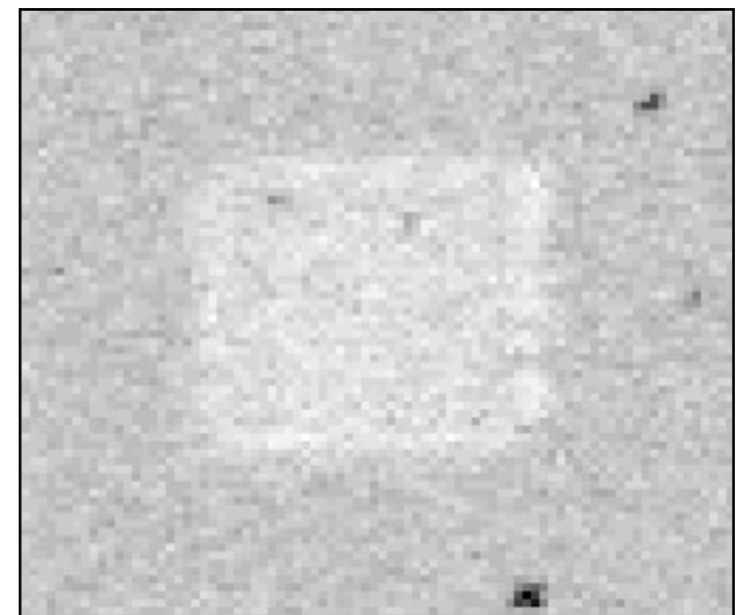
- Beetz and Jacobsen, J. Synchrotron Radiation **10**, 280 (2003)
- Repeated sequence: dose (small step size, long dwell time), spectrum (defocused beam)
- Images: dose region (small square) at end of sequence



Room temperature: mass loss immediately visible



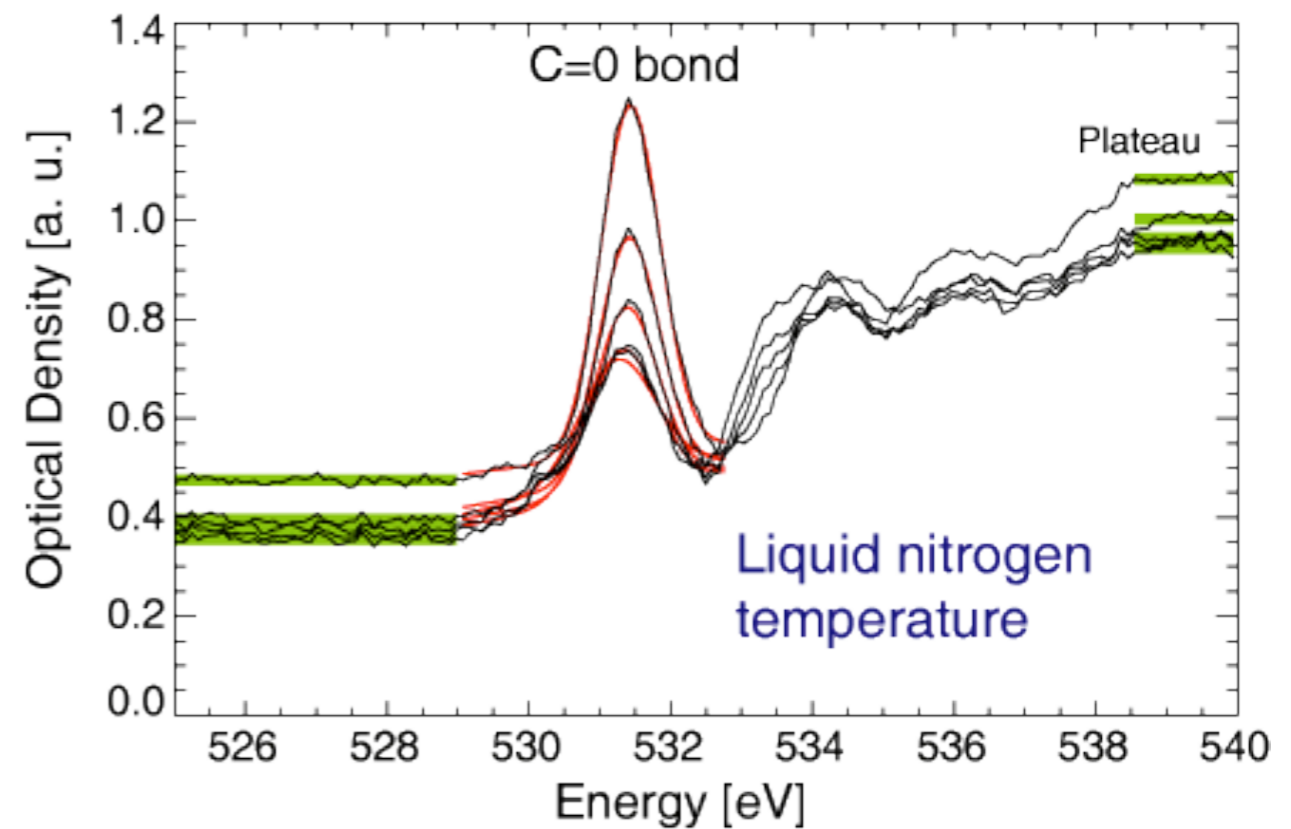
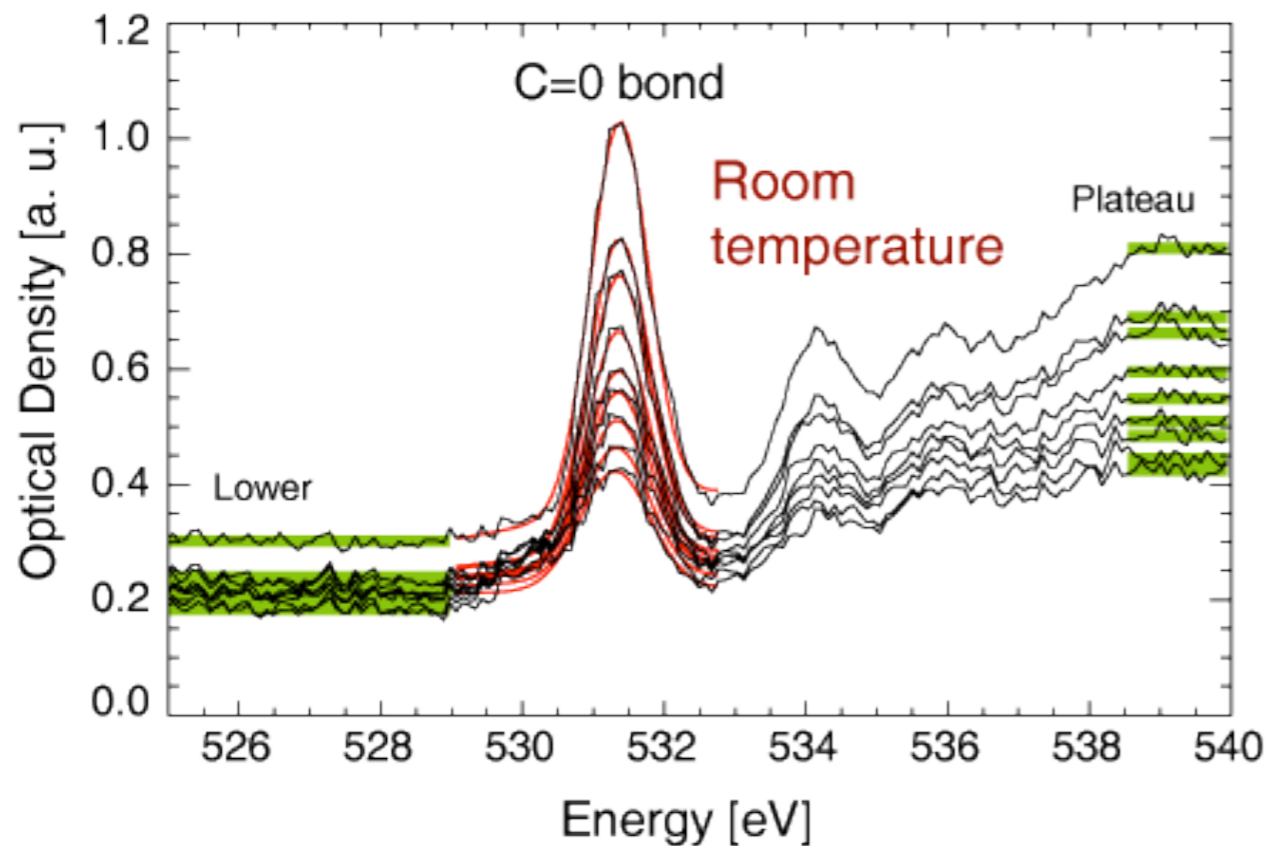
LN2 temperature: no mass loss immediately visible



After warm-up: mass loss becomes visible

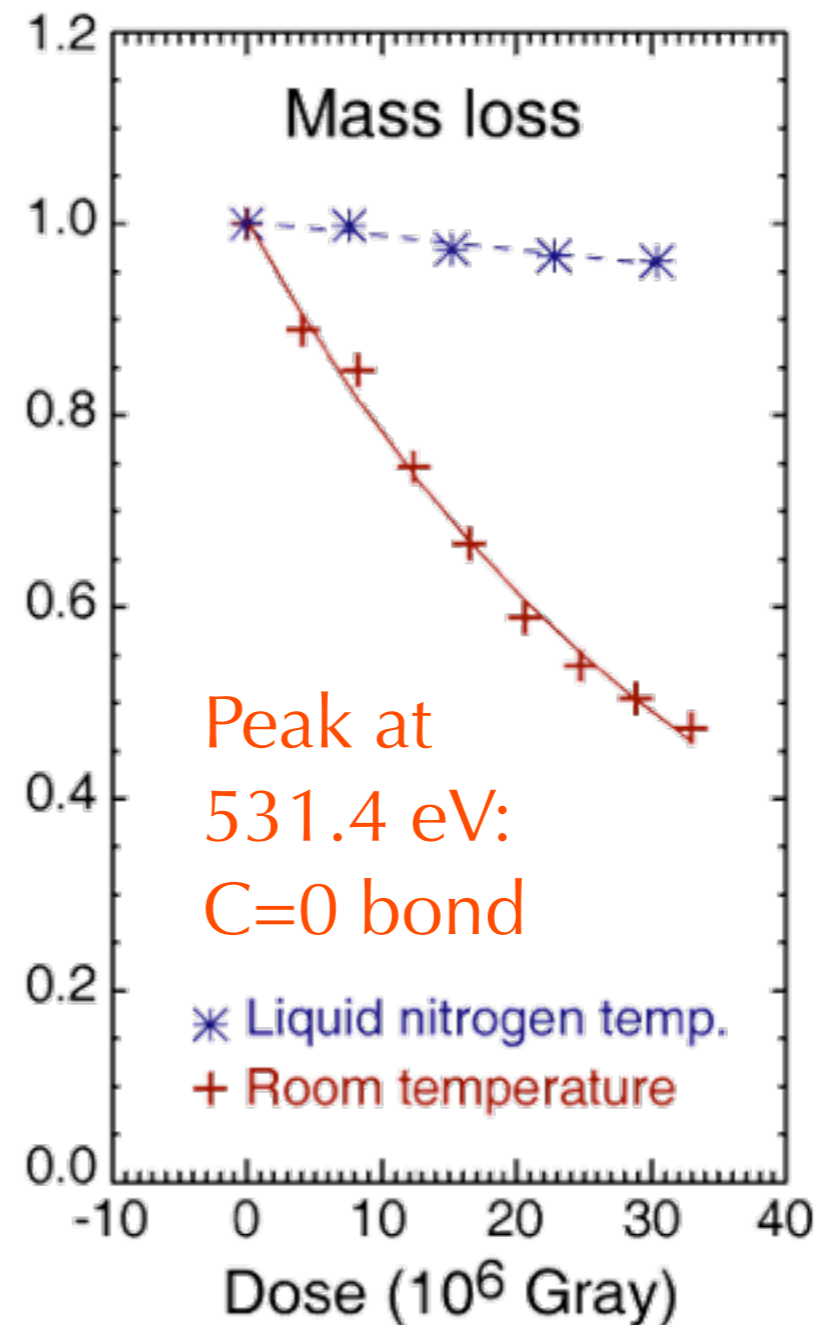
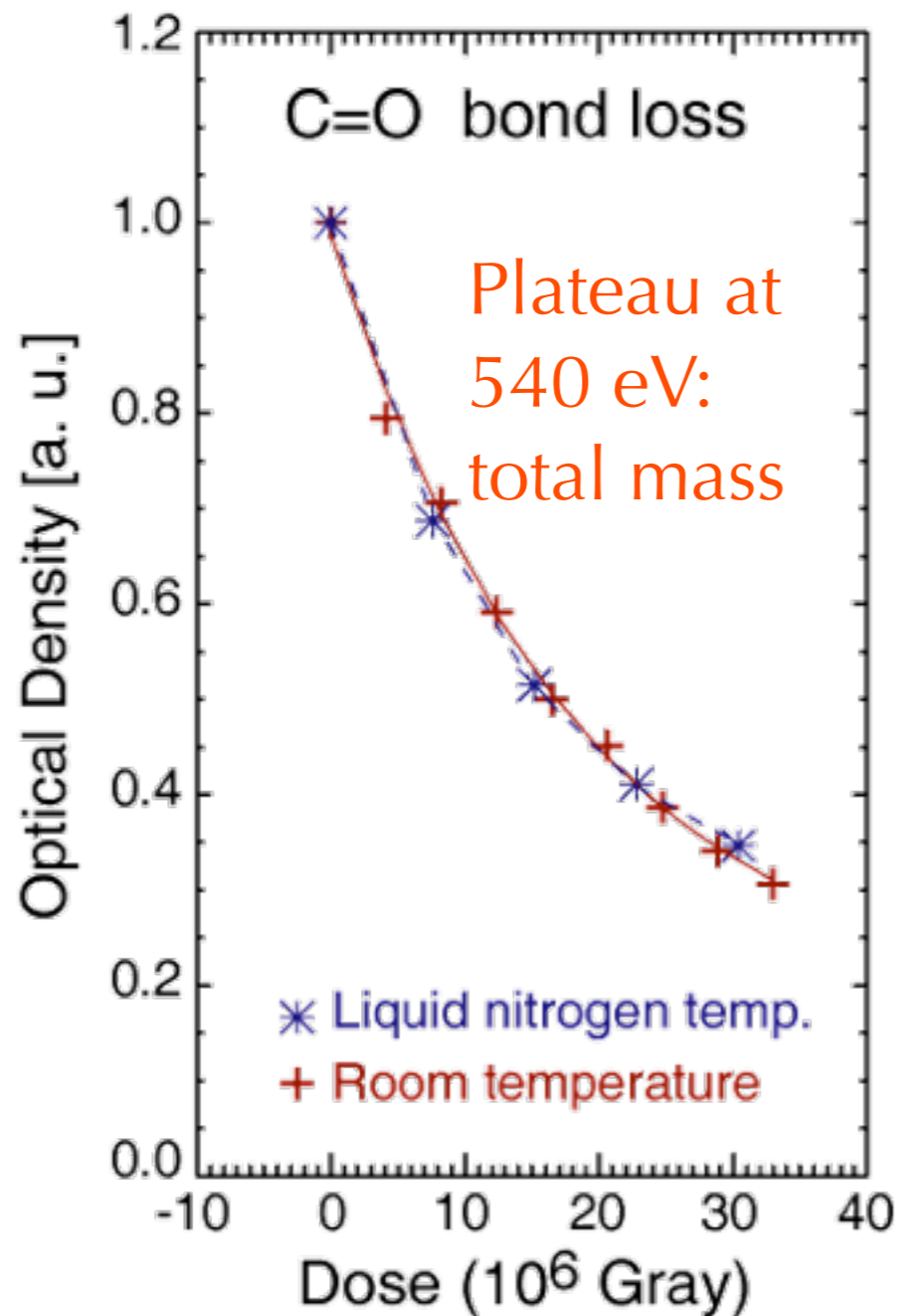
# PMMA at LN2, room temperature: XANES spectra

- Peak at 531.4 eV: C=O bond
- Plateau at 540 eV: total mass (plus some emphasis on oxygen  $\sigma^*$  bonds)
- Beetz and Jacobsen, J. Synchrotron Radiation **10**, 280 (2003)



# Results from fitting spectra

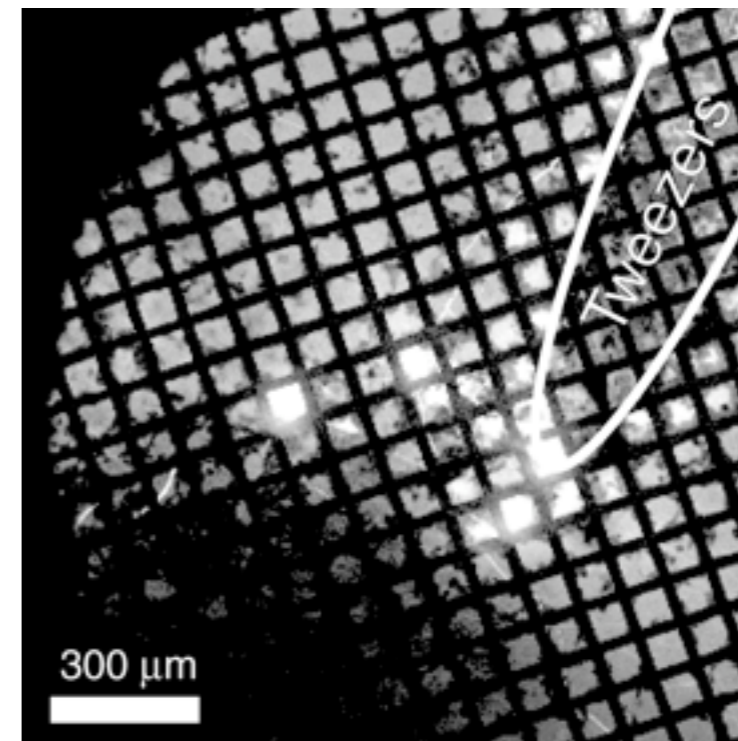
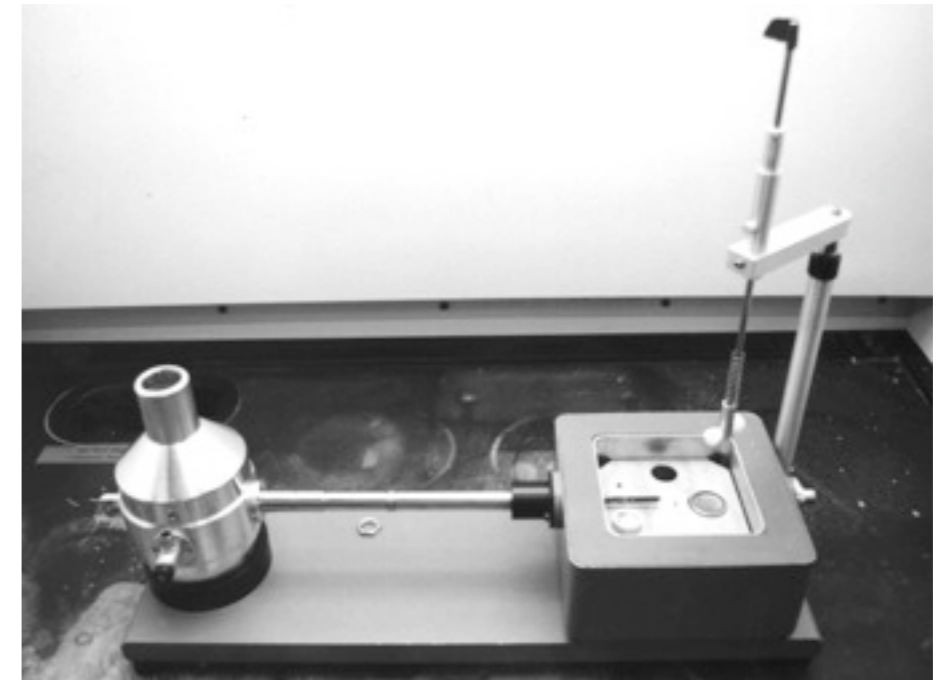
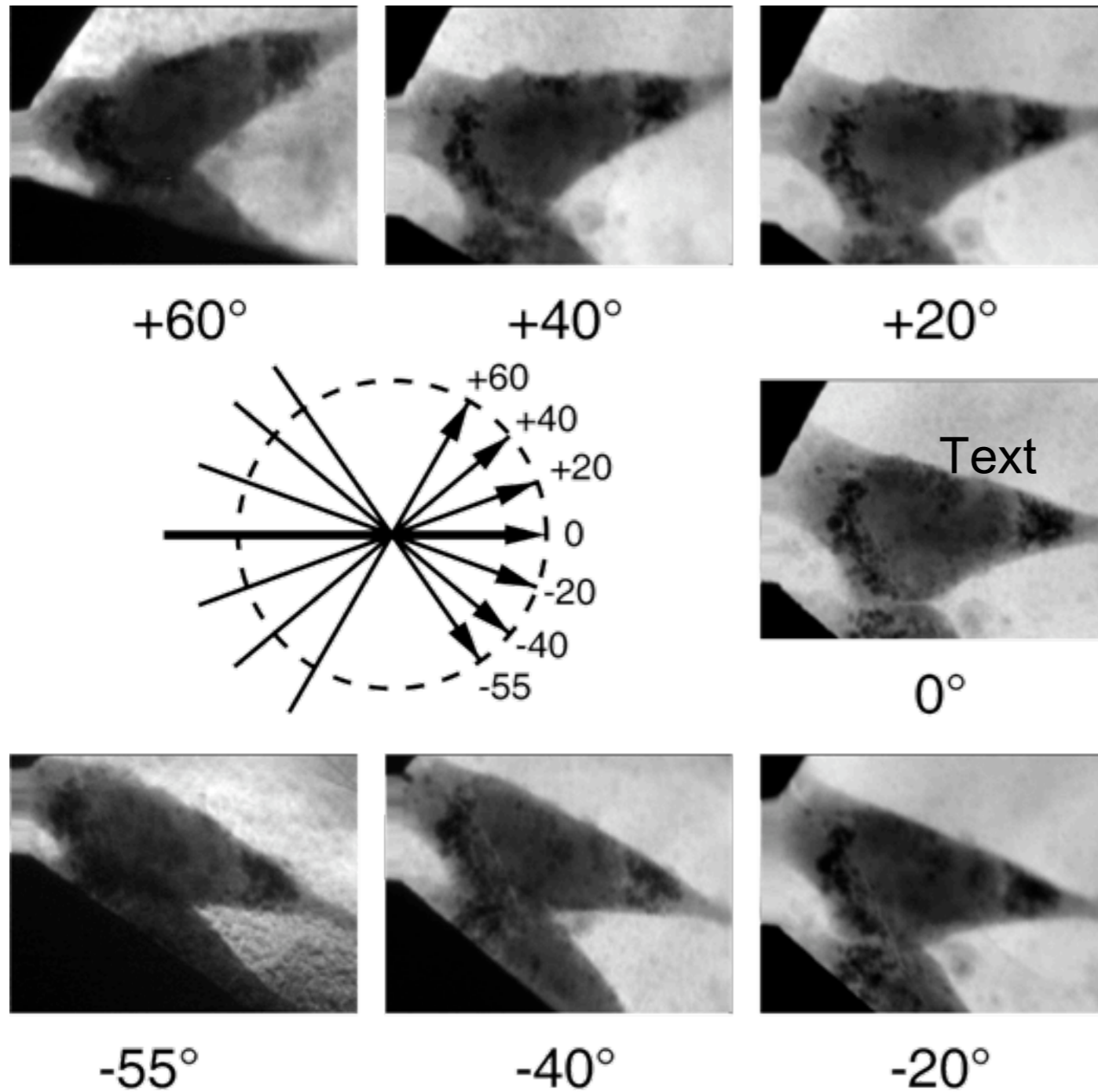
LN<sub>2</sub> temp: protection against mass loss, but not against breaking bonds  
(at least C=O bond in dry PMMA)



Beetz and Jacobsen, *J. Synchrotron Radiation* **10**, 280 (2003)

# Tomography: projections in a microscope

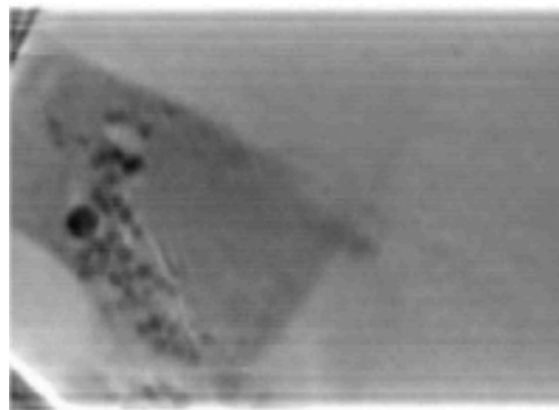
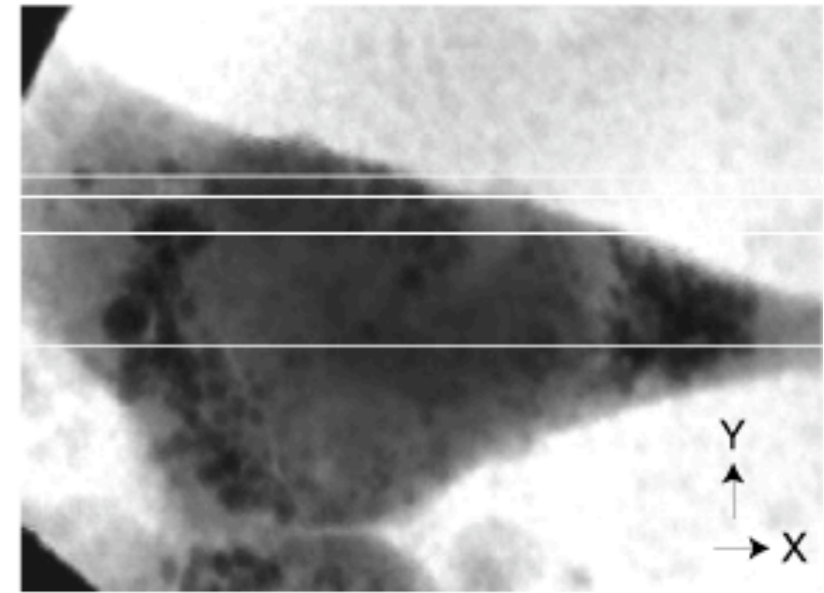
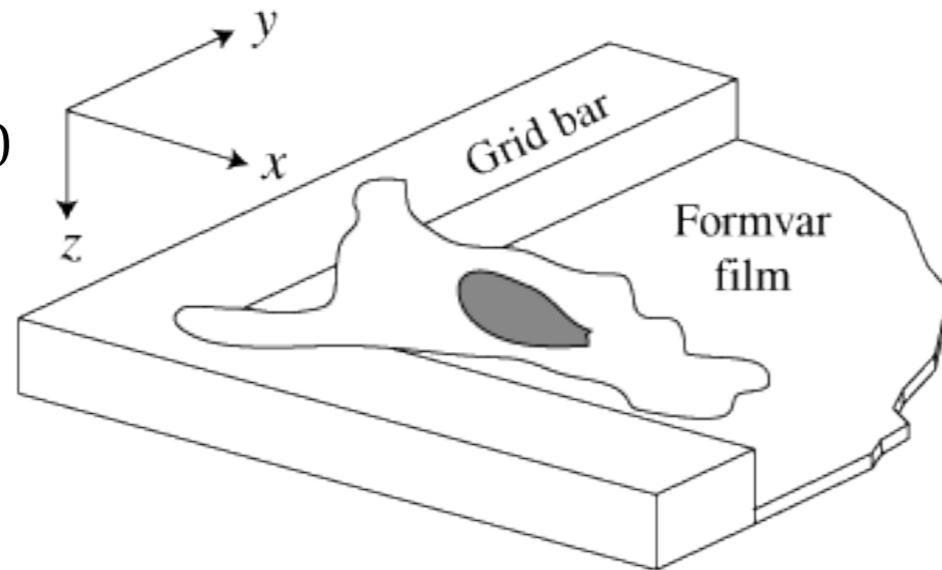
Projections of a frozen hydrated 3T3 fibroblast. Y. Wang *et al.*, *J. Microscopy* **197**, 80 (2000)



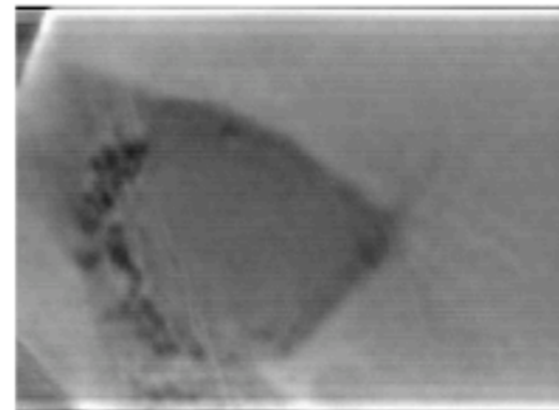
Maser *et al.*, *J. Micros.* **197**, 68 (2000)

# Fibroblast reconstruction: Z slices

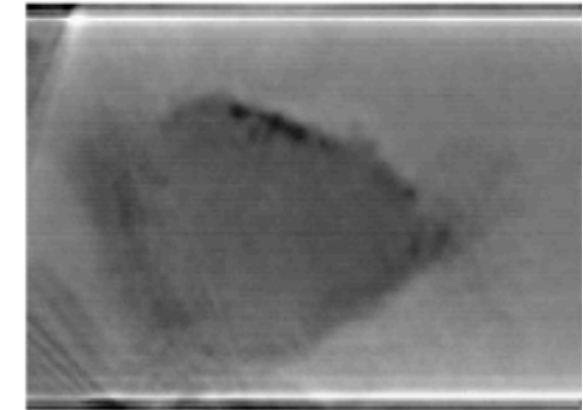
Y. Wang et al., J.  
Microscopy **197**, 80  
(2000)



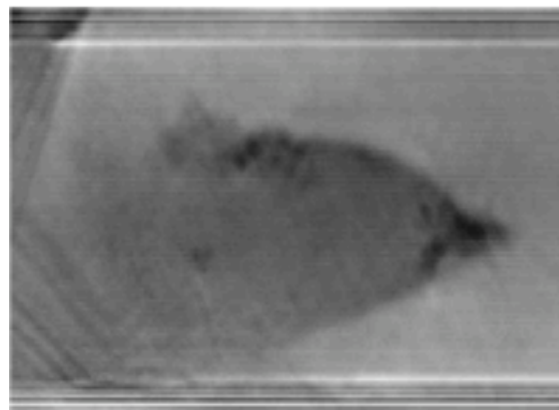
$z = 12.7 \mu\text{m}$



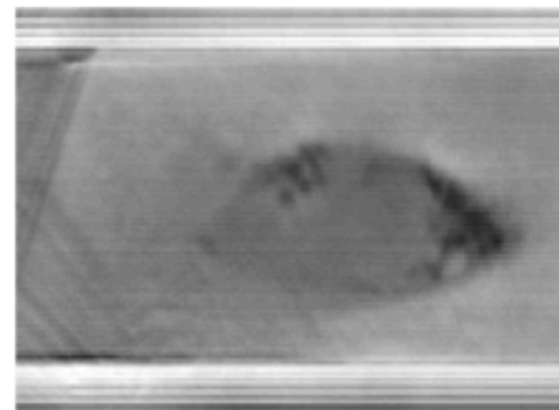
$z = 15.1 \mu\text{m}$



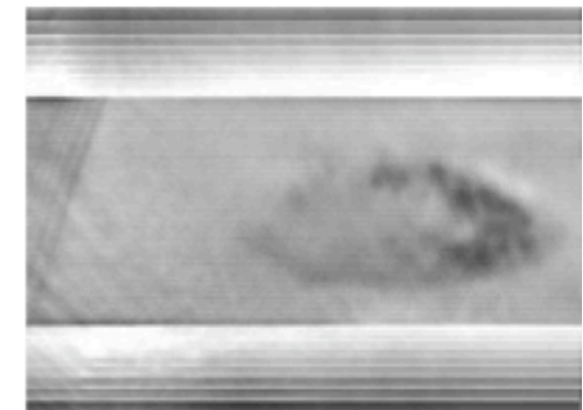
$z = 17.6 \mu\text{m}$



$z = 20.0 \mu\text{m}$



$z = 21.6 \mu\text{m}$



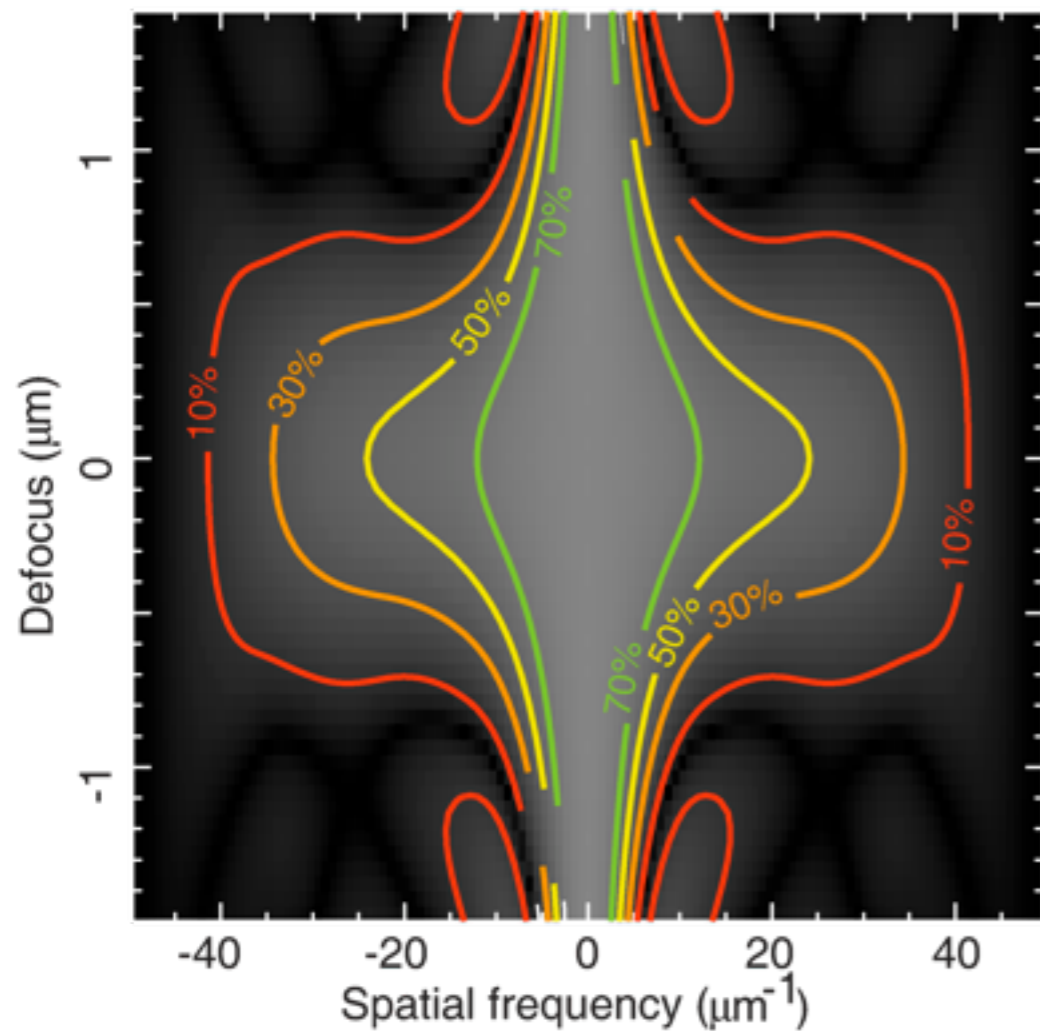
$z = 23.1 \mu\text{m}$

# 3D imaging with lenses

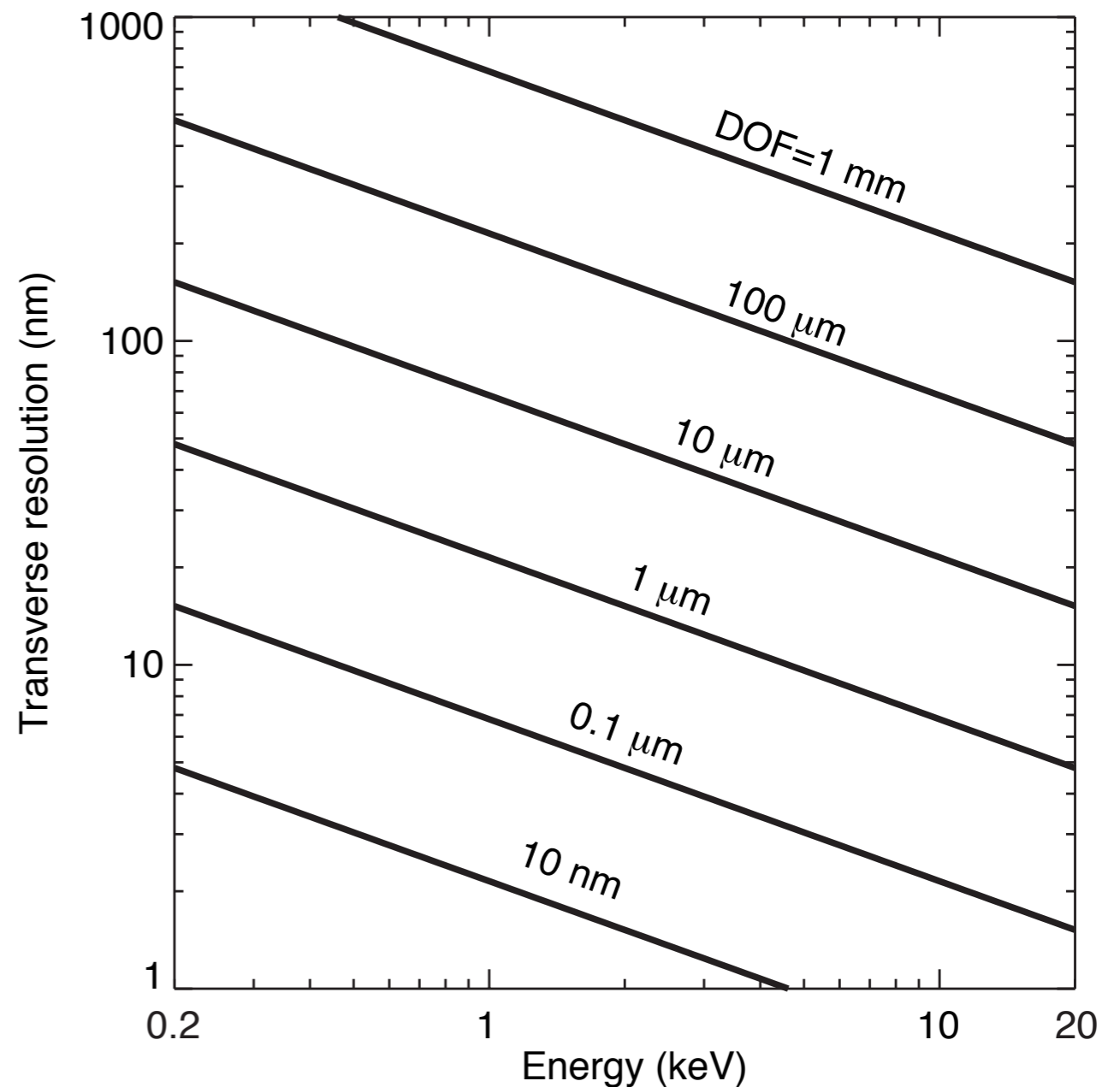
Transverse:  $\Delta_t \Rightarrow \frac{\lambda}{4\theta} = \frac{\Delta_{rN}}{2}$

Longitudinal:  $\Delta_\ell \Rightarrow \frac{\lambda}{\theta^2} = 4\Delta_{rN} \frac{\Delta_{rN}}{\lambda}$

Contrast versus defocus:  
 $\delta_{rN}=20 \text{ nm}, \lambda=2.5 \text{ nm}$



20 nm resolution at 520 eV: depth of field  $\sim 1 \mu\text{m}$

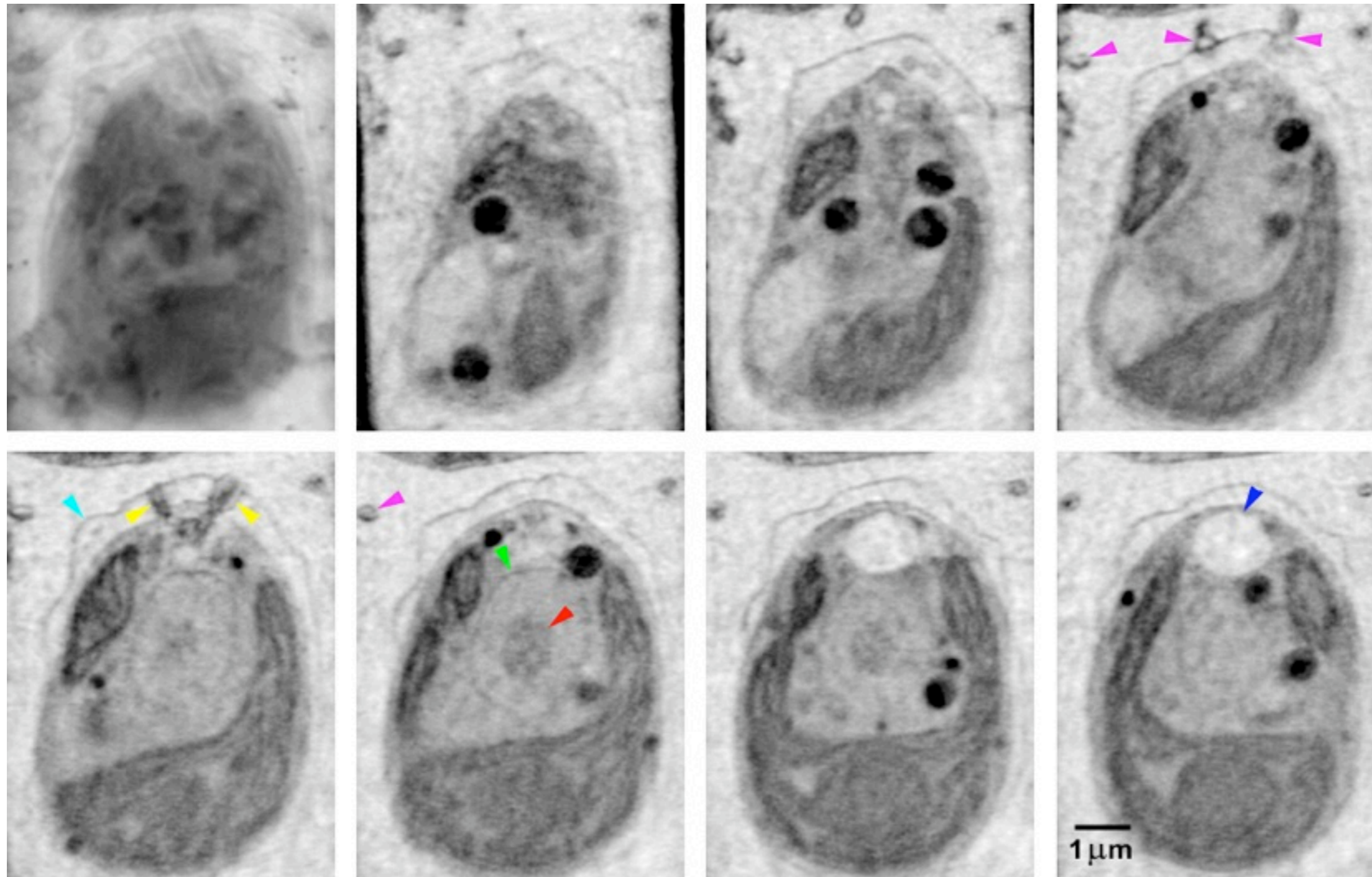


Through-focus deconvolution with lenses:

- Confocal: fully incoherent (fluorescence)
- EM: phase only, coherent
- TXM: partially coherent, equal absorption and phase contrast, need for experimental CTF



# Soft x-ray tomography of algae shock-frozen in liquid ethane: Slices through a tomographic reconstruction



- Vacuole
- Nuclear membrane
- Nucleolus
- Flagellar roots and neuromotor
- Cell wall
- Flagella

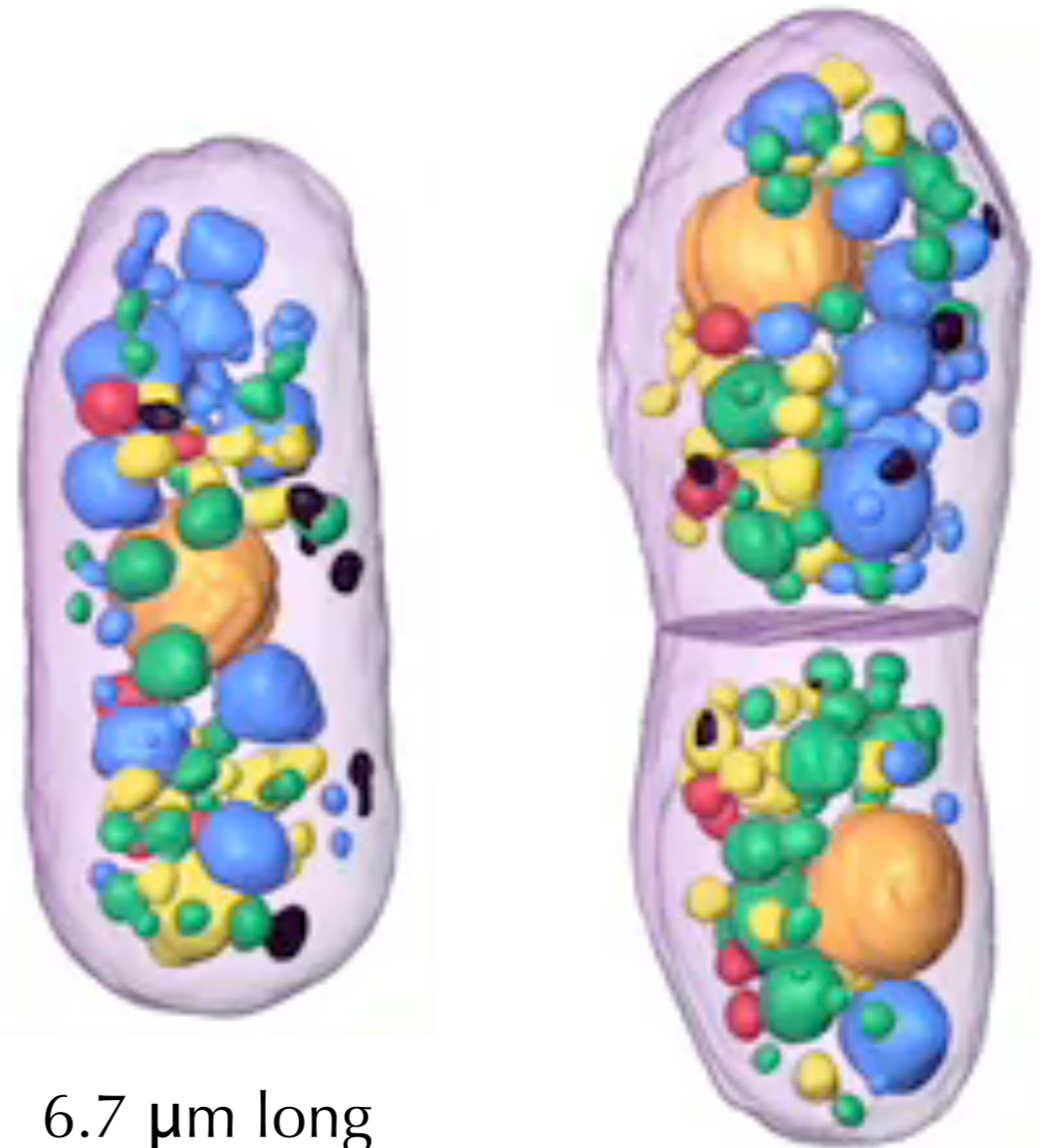
Weiss, Schneider et al., *Ultramicroscopy* **84**, 185 (2000).

See also Larabell and Le Gros, *Molecular Biology of the Cell* **115**, 957 (2004)

# National Center for X-ray Tomography

DoE/BER and NIH funded center at Advanced Light Source in Berkeley;  
sophisticated TXM for cryo tomography; Larabell, LeGros *et al.*

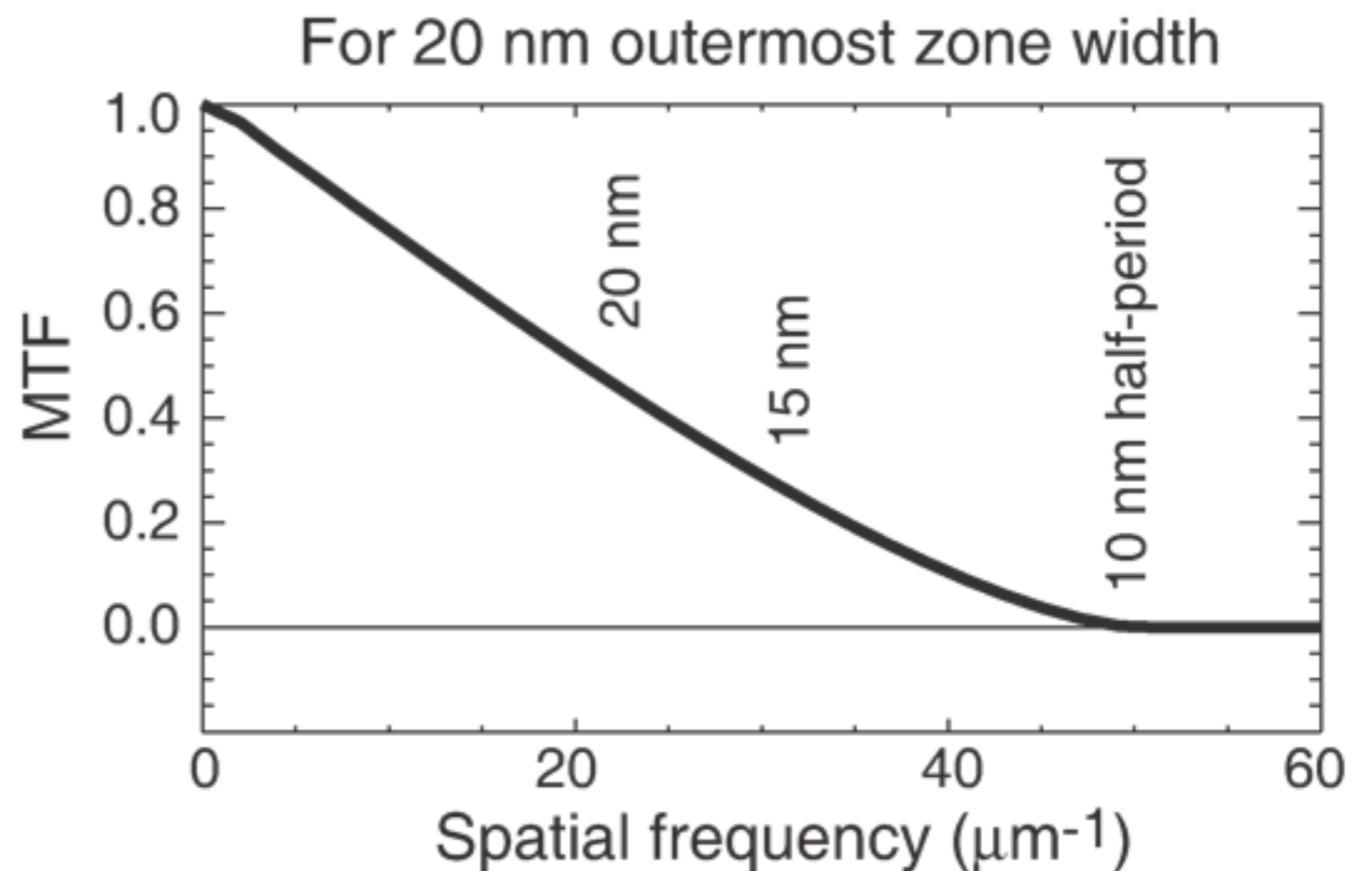
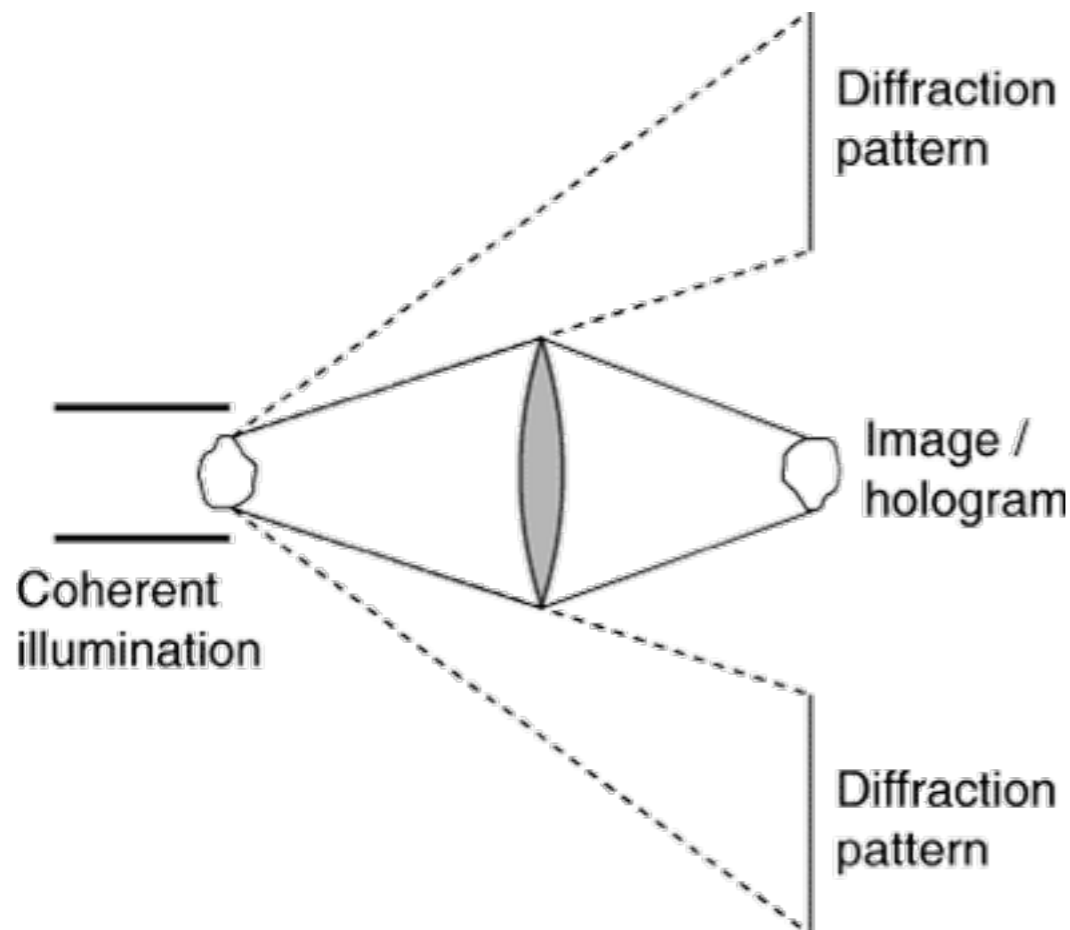
Parkinson *et al.*, *J. Struct. Bio.* **162**, 380  
(2008): fission yeast  
*Schizosaccharomyces pombe*.  
Nuclei, mitochondria, vacuoles...



6.7  $\mu\text{m}$  long

# Radiation damage sets the ultimate resolution limit

- For many specimens, radiation damage sets the ultimate limit on achievable resolution.
- Lenses phase the signal, but lose the signal. Example: 20 nm zone plate with 10% efficiency, 50% window transmission, 20% modulation transfer function (MTF) for 15 nm half-period:  
**net transfer of 1% for high spatial frequencies**
- Can we avoid this ~100x signal loss, and also go beyond numerical aperture limit of available optics?



# Phase matters

Image  $\rightarrow$  Fourier transform  $\rightarrow$  zero magnitude or phase  $\rightarrow$  inverse Fourier transform



Malcolm Howells  
at La Clusaz

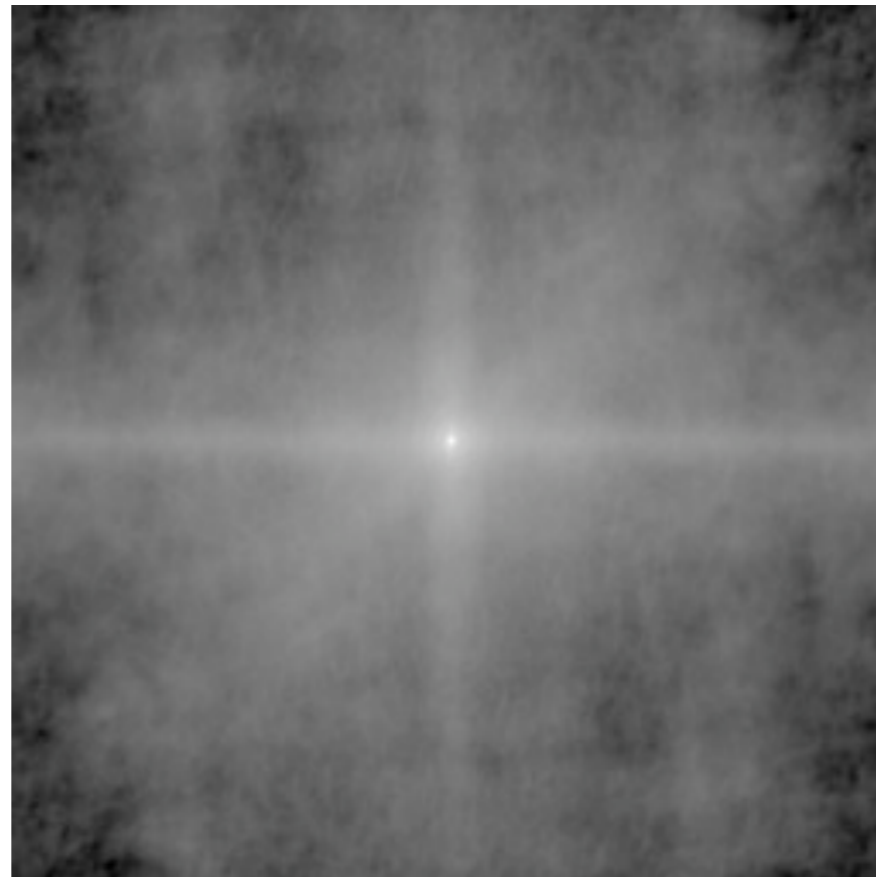


Image using only  
Fourier magnitudes

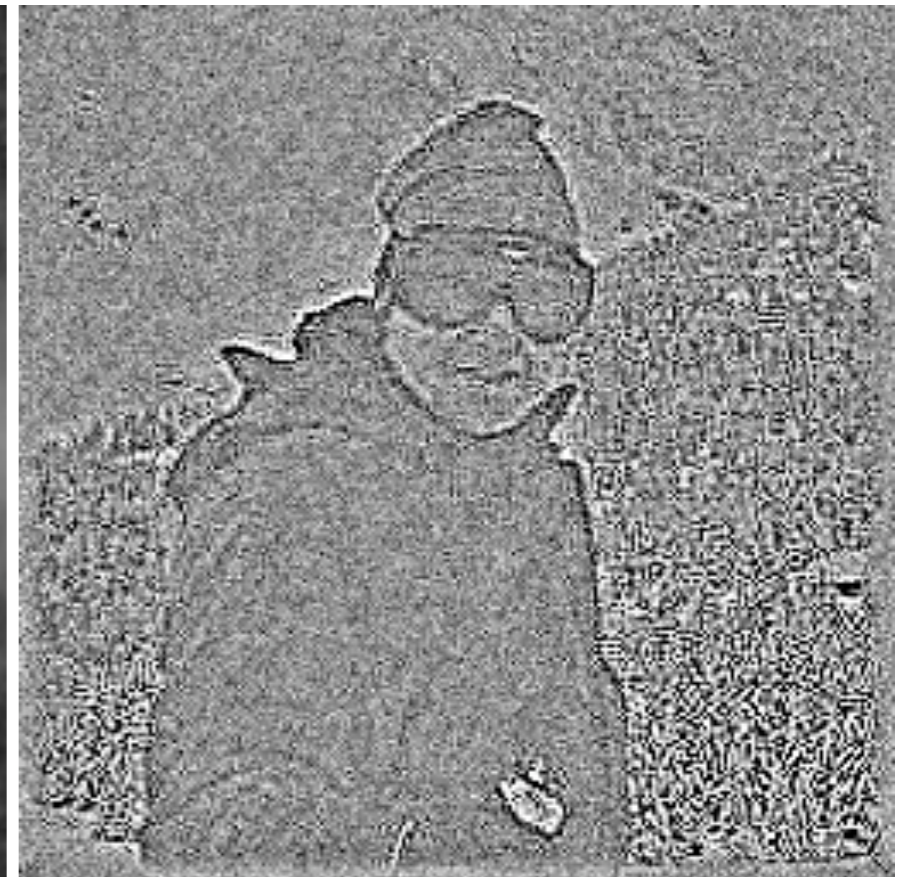
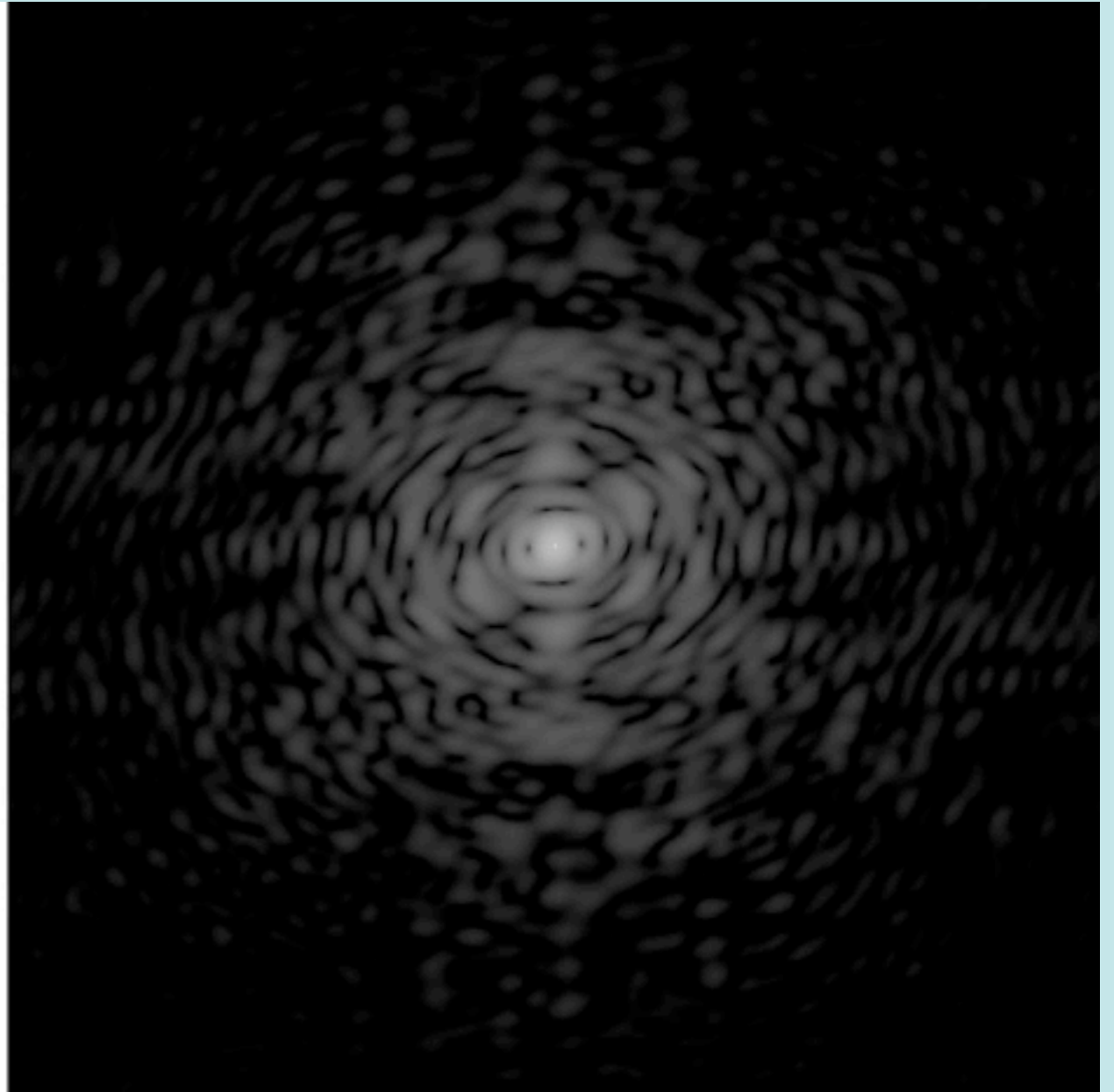
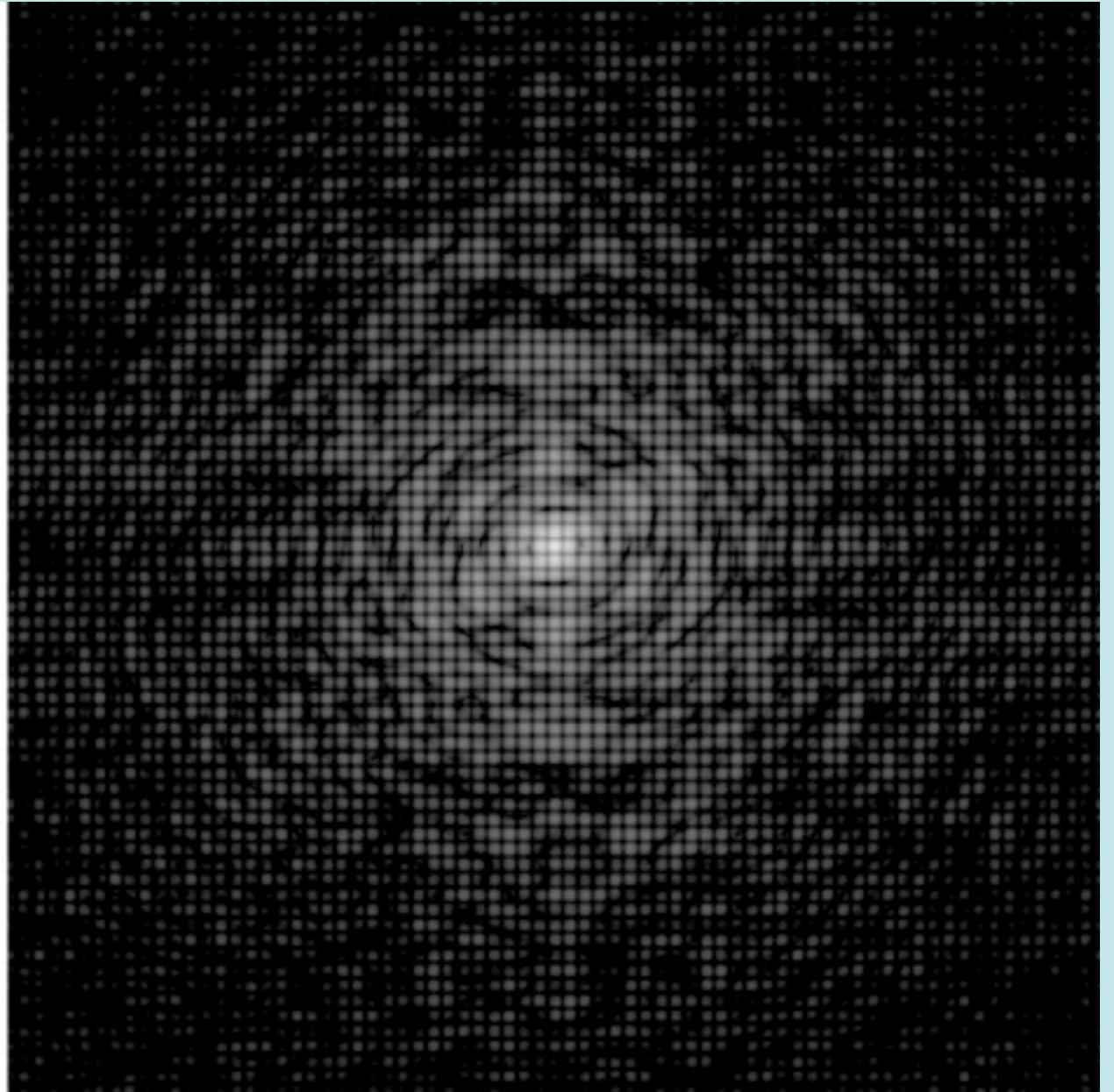


Image using only  
Fourier phases

# 1 unit cell

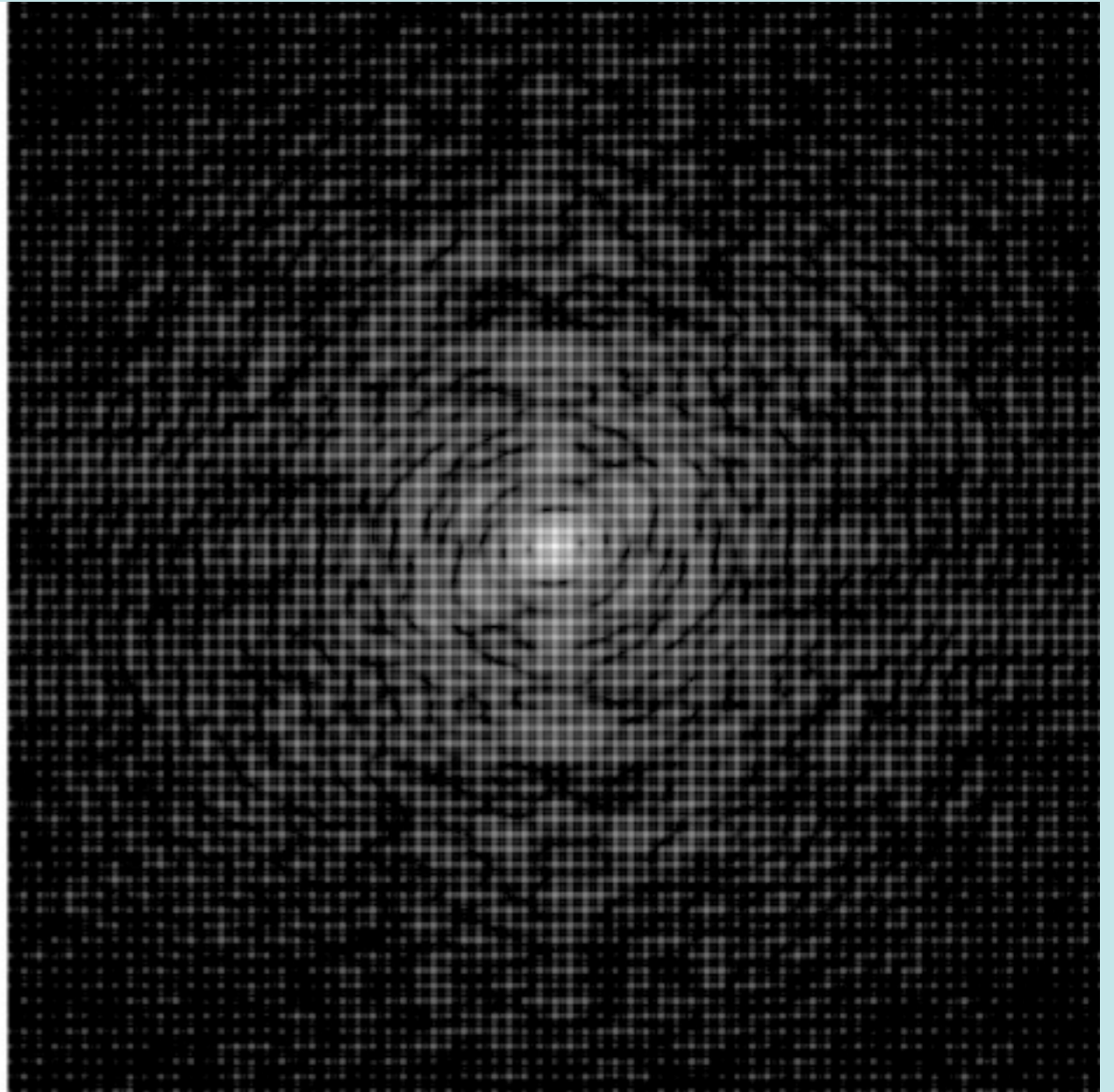


# 2x2 unit cells



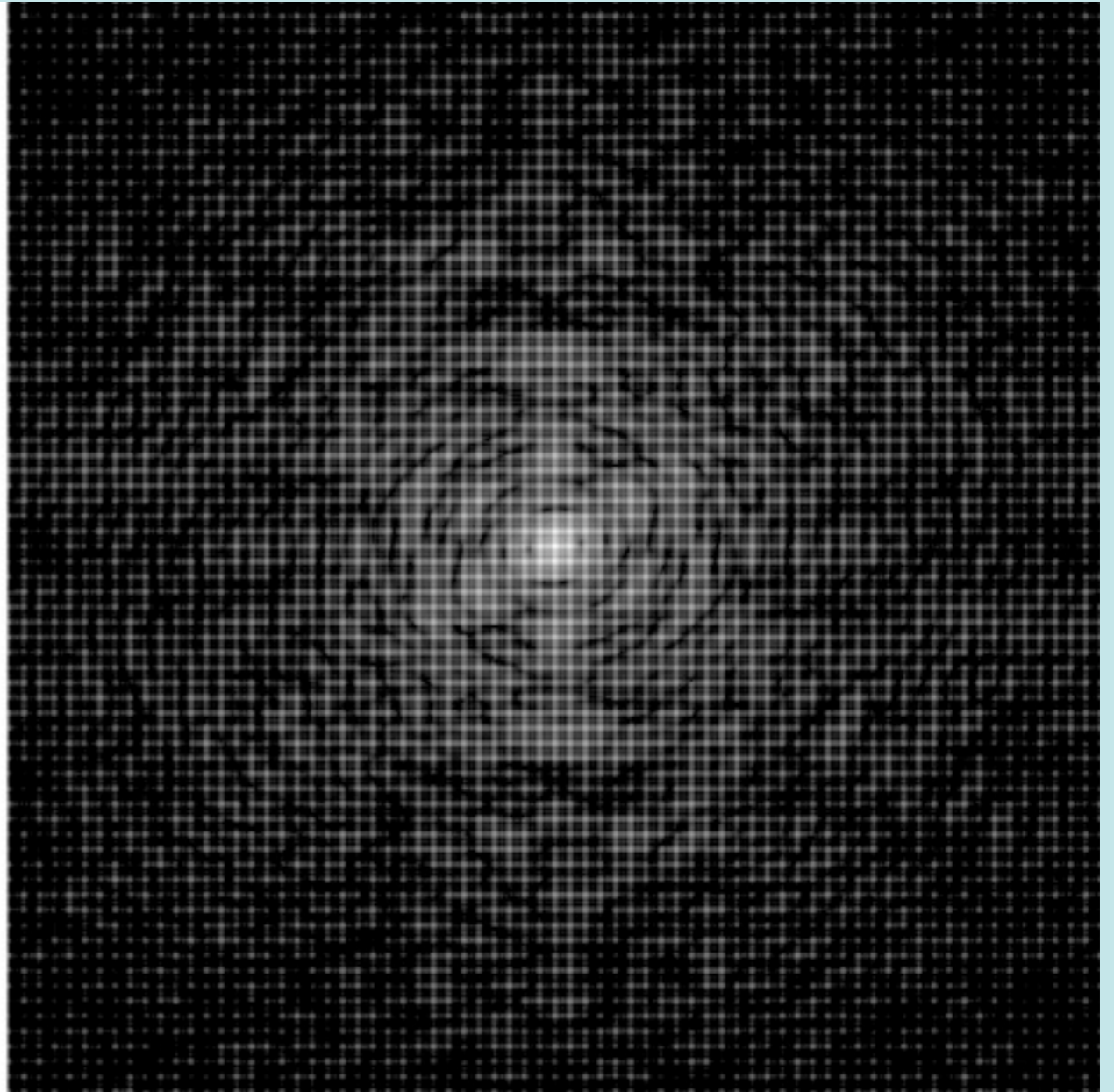
See e.g., D. Sayre, "Some implications of a theorem due to Shannon," *Acta Cryst.* **5**, 843 (1952)

# 3x3 unit cells



See e.g., D. Sayre, "Some implications of a theorem due to Shannon," *Acta Cryst.* **5**, 843 (1952)

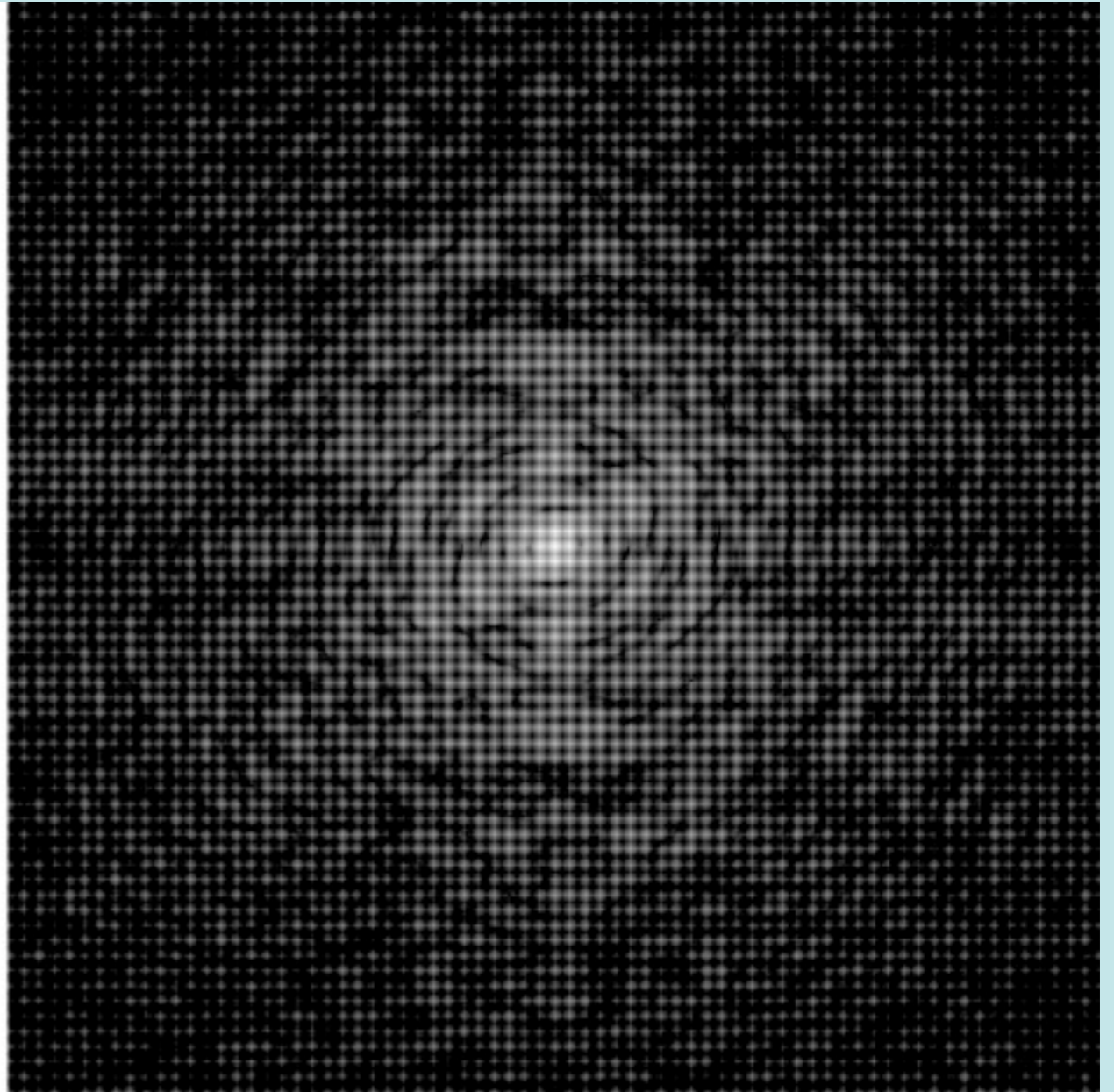
# 4x4 unit cells



See e.g., D. Sayre, "Some implications of a theorem due to Shannon," *Acta Cryst.* **5**, 843 (1952)

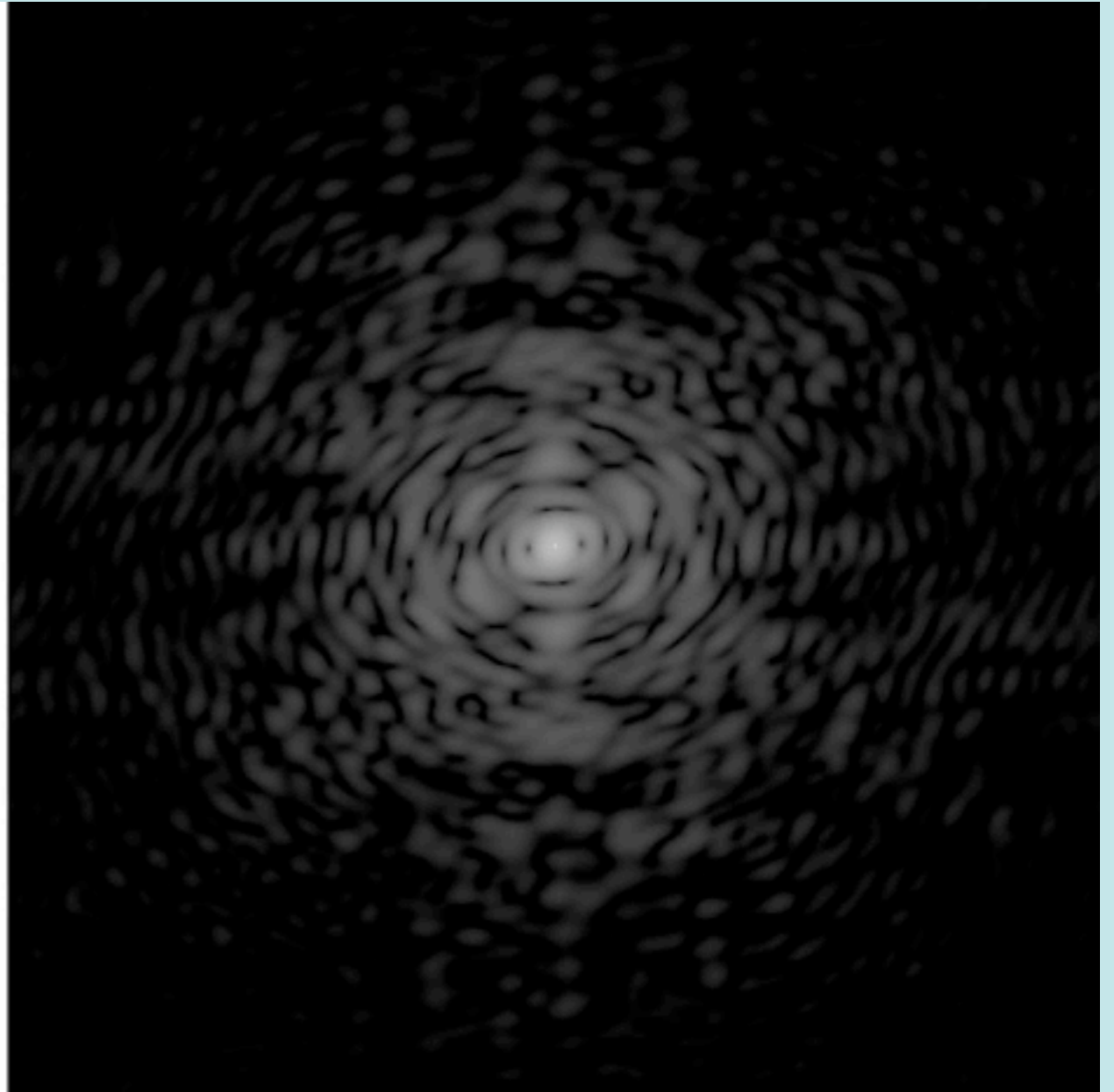


# 5x5 unit cells



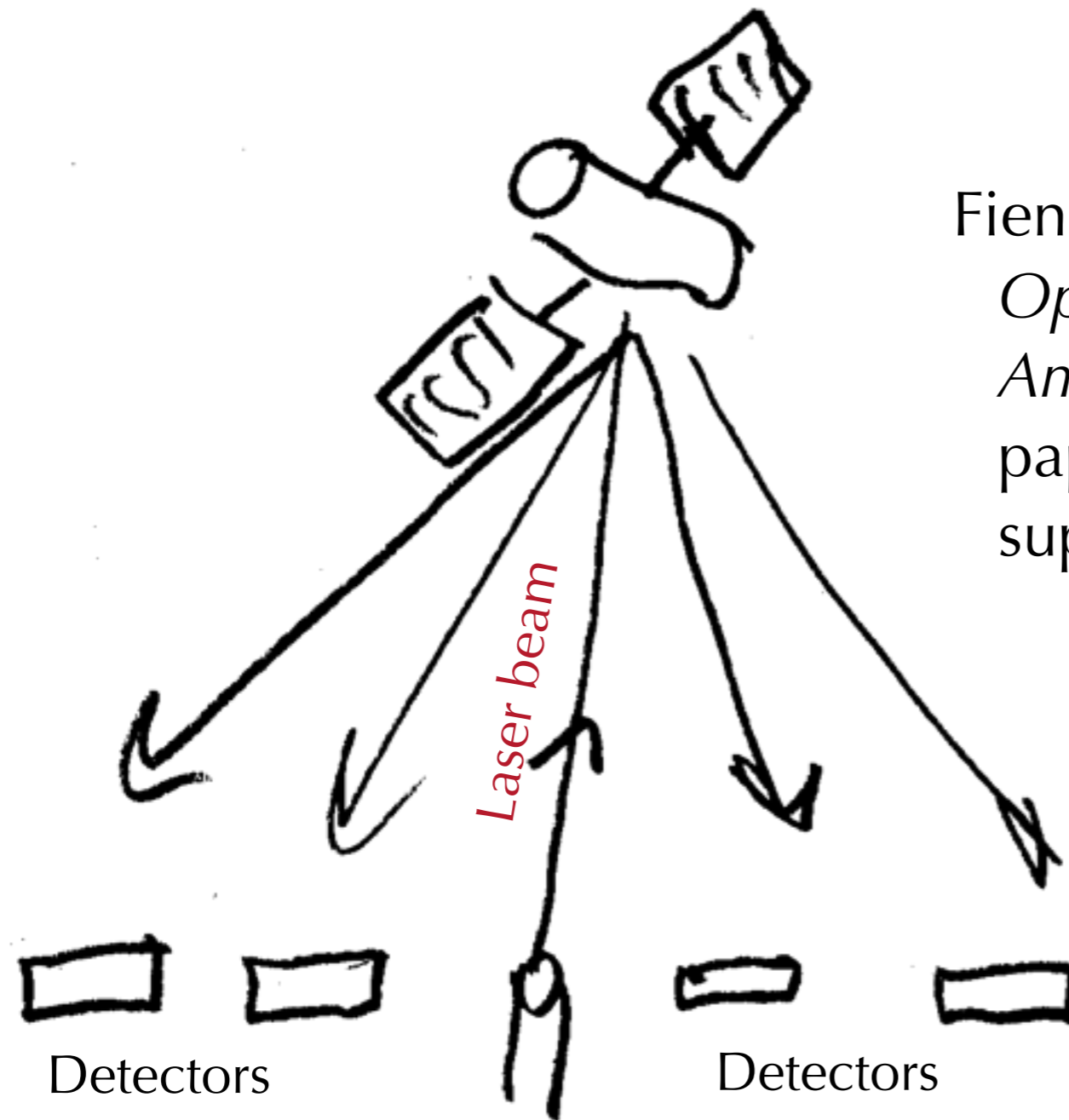
See e.g., D. Sayre, "Some implications of a theorem due to Shannon," *Acta Cryst.* **5**, 843 (1952)

# 1 unit cell



See e.g., D. Sayre, "Some implications of a theorem due to Shannon," *Acta Cryst.* **5**, 843 (1952)

# Who else might be interested?



Fienup, *Opt. Lett.* **3**, 27 (1978); *Appl. Opt.* **21**, 2758 (1978); *J. Opt. Soc. Am. A* **4**, 118 (1987); and other papers. Introduces the use of a “finite support”.

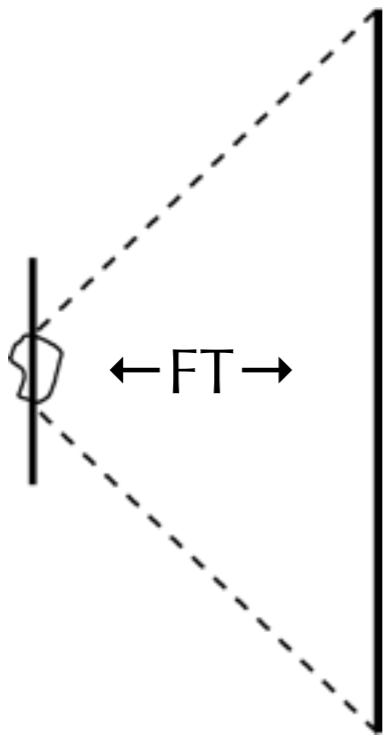
Turbulent atmosphere degrades phase

Cartoon based on presentations by Fienup from ERIM (Environmental Research Institute of Michigan). Fienup is now at U. Rochester

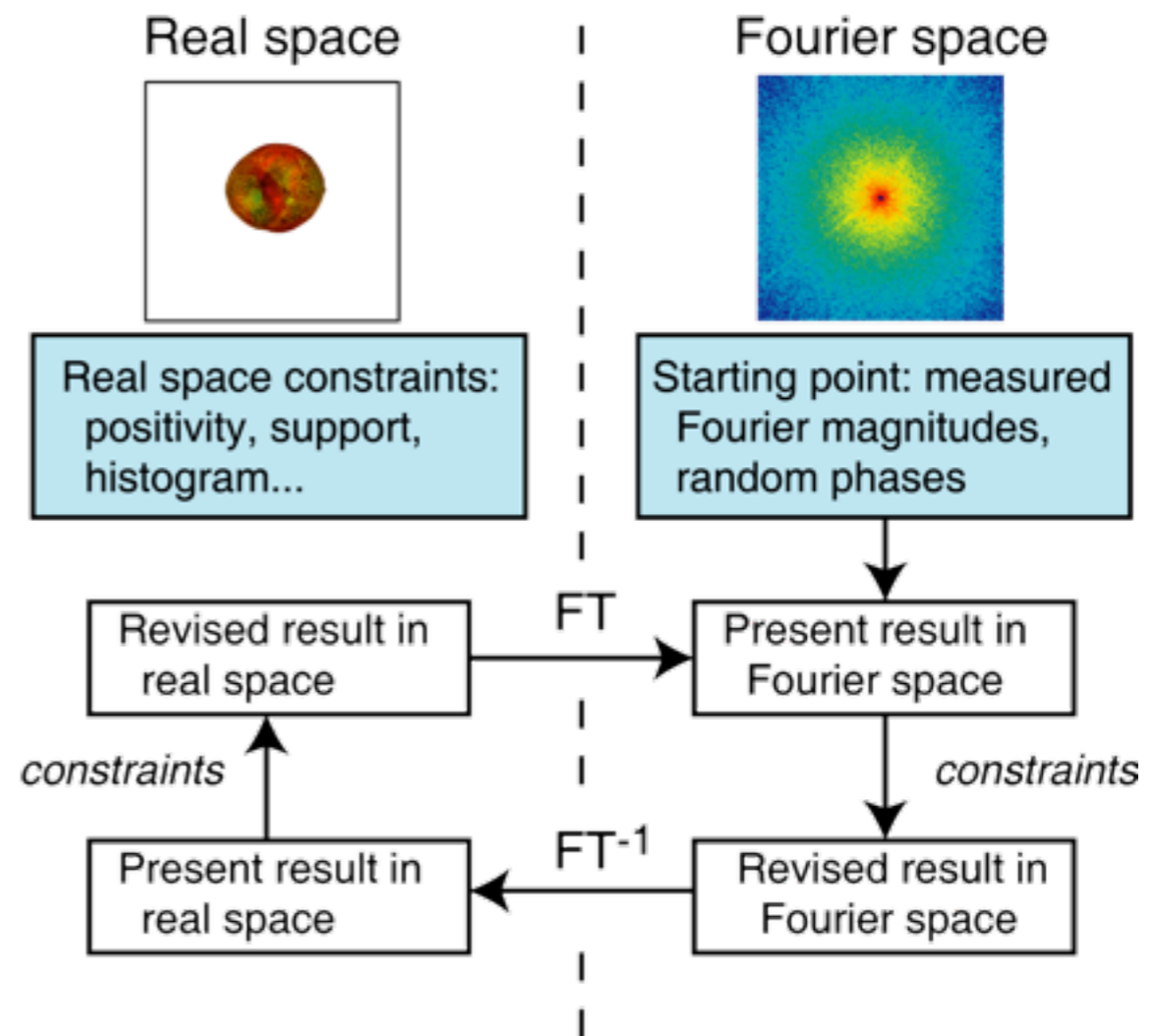
# Imaging without lenses

- Avoid losses of lens efficiency and transfer function
- Must phase the diffraction intensities

Real space: finite support  
(or other constraints)



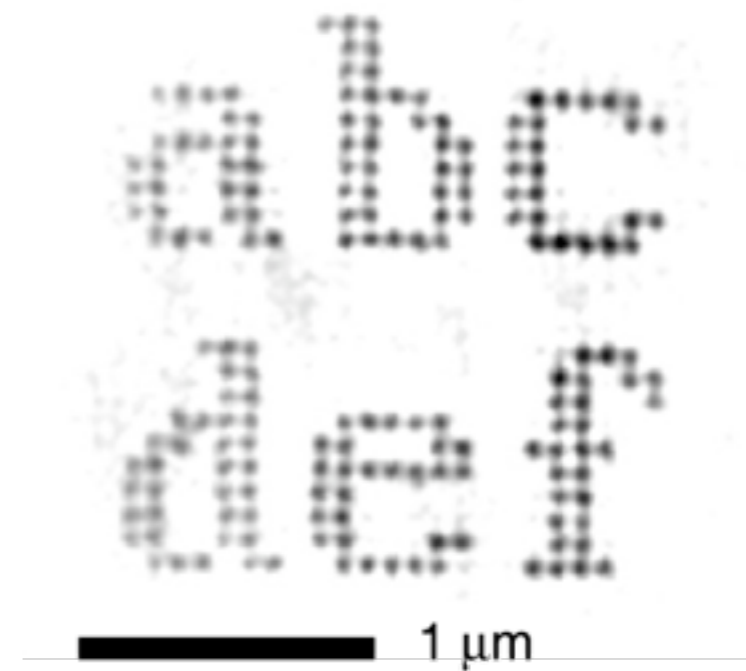
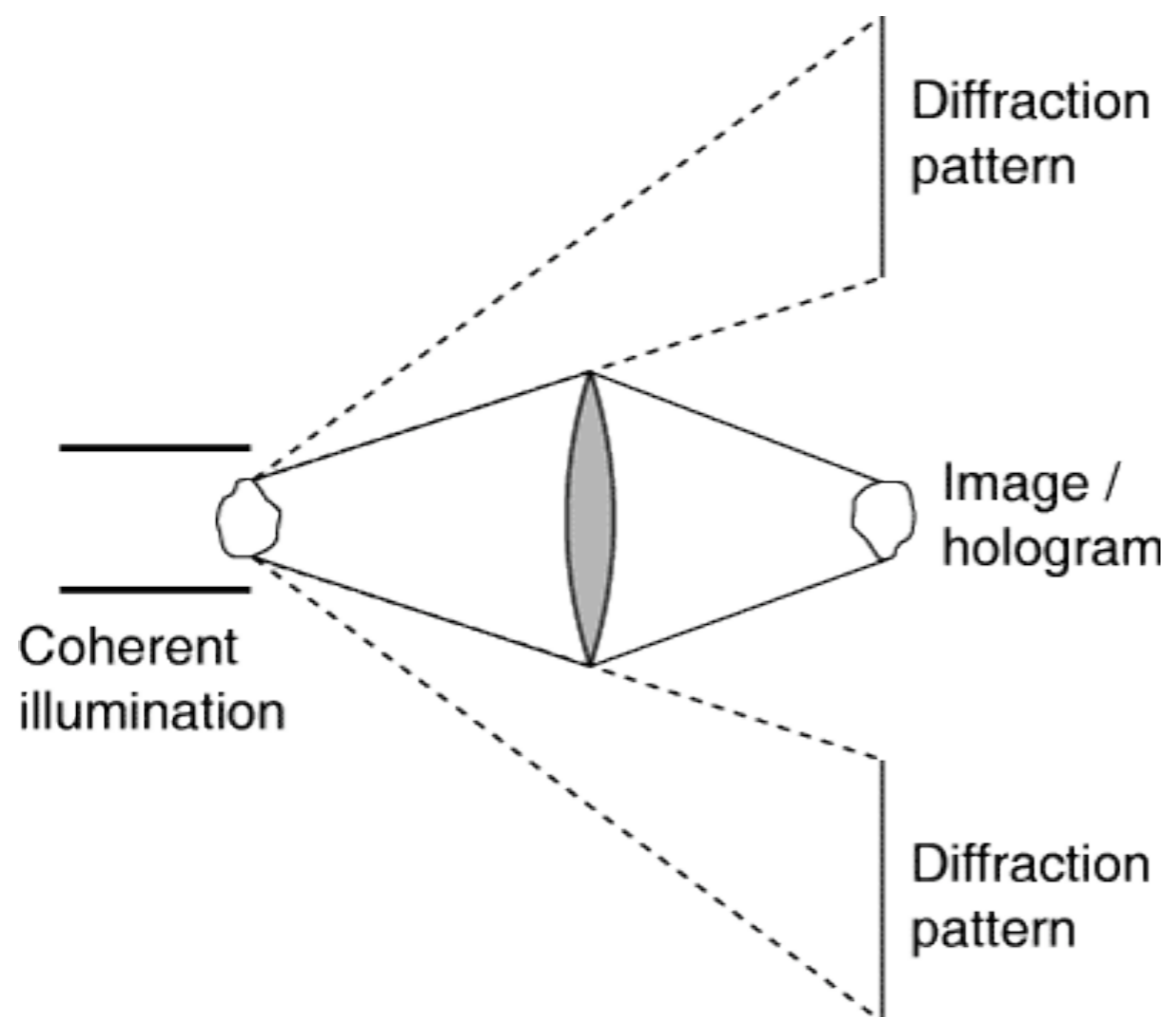
Fourier space: magnitudes  
known, but phases are  
not



Phasing algorithms: Feinup, *Opt. Lett.* **3**, 27 (1978); Elser, *JOSA A* **20**, 40 (2003); and others. First x-ray demonstration: Miao *et al.*, *Nature* **400**, 342 (1999).

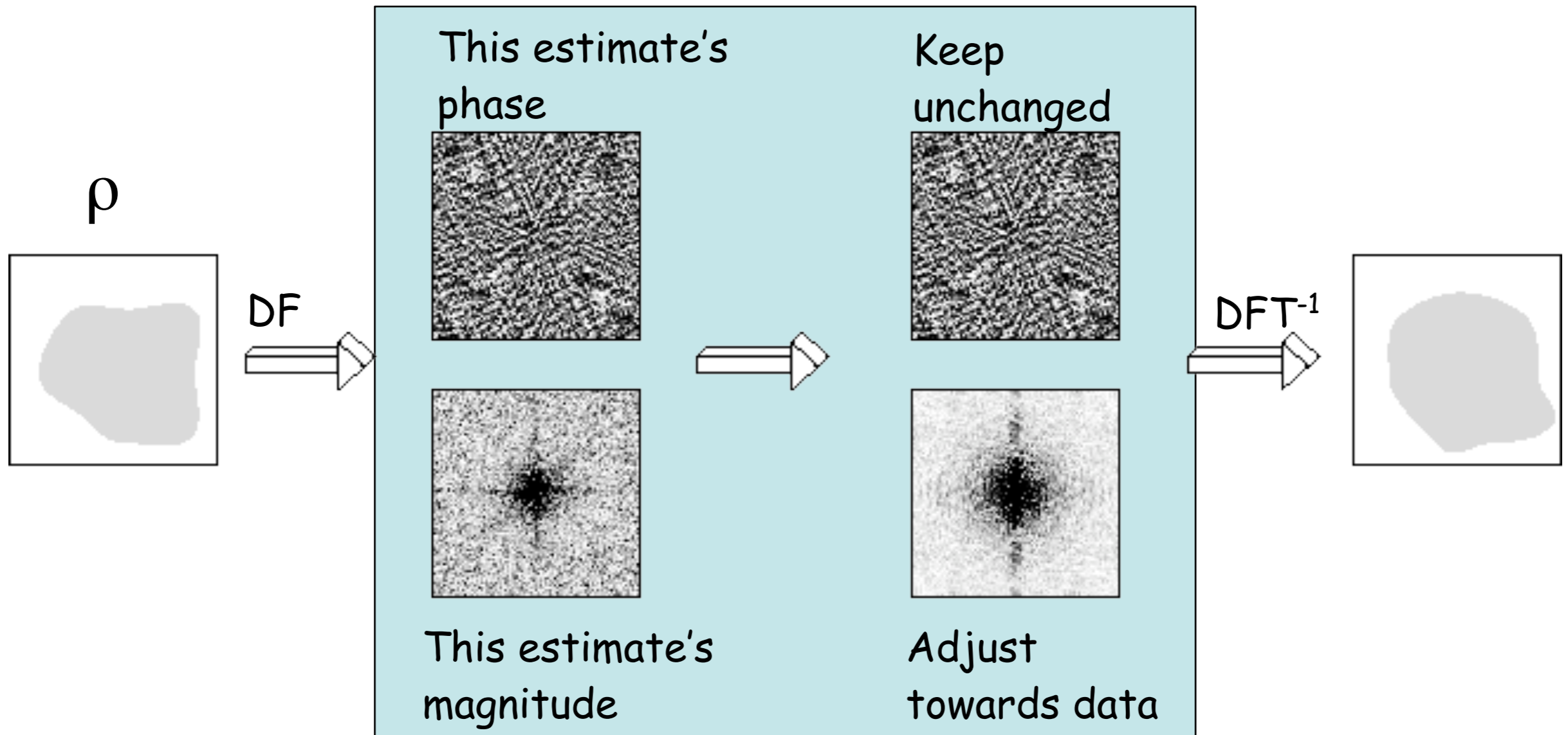
# X-ray diffraction microscopy

- Proposed by Sayre (in Schlenker, ed., **Imaging and Coherence Properties in Physics**, Springer-Verlag, 1980)
- Through 1999: experiments by Sayre, Kirz, Yun, Chapman, Miao



First x-ray reconstruction: Miao, Charalambous, Kirz, and Sayre, *Nature* **400**, 342 (1999)

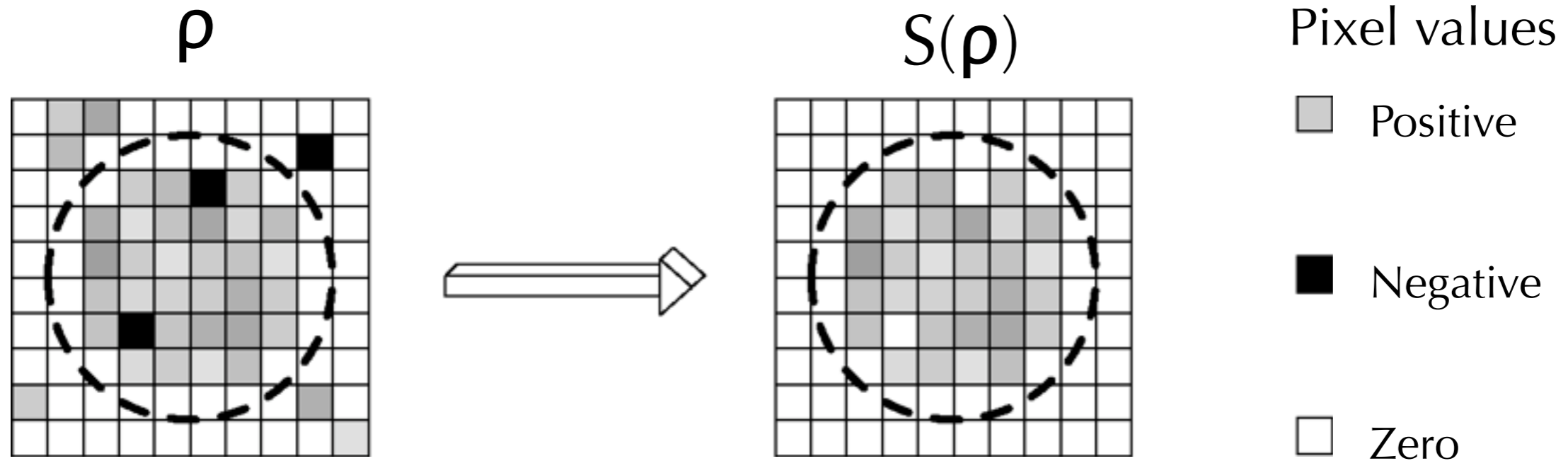
# Fourier modulus constraint



(Enju Lima, Stony Brook)

# Real space constraints

Support, positivity (if positivity is applicable)



**Histogram constraint**

$$\rho_i \rightarrow H_i$$

(V. Elser)

$$\rho = \begin{array}{|c|c|c|c|c|c|} \hline 0 & 4 & 2 & 1 & 13 & 0 \\ \hline \end{array}$$

↓  $H = \{10, 7, 2, 0, 0, 0\}$

$$H(\rho) = \begin{array}{|c|c|c|c|c|c|} \hline 0 & 7 & 2 & 0 & 10 & 0 \\ \hline \end{array}$$

(Enju Lima, Stony Brook)

# Phase retrieval particulars

- Our favored approach: difference map algorithm [V. Elser, J. Opt. Soc. Am. A **20**, 40 (2003)]

- Generalized description based on set projections

- Do modulus then support, and support then modulus, and compare:

$$\psi_{n+1} = \psi_n + \beta \Delta \{\psi_n\}$$

$$\Delta = \Pi_{\text{sup}}[(1 + \gamma_2)\Pi_{\text{mod}} - \gamma_2] \\ - \Pi_{\text{mod}}[(1 + \gamma_1)\Pi_{\text{sup}} - \gamma_1]$$

- With orthogonal projections,  $\beta=1$ . In general,

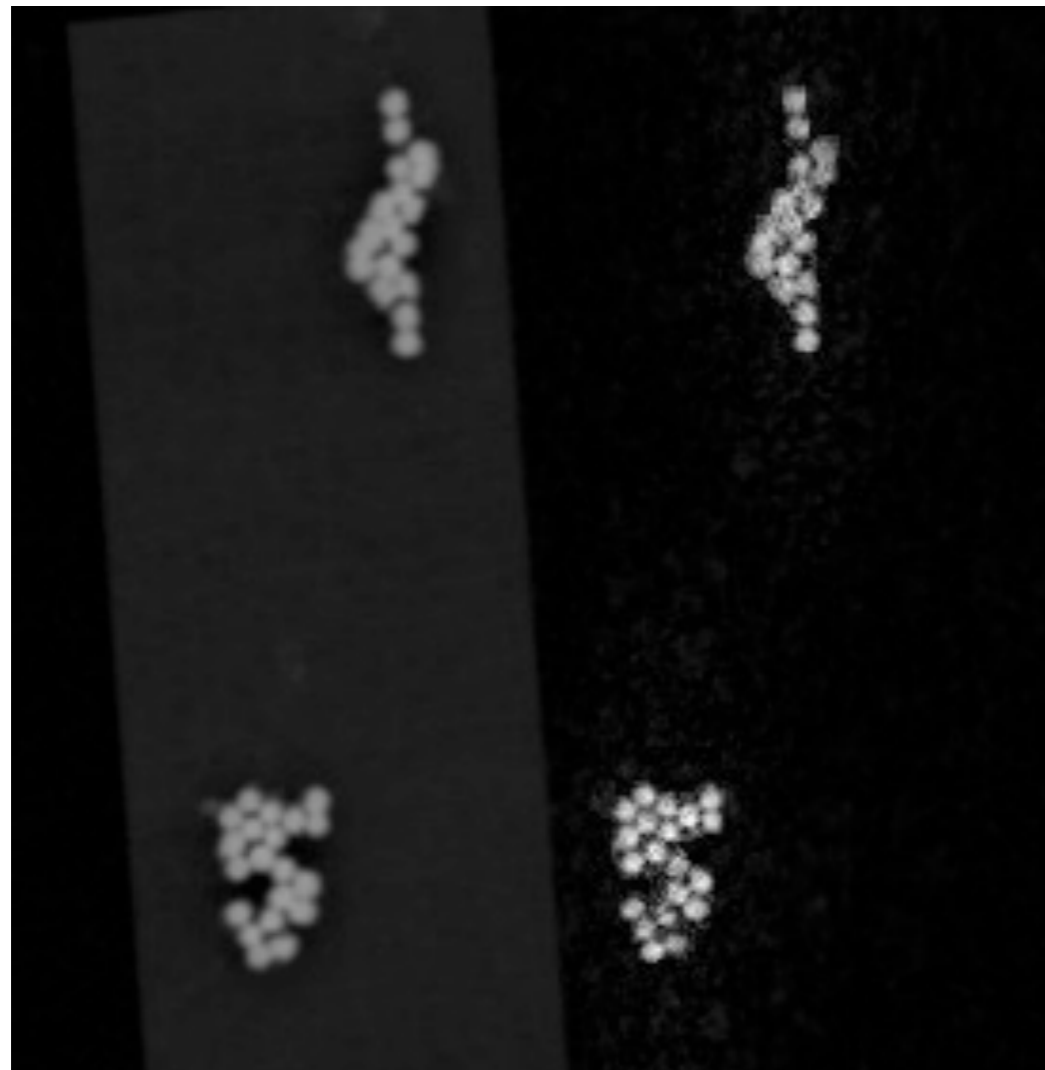
$$\gamma_1 = -\beta^{-1} \quad \gamma_2 = \beta^{-1}$$

- Additional good algorithms: Bauschke et al., J. Opt. Soc. Am. A **20**, 1025 (2003).

- Discussion of phase retrieval in imaging and crystallography: Millane, J. Opt. Soc. Am. A **7**, 394 (1990).



# RECONSTRUCTED X-RAY IMAGE AND SEM PICTURE OF THE SAMPLE FOR COMPARISON



↑  
SEM

↑  
X-ray  
reconstruction



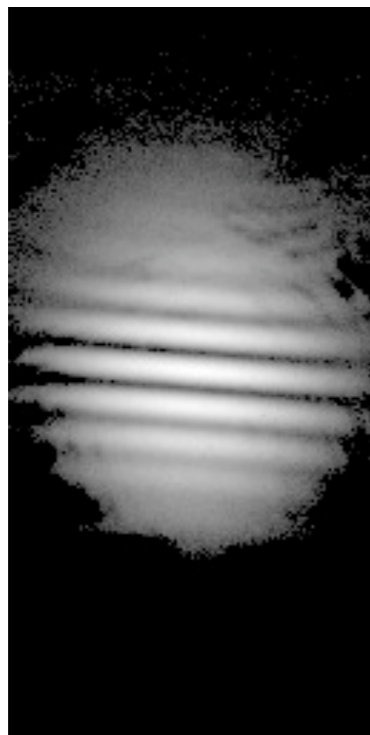
↑  
Tight  
support

- Sample consisting of 50 nm gold balls mounted on a  $75 \mu\text{m}$  square  $\text{Si}_3\text{N}_4$  window
- The sample was intentionally arranged in this form by means of sweeping the balls around on the window using an atomic force microscope
- Stage 1 reconstruction using the two-ellipse support derived from the autocorrelation (100 iterations)
- Stage 2 final reconstruction using the tight support (left) derived from the preliminary form of the reconstruction. Shrink-wrap: S. Marchesini (53 iterations)
- No positivity constraint was used on either real or imaginary part
- The data points blocked by the beam stop were not constrained but left to float

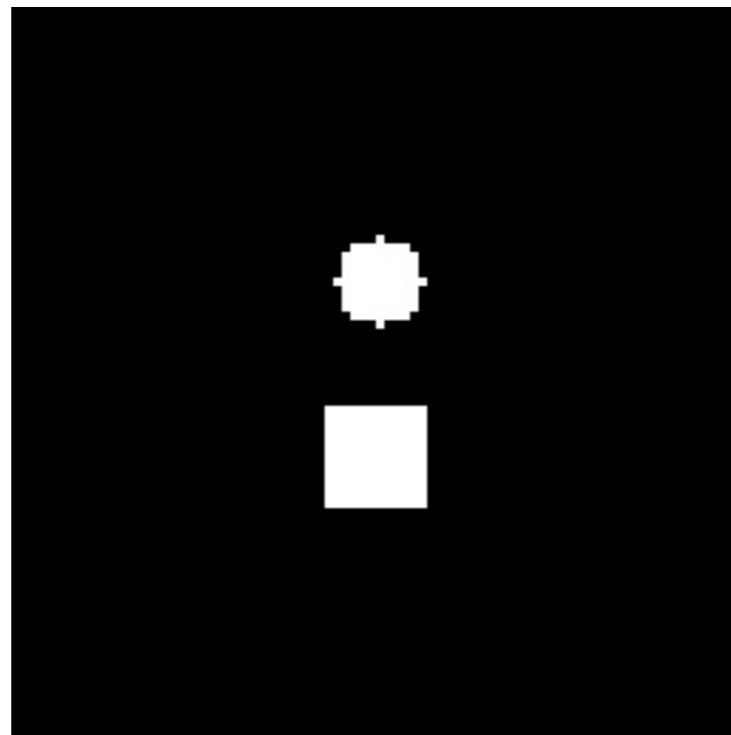
(From Malcolm Howells)

# Iterative phasing: simple example

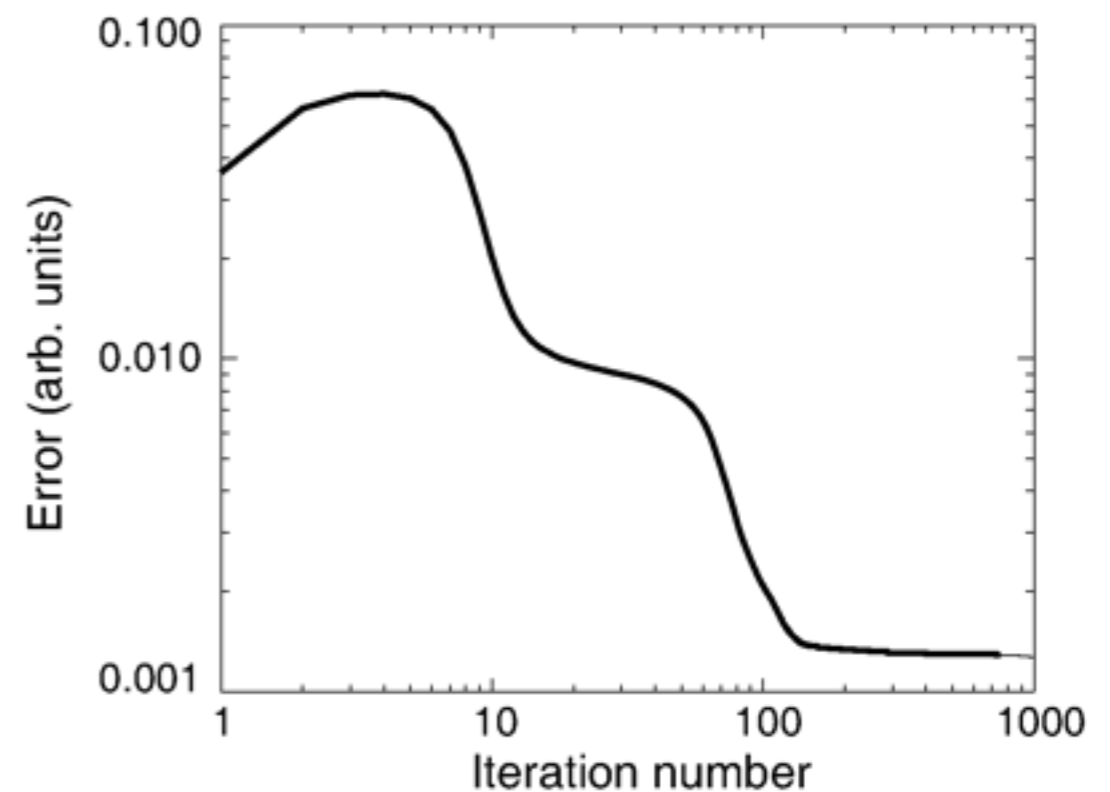
- High harmonic generation of XUV radiation from femtosecond lasers, illuminating two pinholes.
  - R. Bartels, A. Paul, H. Green, H.C. Kapteyn, M.M. Murnane, S. Backus, I.P. Christov, Y. Liu, D. Attwood, C. Jacobsen, *Science* **297**, 376 (2002)



Data

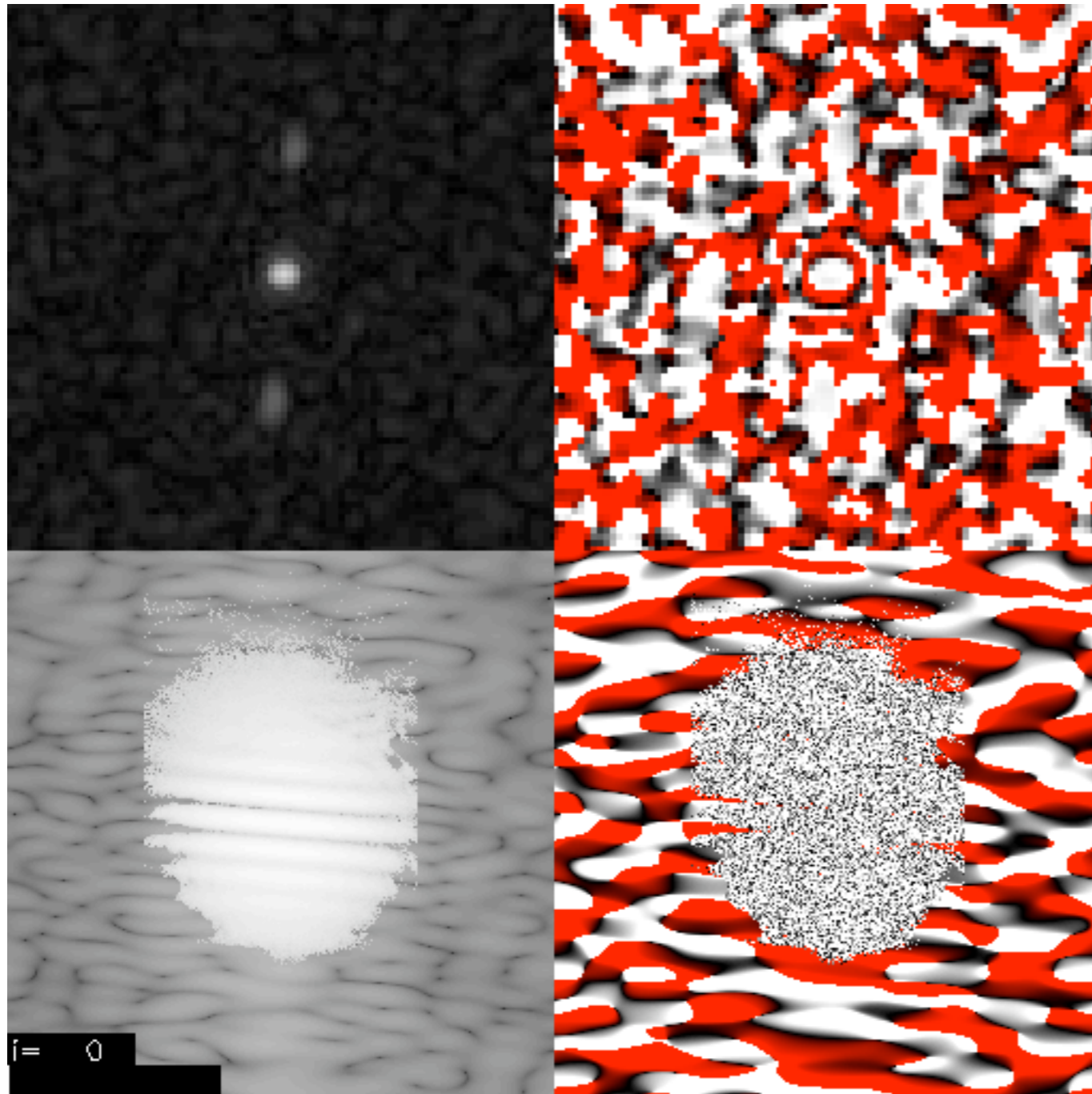


Support constraint  
(very loose)



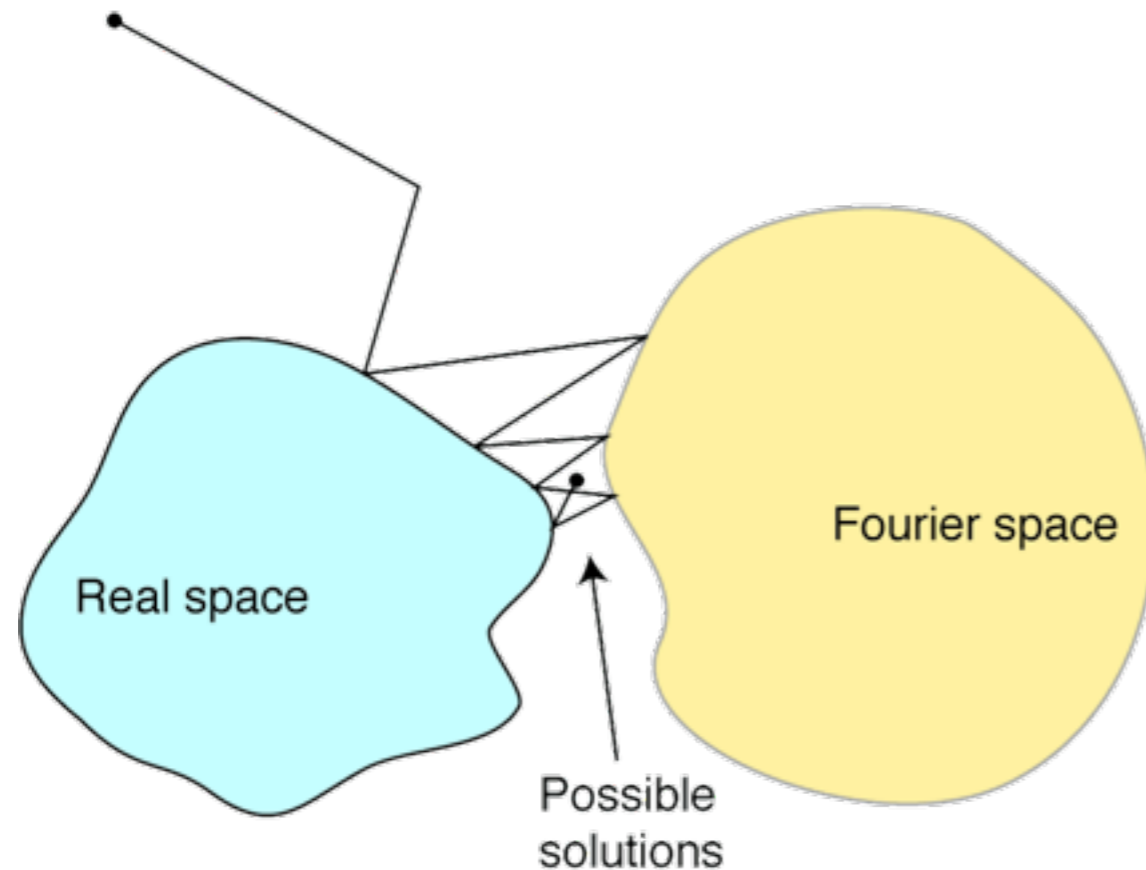
Reconstruction error

# The reconstruction

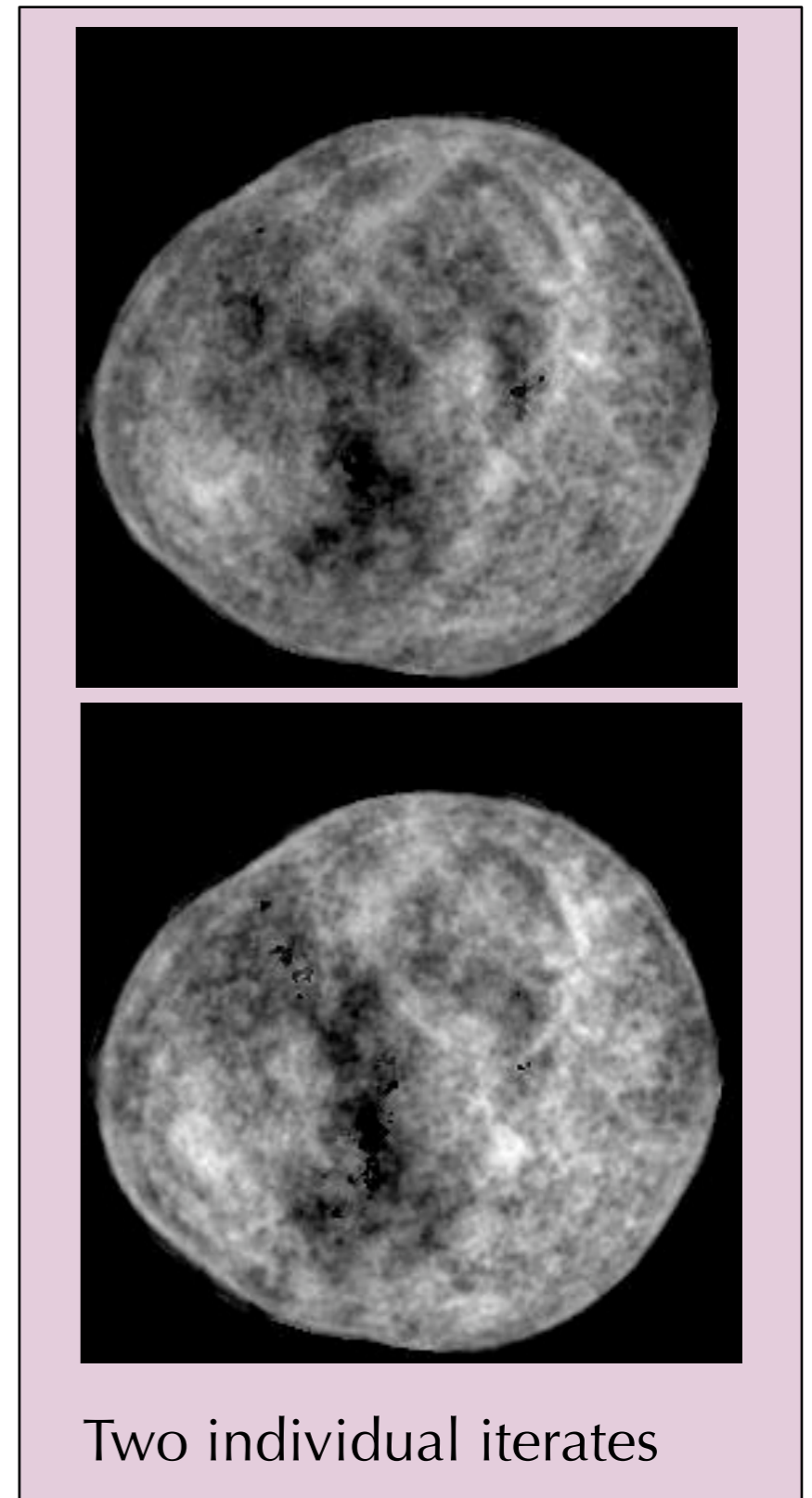


Real space Magnitude	Real space Phase
Far field Magnitude	Far field Phase

# Fluctuating solutions

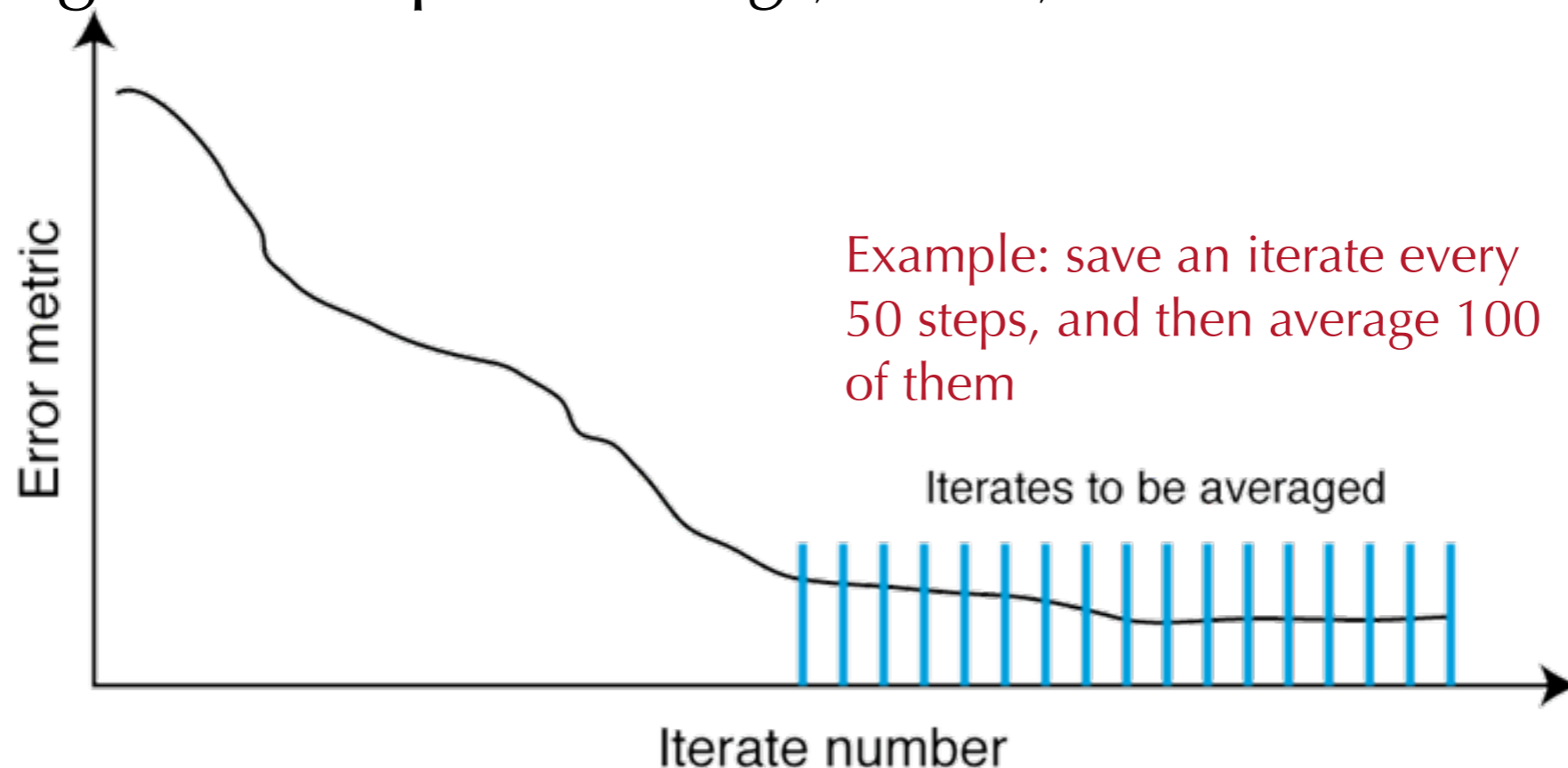


- Ideally, there would be a single point of best agreement between various constraints.
- Noise and incomplete constraints only provide a neighborhood of acceptable solutions.
- Choosing one iterate from one random starting phase as “the” solution is unwarranted!

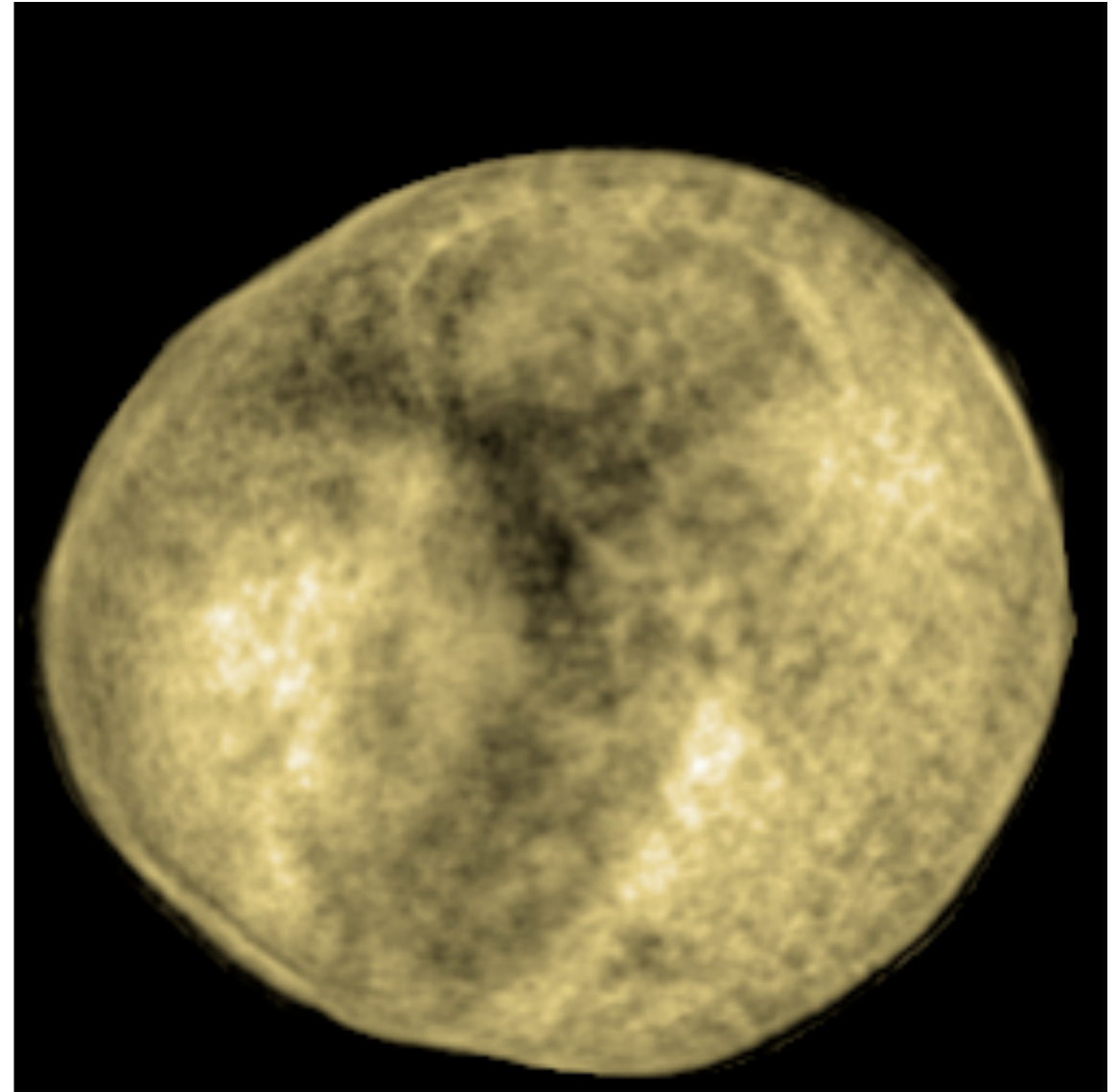
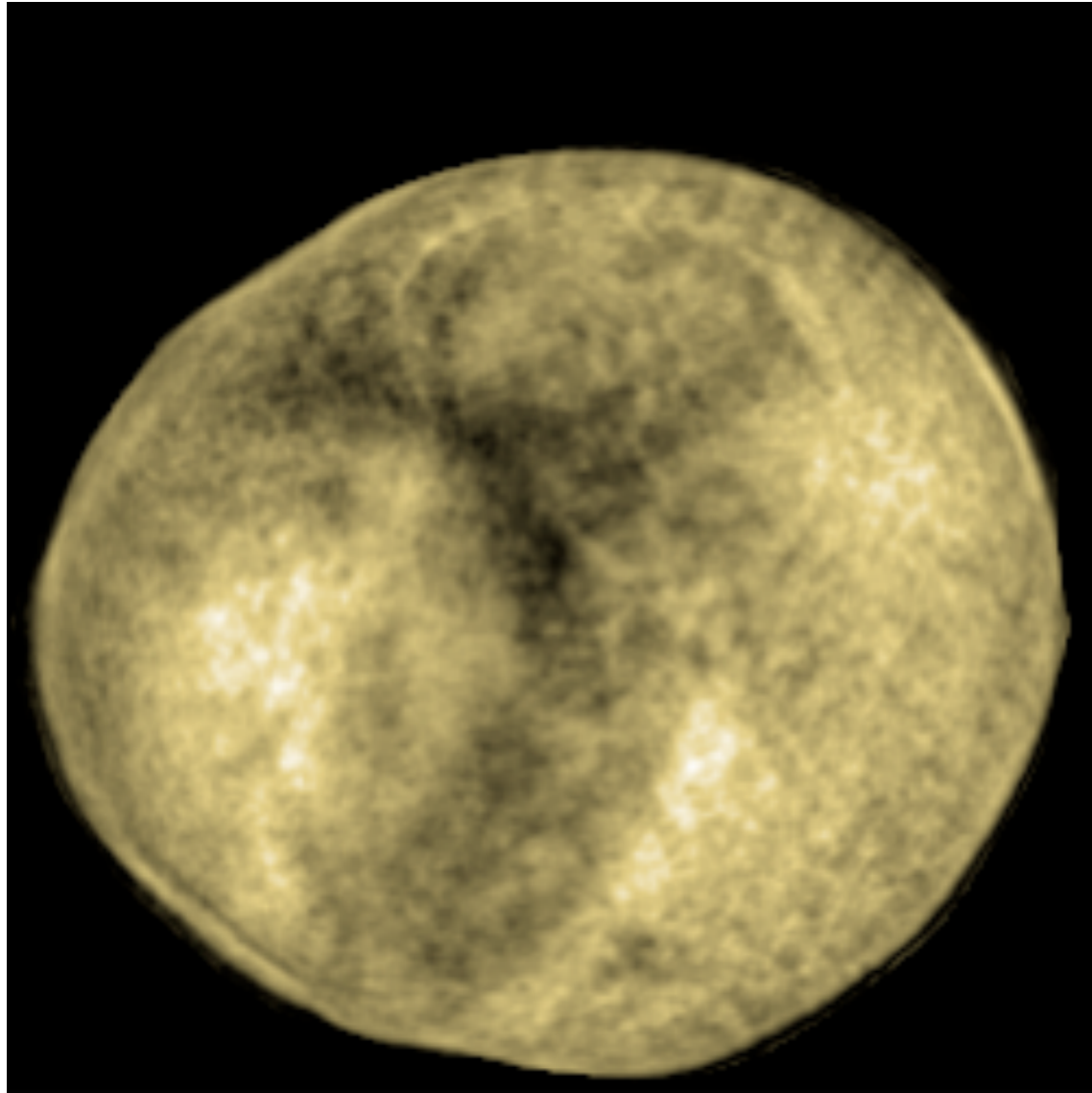


# Iterate averaging

- If the solution fluctuates, let's take many samples and average them!
- Non-reproducible phases get washed out; reproducible phases get reinforced
- Thibault, Elser, Jacobsen, Shapiro, and Sayre, *Acta Crystallographica A* **62**, 248 (2006)
- Other approaches: compare results from several different starting random phases (e.g., Miao, Robinson)



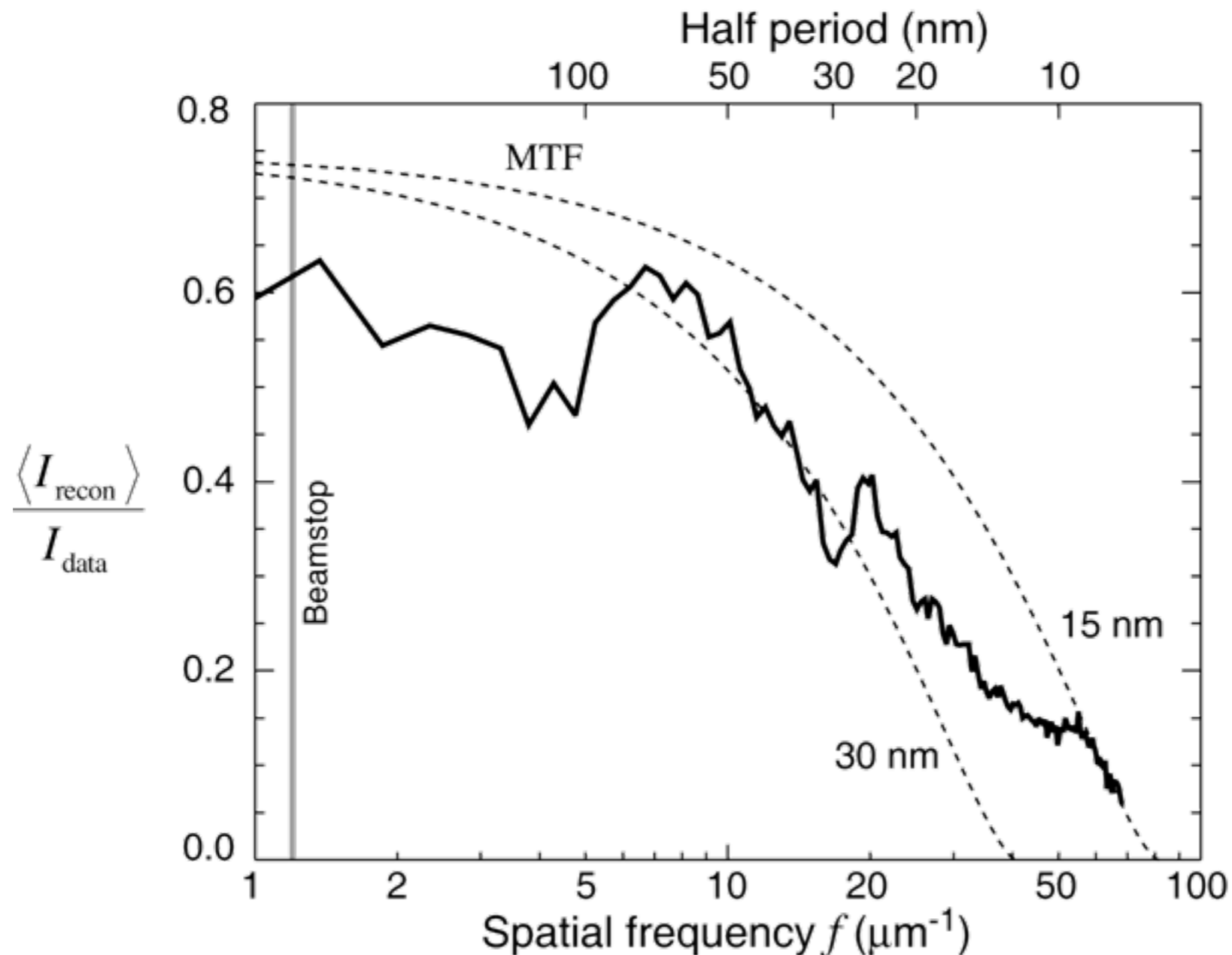
# Different starting random phases



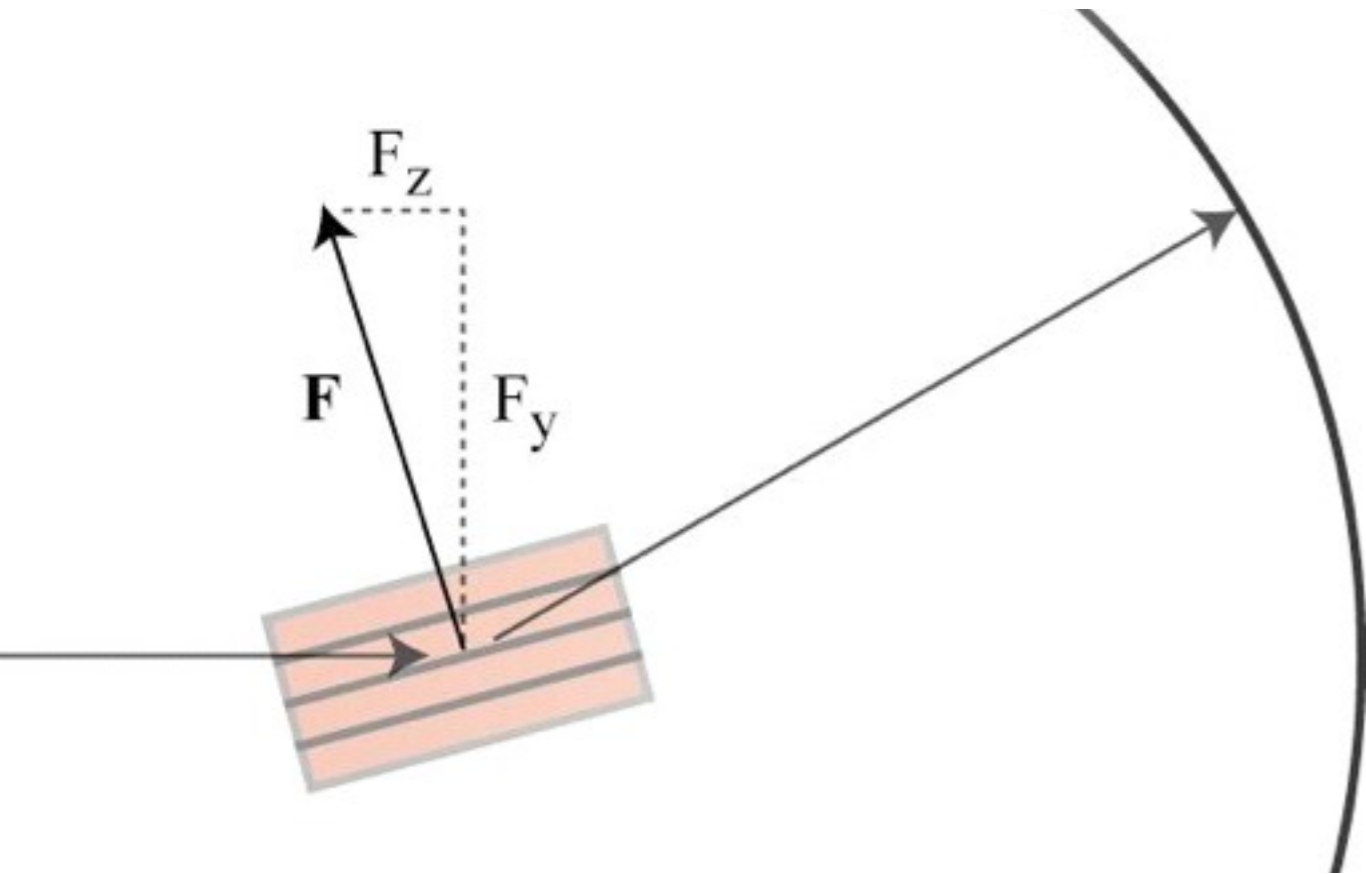
Two separate runs of algorithm with different random starting phases. In both cases, 125 iterates spaced 40 iterations apart were averaged (E. Lima).

# What is the resolution?

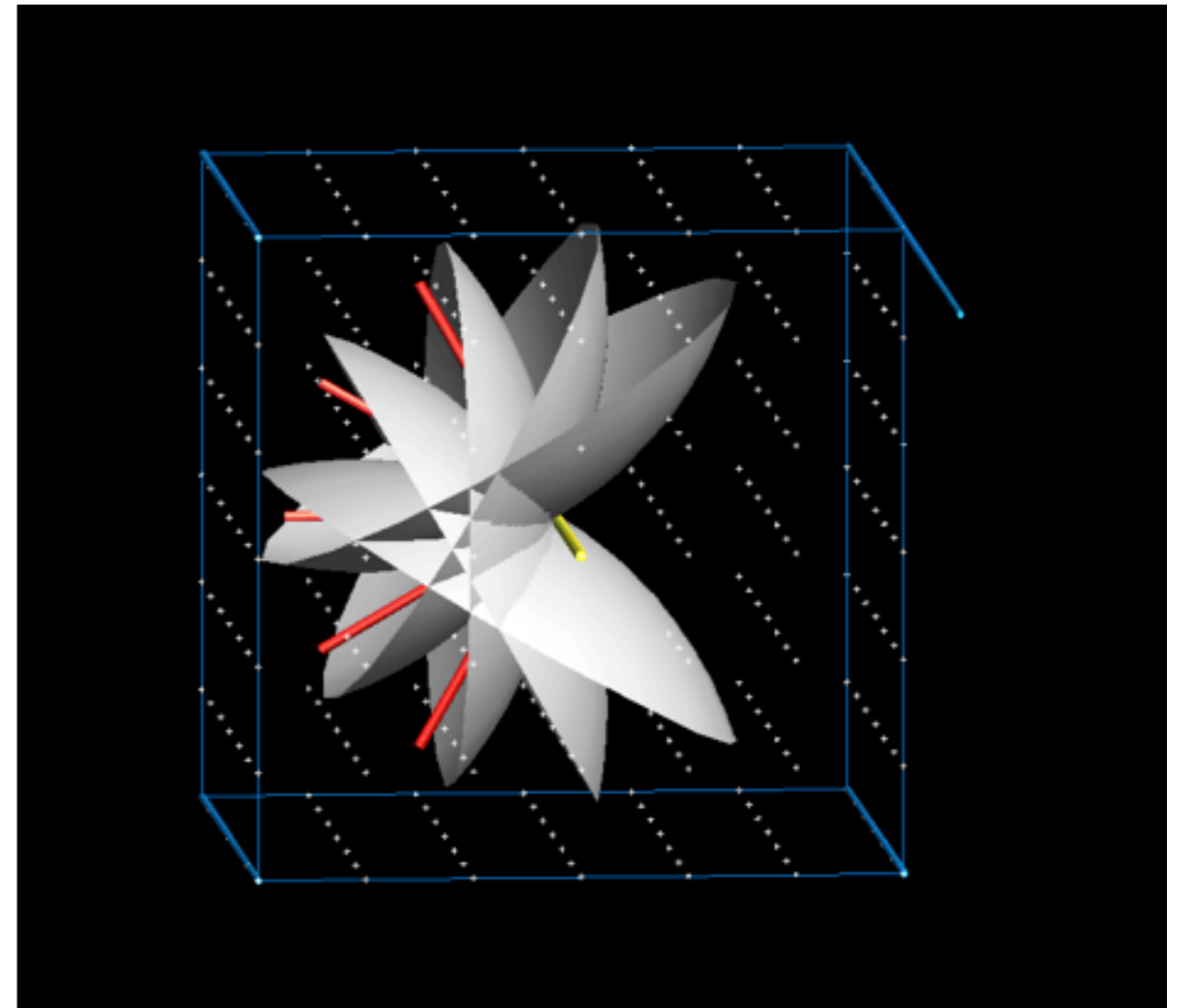
- We do *not* claim maximum angle of speckles as the resolution of the reconstructed image.
- Instead, one can look at how much iterate preserves Fourier intensities at various spatial frequencies – like an MTF.
- Equivalent alternative: phase error versus spatial frequency (Chapman *et al.*)



# Diffraction microscopy in 3D



Bragg gratings that diffract to a certain angle represent a specific transverse and longitudinal periodicity (Ewald sphere)

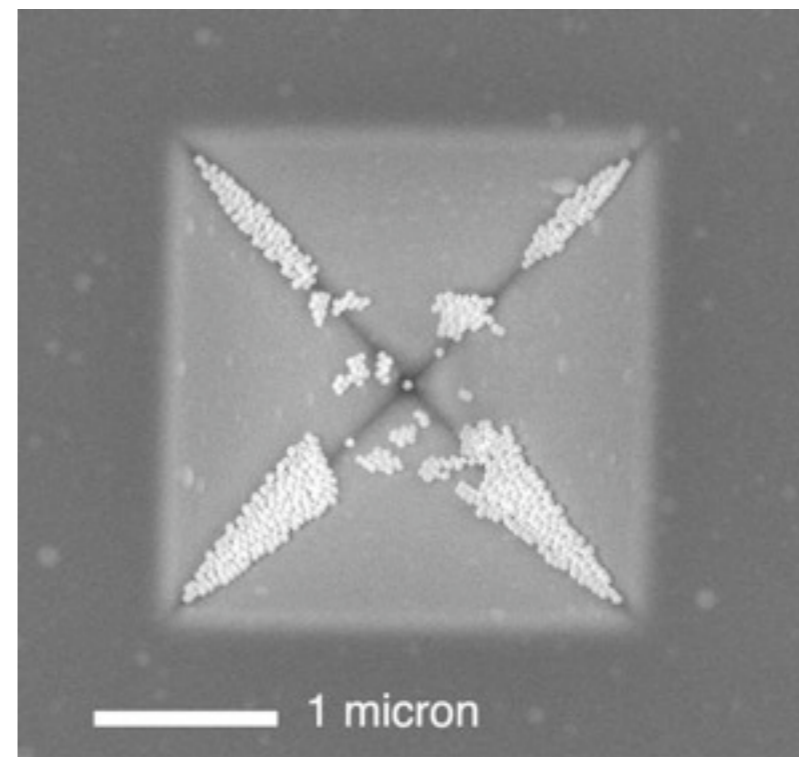
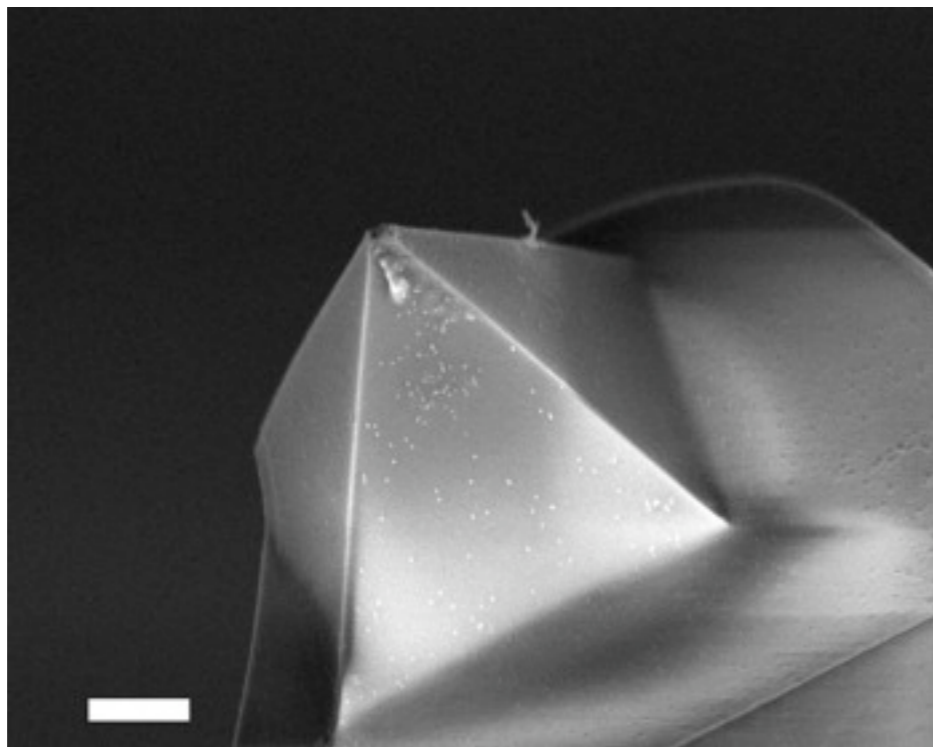


Data collection over a series of rotations about an axis fills in 3D Fourier space for phasing



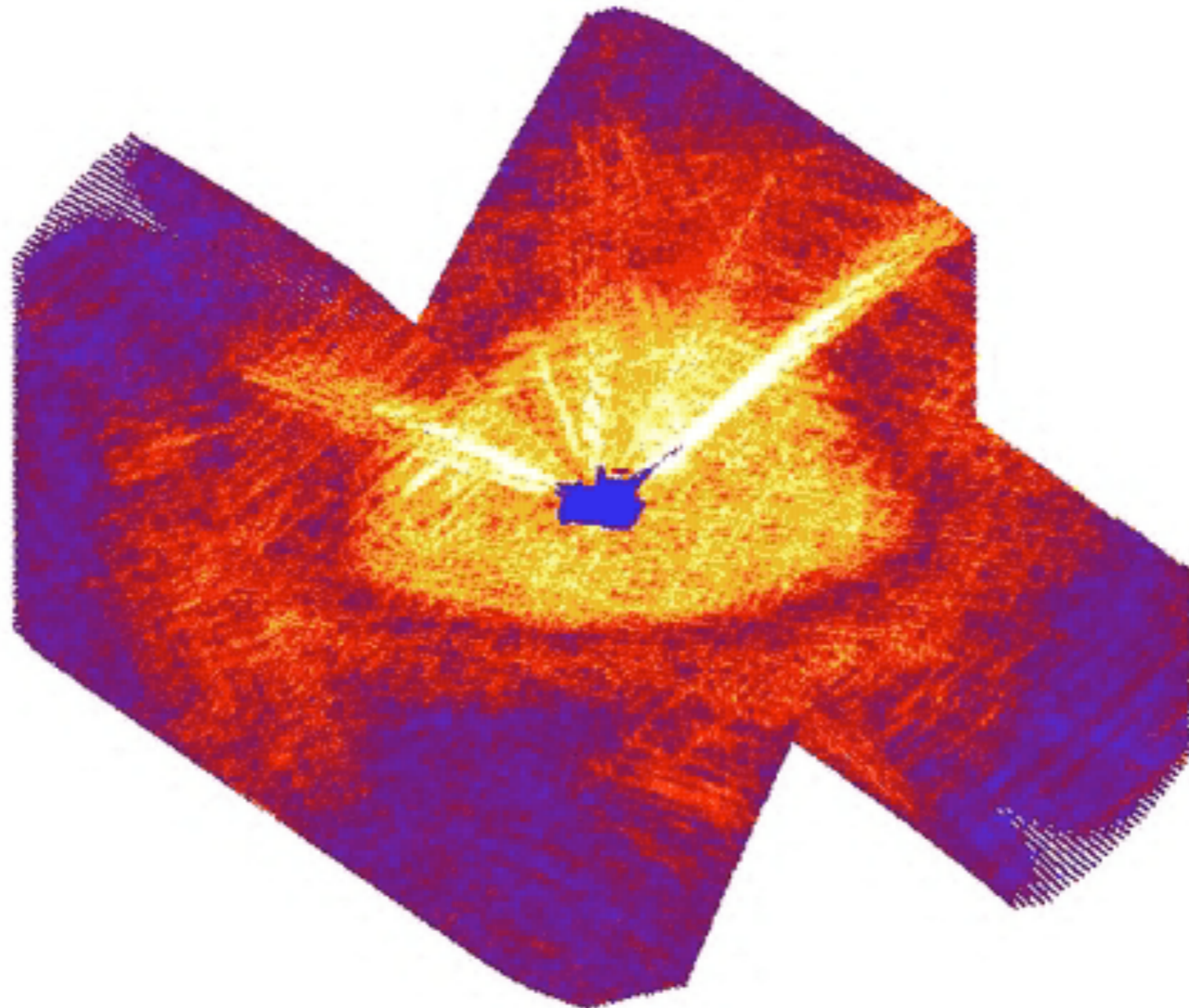
# 3D diffraction microscopy of materials science specimens

- Chapman, Barty, Marchesini, Noy, Hau-Riege, Cui, Howells, Rosen, He, Spence, Weierstall, Beetz, Jacobsen, Shapiro, *J. Opt. Soc. Am. A* **23**, 1179 (2006)
- 50 nm gold spheres placed on hollowed AFM tip “pyramid”
- Data taken using Stony Brook apparatus at ALS beamline 9.0.1



# 3D data cube

Chapman, Barty, Marchesini, Noy, Hau-Riege, Cui, Howells, Rosen, He, Spence, Weierstall, Beetz, Jacobsen, Shapiro, *J. Opt. Soc. Am. A* **23**, 1179 (2006)



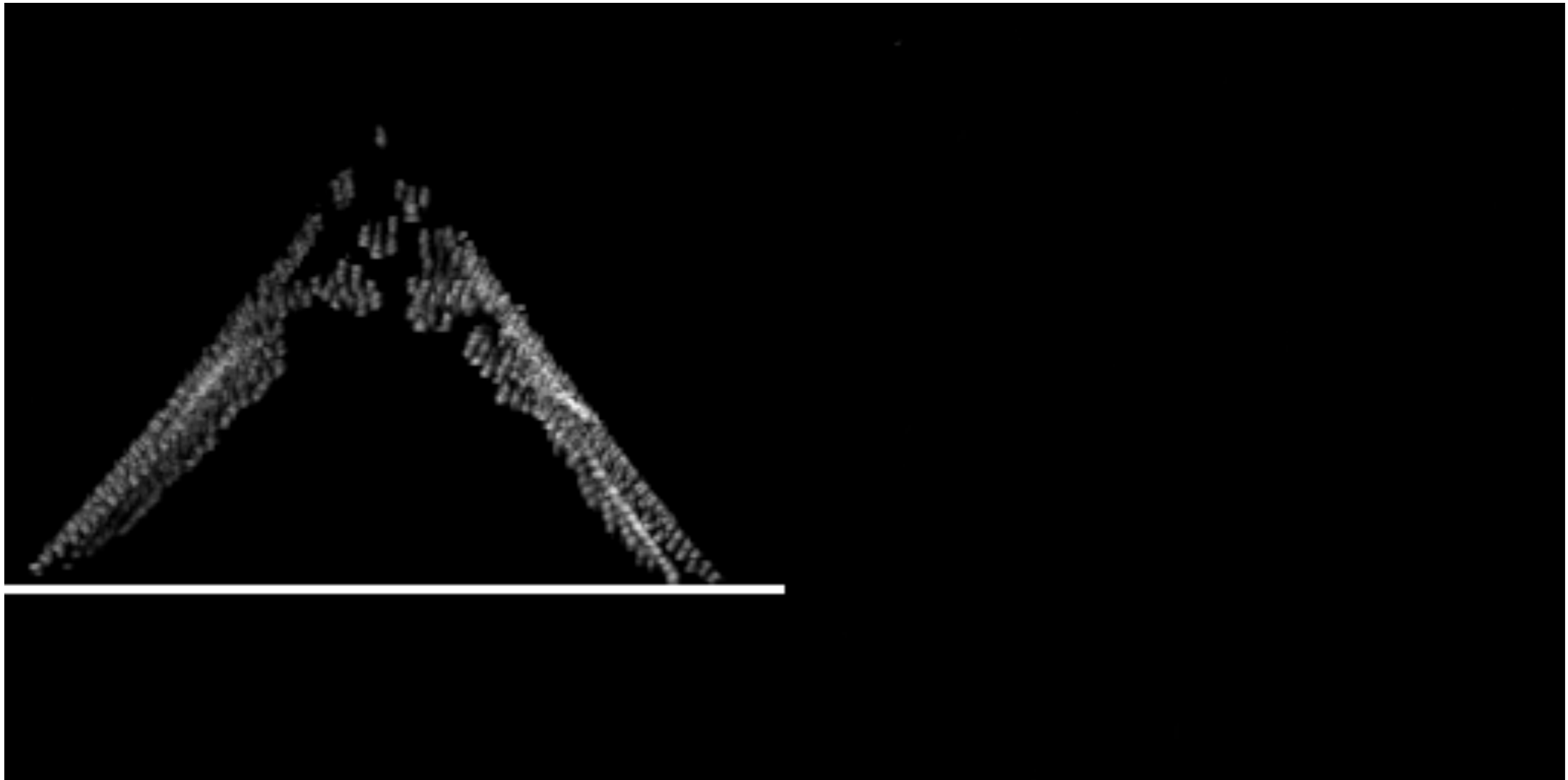
# Reconstruction

Chapman, Barty, Marchesini, Noy, Hau-Riege, Cui, Howells, Rosen, He, Spence, Weierstall, Beetz, Jacobsen, Shapiro, *J. Opt. Soc. Am. A* **23**, 1179 (2006)



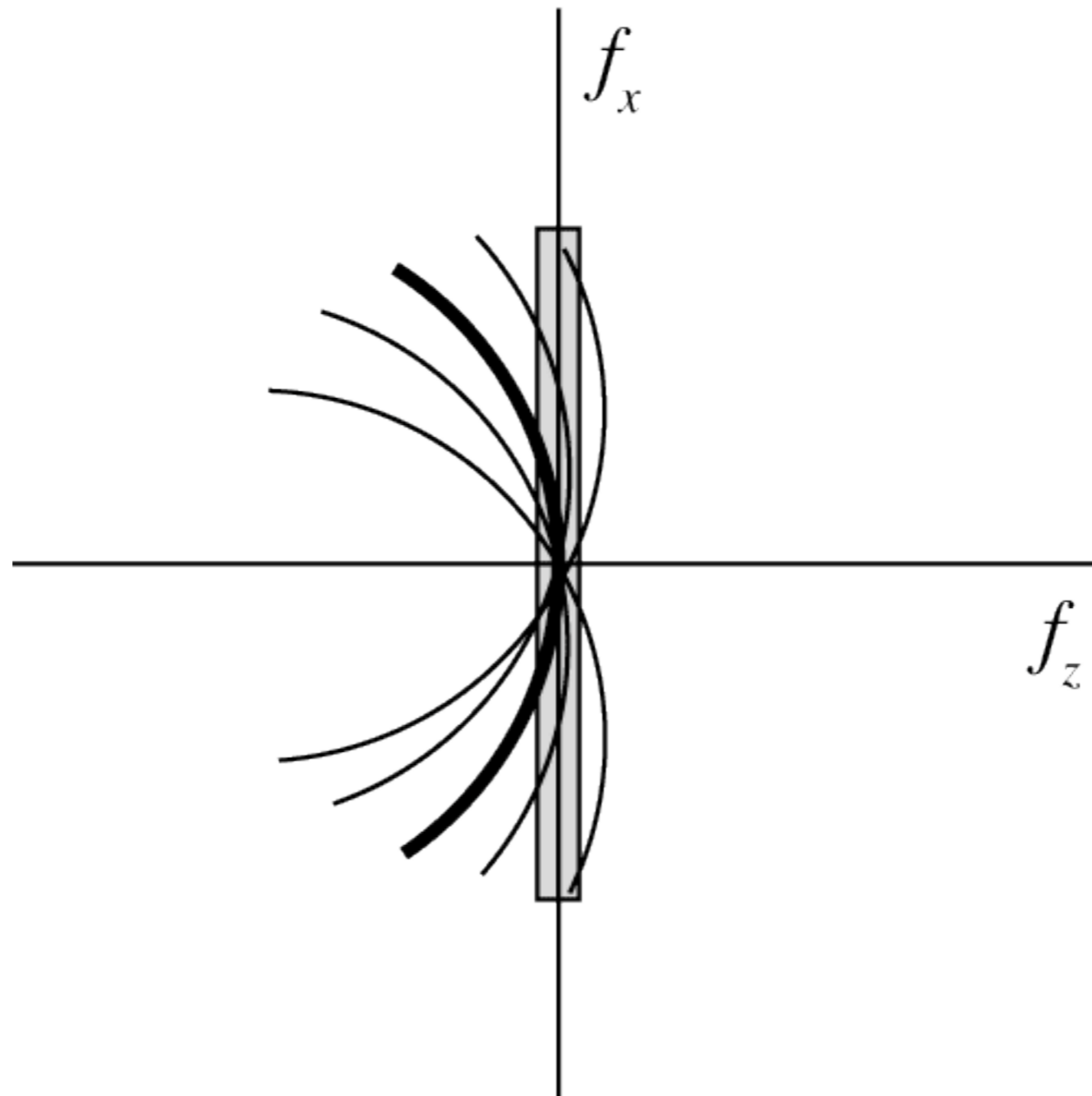
# Slices through reconstruction

- Chapman, Barty, Marchesini, Noy, Hau-Riege, Cui, Howells, Rosen, He, Spence, Weierstall, Beetz, Jacobsen, Shapiro, *J. Opt. Soc. Am. A* **23**, 1179 (2006)
- Resolution  $\sim 10 \times 10 \times 50$  nm

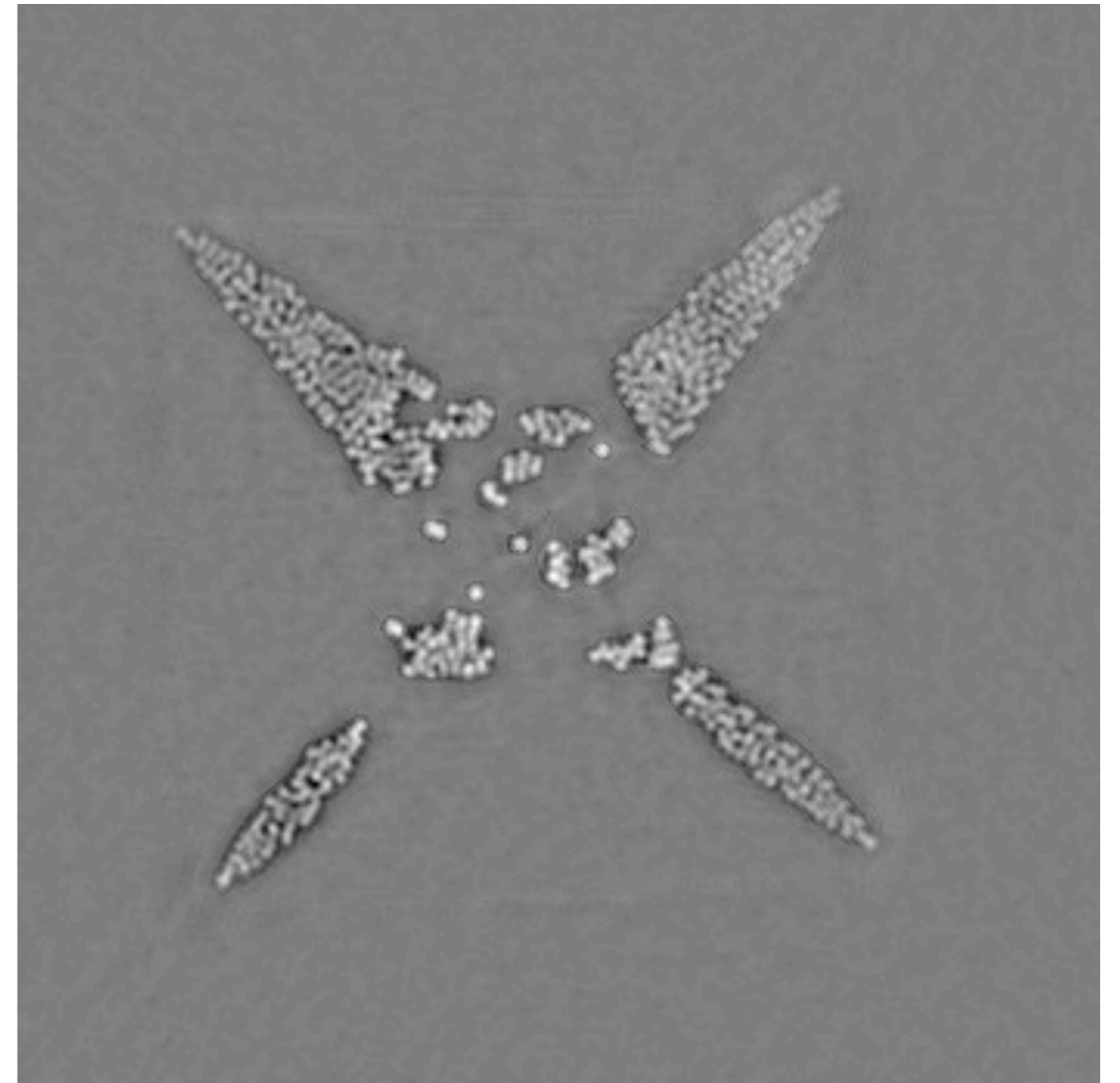
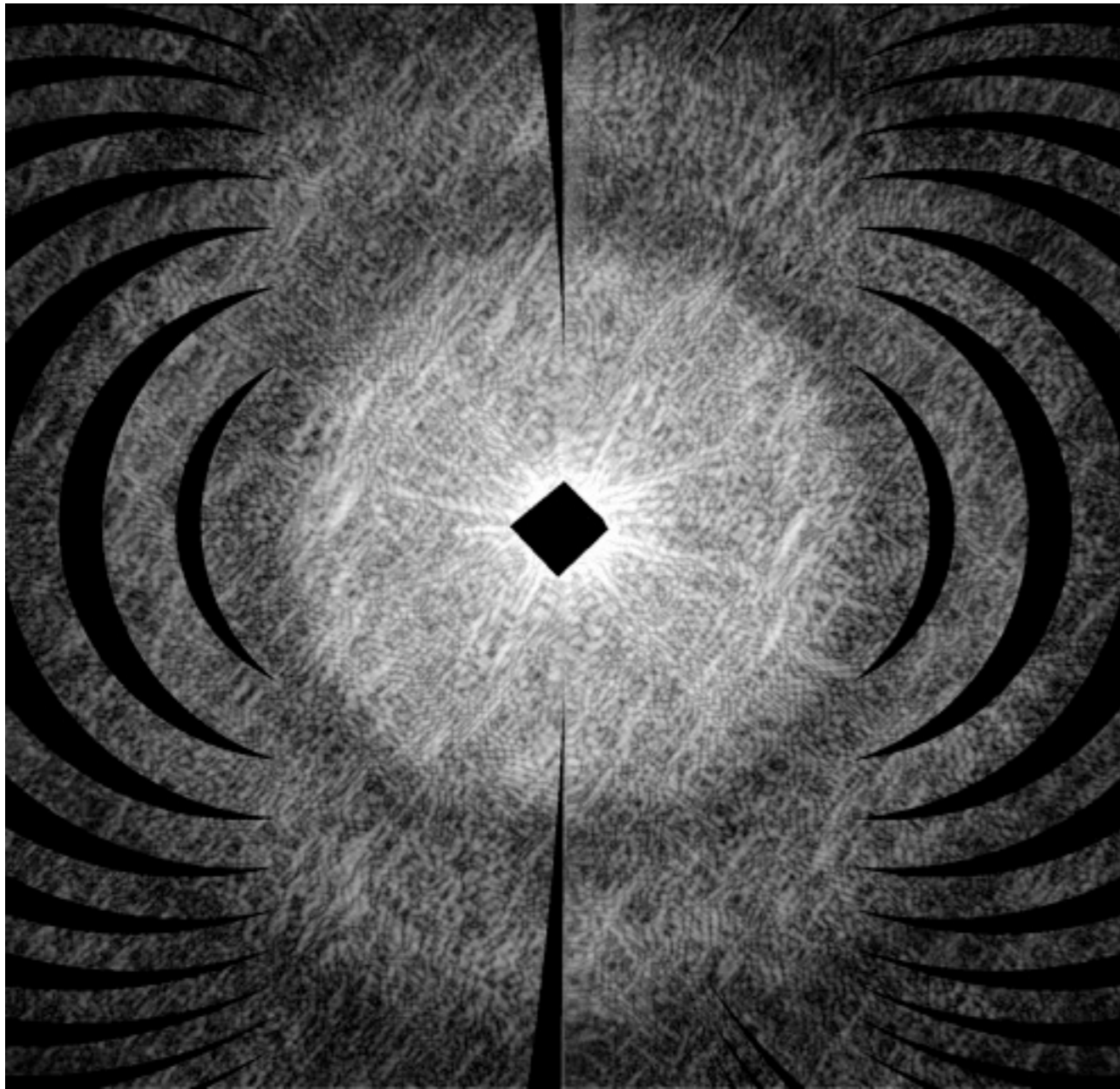


# Pure projections from phased 3D data

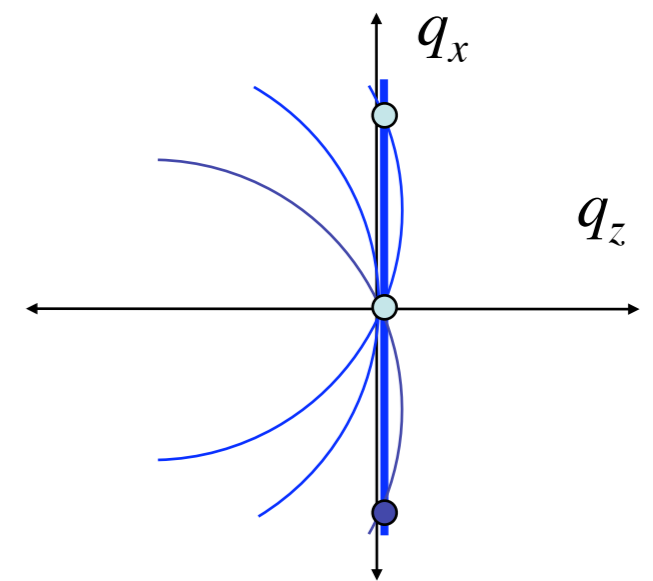
Chapman, Barty, Marchesini, Noy, Hau-Riege, Cui, Howells, Rosen, He, Spence, Weierstall, Beetz, Jacobsen, Shapiro, *J. Opt. Soc. Am. A* **23**, 1179 (2006)



# Experimental realization

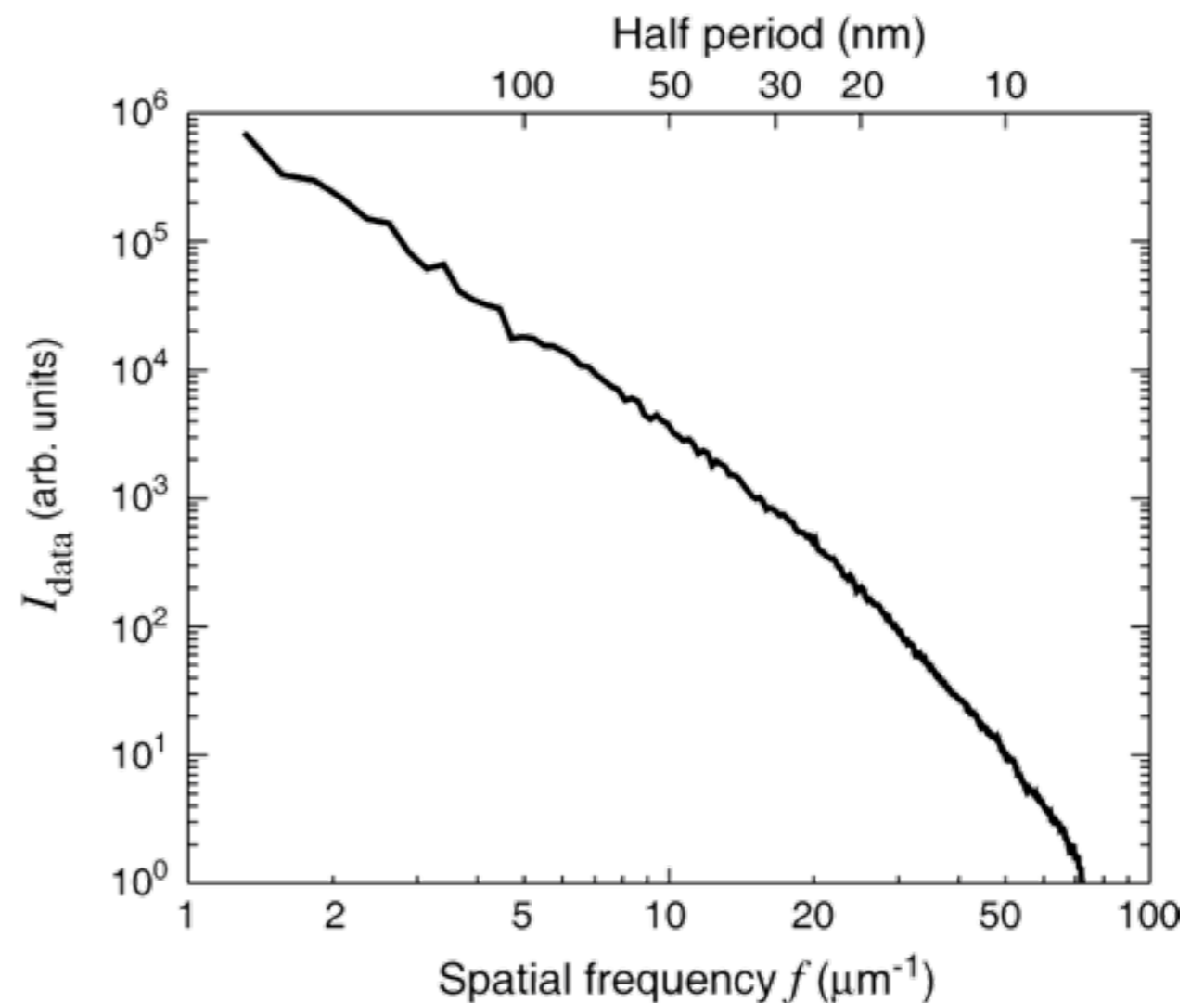
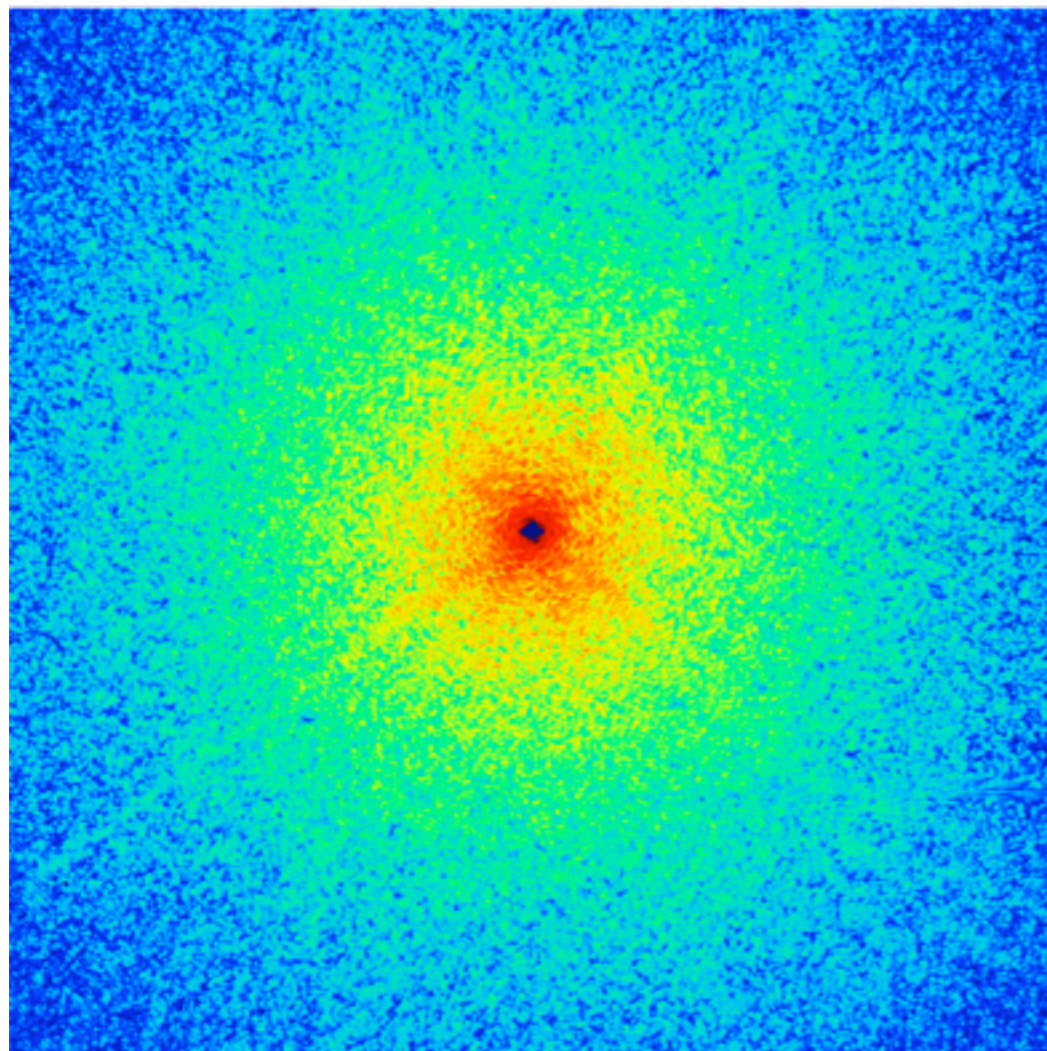


Chapman, Barty, Marchesini, Noy, Hau-Riege, Cui, Howells, Rosen, He, Spence, Weierstall, Beetz, Jacobsen, Shapiro, *J. Opt. Soc. Am. A* **23**, 1179 (2006)

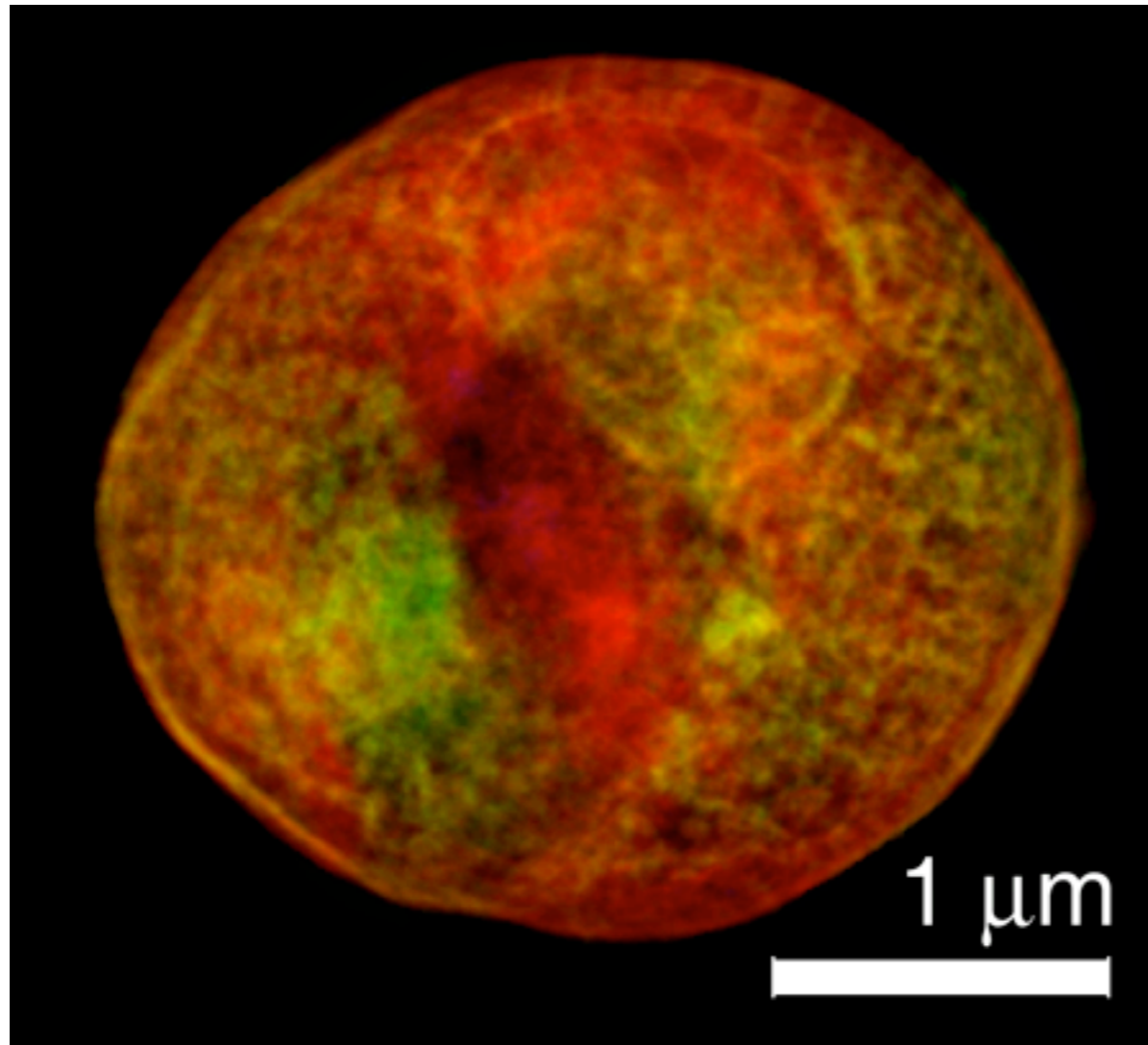


# Diffraction from a yeast cell

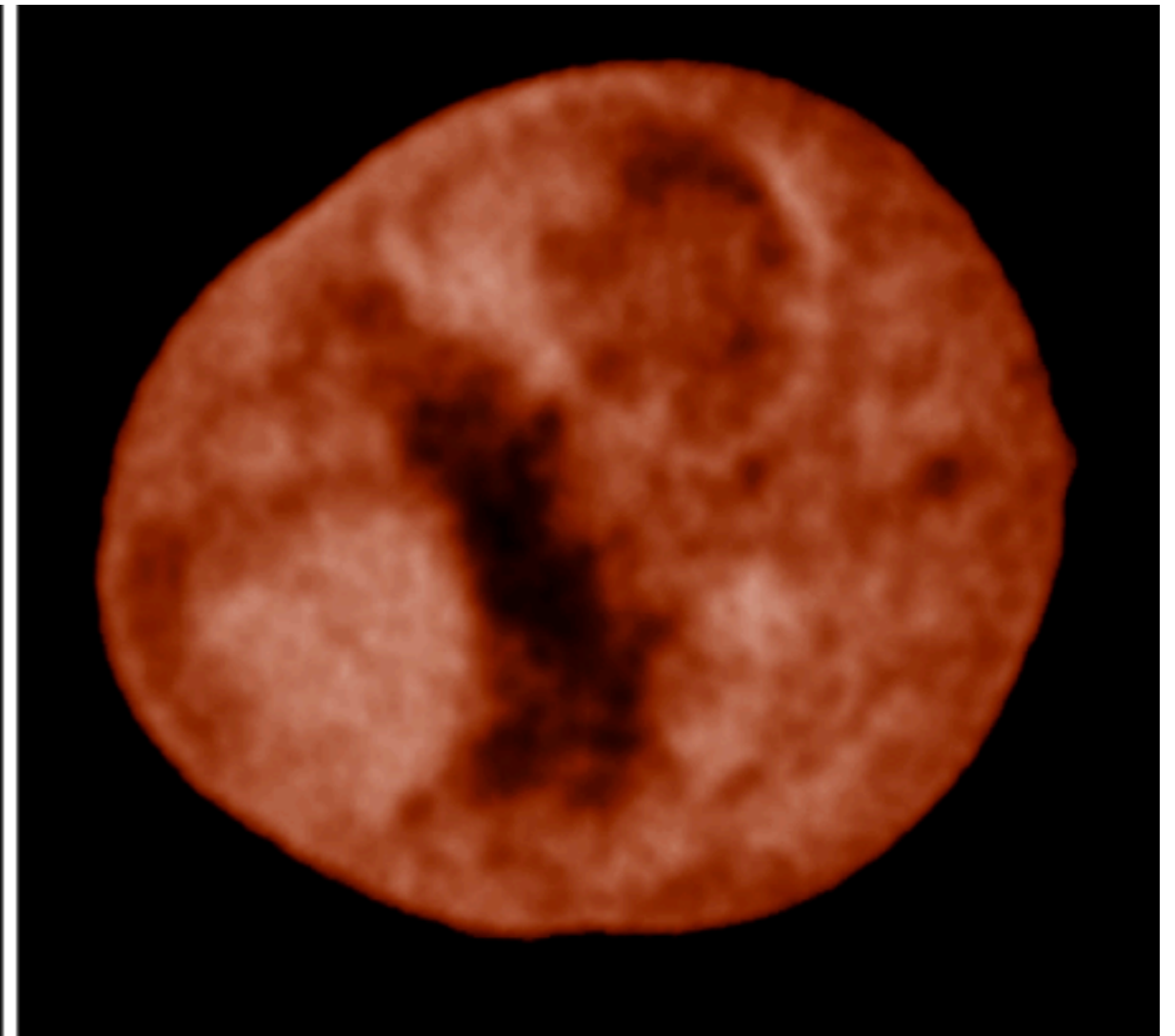
- Shapiro, Thibault, Beetz, Elser, Howells, Jacobsen, Kirz, Lima, H. Miao, Nieman, Sayre, *Proc. Nat. Acad. Sci.* **102**, 15343 (2005). ALS beamline 9.0.1 operated at 750 eV
- Total dose to freeze-dried, room temperature, unstained cell around  $10^8$  Gray



# Freeze-dried dwarf yeast



Diffraction reconstruction (data taken at 750 eV; absorption as brightness, phase as hue).



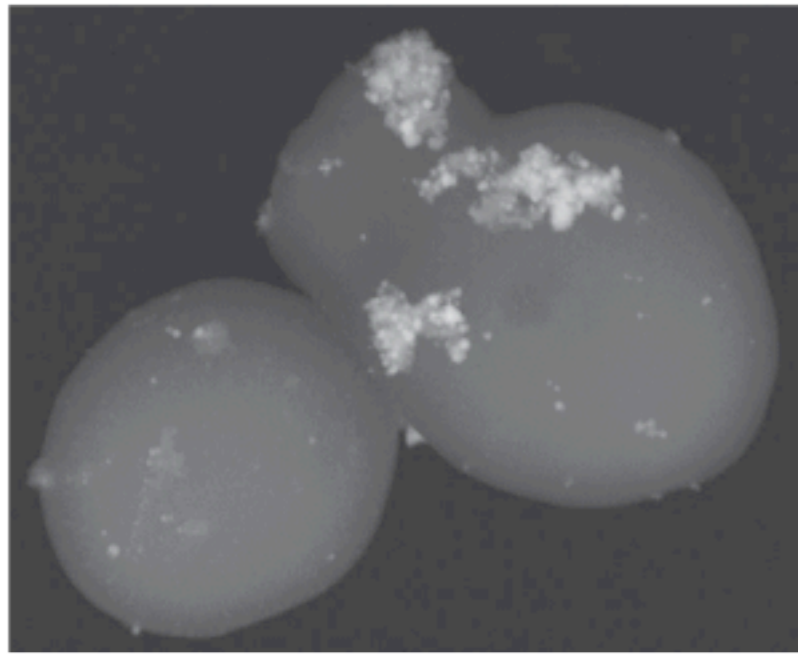
Stony Brook/NSLS STXM image with 45 nm Rayleigh resolution zone plate at 520 eV (absorption as brightness)

Shapiro *et al.*, *Proc. Nat. Acad. Sci.* **102**, 15343 (2005).

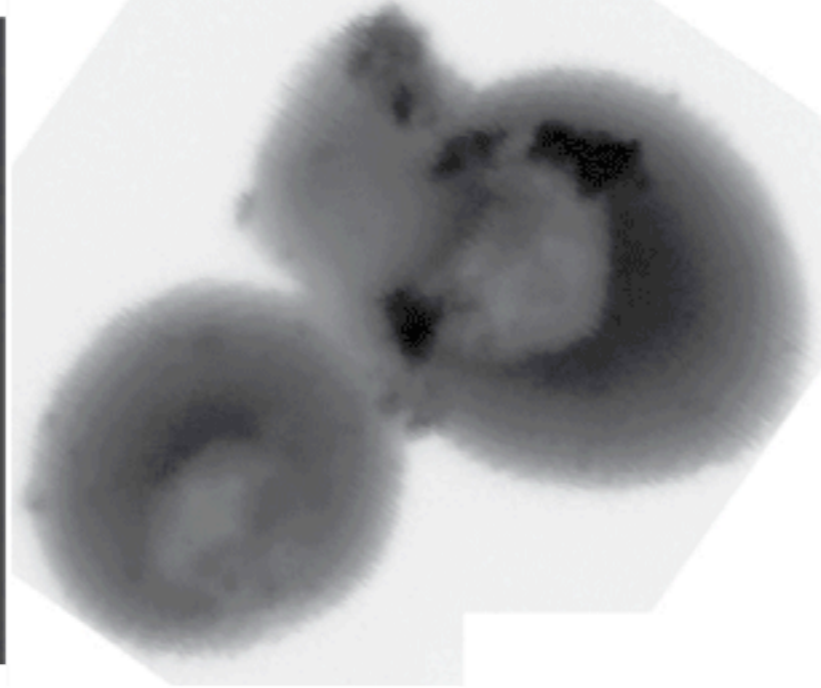


# X-ray diffraction microscopy at Stony Brook

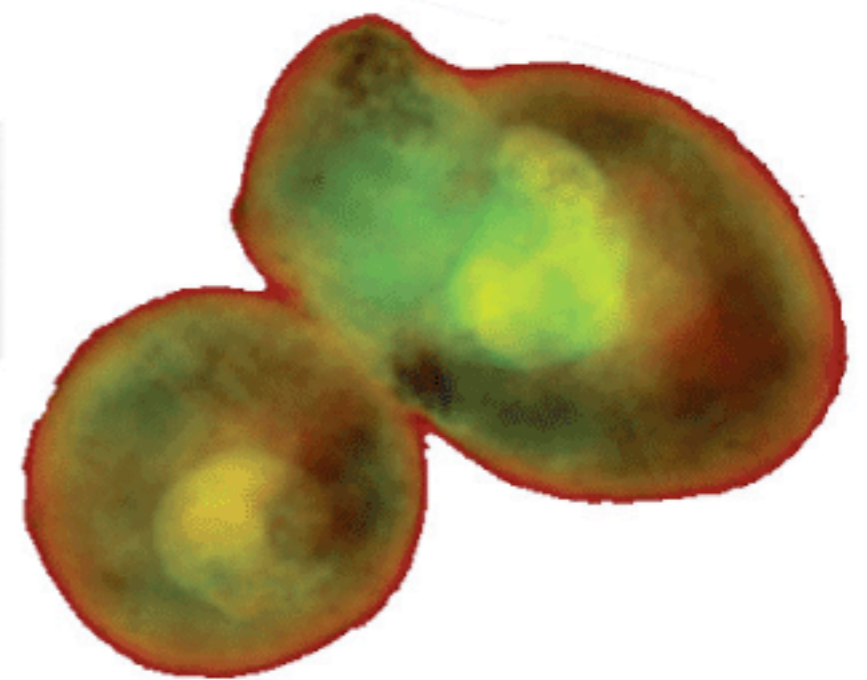
Gold labeling for surface proteins on yeast (dried; J. Nelson)



SEM

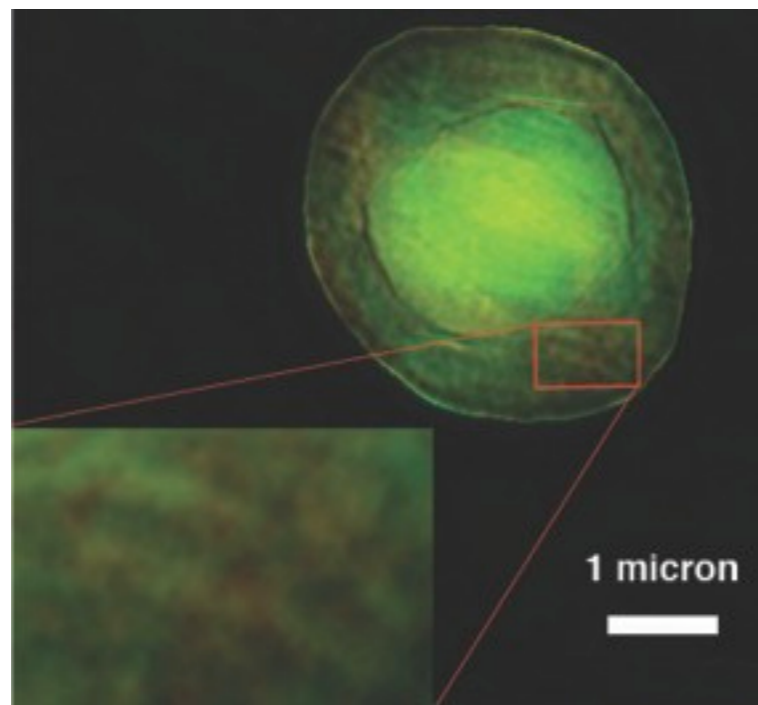


STXM



XDM

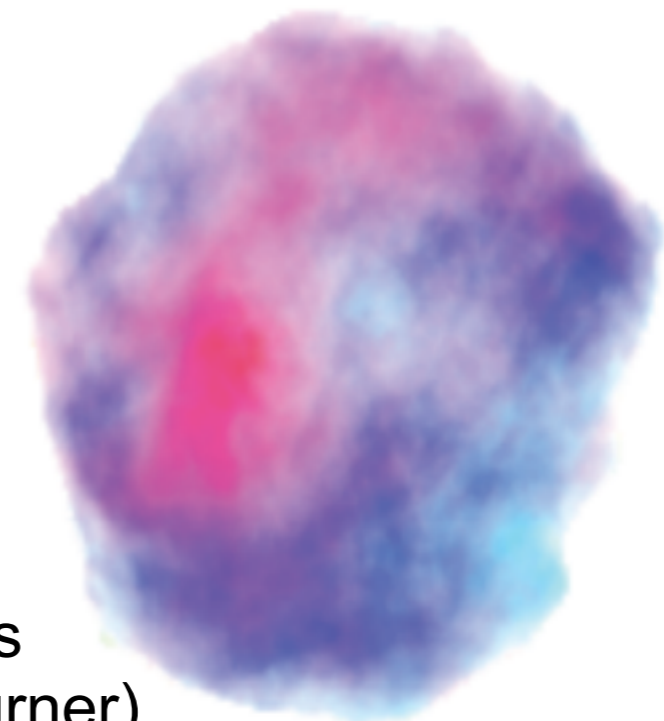
Frozen-hydrated yeast (X. Huang)



0.5  $\mu\text{m}$



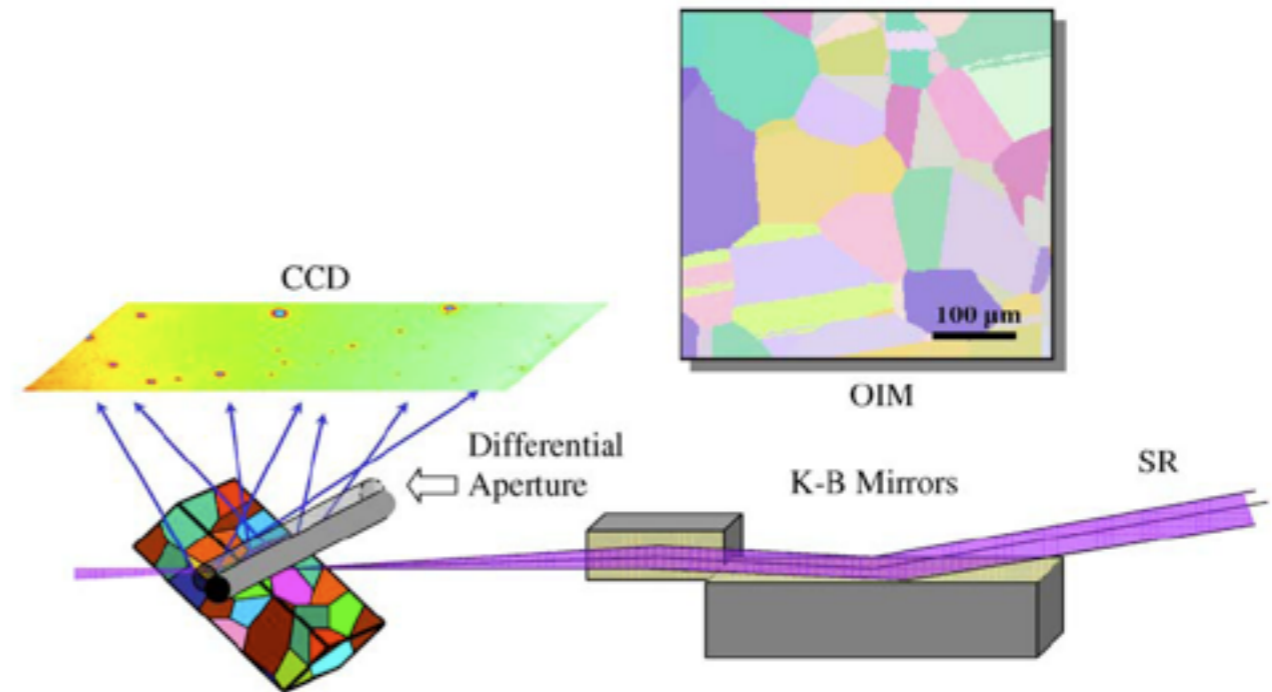
Nanoporous glass (J. Turner)



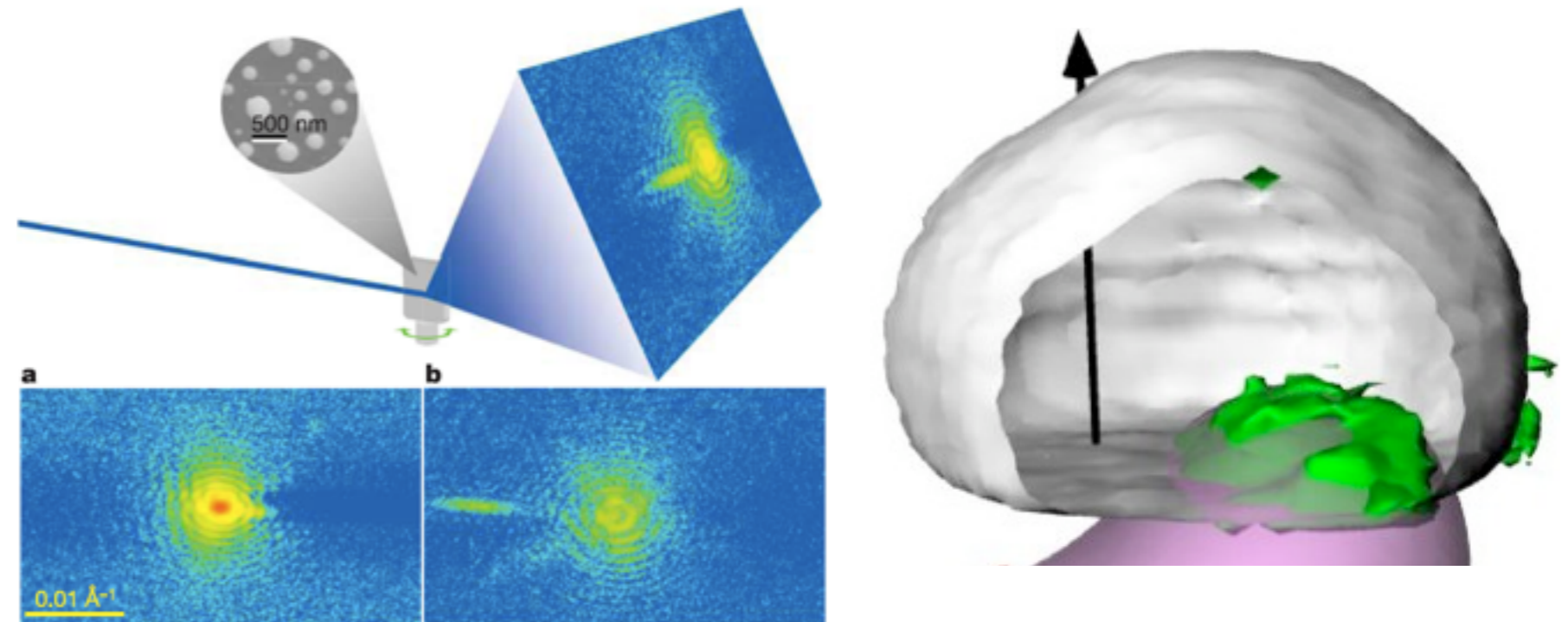
# Crystallinity, and strain within nanocrystals

W. Liu et al. / *Ultramicroscopy* 103 (2005) 199–204

Domain boundaries in polycrystalline materials: Liu et al., *Ultramicroscopy* **103**, 199 (2005).



Coherent diffraction about a Bragg peak reveals the shape of and strain within a nanocrystalline domain at 40 nm resolution. Pfeiffer et al., *Nature* **442**, 63 (2006).



# Ptychography

## High-Resolution Scanning X-ray Diffraction Microscopy

Pierre Thibault,<sup>1\*</sup> Martin Dierolf,<sup>1</sup> Andreas Menzel,<sup>1</sup> Oliver Bunk,<sup>1</sup> Christian David,<sup>1</sup> Franz Pfeiffer<sup>1,2</sup>

Coherent diffractive imaging (CDI) and scanning transmission x-ray microscopy (STXM) are two popular microscopy techniques that have evolved quite independently. CDI promises to reach resolutions below 10 nanometers, but the reconstruction procedures put stringent requirements on data quality and sample preparation. In contrast, STXM features straightforward data analysis, but its resolution is limited by the spot size on the specimen. We demonstrate a ptychographic imaging method that bridges the gap between CDI and STXM by measuring complete diffraction patterns at each point of a STXM scan. The high penetration power of x-rays in combination with the high spatial resolution will allow investigation of a wide range of complex mesoscopic life and material science specimens, such as embedded semiconductor devices or cellular networks.

SCIENCE VOL 321 18 JULY 2008 379

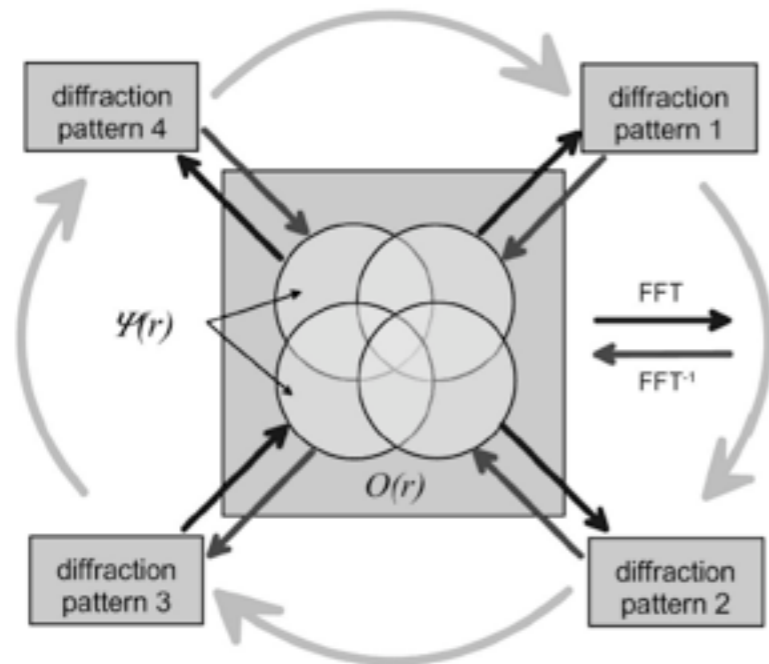
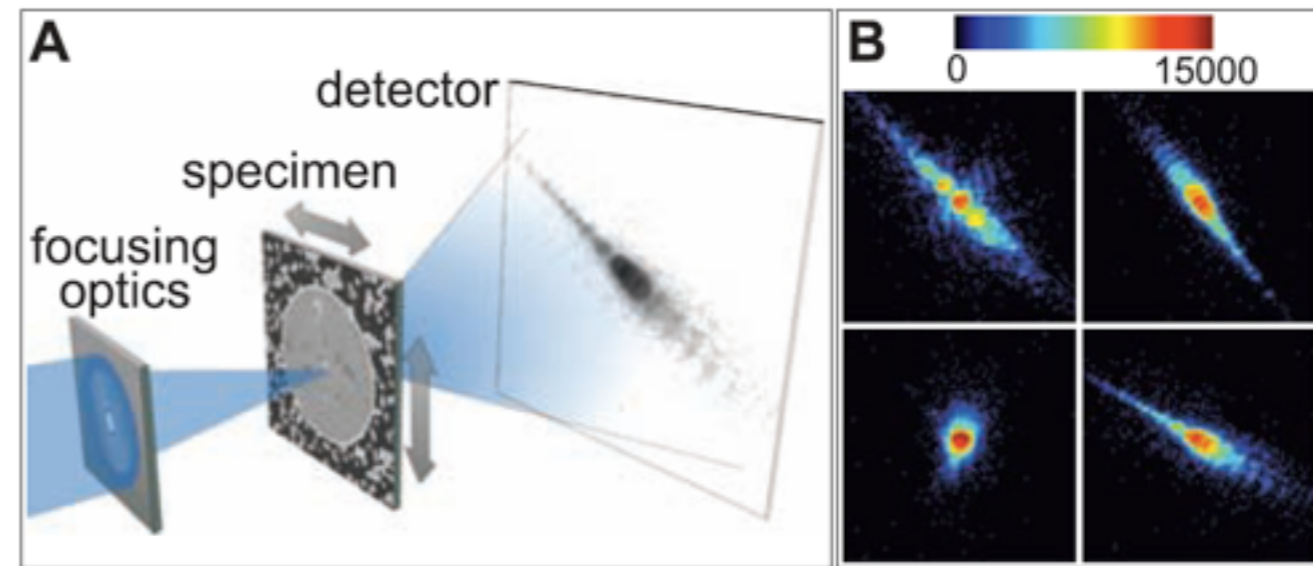
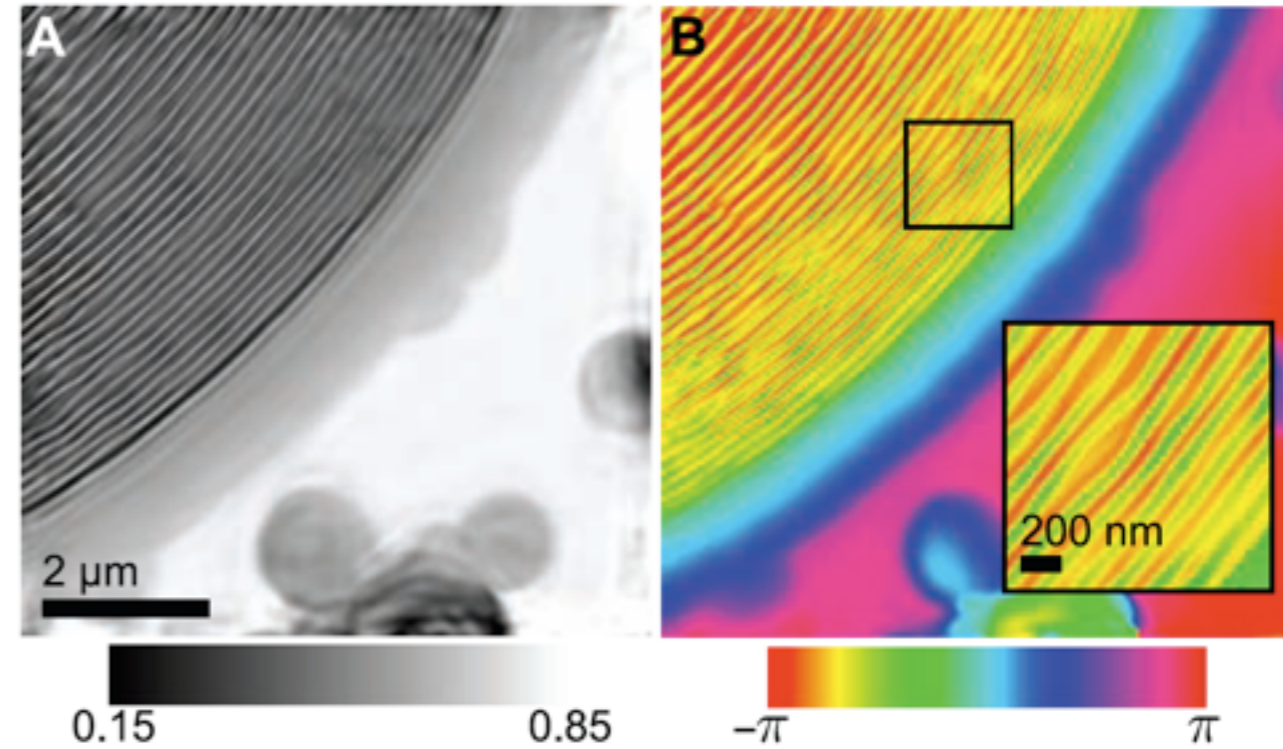


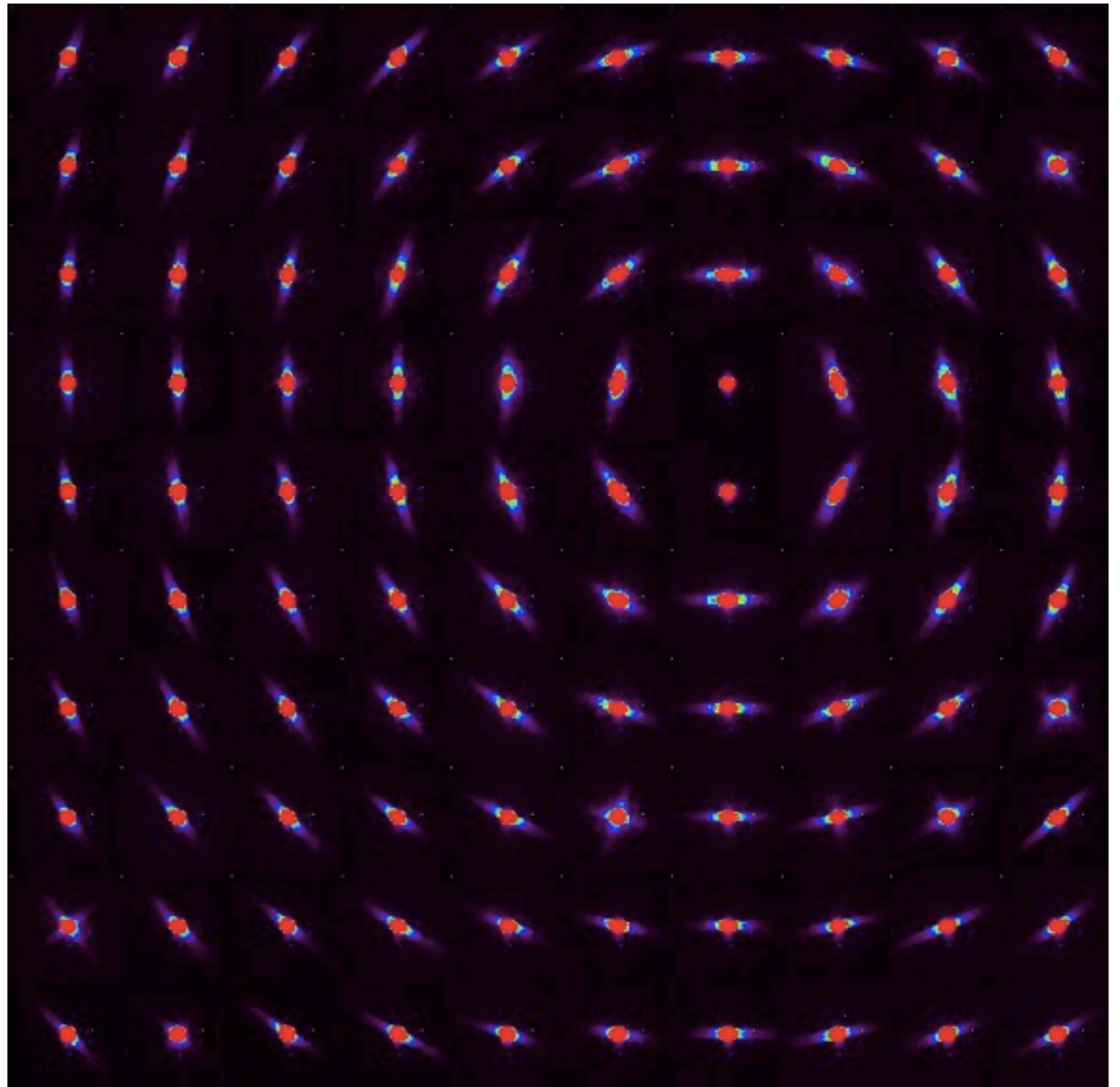
FIG. 2. Diagram of the phase-retrieval algorithm. The outer circular arrows indicate the position stepping within one iteration. The arrows within indicate (inverse) Fourier transforms and the desired input-output information.



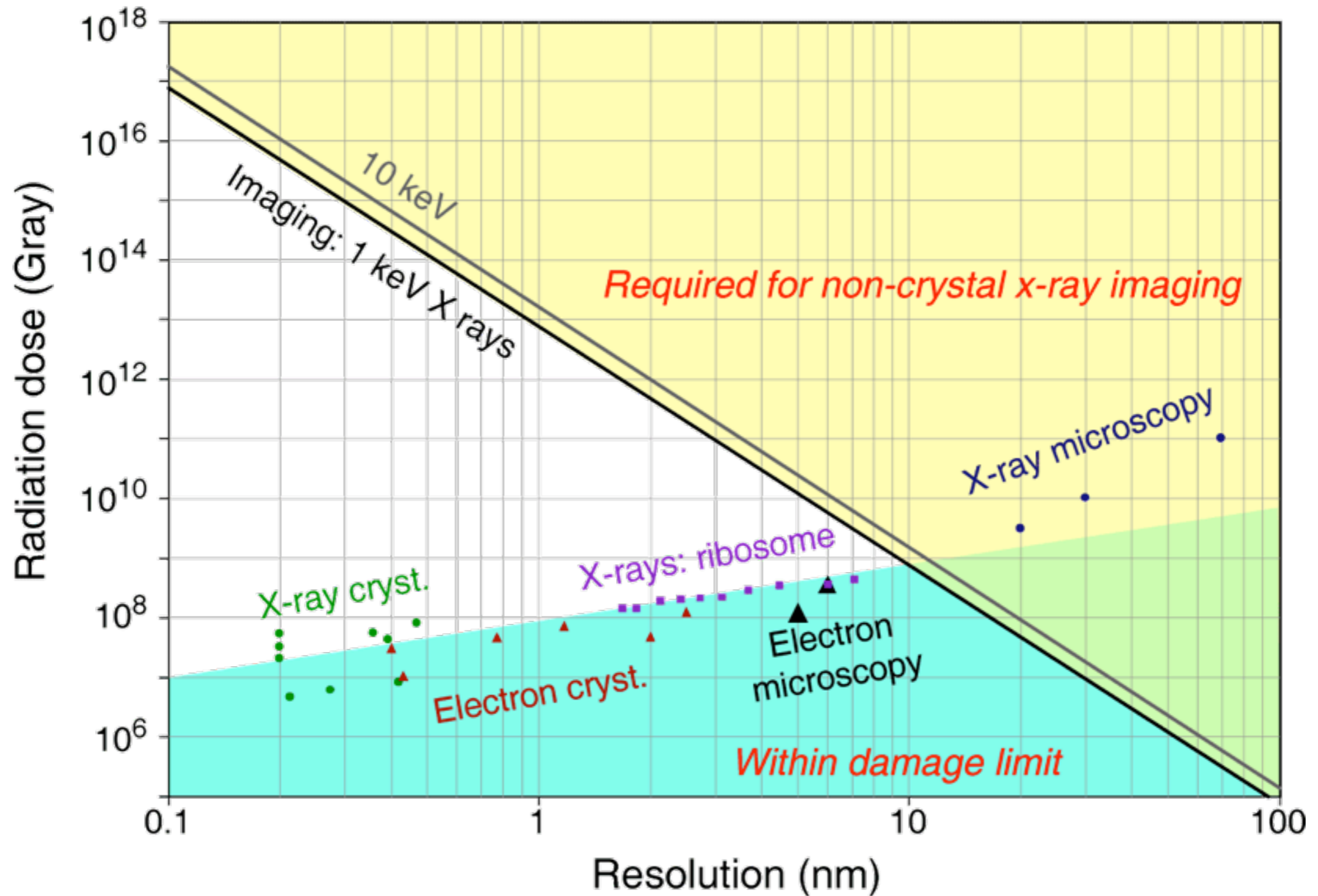
Rodenburg *et al.*, *Phys. Rev. Lett.* **98**, 034801 (2007)

# Ptychography with the Cornell PAD

- Cornell PAD (Gruner *et al.*): hybrid digital/analog electronics *per pixel* for unlimited dynamic range, fast scanning (msec/pixel)
- Experiments at APS/Argonne in April 2009: coherent diffraction series from sequential positions on a spoke pattern (Holzner, Steinbrener, Tate, McNulty...)



# What's the limit for cells?

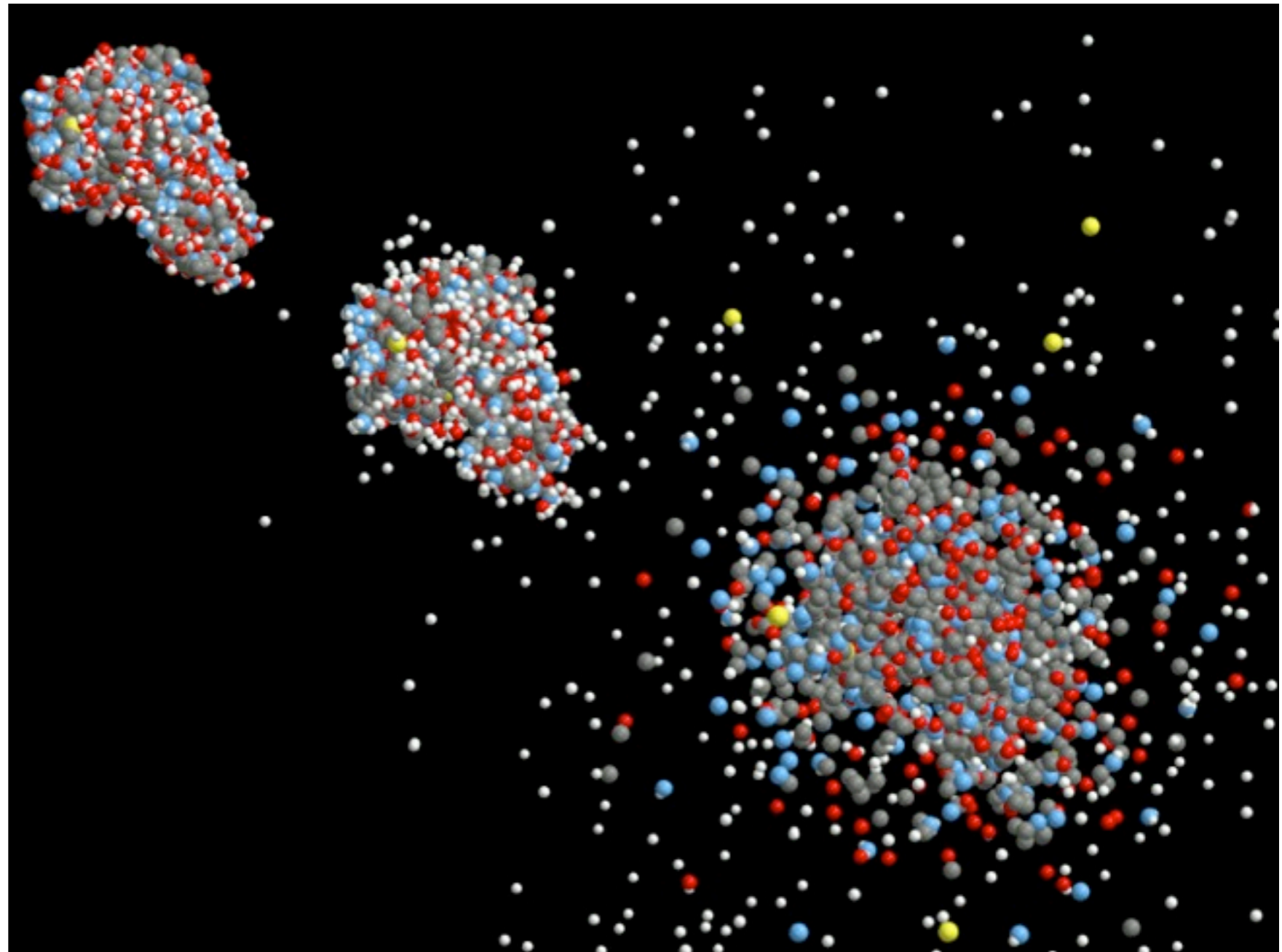


Howells et al., *JESRP* (submitted).

See also Shen et al., *J. Sync. Rad.* **11**, 432 (2004)

# How does Lysozyme react to an XFEL pulse?

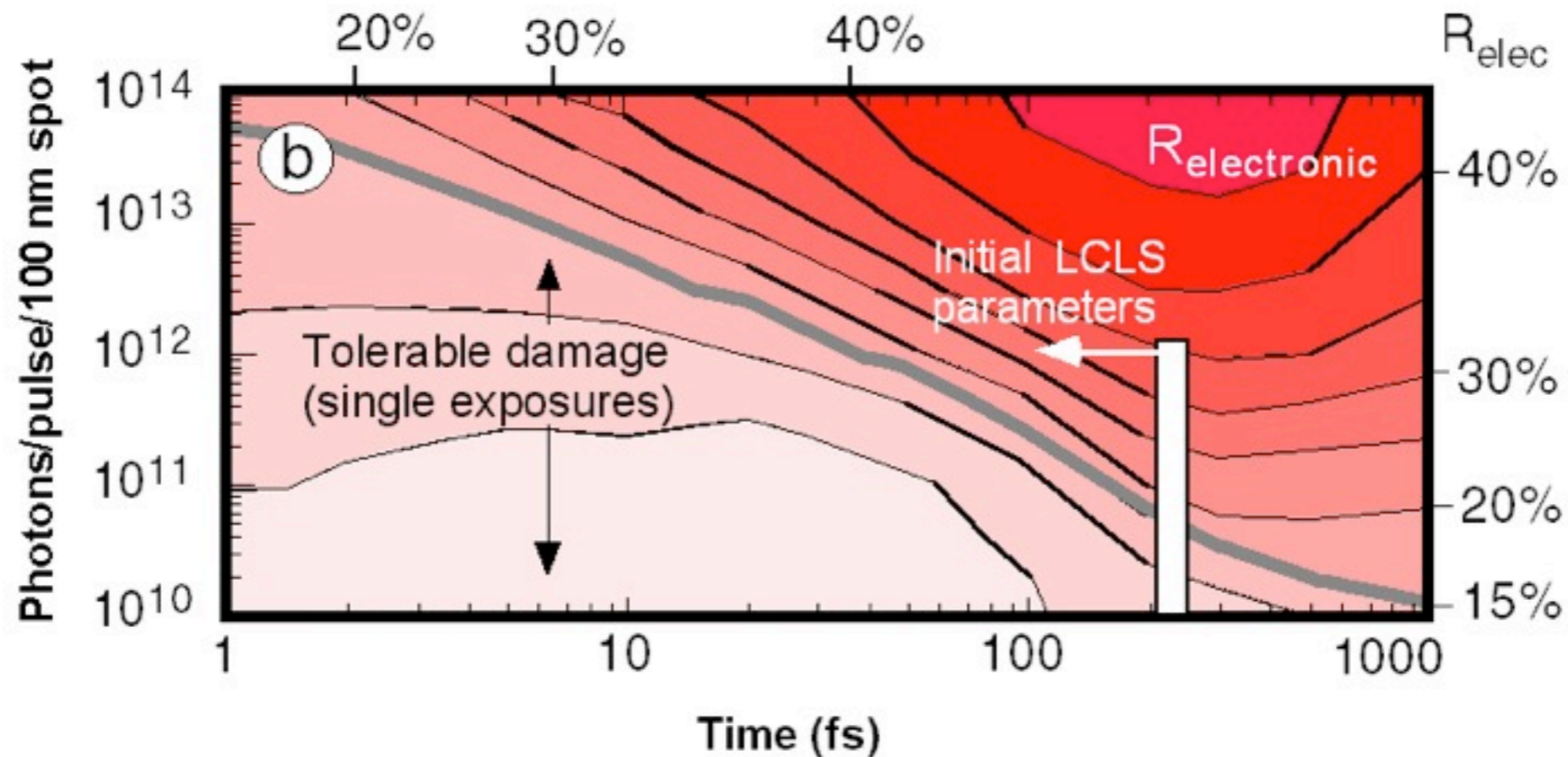
- **Violently!**
- Extension of GROMACS molecular dynamics program, with electrons removed by x rays
- Does not include any electron recombination.
- Lysozyme explodes in  $\sim 50$  fsec
- R. Neutze et al., Nature **406**, 752 (2000)



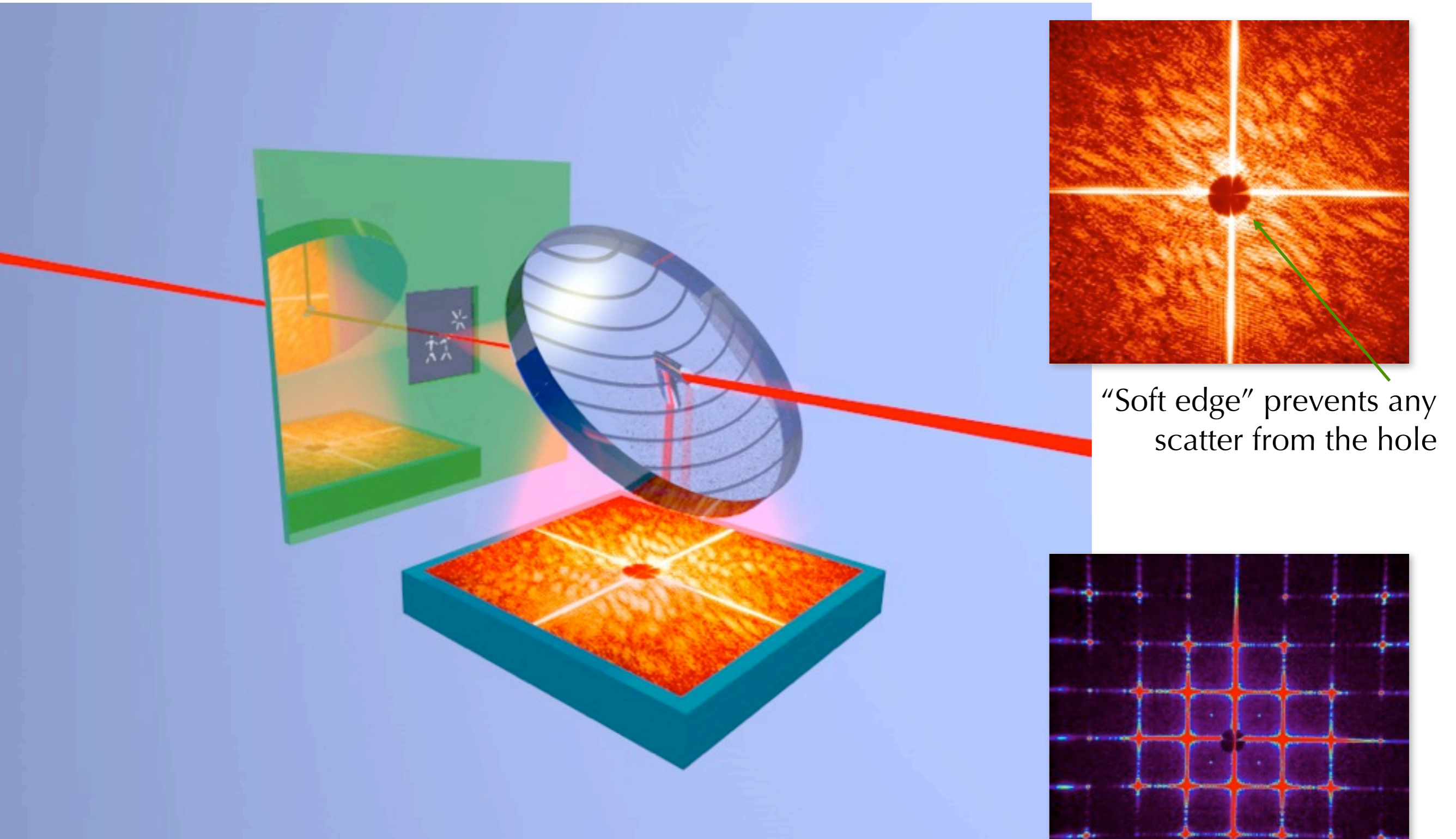
# Single molecule imaging: what's needed?

- Lots of coherent photons in a short pulse! 50 fsec is OK; 150 fsec is not.
- LCLS (Stanford), TESLA (Hamburg) X-FEL experiment proposals led by J. Hajdu (Uppsala)

$$R = \frac{|\sqrt{I(t)} - \sqrt{I_0}|}{\sqrt{I_0}}$$



# Experiments at FLASH by Chapman *et al.*, LLNL



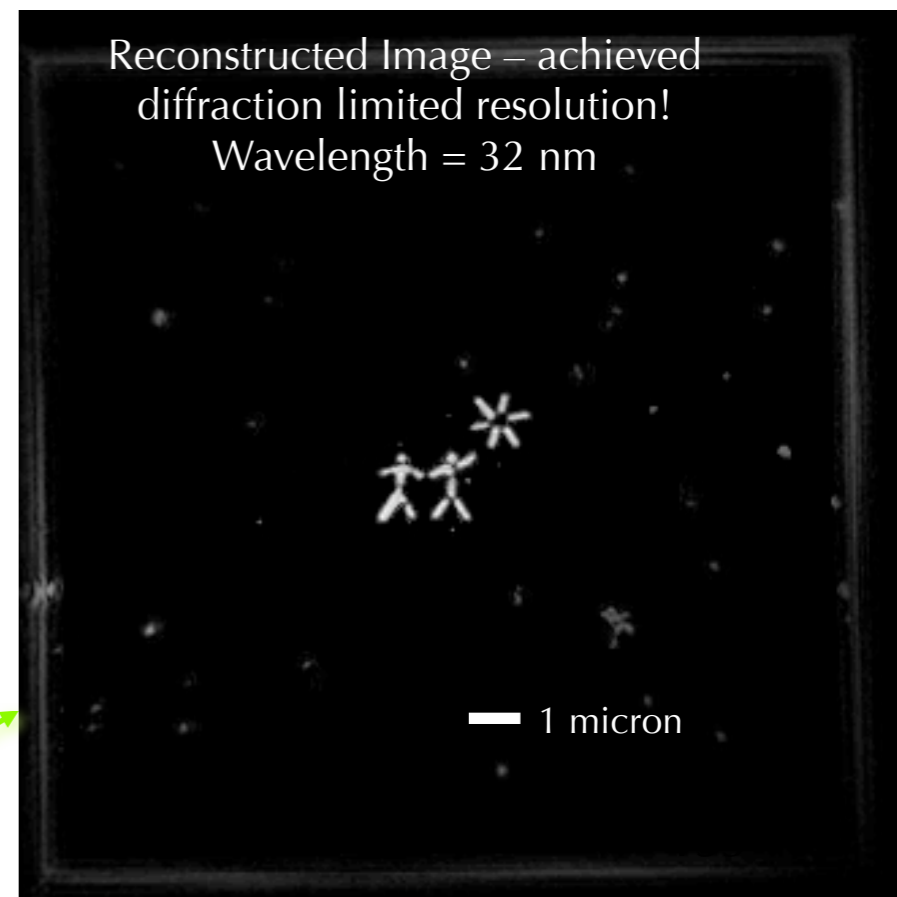
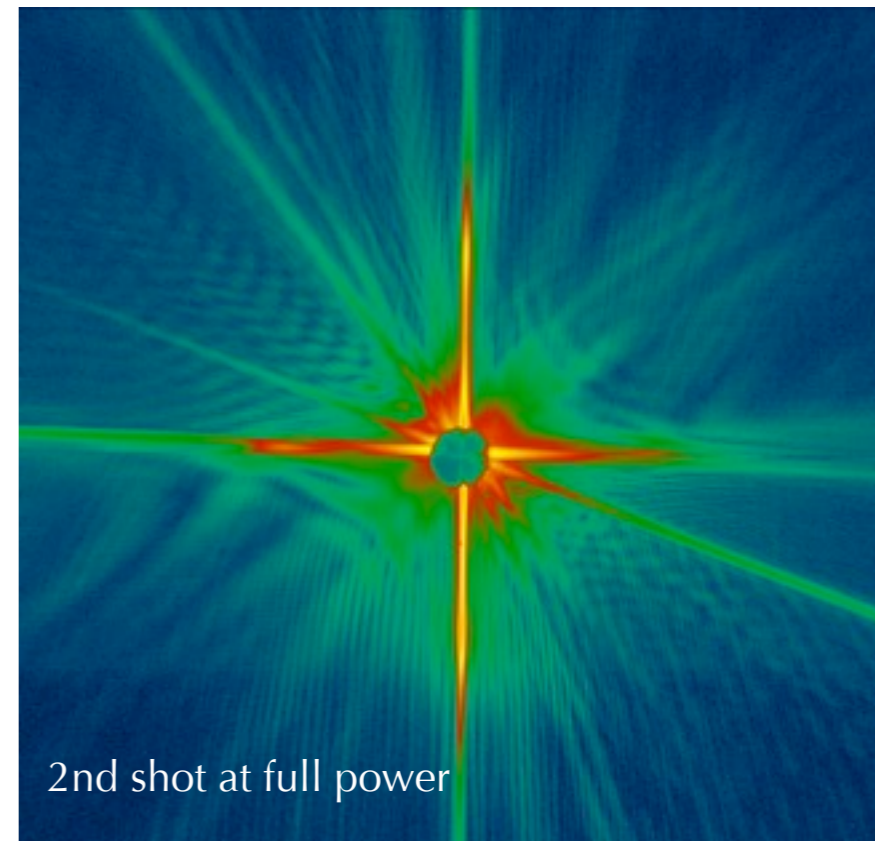
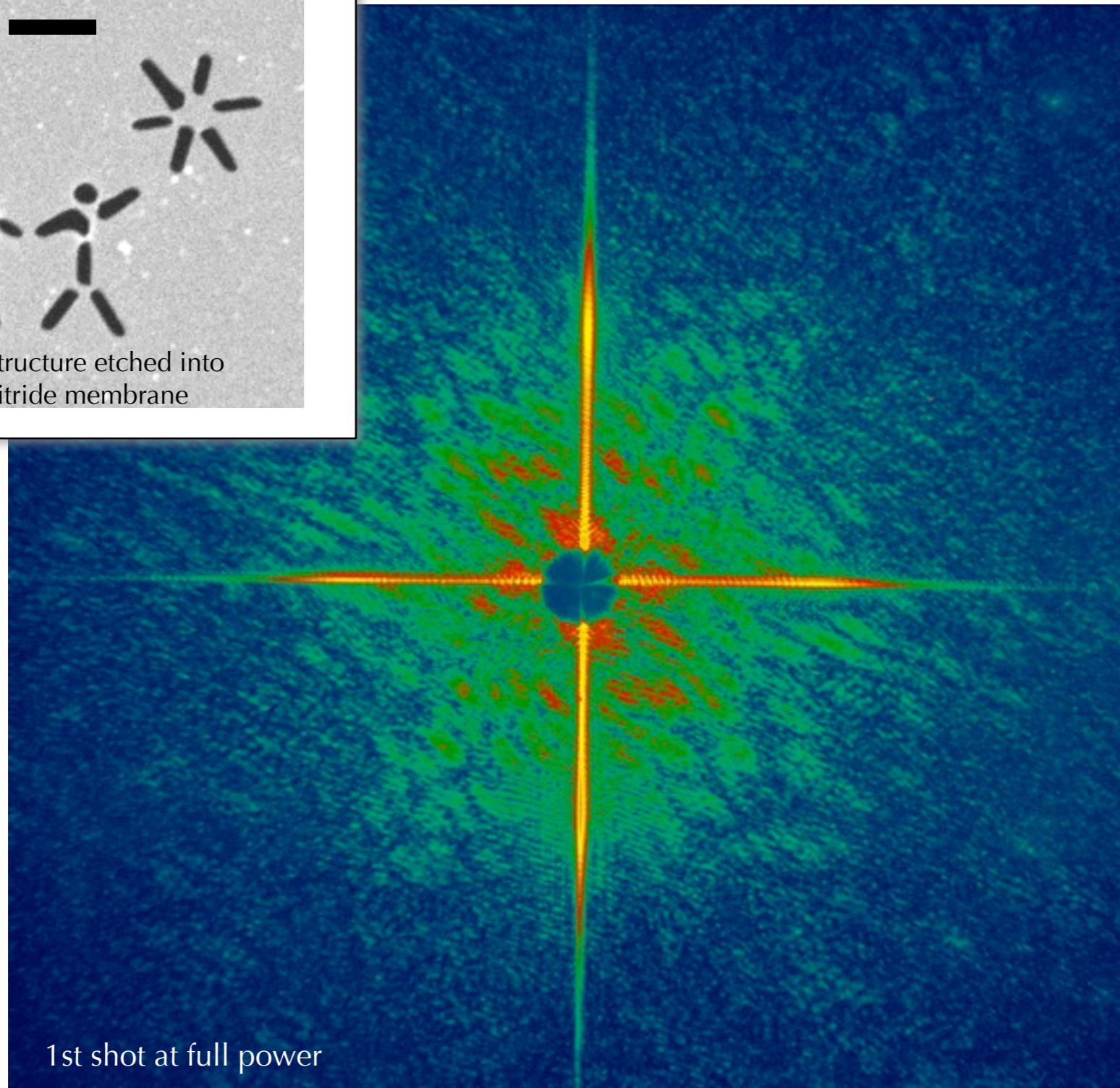
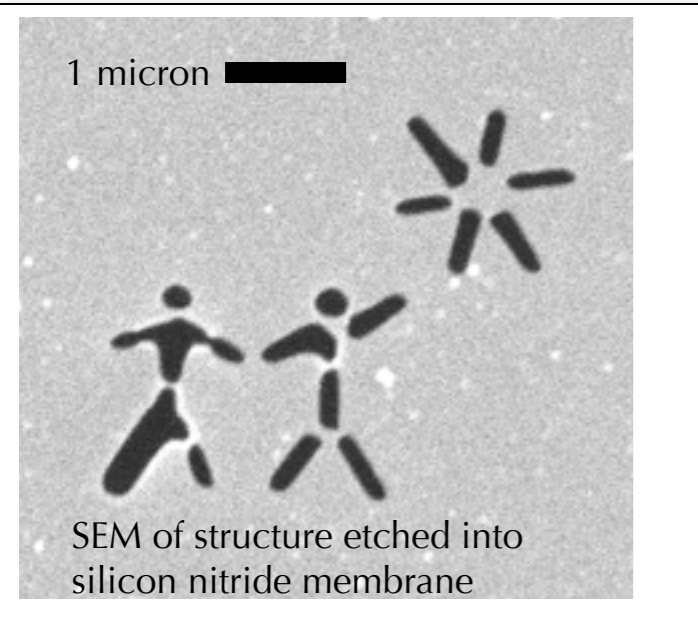
“Soft edge” prevents any scatter from the hole

Mirror/CCD: Bajt *et al.*,  
*Applied Optics* **47**, 1673  
(2008).

Multilayer reflectivity is uniform across  
the 30° to 60° gradient



# Data collected from a single pulse



Chapman *et al.*, *Nature Physics* **2**, 839 (2006)

Edge of membrane support also reconstructed

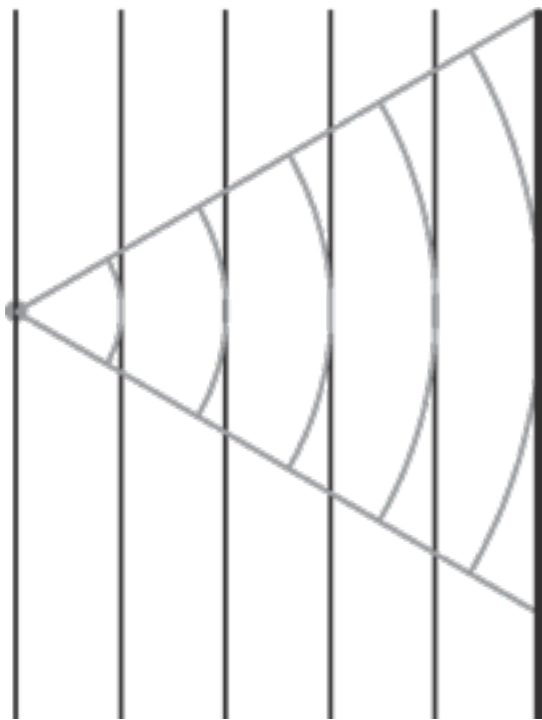


# X-ray holography

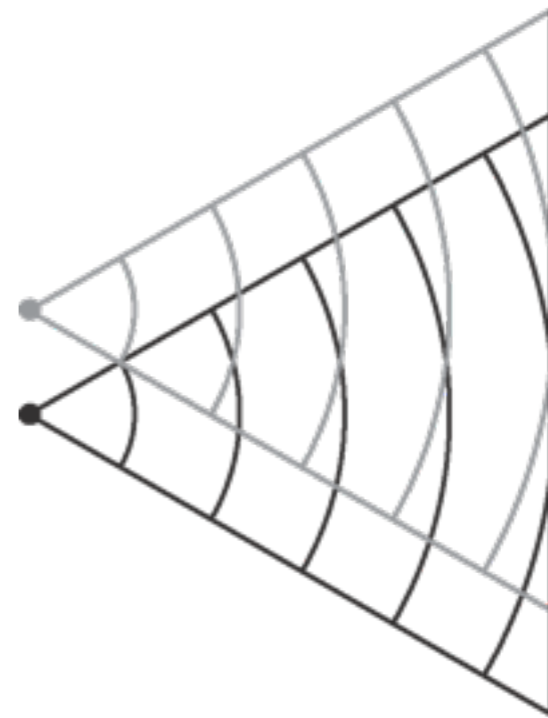
- Holography gives amplitude *and* phase of object
- Reference wave  $r$  should be stronger than object wave  $o$ :

$$I = (o + r)(o + r)^* = oo^* + rr^* + or^* + o^*r$$

- In holography, you must do *something* at high resolution



Plane reference wave:  
detector sets resolution limit



Spherical reference wave:  
point source sets resolution limit

Exciting recent progress! Eisebitt *et al.*, *Nature* **432**, 885 (2004)